

1995

Synthesis and study of novel silicon-based unsaturated polymers

Jibing Lin

Iowa State University

Follow this and additional works at: <https://lib.dr.iastate.edu/rtd>

 Part of the [Organic Chemistry Commons](#), and the [Polymer Chemistry Commons](#)

Recommended Citation

Lin, Jibing, "Synthesis and study of novel silicon-based unsaturated polymers" (1995). *Retrospective Theses and Dissertations*. 10925.
<https://lib.dr.iastate.edu/rtd/10925>

This Dissertation is brought to you for free and open access by the Iowa State University Capstones, Theses and Dissertations at Iowa State University Digital Repository. It has been accepted for inclusion in Retrospective Theses and Dissertations by an authorized administrator of Iowa State University Digital Repository. For more information, please contact digirep@iastate.edu.

INFORMATION TO USERS

This manuscript has been reproduced from the microfilm master. UMI films the text directly from the original or copy submitted. Thus, some thesis and dissertation copies are in typewriter face, while others may be from any type of computer printer.

The quality of this reproduction is dependent upon the quality of the copy submitted. Broken or indistinct print, colored or poor quality illustrations and photographs, print bleedthrough, substandard margins, and improper alignment can adversely affect reproduction.

In the unlikely event that the author did not send UMI a complete manuscript and there are missing pages, these will be noted. Also, if unauthorized copyright material had to be removed, a note will indicate the deletion.

Oversize materials (e.g., maps, drawings, charts) are reproduced by sectioning the original, beginning at the upper left-hand corner and continuing from left to right in equal sections with small overlaps. Each original is also photographed in one exposure and is included in reduced form at the back of the book.

Photographs included in the original manuscript have been reproduced xerographically in this copy. Higher quality 6" x 9" black and white photographic prints are available for any photographs or illustrations appearing in this copy for an additional charge. Contact UMI directly to order.

UMI

**A Bell & Howell Information Company
300 North Zeeb Road, Ann Arbor, MI 48106-1346 USA
313/761-4700 800/521-0600**



Synthesis and study of novel silicon-based unsaturated polymers

by

Jibing Lin

**A Dissertation Submitted to the
Graduate Faculty in Partial Fulfillment of the
Requirements for the Degree of
DOCTOR OF PHILOSOPHY**

**Department: Chemistry
Major: Organic Chemistry**

Approved:

Signature was redacted for privacy.

In Charge of Major Work

Signature was redacted for privacy.

For the Major Department

Signature was redacted for privacy.

For the Graduate College

**Iowa State University
Ames, Iowa**

1995

UMI Number: 9531761

UMI Microform 9531761

Copyright 1995, by UMI Company. All rights reserved.

**This microform edition is protected against unauthorized
copying under Title 17, United States Code.**

UMI

**300 North Zeeb Road
Ann Arbor, MI 48103**

DEDICATION

TO THE MEMORY OF MY PARENTS,

TO LINGHUA

TABLE OF CONTENTS

INTRODUCTION	1
I. POLYSILAALLENE AND CYCLIC BISALLENES	2
Literature Survey	2
Results and Discussion	6
Conclusions	18
Experimental	19
II. SYNTHESIS, THERMAL ISOMERIZATION, AND RING OPENING POLYMERIZATION OF 1,1,3,3-TETRAMETHYL-2,4-DIMETHYLENE-1,3- DISILACYCLOBUTANE	29
Literature Survey	29
Results and Discussion	44
Conclusions	76
Experimental	77
III. THE FIRST SYNTHESIS AND STUDY OF CUMULENE-CONTAINING POLYMERS	88
Literature Survey	88
Results and Discussion	108
Conclusions	180
Experimental	181
FUTURE WORK	208
REFERENCES	212
ACKNOWLEDGMENTS	223

INTRODUCTION

Three separate studies are included in this thesis.

The first section of this thesis addresses the synthesis and study of a polysilaallene, 10- and 8-membered ring cyclic bisallenes. The polysilaallene was characterized by GPC, TGA, NMR, UV, and FTIR. The structure of strained, cyclic bisallenes were studied by X-ray diffraction. Photolysis and thermolysis of the cyclic bisallenes were investigated. Attempted synthesis and isolation of a 6-membered ring cyclic allene, 1,3-bis(trimethylsilyl)-4,4,6,6-tetramethyl-5-oxy-4,6-disilacyclohexa-1,2-diene, is also presented.

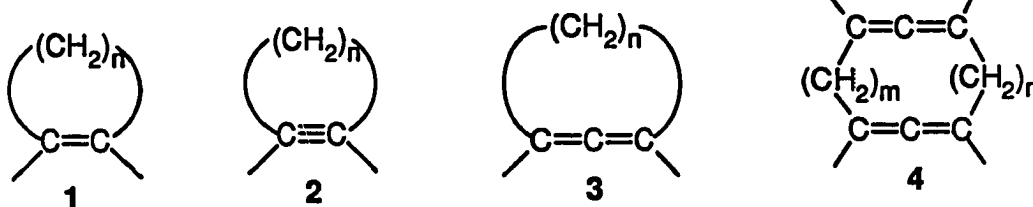
The second section deals with the synthesis, mechanism and kinetics of the thermal isomerization of 1,1,3,3-tetramethyl-2,4-dimethylene-1,3-disilacyclobutane. The reexamination and kinetics study of the thermal rearrangements of 1,1-dimethyl-2-methylene-1-silacyclobutane were also conducted. The question as to why the carbon analogs of the four membered rings does not isomerize under the same conditions was probed theoretically. Anionic and catalytic ring opening polymerization of the dimethylenedisilacyclobutane were also conducted.

The last section of this thesis involves the first synthesis and study of cumulene-containing polymers. To improve the solubility and processability of the polymers, alkoxy side chains or flexible blocks as main chain building segments were introduced. All the polymers synthesized were characterized by GPC, DSC, NMR, UV-VIS, and FTIR. The doped conductivity and the high third-order nonlinear optical response of conjugated cumulene-containing polymers measured by Z-scan technique are discussed. Finally, comparative studies were conducted on a 1,2,3-butatriene-containing polymer and a 1,3-butadiene-containing polymer, a formal partial reduction product of the former.

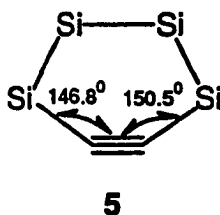
I. POLYSILAALLENE AND CYCLIC BISALLENES

Literature Survey

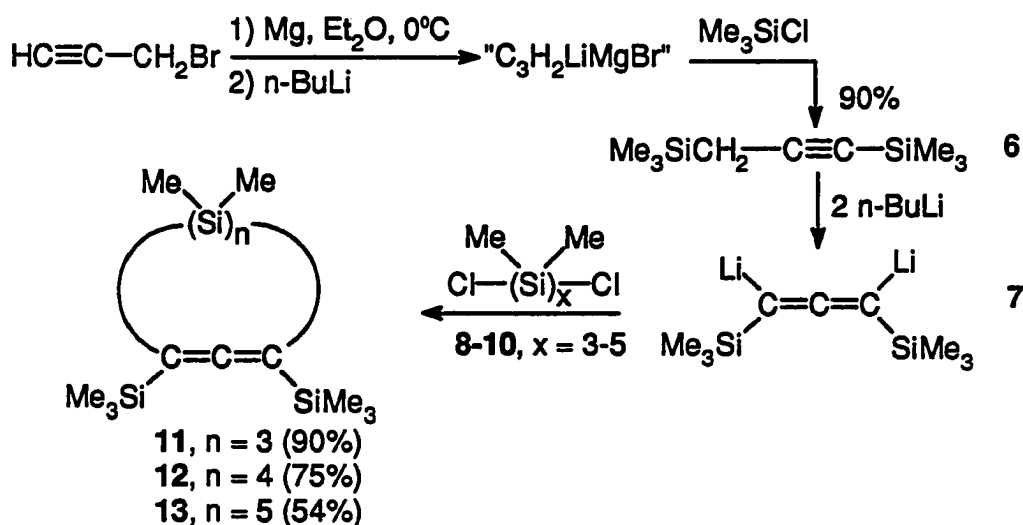
Highly strained, unsaturated cyclic molecules have drawn considerable attention because of the interest in their structural limitation and reactivities.¹ There is no limitation in the ring size of cycloalkenes (1), the readily prepared and isolated cyclopropenes have ring strain energy > 50 kcal/mol.²



The smallest isolated all carbon cycloalkyne (2) is a seven-membered ring.³ Smaller ring size cycloalkynes have been subjects of theoretical study.⁴ Cyclobutyne, as a ligand of a metal complex, has been synthesized.⁵ Recently, the synthesis and characterization of a six-membered ring polysilacycloalkyne was reported independently by two groups.^{6,7} X-ray structural analysis revealed the Si-C \equiv C bond angles of 146.8° and 150.5° in compound 5 where the asymmetry was produced from the crystal packing.⁶ The smaller bond angle of 146.8° may be compared with the C-C \equiv C angle of cyclooctyne,⁸ 158.5° , and the smallest angle, $145.8 \pm 0.7^\circ$ measured in 3,3,6,6-tetramethyl-1-thia-4-cycloheptyne.³

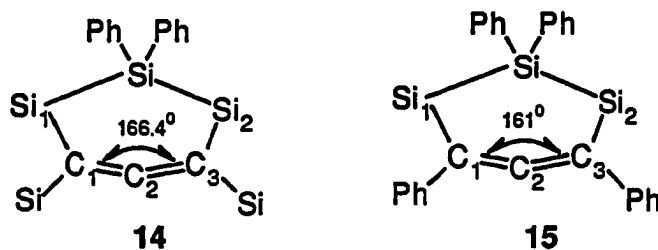


While in cycloalkynes the carbon-carbon triple bond unit can only be bent, the allene unit in cycloallenes (**3**) is usually both bent and twisted.⁹ The smallest isolated all carbon cycloallene is the eight-membered ring.¹⁰ The smallest isolated cycloallene, six-membered ring tetrasilacycloallene, was recently reported by two groups.^{11,12} The synthetic route shown in Scheme 1¹¹ is based on the quantitative conversion of 1,3-bis(trimethylsilyl)-1-propyne (**6**) to the allenyl dianion (**7**) upon treatment with two equivalents of *n*-BuLi in ether. Quenching of **7** with dichloropolysilanes (**8-10**) gives good yield of allene cyclics (**11-13**).

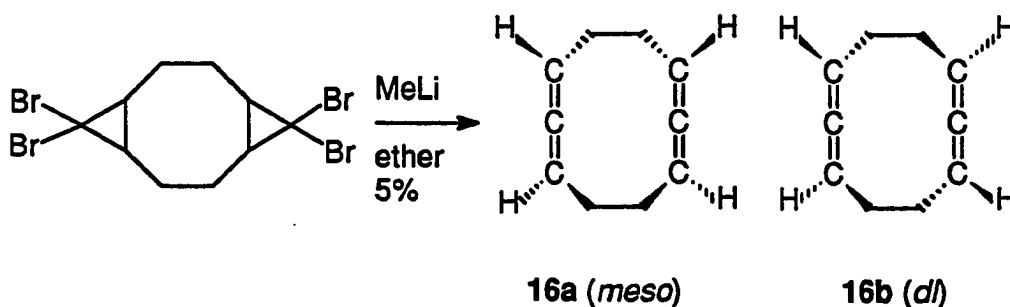


Scheme 1. Synthesis of polysilacycloallenes.

In compound **14**,¹¹ the allene unit was bent to 166.4° and the twisting dihedral angle defined by the $\text{Si}_1\text{-C}_1\text{-C}_2$ and $\text{Si}_2\text{-C}_3\text{-C}_2$ planes is 64.6° . In compound **15**,¹² the allene unit was bent to 161° and the twisting dihedral angle defined by the $\text{Si}_1\text{-C}_1\text{-C}_3$ and $\text{Si}_2\text{-C}_3\text{-C}_1$ planes is 52.2° . The allene units in the two slightly different six-membered ring systems, were bent $15\text{-}20^\circ$ away from the normal linear geometry. Even though the twisting was defined differently in the two systems, the twisting was very removed from the normal vertical geometry.



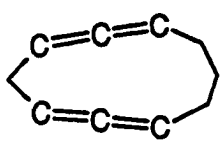
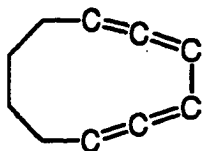
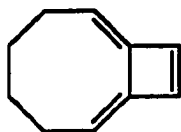
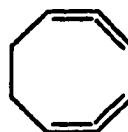
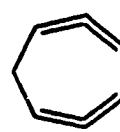
In the cyclic bisallenes (4), both allenic units can bend and twist to accommodate the ring strain. Skattebol reported the synthesis of the first cyclic bisallene **16** ($m = n = 2$ in **4**) based on the reaction of *gem*-dibromocyclopropane with methyllithium (Scheme 2).¹³ Compound **16** obtained consists of an approximate one-to-one mixture of *meso* and *dl* pair isomers. The stereoselective synthesis of compound **16** was also reported recently.¹⁴ An X-ray structure¹⁵ of the *meso* isomer **16a** shows the allene bond is bent to 174° , which implies very modest strain. The distance between the two allenic central carbon atoms in **16a** is 3.208 \AA which is a little long for proximity interactions (Van der Waal's radii for the allenic center carbon should be similar to the acetylenic carbon, which is $\sim 1.5 \text{ \AA}$).



Scheme 2. Synthesis of cyclic bisallene from *gem*-dibromocyclopropane.

The ten-membered ring cyclic bisallene **17** was also isolable.¹⁶ An attempt to synthesize **18**, however, was not successful since it tautomerized to the bicyclic valence tautomer **19**

even at low temperature.¹⁷ A few smaller cyclic bisallenenes such as **20**¹⁸ and **21**¹⁹ have only been postulated as reaction intermediates.

**17****18****19****20****21**

Results and Discussion

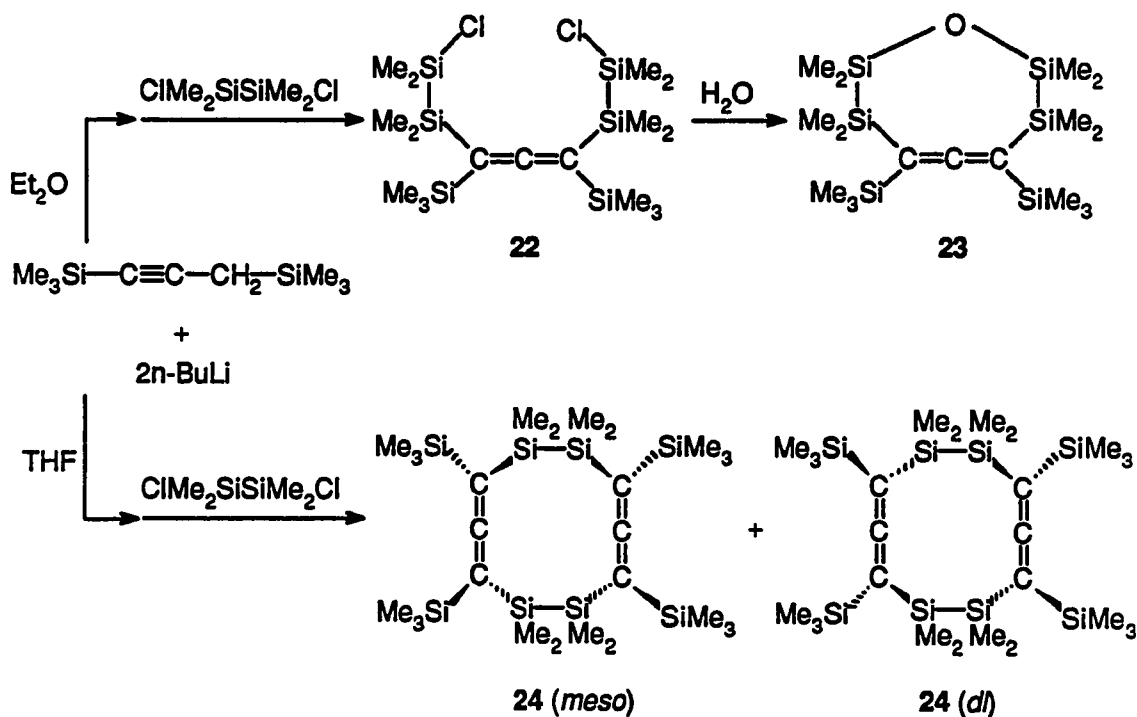
Synthesis and structure study of polysilaallene and cyclic bisallene.

Although our group has recently reported the surprising observations that 1,3-dilithio-1,3-bis(trimethylsilyl) allene **7** cleanly condenses with α -, ω -dichlorosilanes **8-10** to produce the strained silacycloallenes **11-13** (Scheme 1),¹¹ we assumed that polymerization, not cyclization, was the only reasonable option for the condensation of **7** and ClMe₂SiSiMe₂Cl or Me₂SiCl₂.

In contrast to this assumption, the reaction of **7** and ClMe₂SiSiMe₂Cl in ether was not complete, and compound **22** was obtained as the major product. When two equivalents of dichlorodisilane were used to quench the dianion **7** in ether, compound **22** was obtained in excellent yield. Upon work up, compound **22** was quantitatively converted to compound **23**, a cyclic allene containing a siloxane unit.

However, reaction of dianion **7** and dichlorodisilane in THF affords in combined 57% yield an approximate one-to-one mixture of diastereomers **24** (*meso*) and **24** (*dl*) (Scheme 3). One of these diastereomers could be purified by fractional crystallization, thus allowing subtraction for the spectral features of the other.

Assignment of structure of compounds **24** could not be accomplished by NMR as chiral shift reagents were ineffective, but the *meso* structure was established for the selectively crystallized isomer by X-ray diffraction²⁰ and the molecular structure is shown in Figure 1. The allene unit is bent only slightly from linearity to 178.6° but is twisted to produce a dihedral angle of 80.6° as defined as plane Si₍₁₎C₍₁₎C₍₂₎ vs. Si₍₄₎C₍₃₎C₍₂₎. However a dihedral angle of 86.1° is obtained from plane Si₍₁₎C₍₁₎Si₍₂₎ vs. Si₍₃₎C₍₃₎Si₍₄₎, and comparison of plane Si₍₂₎C₍₁₎C₍₂₎ and Si₍₃₎C₍₃₎C₍₂₎ yields an apparently normal 89.4°-- a result of both the bending and apparent rehybridization of the allene carbons as evidenced both by the bond angles and pyramidalization.



Scheme 3. Reaction of dianion and dichlorodisilane.

Condensation of Me_2SiCl_2 and dianion **7** in Et_2O produced in 32% yield the polysilaallene **25** along with a trace of 1,3,5,7-tetrakis(trimethylsilyl)-4,8-bis(dimethylsila)cycloocta-1,2,5,6-tetraene **26**. The same condensation conducted in THF afforded **26** in 33% yield as crystalline needles, mp 115-117°C. The ^1H NMR spectrum of **26** (Table I) revealed a symmetrical structure which could be rationalized as a rapidly equilibrating chair form which, however, was not supported by NMR studies down to -42°C.

Polymer **25** was characterized by GPC, TGA, FTIR and NMR (^1H and ^{13}C). It has relatively low molecular weight ($M_w = 6,900$, $M_n = 6,500$) and narrow molecular weight distribution (PDI = 1.06). However, polymer **25** proved not to be a good precursor to silicon carbide, because thermogravimetric analysis (TGA) shows its fast decomposition starts at 334°C and its complete decomposition at 500°C with no significant char yield.

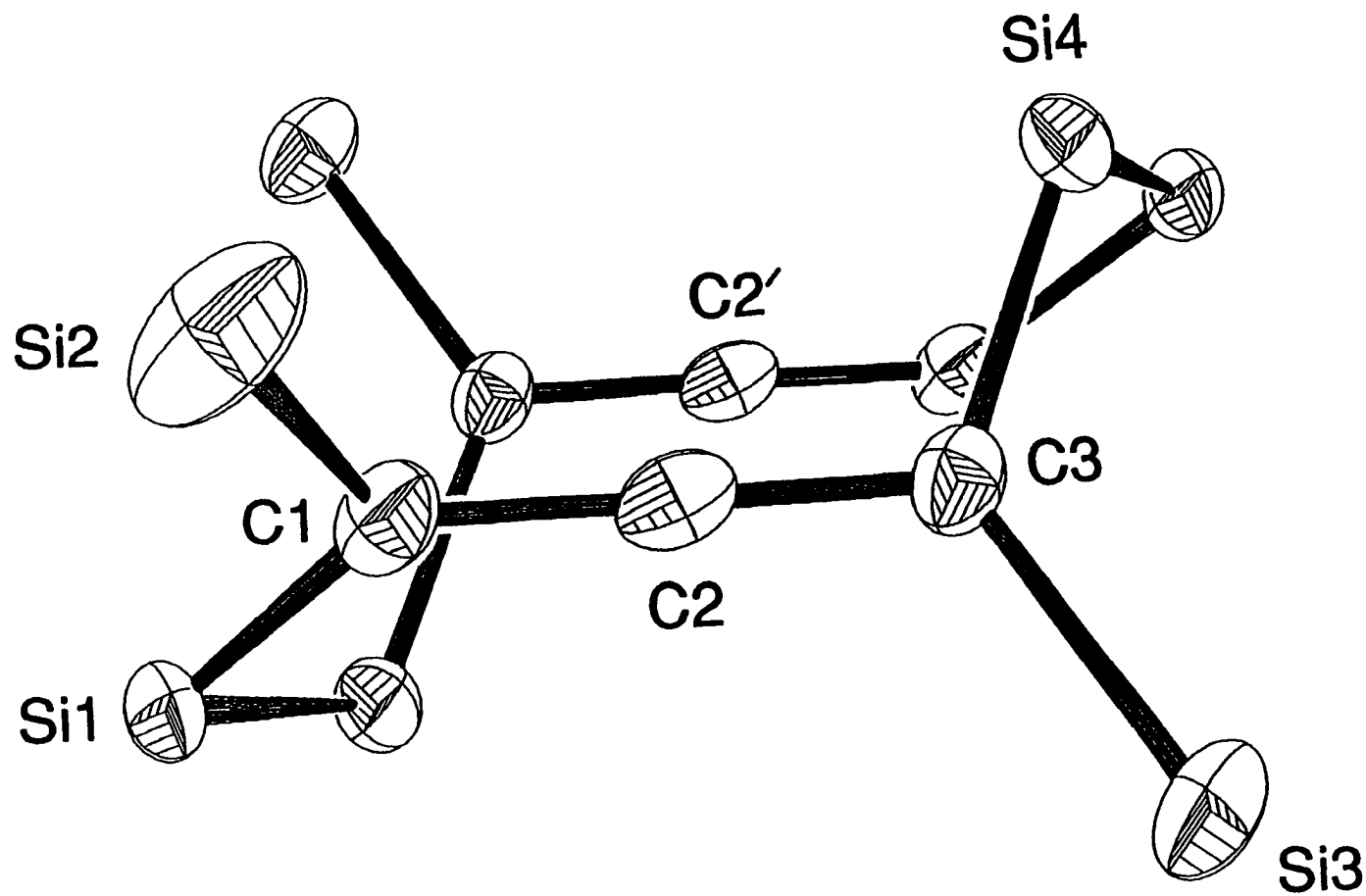
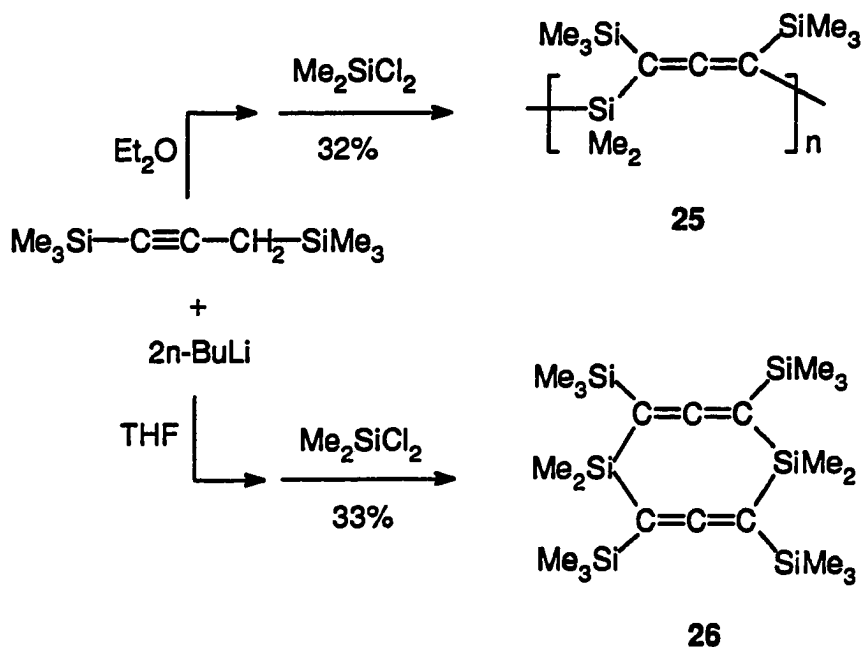


Figure 1. ORTP drawing of **24** (*meso*). The methyl groups have been omitted for clarity. Selected bond distances (Å) and angles (degree) are Si(1)-C(1) = 1.866(4), C(1)-C(2) = 1.305(5), Si(2)-C(1) = 1.879(4), C(2)-C(2') = 4.162, Si(1)-C(1)-Si(2) = 124.5(2), Si(1)-C(1)-C(2) = 118.9(3), Si(2)-C(1)-C(2) = 116.6(3), C(1)-C(2)-C(3) = 178.6.



Scheme 4. Reaction of dianion 7 with dimethyldichlorosilane.

The molecular structure of **26** was solved by X-ray diffraction²¹ and is shown in Figure 2. Of greatest interest is the allene bend of 175.2° and twist of 78.1° , as defined by the $\text{Si}_{(2)}\text{-C}_{(1)}\text{-C}_{(2)}$ and $\text{Si}_{(4)}\text{-C}_{(3)}\text{-C}_{(2)}$ planes. In addition, to accommodate two allenes in an 8-membered ring, the terminal carbons have undergone apparent rehybridization to decrease the internal bond angles with a concomitant increase in the external (Si-C-SiMe) angles (Figure 3).

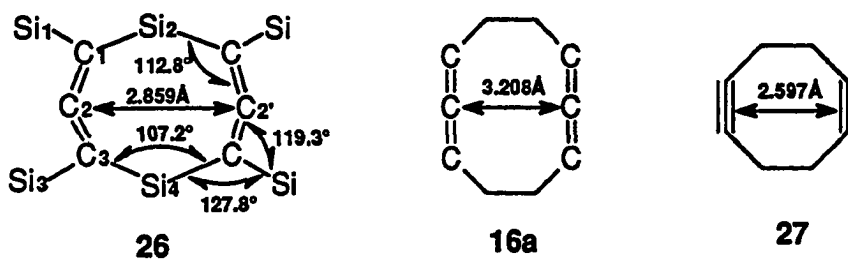


Figure 3. Comparison of transannular distances between *sp*-carbons in strained, cyclic bisallenenes and 1,5-cyclooctadiene.

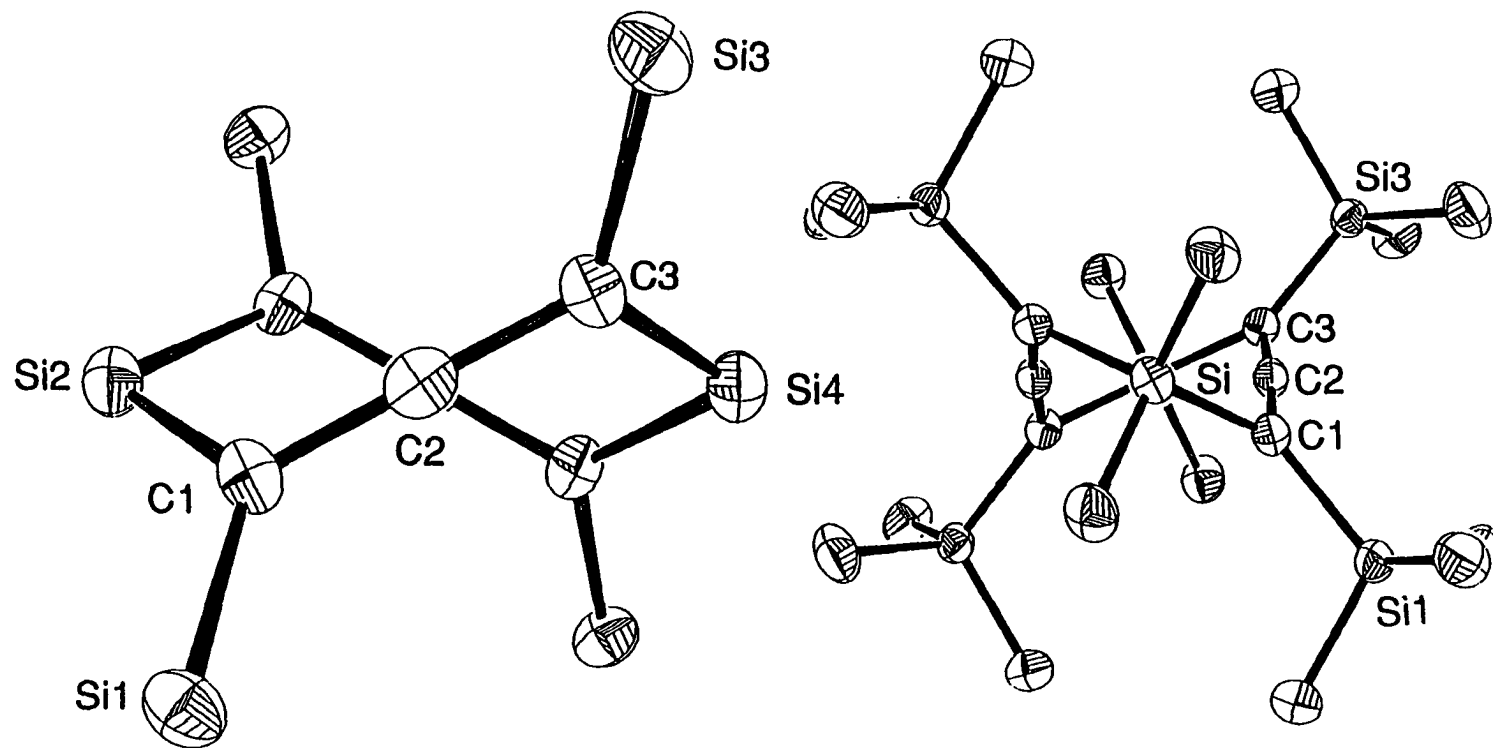


Figure 2. ORTP drawings of 26. Selected bond length (\AA) and bond angles (deg) are $\text{Si}(1)\text{-C}(1) = 1.861(2)$, $\text{Si}(2)\text{-C}(1) = 1.881(2)$, $\text{C}(1)\text{-C}(2) = 1.311(3)$, $\text{C}(1)\text{-C}(2)\text{-C}(3) = 175.2(2)$.

Table I. Selected spectral features of tetrakis(trimethylsilyl)allene, **24** (*meso*) and **26**.

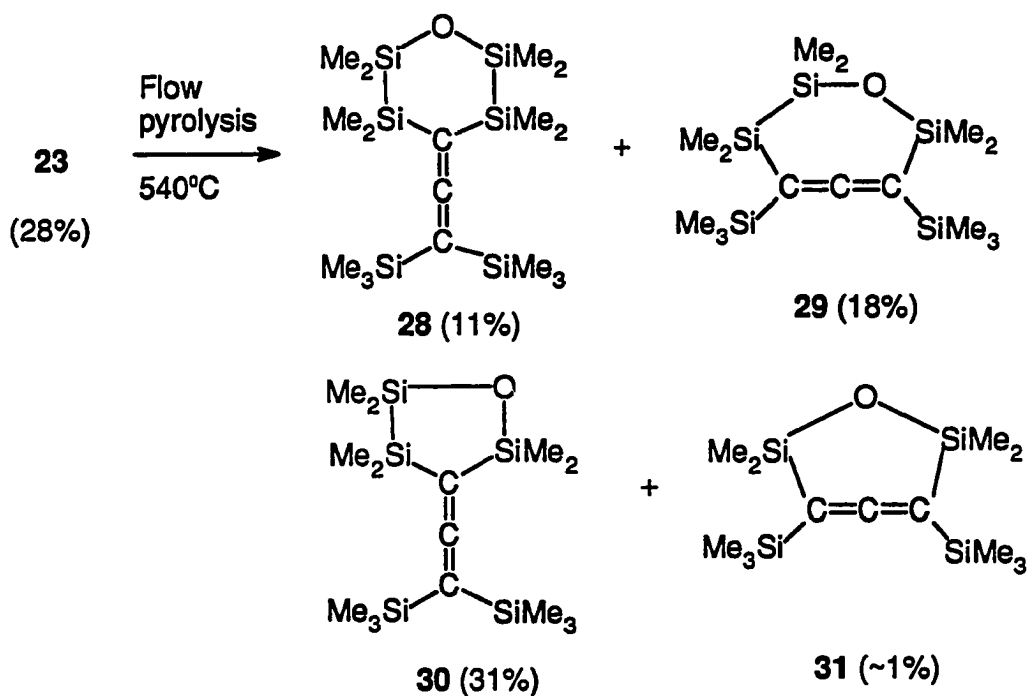
	IR(cm ⁻¹)	¹ H NMR (δ)	¹³ C NMR (δ)	²⁹ Si NMR (δ)
(Me ₃ Si) ₄ C ₃	1870		0.40 (12C) 64.03 (2C) 203.64 (1C)	-3.93
24 (<i>meso</i>)	1867	0.12 (s, 36H) 0.17 (s, 12H) 0.22 (s, 12H)	-0.56 (4C) 0.05 (4C) 0.97 (12C) 62.21 (4C) 203.72 (2C)	-22.75 (4Si) -3.24 (4Si)
26	1871	0.09 (s, 36H) 0.23 (s, 12H)	0.55 (12C) 2.24 (4C) 66.0 (4C) 205.38 (2C)	-5.06 (4Si) 0.20 (2Si)

All-carbon, cyclic bisallenes have been reported, with the smallest isolated being the 10-membered ring **16**. As the crystal structure of **16a** has been determined, the transannular distances between the central carbon atoms may be compared. As expected, the longer bonds associated with silicon produce a significantly longer C₍₂₎-C_(2') distance of 4.162 Å in **24** as opposed to 3.208 Å in **16a**. However, this transannular distance in **26**, 2.859 Å, is notably shorter than in **16a**, but slightly longer (0.26 Å) than the transannular *sp*-carbon distances in the smallest cyclic diyne for which structural information is available, 1,5-cyclooctadiyne, **27**.²² The *sp*-carbons of **27** (δ 95.8) are considerably shifted downfield from those of normal acetylenes, an effect which has been ascribed to the olefinic character for the bent acetylenes in **27** rather than to a "proximity effect".²³ Although no large shifts are observed in the ¹³C NMR of **26** relative to **24**, future efforts at probing the chemistry of these cyclic bisallenes will seek evidence for proximity interactions.

Flow pyrolysis of compound 23.

Compound **22** was obtained from the reaction of dianion **7** and two equivalents of dichlorodisilane in excellent yield (92% purity according to GC). Upon hydrolysis, and purification by flashing through a neutral alumina column, cyclic siloxane **23** was obtained in 75% isolated yield.

Gas-phase flow pyrolysis of compound **23** at 540°C produced compounds **28-31** (Scheme 5). While isomerization of **23** to **28** represents a formal dyatropic rearrangement, compound **29** represents a dimethylsilylene extrusion product from **23**. Exocyclic allene **30** could either have been produced by dimethylsilylene extrusion from **28** or by isomerization of **29**. Only a trace amount of the six-membered ring cyclic allenic compound **31**, which represents two dimethylsilylene extrusion product, was observed.

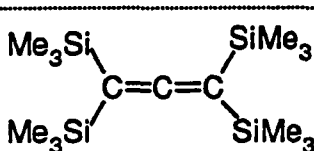


Scheme 5. Flow pyrolysis of compound **23**.

Only compound **30** was isolated by preparative GC. Compound **28** was separated by preparative GC as a mixture with starting material **23** and spectral features were obtained by subtraction. Compound **29** also was separated by preparative GC only as a mixture with compound **30** and spectral features were also obtained by subtraction. Attempts to isolate compound **31** from the reaction mixture failed and it was only characterized by GC-IR-MS.

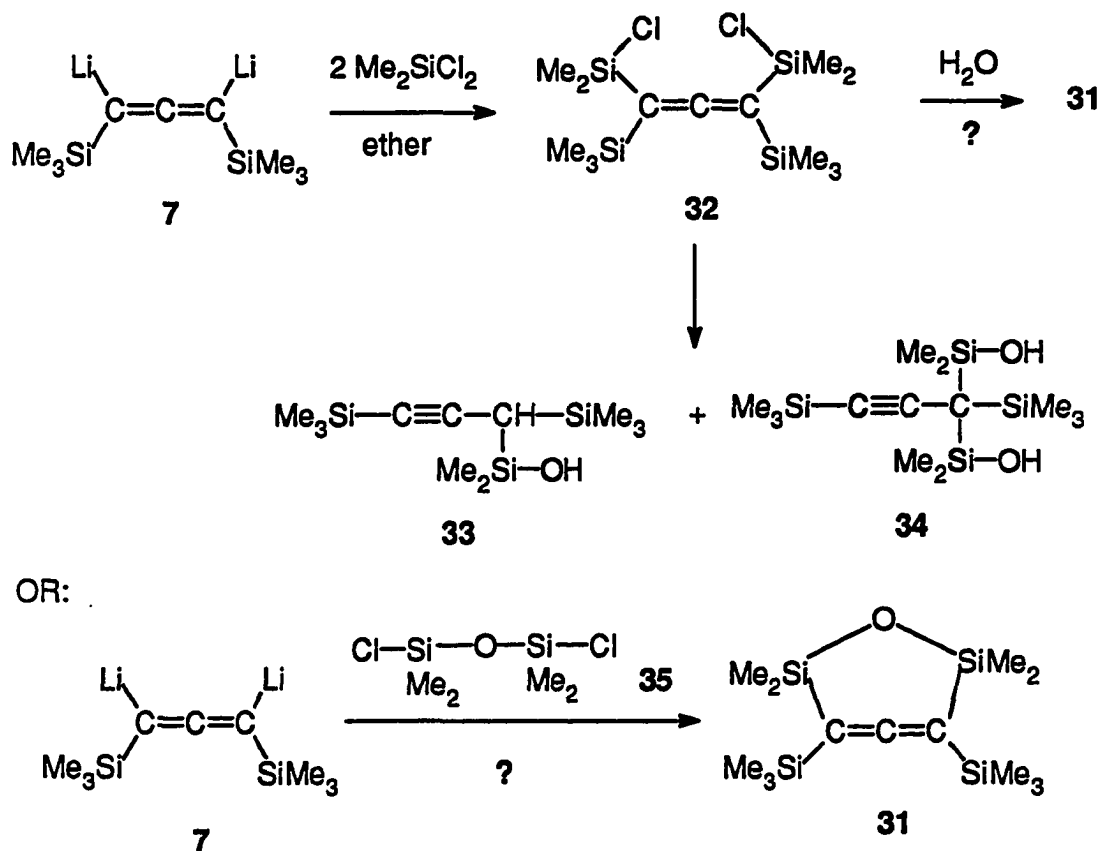
The existence of compound **31** was supported by the absorption position of the allene unit in the IR spectrum. As shown in Table II, in acyclic tetrakis(trimethylsilyl)allene, allene stretching is at 1870 cm^{-1} . In silacyclicallenes, as the ring size goes down from 8 to 7 to 6 from compound **11** to **13**, the ring strain increases, and the allene absorption shifts from 1860 to 1840 cm^{-1} . Thus for compounds **23** to **29** to **31**, the ring size decreases from 8 to 7 to 6 and the allene absorption changes from 1863 to 1860 to 1821 cm^{-1} . This implies a significant increase in ring strain in compound **31** compared to **11**, which is the smallest isolated cyclic allene.¹¹

Table II. IR absorption of allenic unit.

	GC-IR (ν , cm^{-1})
	1870
11	1860
12	1860
13	1840
23	1863
29	1860
31	1821

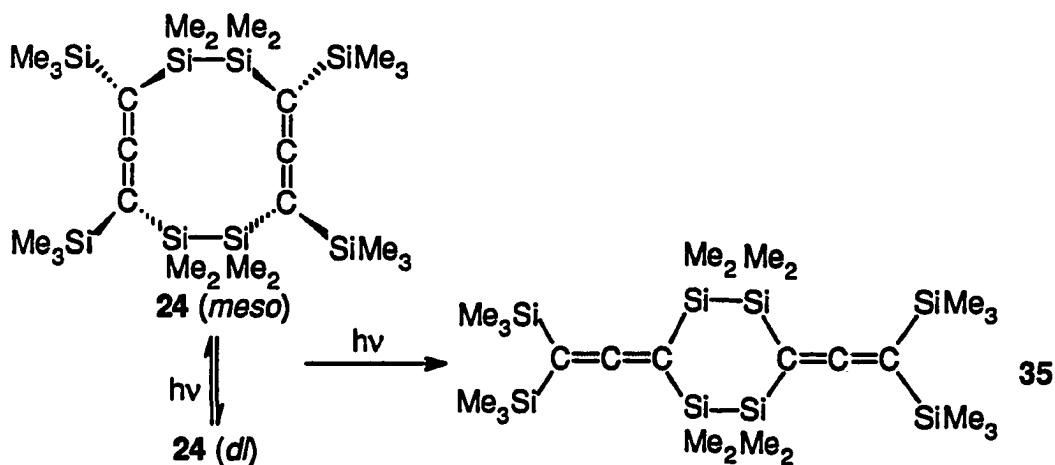
Attempted synthesis of compound 31.

Compound **31** is of the most interest among the pyrolysis products from compound **23** because the Si-O bond is shorter than the Si-Si bond and more ring strain should be present than in tetrasilacycloallene **11**. Two different routes were attempted to synthesize compound **31** (Scheme 6). In the first attempt, compound **32**, a plausible precursor to **31**, was produced solely from the reaction of dianion **7** and dimethyldichlorosilane in ether (96% purity according to GC). However, when hydrolysis of dichlorosilane **32** was performed under acidic, basic, or neutral conditions, compounds **33**, and **34** were observed as the major products on GC, GC-IR-MS; no trace amount of compound **31** was observed. The second attempt by condensation of dianion **7** and dichlorosilane **35** yields only oligomers.

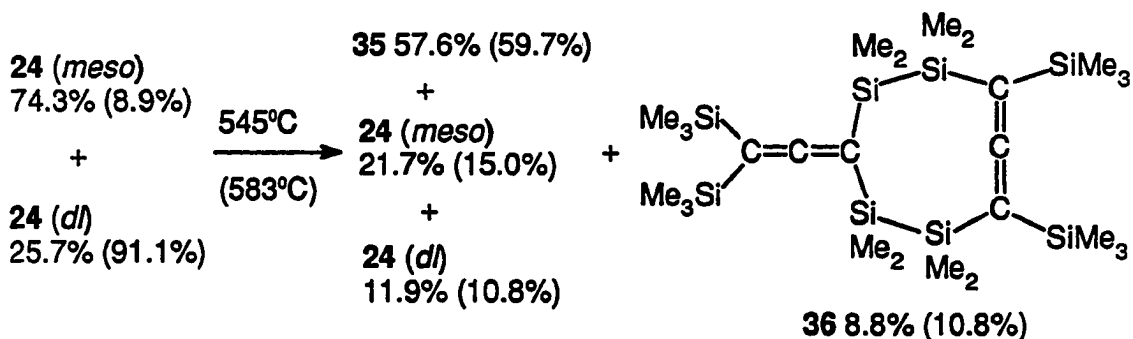
Scheme 6. Attempted synthesis of compound **31**.

Photolysis and flow pyrolysis of compounds 24. and 26.

Photolysis of **24** (*meso*) or **24** (*dl*) in hexane with a low pressure Hg-arc lamp produced an approximately 1:1 mixture of the two diastereomers. After about two hours of irradiation a third isomer, **35**, was observed in the mixture (14% after 24 hours). The photoinduced racemization of allene is well established,²⁴ but the photoisomerization of **24** to **35** is to our knowledge unprecedented and formally represents two dyatropic rearrangements. Under the same photolysis conditions, **23** and **26** failed to react.

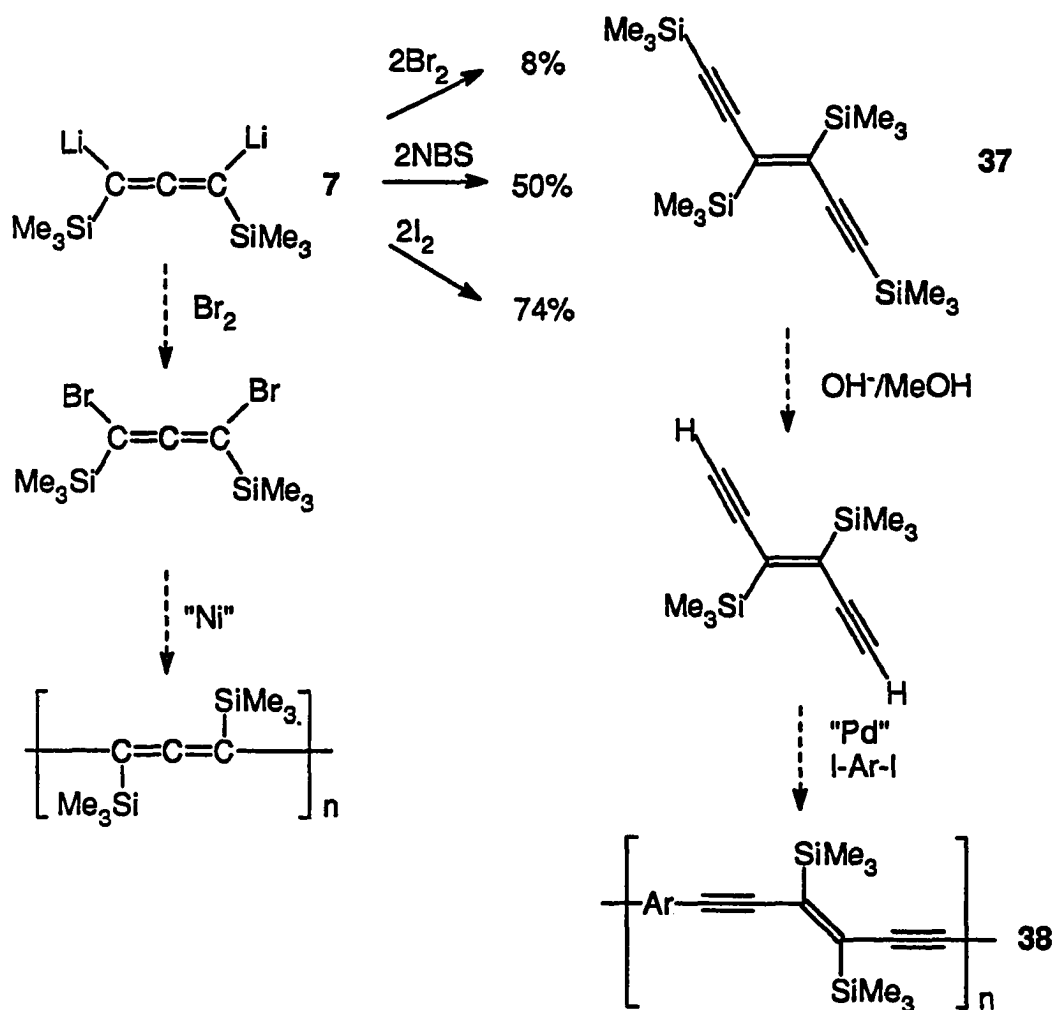


Gas-phase flow pyrolysis of two different mixtures of **24** (*meso*) and **24** (*dl*), one at 545°C and one at 585°C, also produced **35** as the major product along with a significant amount of **36** which is assumed to be an intermediate in the **24**-to-**35** conversion. Bisallene **26** was unchanged upon pyrolysis at 600°C and at 650°C began to decompose to a myriad of products.



Miscellaneous chemistry of dianion 7.

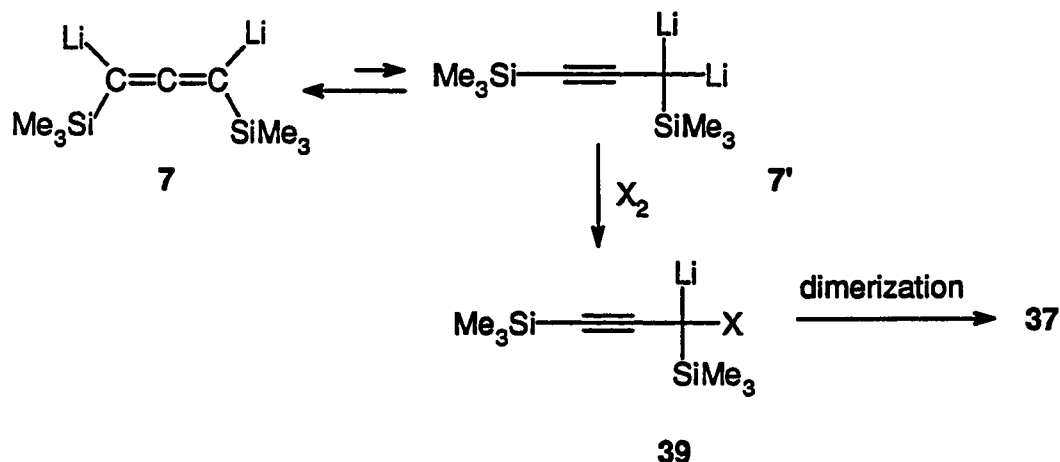
When dianion **7** was reacted with bromine, 1,3-dibromoallene (which could be used to make polyallene by Ni-catalyzed coupling reaction) was the expected product. However, the major identified product is 1,3,4,6-tetrakis(trimethylsilyl)-3-ene-1,5-diyne (**37**) (Scheme 7). The yield of compound **37** was improved when NBS or iodine was used instead of bromine to couple **7**. Compound **37**, after selective desilylation of the acetylenic silyl group, could be used as a building block for the construction of conjugated polymers with repeating units such as **38** based on the palladium catalyzed coupling reaction.



Scheme 7. Reaction of dianion **7** with bromine, NBS, and iodine.

The *trans* instead of *cis* assignment of compound **37** was based on the comparison of its IR and Raman spectra. There is a strong absorption for the central double bond at 1465 cm^{-1} in the Raman spectrum while very weak absorption at 1406 cm^{-1} was observed in the IR spectrum. The difference in absorptivity in Raman and IR for the central double bond shows this compound is central symmetric and so *trans* structure was assigned. The acetylenic absorption is at 2122 cm^{-1} in the IR and 2102 cm^{-1} in the Raman.

One possible mechanism for the formation of compound **37** is proposed in Scheme 8, where intermediate **39** is formed from the reaction of the isomeric dianion **7'** and halogen or NBS. Dimerization of **39** produced **37**.



Scheme 8. A possible mechanism for the formation of compound **37**.

Notes

Shortly after our results on the synthesis and structural study of strained, cyclic bisallenes were published,²⁶ Ando's group reported the synthesis and structural study of analogs of compound **24** (*meso*) and **24** (*dl*) where phenyl substituents instead of trimethylsilyl substituents are attached to the allene unit.²⁷ However, only semiempirical PM3 calculation results were reported on the analog of the smaller cyclic bisallene **26** were reported.

Conclusions

Polysilaallene, 10- and 8-membered ring cyclic bisallenes were synthesized from the condensation of 1,3-dilithio-1,3-bis(trimethylsilyl)allene and the corresponding dichlorosilanes. TGA of polysilaallene proved it not to be a good silicon carbide precursor with complete decomposition at -500°C . The X-ray determined structure of the *meso* diastereomer of the 10-membered ring cyclic bisallene reveals it to be relatively unstrained. The molecular structure (X-ray) of the highly strained 8-membered cyclic bisallene contains allenes which are both bent (175.2°), twisted (dihedral angle of 78.1°) and rehybridized at the “*sp*²” carbons to accommodate decreased internal bond angles. The transannular distance between the central allenic carbons is only 2.859 Å. Photolysis and thermolysis of the 10-membered ring cyclic bisallene afforded both isomerization between *meso* and *dl*-forms and conversion to a 6-membered ring with two exocyclic allene units.

The 6-membered cyclic allene, 1,3-bis(trimethylsilyl)-4,4,6,6-tetramethyl-5-oxy-4,6-disilacyclohexa-1,2-diene, was produced as the bis(dimethylsilylene)-extrusion product from the pyrolysis of the 8-membered cyclic allene. However, attempts to isolate or synthesize this 6-membered ring failed. 1,3,4,6-Tetrakis(trimethylsilyl)-3-ene-1,5-diyne (37), a potentially useful building block for the construction of conjugated polymers, was synthesized from the reaction of 1,3-dilithio-1,3-bis(trimethylsilyl)allene with NBS or iodine.

Experimental

^1H , ^{13}C , and ^{29}Si -NMR spectra were acquired on a Varian VXR-300 spectrometer. In order to assure the quantitative features of the ^{13}C -NMR and ^{29}Si -NMR spectra, the relaxation reagent chromium (III) acetylacetonate was used in CDCl_3 with a repeat delay of 5 seconds. TMS was used as the external standard for ^{29}Si -NMR. Preparative GC separation was performed on a Varian Model 920 instrument with a 8-foot long copper column (1/4" radii) with 14% SE-30 on chromosorb WHP packing. Routine GC was performed on a Hewlett Packard 5890 GC spectrometer. Routine GC-IR-MS spectra were obtained on a Hewlett Packard GC-IR-MS spectrometer (5890 GC spectrometer, 5965A IR spectrometer, 5970 MS spectrometer). UV spectra were obtained on a Hewlett Packard 8452 A Diode Array spectrometer. Flow pyrolysis experiments were performed by slowly dripping the starting material solution into a vertical quartz tube packed with quartz chips under argon flow. The pyrolysate was collected in a trap at -78°C .

Molecular weights of the polymers were determined by gel permeation chromatography (GPC) with 4 Microstyrigel columns in series of 500 A, 2×10^3 A, 2×10^4 A, 2×10^5 A. THF was used as eluent at a flow rate of 10 mL/min. The system was calibrated by polystyrene standards. GPC analysis was performed on a Perkin-Elmer series 601LC equipped with Beckman solvent delivery system, a Walter Associate R401 refractive index detector and a Viscotek viscometer.

THF was distilled from lithium aluminum hydride and ether was distilled over calcium hydride immediately before use. Commercially available reagents were used as received unless otherwise noted.

General procedure for flow pyrolysis (Flow pyrolysis of compound 24 as an example).

A 70 mg mixture of 24 (*meso*) and 24 (*dl*) was dissolved in 3 mL hexanes. The solution was added dropwise (ca. 10 drops/min) into a quartz tube (40 cm, packed with quartz chips) under argon flow (28 mL/min) while the tube was maintained at the desired temperature in a vertical

oven. The pyrolysate was collected in a trap cooled to -78°C . Most of the hexanes solvents were removed from the pyrolysis products on a rotatory evaporator. The product **35** slowly crystallized out from the mixture as colorless crystals, m.p. $190\text{-}191^{\circ}\text{C}$.

General procedure for photolysis (Photolysis of **24** as an example). A solution of 5 mg of bisallene **24** (100% pure) and 5 mg decane (serving as the internal standard) dissolved in 2 mL hexanes (HPLC grade) was prepared in a quartz tube equipped with a septum. The tube was filled with argon by the freezing and thawing technique (three times). The tube was then connected to an argon balloon and exposed to UV irradiation (a Rayonet photochemical reactor equipped with sixteen 5W low pressure Hg lamp). The reaction was monitored by frequent sampling and analysis by a capillary GC.

General procedure for preparation of 1,3-dilitho-1,3-bis(trimethylsilyl)allene (**7**). In a 25 mL oven-dried, argon-flushed flask equipped with a magnetic stirrer and a septum, 0.92 g 1,3-bis(trimethylsilyl)propyne (**6**, 5 mmol, the synthesis is shown below) and 10 mL THF or 10 mL ether (freshly distilled over LiAlH_4) were charged. After the solution was cooled to -78°C by a dry-ice/isopropanol bath, 4.0 mL n-BuLi (2.5 M solution in hexanes, 10 mmol) was added dropwise. After stirring at -78°C for 20 minutes, the solution was gradually warmed to room temperature and then stirred for an additional 2 hours. An aliquot was taken by syringe and quenched by excess trimethylchlorosilane. The analysis of the quenching products by GC-IR-MS showed that $(\text{Me}_3\text{Si})_2\text{C}=\text{C}=\text{C}(\text{SiMe}_3)_2$ was the major product (ca. 60% according to GC for THF as solvent, 90% for ether as solvent).

Synthesis of 1,3-bis(trimethylsilyl)propyne (**6**). To a 250 mL 2-necked oven-dried, argon-flushed flask equipped with a mechanical wire-stirrer and an additional funnel, 60 mL ether (freshly distilled over LiAlH_4) and 2.916 g magnesium turning (0.12 mol) were charged. 0.11 g mercury(II) chloride²⁵ was added and the mixture was stirred for 30 minutes at room temperature. The mixture was cooled to 0°C and 0.8 mL of the 9.8 mL propargyl bromide

(0.11 mol) was added. The mixture was stirred vigorously at 0°C for 30 min. and the magnesium surface became dark which indicated the reaction had started. The rest of the propargyl bromide was added dropwise during a 2 hour period at 0°C. After this addition the mixture was stirred for an additional 45 minutes at 0°C. At this time all the magnesium metal was consumed. The gray Grignard solution obtained was then cooled to -10°C and 44 mL of n-butyllithium (2.5 M solution in hexanes, 0.11 mol) was added dropwise. After gradually warming to room temperature and stirring for 2 hours, the reaction mixture was a white slurry. This slurry was cooled to below -10°C and 29.1 mL trimethylchlorosilane (0.23 mol) was added dropwise. Following the addition, the mixture was stirred at -10°C for 20 minutes, then at room temperature overnight. The reaction mixture was slowly added at 0°C to a 250 mL flask containing 50 mL cold 0.5 M HCl aqueous solution and 50 mL pentane. The organic layer was separated and washed twice with cold dilute aqueous HCl (25 mL each time). Finally the organic layer was dried over Na₂SO₄. Fractional distillation gave 1,3-bis(trimethylsilyl)-1-propyne as a colorless liquid, b.p. 92-94°C/50 mmHg, yield 90%. The product was contaminated only by ca. 3% Me₃Si-C≡C-CH₂-CH=C=CH₂ as indicated by GC-IR-MS. GCMS *m/z* 185(2), 184(8, M), 171(2), 170(4), 169 (20, M-Me), 97(6), 96 (26), 73 (100); GC-FTIR ν (cm⁻¹): 2965(s), 2899(w), 2156(s), 1403(w), 1260(s), 1153(w), 1035(w), 849(vs); ¹H-NMR (300 MHz, CDCl₃) δ : 1.53(s, 2H), 0.11(s, 9H), 0.09(s, 9H); ¹³C-NMR (75.429 MHz, CDCl₃) δ : -2.28(3C), 0.21(3C), 8.62(1C), 83.04(1C), 105.69(1C).

Synthesis of 1,2-dichlorotetramethyldisilane. In a 250 mL three-necked round bottom flask, equipped with a condenser, mechanical stirrer and addition funnel, 40.2 mL hexamethyldisilane (0.2 mol) and 53.0 g aluminum chloride (0.4 mol) were charged under argon atmosphere. Under stirring, 32.0 mL acetylchloride (0.45 mol) was added dropwise to the slurry (**exothermic reaction, add slowly!**) The reaction was stirred at room temperature overnight. Crude product was distilled out via vacuum distillation (85 mmHg at 85°C water bath) from the reaction slurry. Fractional distillation gives 35.5 g (95% yield) 1,2-dichlorotetramethyldisilane as a colorless liquid (b.p. 148-151°C).

Synthesis of 1,3-bis(trimethylsilyl)-4,4,5,5,7,7,8,8-octamethyl-6-oxy-4,5,7,8-tetrasilacycloocta-1,2-diene (23). The yellow orange dianion **7** (5 mmol) solution in 10 mL ether made according to procedure described earlier was cooled back to 0°C by an ice-water bath, and 1.87 g 1,2-dichlorotetramethyldisilane (10 mmol) was added dropwise. After stirring at 0°C for an additional 20 minutes, the temperature was gradually raised to room temperature and the reaction mixture was stirred overnight. A lot of salts precipitated from the reaction. Compound **22**, which was not isolated, was produced as the major product (96% purity according to GC). Compound **22**: GCMS m/z 469(2, M-Me), 394(12), 393(31), 392(23), 391(54), 221(15), 201(21), 93(22), 73(100).

The above reaction mixture was poured into a mixture of 20 mL hexane and 20 mL ice-cold, dilute aqueous HCl. After washing by dilute aqueous HCl one more time, the organic layer was mixed with 5 mL water and stirred at room temperature. The hydrolysis process was monitored by GC and it was finished after 5 hours of stirring. The organic layer was then washed twice with cold water and dried over anhydrous Na₂SO₄. After removing the solvents, the product was then purified by flashing through a neutral alumina column (hexanes as eluent). Cyclicallene **23** was obtained as yellow wax-like material (1.62g, 75% yield). Compound **23**: GCMS m/z 431(12, M+1), 430(24, M), 416(12), 415(25), 359(25), 358(40), 357(100), 327(18), 275(17), 245(14), 187(17), 73(64); HRMS cal. for C₁₇H₄₂OSi₆, 430.18514, measured 430.18473 (Kratos 50); GC-FTIR $\nu(\text{cm}^{-1})$, 2959(m), 2902(w), 1863(vs), 1254(s), 1050(s), 890(s), 843(s); ¹H-NMR (300 MHz, CDCl₃) δ 0.12(s, 18H), 0.14(s, 6H), 0.16(s, 6H), 0.18(s, 6H), 0.20(s, 6H); ¹³C-NMR (75.429 MHz, CDCl₃) δ -1.74(2C), -1.03(2C), 0.61(6C), 2.26(2C), 2.89(2C), 61.19(2C), 203.72(1C); ²⁹Si-NMR (59.591 MHz, CDCl₃, TMS as external standard) δ -19.75(2Si), -4.03(2Si), 3.96(2Si).

Synthesis of 1,3,6,8-tetrakis(trimethylsilyl)-4,4,5,5,9,9,10,10-octamethyl-4,5,9,10-tetrasilacyclodeca-1,2,6,7-tetraene (24, *meso* and *dD*). A yellow-orange solution of dianion **7** (5 mmol) in 10 mL THF (procedure described earlier) was cooled to 0°C by an ice-water bath, and 0.934 g 1,2-dichlorotetramethyldisilane (5 mmol) was added dropwise. After

stirring at 0°C for an additional 20 minutes, the temperature was gradually raised to room temperature and the reaction mixture was stirred overnight. A lot of salts precipitated from the reaction mixture. The reaction mixture was poured into a mixture of 20 mL hexane and 20 mL ice-cold dilute HCl aqueous solution. The organic layer was washed twice with cold water and dried over anhydrous Na₂SO₄. After removing the solvents, the crude product was a white solid. After purification by silica gel chromatography (hexanes as eluent), a mixture of **24** (*meso*) and **24** (*dl*) (ratio ca. 1:1) was obtained as colorless crystals in 57% total yield. The compound **24** (*meso*), m.p. 215-216°C, was separated from the mixture of two isomers since it crystallized out first as a colorless crystal. The NMR spectra of the compound **24** (*dl*) was obtained by subtracting the spectra of the compound **24** (*meso*) from the spectra of the mixture of the two isomers. Both ¹³C-NMR and ²⁹Si-NMR spectra were taken under quantitative conditions.

Characterization of 1.3.6.8-tetrakis(trimethylsilyl)-4.4.5.5.9.9.10.10-octamethyl-4.5.9.10-tetrasilol-3.4.8.9-cyclodeca-1.2.6.7-tetraene **24** (*meso*). m.p. 215-216°C; GCMS *m/z* 527(2), 525(8), 525(22), 524(33), 523(57, M-SiMe₃), 342(13), 341(31), 283(19), 225(11), 185(18), 171(20), 155(13), 141(11), 73(100); HRMS *m/z* cal. for C₂₆H₆₀Si₈ 596.28493, measured 596.28455 (Kratos 50); GC-FTIR ν (cm⁻¹): 2959(m), 2904(w), 1867(vs), 1404(w), 1254(m), 881(s), 844(s); ¹H-NMR (300 MHz, CDCl₃) δ 0.12(s, 36H), 0.17(s, 12H), 0.22(s, 12H); ¹³C-NMR (75.429 MHz, CDCl₃) δ -0.56(4C), 0.05(4C), 0.97(12C), 62.21(4C), 203.72(2C); ²⁹Si-NMR (59.591 MHz, CDCl₃, TMS as external standard) δ -22.75(4Si), -3.24(4Si); The UV spectrum (hexanes, nm): λ_{max} = 202 (5.80 x 10⁴), λ_{sh} = 258 (7.2 x 10³).

Characterization of cyclic bisallene **24** (*dl*). GCMS *m/z* 527(3), 526(9), 525(23), 524(33), 523(57, M-SiMe₃), 342(13), 341(34), 225(10), 185(16), 171(18), 155(13), 73(100); GC-FTIR ν (cm⁻¹) 2960(m), 2905(w), 1864(vs), 1402(w), 1255(m), 874(s), 846(s), 790(m); ¹H-NMR (300 MHz, CDCl₃) δ 0.14(s, 36H), 0.17(s, 12H), 0.23(s, 12H); ¹³C-NMR (75.429

MHz, CDCl₃) δ -0.24(4C), 0.14(4C), 1.30(12C), 61.81(4C), 203.78(2C); ²⁹Si-NMR (59.591 MHz, CDCl₃, TMS as external standard) δ -18.62(4Si), -2.33(4Si).

Synthesis of poly[dimethylsilylene 1,3-bis(trimethylsilyl)-1,2-diene] (25). The yellow-orange solution of dianion **7** (10 mmol) in 10 mL ether (procedure described earlier) was cooled to 0°C by an ice-water bath, and 1.29 g dichlorodimethylsilane (10 mmol) was added dropwise. After stirring at 0°C for an additional 20 min., the temperature was gradually raised to room temperature and the reaction mixture was stirred overnight. A lot of salts precipitated from the reaction mixture. The reaction mixture was poured into a mixture of 20 mL hexane and 20 mL ice-cold dilute HCl aqueous solution. The organic layer was washed twice with cold water and dried over anhydrous Na₂SO₄. After removal of all the solvents, the viscous liquid obtained was dissolved in a minimum amount of THF and the polymer was precipitated in methanol. 0.76 g of polymer **25** was obtained as a white solid (32% yield). GPC: $M_w = 6900$, $M_n = 6500$, PDI = 1.06; FTIR (film on KBr) ν (cm⁻¹) 2959(m), 2903(w), 1846(vs), 1248(s), 893(s), 839(s), 793(s); ¹H-NMR (300 MHz, CDCl₃) δ 0.16(s, ~18H), 0.26(s, ~6H); ¹³C-NMR (75.429 MHz, CDCl₃) δ 1.37(overlapped with the peak at 1.44), 1.44, 65.83(2C), 204.85(1C); TGA shows its fast decomposition starts at 334°C and its complete decomposition at 500°C with no significant char yield.

Synthesis of 1,3,5,7-tetrakis(trimethylsilyl)-4,4,8,8-tetramethyl-4,8-disilacycloocta-1,2,5,6-tetraene (26). The synthesis follows the same procedure as the synthesis of compound **24**. After purification on a silica-gel column (hexanes as eluents), compound **26** was obtained as colorless crystals, m.p. 115-117°C, in 33% isolated yield. GCMS m/z 483(8), 482(22), 480(66, M), 467(18), 466(28), 465(53, M-Me), 155(10), 73(100); HRMS m/z cal. for C₂₂H₄₈Si₆ 480.23718, measured 480.23697 (Kratos 50); GC-FTIR ν (cm⁻¹): 2961(m), 2905(w), 1871(vs), 1406(w), 1258(m), 904(s), 844(s); ¹H-NMR (300 MHz, CDCl₃) δ 0.09(s, 36H), 0.23(s, 12H); ¹³C-NMR (75.429 MHz, CDCl₃) δ 0.55(12C), 2.24(4C), 66.00(4C),

205.38(2C); $^{29}\text{Si-NMR}$ (59.591 MHz, CDCl_3 , TMS as external standard) δ -5.06(4Si), 0.20(2Si); The UV spectrum (hexanes, nm): $\lambda_{\text{max}} = 204$ (5.34×10^4) $\lambda_{\text{sh}} = 252$ (2.94×10^3).

Characterization of compound 28. GCMS m/z 432(7), 431(12), 430(24, M), 415(25), 416(12), 359(25), 358(40), 357(100), 327(18), 245(14), 187(17), 73(64); GC-FTIR $\nu(\text{cm}^{-1})$ 2961(m), 2902(w), 1868(vs), 1256(s), 1026(s), 879(s), 843(s); Partial NMR spectra of compound 28 was obtained by subtraction of the spectra of compound 23 from that of the mixture of 23 and 28. The $^1\text{H-NMR}$ could not be obtained by subtraction; $^{13}\text{C-NMR}$ (75.429 MHz, CDCl_3 , only the allenic carbons were obtained by subtraction) δ 60.00(1C), 64.61(1C), 201.73(1C); $^{29}\text{Si-NMR}$ (59.591 MHz, CDCl_3) δ -29.35(1Si), -3.78(1Si), 7.91(1Si).

Characterization of compound 29. GCMS m/z 374(9), 373(12), 372(55, M), 359(25), 358(40), 357(100), 299(24), 269(12), 187(22), 73(72); GC-FTIR $\nu(\text{cm}^{-1})$ 2961(m), 2903(w), 1860(vs), 1256(s), 1021(s), 906(s), 842(s); NMR spectra of compound 29 was obtained by subtraction of the spectra of compound 30 from that of the mixture of 29 and 30; $^1\text{H-NMR}$ (300 MHz, CDCl_3) δ 0.10(s, 9H), 0.11(s, 9H), 0.169(s, 3H), 0.172(s, 3H), 0.18(s, 3H), 0.20(s, 3H), 0.21(s, 3H), 0.25(s, 3H); $^{13}\text{C-NMR}$ (75.429 MHz, CDCl_3) δ -1.73(1C), -0.88(1C), 0.18(3C), 0.43(3C), 1.75(1C), 1.82(1C), 2.50(1C), 3.05(1C), 63.61(1C), 65.88(1C), 206.81(1C); $^{29}\text{Si-NMR}$ (59.591 MHz, CDCl_3 , TMS as external standard) δ -21.57(1Si), -6.36(1Si), -5.06(1Si), -1.03(1Si), 3.46(1Si).

Characterization of compound 30. GCMS m/z 374(13), 373(21), 372(49, M), 359(26), 358(39), 357(100), 299(22), 269(20), 187(25), 73(62); HRMS m/z cal. for $\text{C}_{15}\text{H}_{36}\text{OSi}_5$ 372.16126, measured 372.16102 (Kratos 50); GC-FTIR $\nu(\text{cm}^{-1})$ 2961(m), 2903(w), 1875(vs), 1255(m), 955(s), 894(m), 848(s); $^1\text{H-NMR}$ (300 MHz, CDCl_3) δ 0.10(s, 18H), 0.20(s, 6H), 0.22(s, 6H), 0.25(s, 6H); $^{13}\text{C-NMR}$ (75.429 MHz, CDCl_3) δ -2.62(2C),

0.62(6C), 1.18(2C), 1.87(2C), 62.03(1C), 63.97(1C), 201.00(1C); ^{29}Si -NMR (59.591 MHz, CDCl_3 , TMS as external standard) δ -19.26(1Si), -3.83(2Si), 11.57(1Si), 15.38(1Si).

Characterization of 1,3-bis(trimethylsilyl)-4,4,6,6-tetramethyl-4,6-disila-5-oxy-cyclohexa-1,2-diene (31). GCMS m/z 316(17), 315(34), 314(100, M), 301(12), 300(20), 299(64), 225(14), 211(16), 187(20), 73(40); GC-FTIR ν (cm^{-1}): 2963(m), 2907(w), 1821(vs), 1258(s), 952(s), 894(s), 842(s).

Synthesis of 1,3-bis(chlorodimethylsilyl)-1,3-bis(trimethylsilyl)-1,2-diene (32) and attempted synthesis of 1,3-bis(trimethylsilyl)-4,4,6,6-tetramethyl-4,6-disila-5-oxy-cyclohexa-1,2-diene (31). The yellow orange dianion **7** (5 mmol) solution in ether made according the procedures described earlier was cooled back to 0°C by an ice-water bath, and 2.58 g dichlorodimethylsilane (20 mmol, 100% excess) was added dropwise. After stirring at 0°C for additional 20 minutes, the temperature was gradually raised to room temperature and the reaction mixture was stirred overnight. Some salts precipitated from the reaction mixture. The salts were filtered out and washed by hexanes. After removal of solvents and excess dichlorodimethylsilane by vacuum distillation, compound **32** was obtained in quantitative yield (94% purity according to GC). GCMS m/z 372(2, M+4), 370(9, M+2), 368(10, M), 355(20), 353(24), 263(10), 262(44), 261(25), 260(100), 247(13), 245(26), 73(25); GC-FTIR ν (cm^{-1}) 2965(m), 1877(vs), 1260(s), 899(s), 843(s).

Water (5 mL) was added to the above dichlorosilane **32** solution in hexanes and the reaction was stirred at room temperature and monitored by GC and GC-IR-MS. No trace amount of the desired product **31** was observed. Instead, compounds **33** and **34** were the two identified major products. When the hydrolysis was carried out under acidic or basic conditions (Et_3N was added), the same results were observed.

Characterization of compound 33. GCMS m/z 258(4, M), 243(28, M-Me), 155(18), 153(13), 148(16), 147(100), 75(15), 73(54); GC-FTIR ν (cm^{-1}) 3726(w), 2965(m), 2906(w), 2143(m), 1260(s), 1005(m), 848(vs).

Characterization of compound 34. GCMS m/z 317(2), 229(33), 221(13), 189(10), 184(28), 169(12), 150(14), 149(100), 133(18), 73(43); GC-FTIR ν (cm^{-1}) 3730(w), 2965(m), 2907(w), 2143(m), 1263(s), 1062(s), 1006(m), 846(vs).

Characterization of compound 35. Compound 35 was crystallized out from the pyrolysis mixture of compounds 24 as a colorless crystal (m.p. 190-191°C). GCMS m/z 526(3), 525(14), 523(24, M-SiMe₃), 411(15), 185(11), 155(11), 73(100); HRMS m/z cal. for C₂₆H₆₀Si₈ 596.28493, measured (Kratos 50) 596.28487; GC-FTIR ν (cm^{-1}) 2959(m), 2903(w), 1861(vs), 1254(m), 868(s), 803(s); ¹H-NMR (300 MHz, CDCl₃) δ 0.10(s, 36H), 0.14(s, 24H); ¹³C-NMR (75.429 MHz, CDCl₃) δ -2.24(8C), 0.66(12C), 60.83(2C), 64.43(2C), 201.81(2C); ²⁹Si-NMR (59.591 MHz, CDCl₃, TMS as the external standard) δ -24.52(4Si), -3.98(4Si); The UV spectrum (hexanes, nm): λ_{max} = 208 (5.9×10^4), λ_{sh} = 226 (4.5×10^4), λ_{sh} = 256 (1.8×10^4).

Characterizations of compounds 36. GCMS m/z 526 (7), 525(18), 524(28), 523(49, M-SiMe₃), 341(10), 283(12), 185(13), 73(100); GC-FTIR ν (cm^{-1}) 2954(m), 2902(w), 1860(vs), 1402(w), 1254(m), 891(s), 844(s); The NMR spectra of compound 36 were obtained by subtracting the spectra of 24 (*meso*), 24(*dl*), and 35 from the pyrolysis products. ¹H-NMR(300 MHz, CDCl₃) δ 0.104 and 0.107(singlets, 1:1), 0.12(6H), 0.185 and 0.192(singlets, 2:1); ¹³C-NMR (75.429 MHz, CDCl₃) δ -1.90(2C), -1.74(2C), -0.88(2C), 0.18(2C), 0.59(6C), 0.82(6C), 60.65(1C), 60.67(1C), 61.72(2C), 202.82(1C), 203.81(1C); ²⁹Si-NMR (59.591 MHz, CDCl₃, TMS as the external standard) δ -21.59(2Si), -14.89(2Si), -3.88(2Si), -3.98(2Si).

Synthesis of 1,3,4,6-tetrakis(trimethylsilyl)-3-ene-1,5-diyne (37). A yellow-orange solution of dianion **7** (5 mmol) in 10 mL ether (procedure described earlier) was cooled to -78°C. A solution of 2.67 g of iodine (10.5 mmol) in 15 mL ether was added into the dianion solution at one time and the reaction was slowly warmed to room temperature and stirred overnight. The reaction solution was poured into a mixture of 20 mL water and 20 mL hexanes. The organic layer was washed sequentially with sodium thiosulfate and brine, and then dried over sodium sulfate. After removal of the solvents and purification on a silica-gel column (hexanes as the eluent), the product was obtained as colorless needles, m.p. 92°C, in 74% yield. GCMS *m/z* 366(18, M+2), 365(32, M+1), 364(100, M), 349(22), 276(11), 262(21), 261(73), 179(24), 155(27), 73(47); HRMS *m/z* cal. for C₁₈H₃₆Si₄ 364.18942, measured 364.18961 (Kratos 50); GC-FTIR ν (cm⁻¹) 2965(s), 2906(m), 1410(w), 1256(s), 1094(m), 850(vs), 769(s); IR (KBr disk) ν (cm⁻¹): 2957(m), 2897(w), 2122(s), 1406(vw), 1248(s), 1107(m), 839(vs), 758(m); Raman (λ_{ex} = 488.0 nm) ν (cm⁻¹) 2102(vs), 1465(s), 1141(m); ¹H-NMR (300 MHz, CDCl₃) δ 0.18(18H), 0.26(18H); ¹³C-NMR (75.429 MHz, CDCl₃) δ -1.52(6C), -0.67(6C), 107.80(2C), 110.27(2C), 149.34(2C); ²⁹Si(59.591 MHz, CDCl₃, TMS as the external standard) δ -13.39(2Si), 0.56(2Si).

II. SYNTHESIS, THERMAL ISOMERIZATION, AND RING-OPENING
POLYMERIZATION OF 1,1,3,3-TETRAMETHYL-2,4-DIMETHYLENE-1,3-
DISILACYCLOBUTANE

Literature Survey

Thermal isomerization of olefins to carbenes.

The isomerization of an olefin to carbene is a high energy process. The activation energy of the rearrangement of ethylene to methylcarbene has been calculated to be between 74.2 and 82.1 kcal/mol.^{28,29} When calculations were performed at the HF/6-31G* level (the Hartree-Fock level using the 6-31G* basis set), the barrier for the reverse reaction is 11.8 kcal/mol. Correlation corrections at the fourth order perturbation level (MP4SDQ/6-31G**//6-31G*) with a zero point vibrational correction eliminate the barrier completely (Figure 1).³⁰ However, when correlation is included in the geometry optimization (MP4/6-311+G**//MP2/6-31G**), the barrier for the reverse reaction was found to be 0.8 kcal/mol.³¹

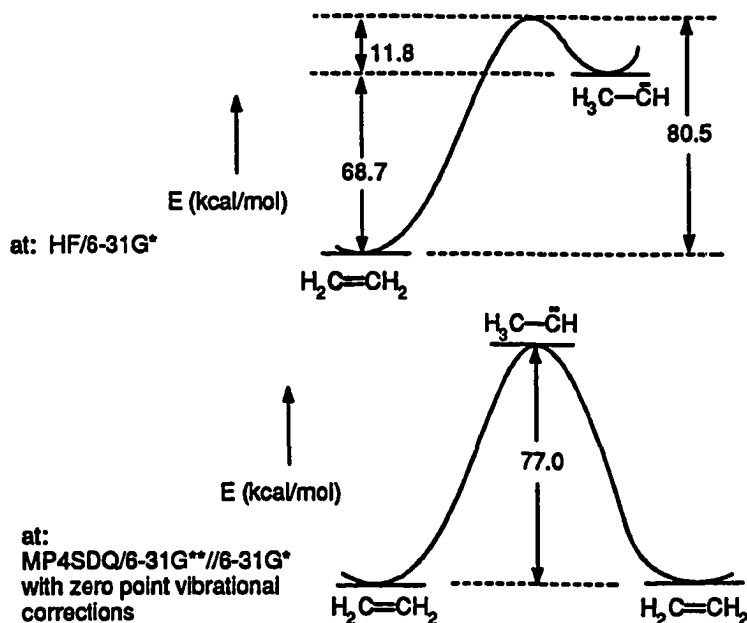
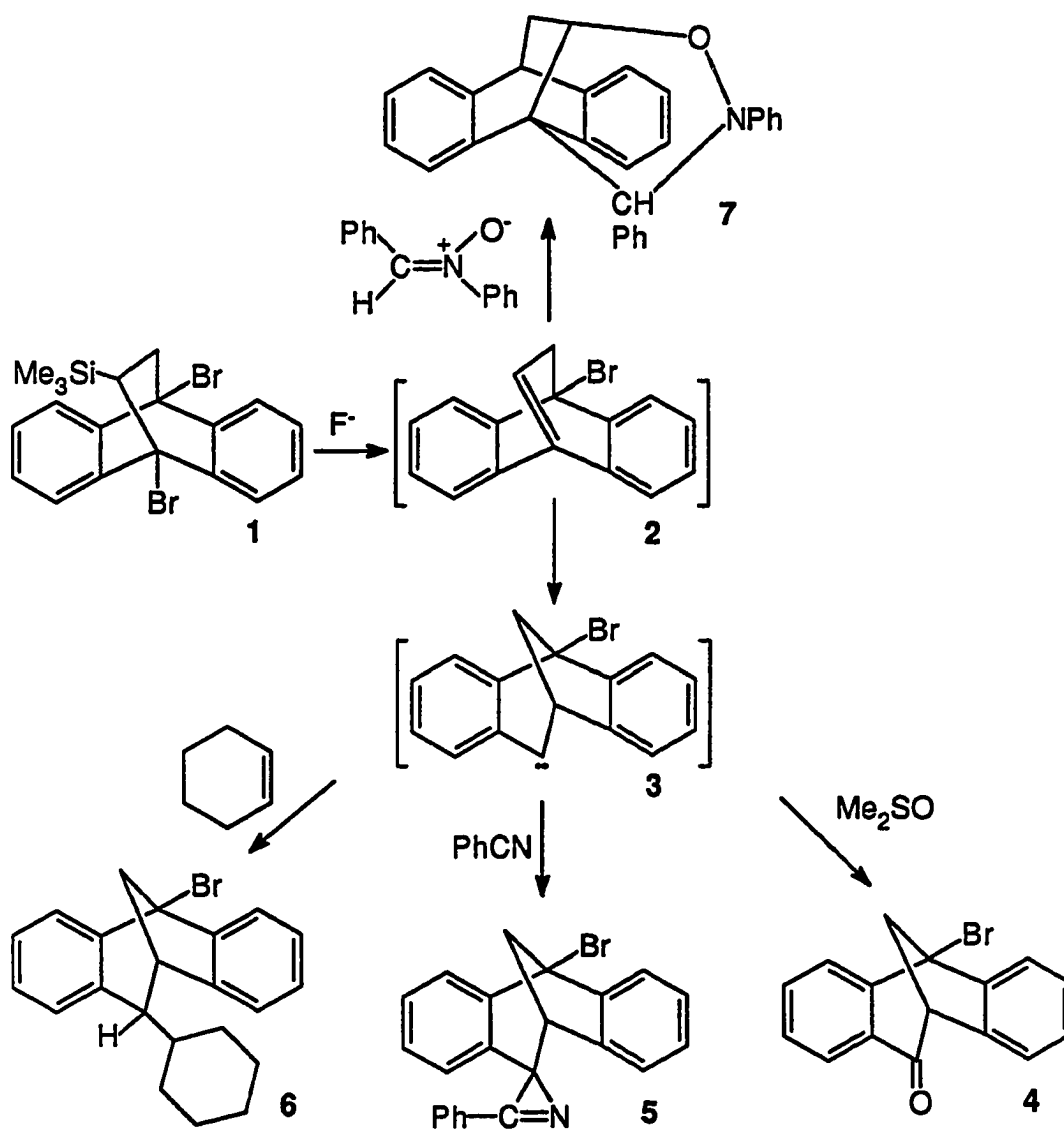
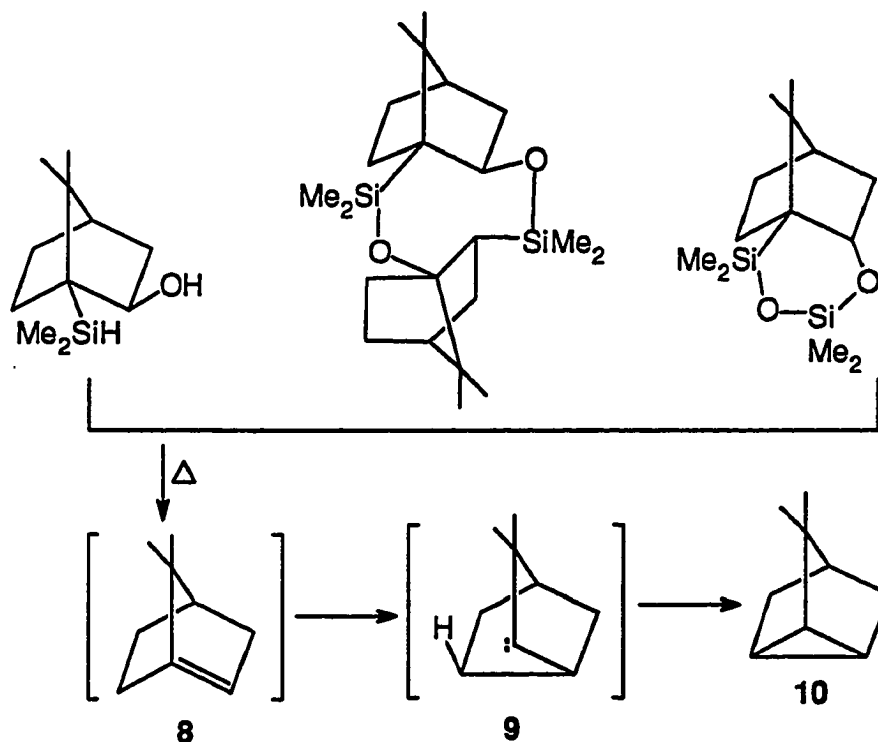


Figure 1. Calculated energies for ethylene and methylcarbene.

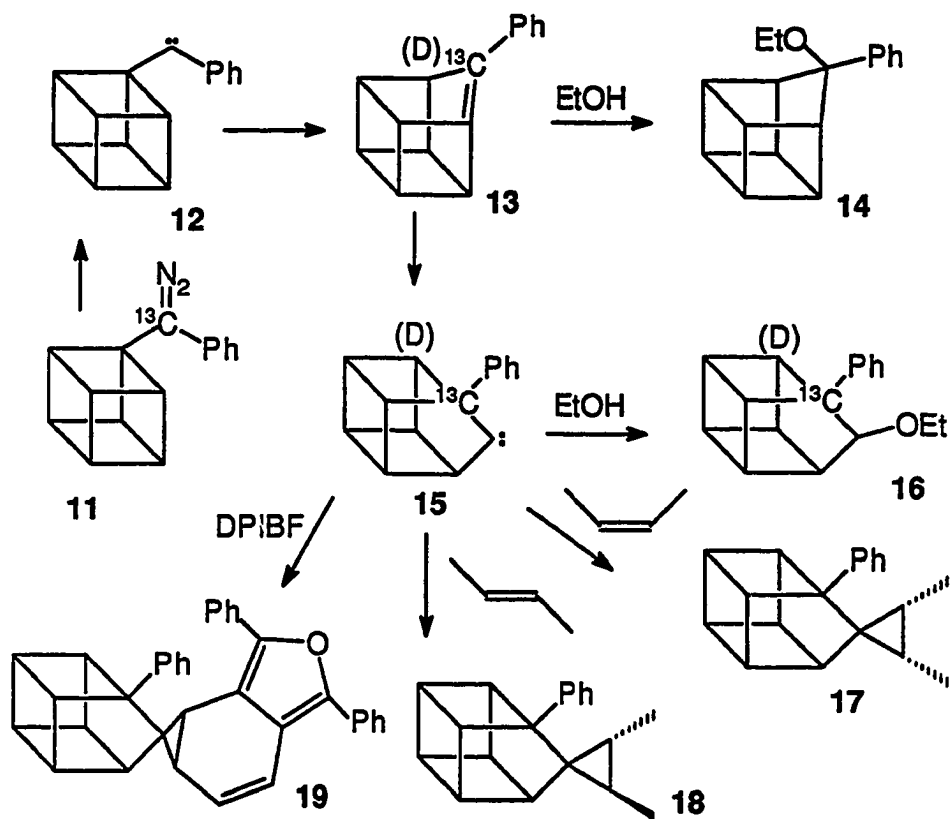
The thermal rearrangement of an olefin to a carbene has been observed in a few strained olefins. Chan and Massuda observed the thermal generation of a carbene from a bridgehead alkene. ³² Fluoride initiated elimination of compound 1 in heated DMSO affords compound 4 which represents an oxidation product of the carbene intermediate 3 by DMSO. Carbene 3 could have been formed via 1,2-aryl shift from the bridgehead alkene 2. Trapping products 5-7 also verified the generation of the bridgehead olefin and carbene.



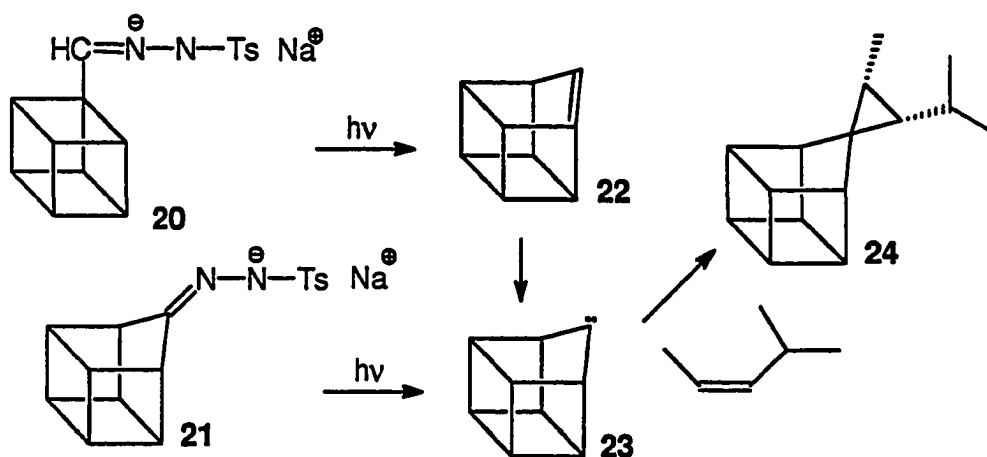
Barton and Yeh reported the thermal decomposition of three precursors to form the bridgehead olefin **8** which then underwent 1,2-alkyl shift to give the 2-norbornylidene **9**.³³ Insertion of the carbene into the γ -CH bond gives the isolated product, nortricyclene **10**.



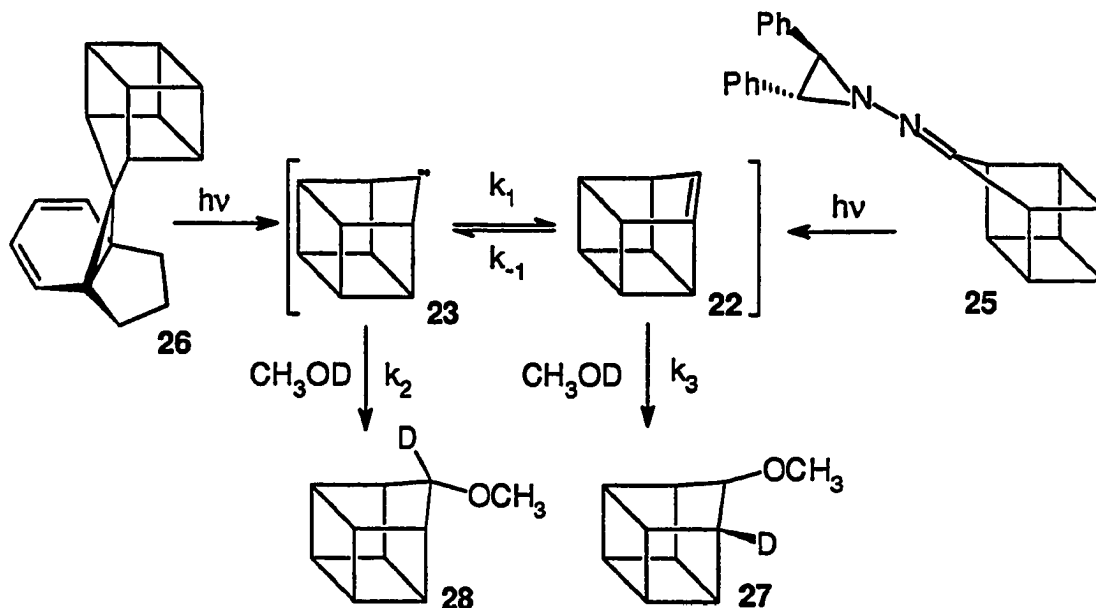
Eaton and Hoffman have studied the rearrangement of the 9-phenyl-1(9)-homocubene **13** which was generated from the cubylphenyldiazomethane **11** photochemically or thermally.³⁴ The highly strained homocubene **13** was trapped by ethanol to form **14**. The conversion of **13** to **15** even takes place at -78°C ! Deuterium-labeling³⁵ and carbon-13-labeling³⁶ experiments established the rearrangement from **13** to **15** is via a 1,2-alkyl migration instead of 1,2-phenyl migration. Formation of **15** was evident from the trapping products **16-19** by ethanol, 2-butenes, and 2,5-diphenylisobenzofuran. Carbene **15** exists as a singlet as indicated by the retention of stereochemistry in the *Z*- or *E*-2-butene adducts. MNDO calculations^{34,37} show that the heat formation for compounds **13** and **15** are 201 kcal/mol and 199 kcal/mol respectively.



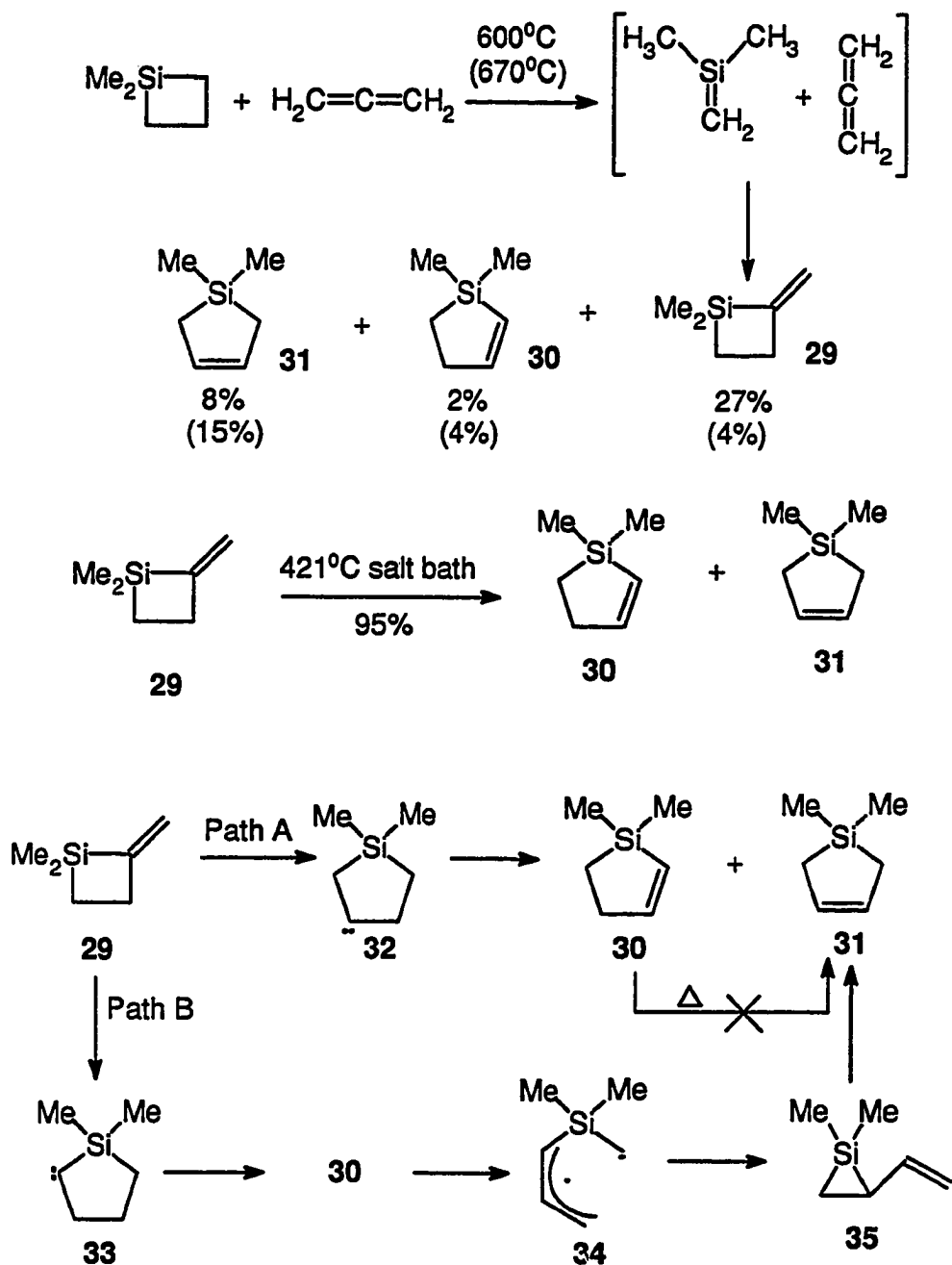
Jones *et al.* complemented Eaton's work by the study of the parent cubyl and homocubyl system.³⁸ Decomposition of tosylhydrazone salts **20** and **21** formed from cubyl carboxaldehyde and homocubanone leads to the trapped product **24** derived from the homocuban-9-ylidene **23**.



Further study established that the rearrangement from homocub-1(9)-ene to homocuban-9-ylidene is reversible.³⁹ While products **27** and **28** from the decomposition of **25** could have come from carbene **23** or from starting material **25**, the generation of trapping products **27** and **28** from the decomposition of **26**, an unequivocal source of homocubylidene, exclusively demonstrates the equilibrium between **22** and **23**. This equilibrium was also observed between 9-phenylhomocub-1(9)-ene **13** and 1-phenylhomocubylidene **15** via the carbon-13-labeling experiments.⁴⁰ A combination of chemical trapping and laser flash photolysis experiments was used to demonstrate the equilibrium between **22** and **23**.^{41, 42} The equilibrium constant was shown to be close to unity at + 20°C ($0.23 \leq K \leq 4.0$).



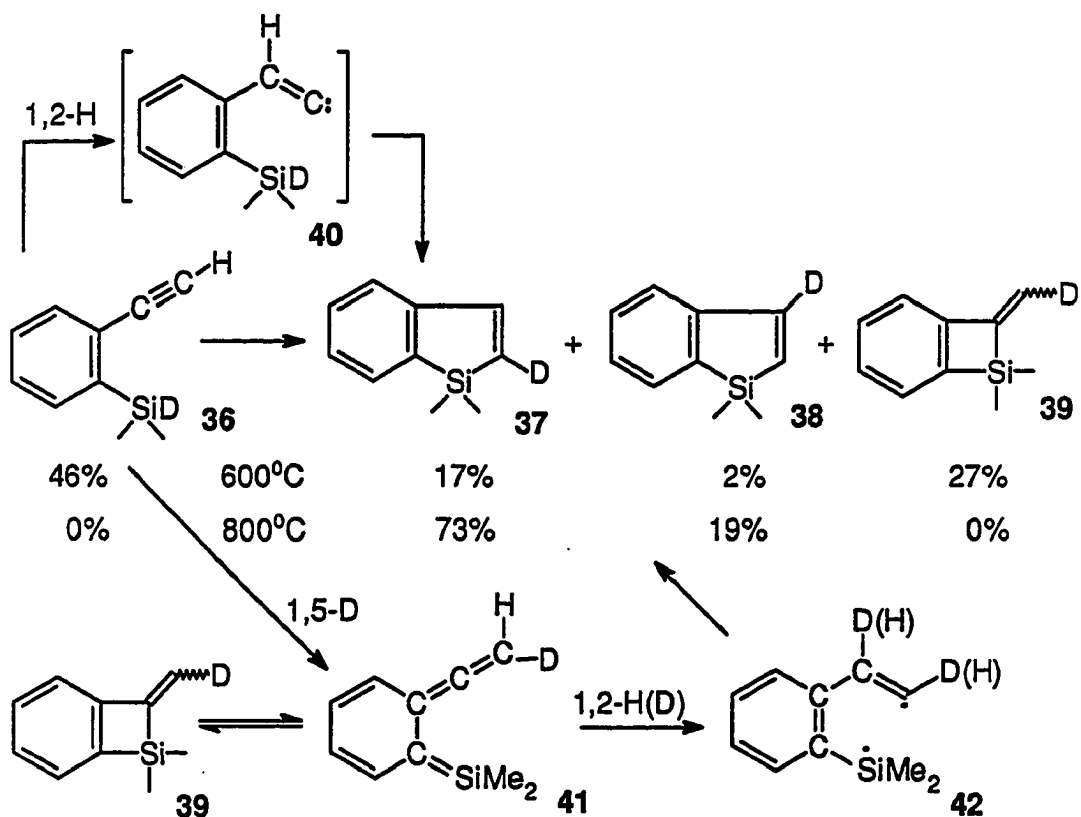
One example of the thermal isomerization of an unstrained olefin to a carbene was observed by Conlin *et al.*⁴³ 1,1-Dimethyl-2-methylenesilacyclobutane **29**, a 2 + 2 adduct of 1,1-dimethylsilene and allene, was obtained together with 1,1-dimethylsilacyclopent-2-ene **30** and 1,1-dimethylsilacyclopent-3-ene **31**. Pyrolysis of **29** alone at 421°C in a salt bath yields the ring expansion dimethylsilacyclopentenes **30** and **31**.



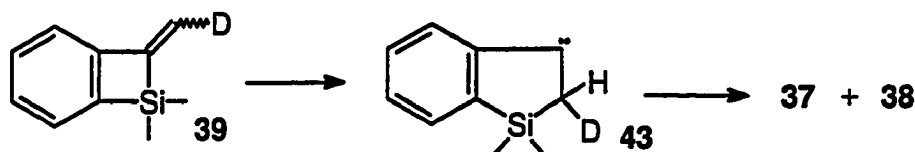
Two possible mechanisms were proposed by Conlin *et al.* for the transformation, each involving carbene intermediacy. Path A involves a β -silyl carbene intermediate, **32**, formed from the vinylic silicon-carbon bond migration. Insertion of the carbene into the adjacent

methylene group gives the isomeric dimethylsilacyclopentenes **30** and **31**. Path B involves the vinylic carbon-carbon bond migration to form the α -silyl carbene, **33**, which can only give one silacyclopentene **30**. The other isomer **31** could be produced from **30** via intermediate **34** and **35**. However, path B was ruled out by the fact that **30** does not isomerize to **31** under the experimental conditions.

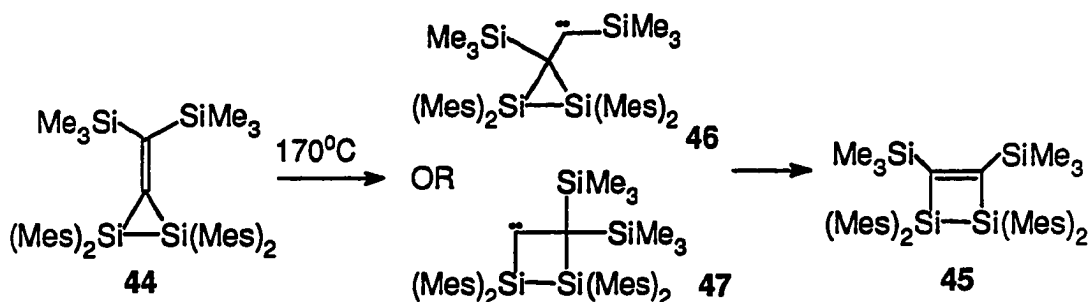
Barton and Groh studied the synthesis of silaindenes by thermally induced acetylene rearrangements.⁴⁴ Deuterium labeling revealed that there are two path ways to silaindenes involving either a 1,2-H shift (**40**) or 1,5-H shift (**41**). The compound, **39**, was converted to **37** and **38** completely at higher temperature.



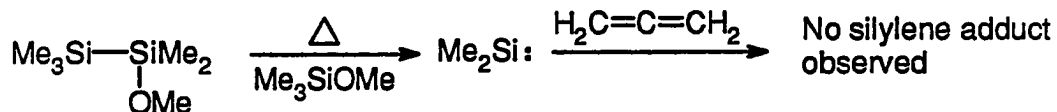
However, given Conlin's study of the thermal isomerization of 2-methylenesilacyclobutane published later,⁴³ the isomerization via a 1,2-silyl shift from compound **39** to **37** and **38** involving carbene **43** should also be considered.

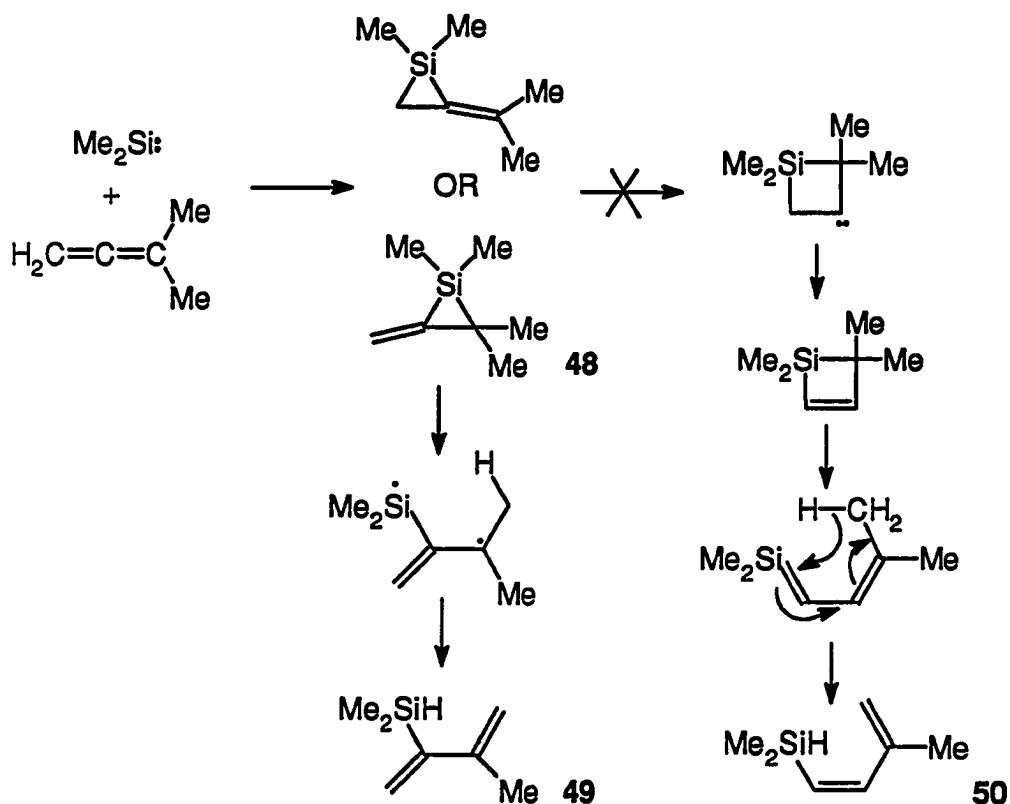


Another example of the thermal isomerization involving a carbene intermediate is the ring expansion of the 1,1,2,2-tetramesityl-3-bis(trimethylsilyl)methylene-1,2-disilacyclopropane **44** to 1,1,2,2-tetramesityl-3,4-bis(trimethylsilyl)-1,2-disilacyclobutene **45** on heating at 170°C.⁴⁵ The mechanism of the transformation of **44** to **45** involving carbene intermediates **46** or **47** was proposed by Barton.⁴⁶

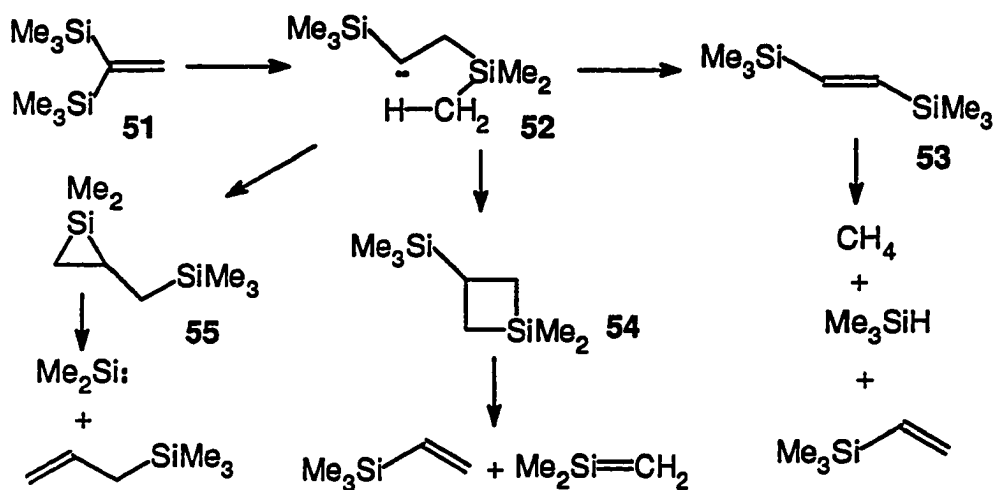


Surprisingly, in the study of the thermal isomerization of the three-membered ring analog of compound **29**, the carbene was ruled out as a possible intermediate from the analysis of the products.⁴⁷ While no silylene adduct was observed when allene was used to trap silylenes, the major product from the flash vacuum pyrolysis (FVP) of adduct of silylene and 1,1-dimethylallene is compound **49**. The formation of compound **49** is explained by a diradical intermediate. Compound **50**, the expected product from the carbene intermediate was not observed and hence the carbene intermediate in the thermal rearrangement of methylenesilacyclopropane was ruled out.



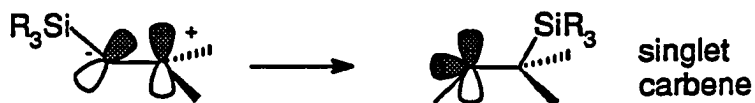


Calculations show that 1,1-disubstituted ethylenes are more strained than *E*-1,2-disubstituted ethylenes, with the strain energy of 1,1-di(*t*-butyl)ethylene being about 12.5 kcal/mol due to the large steric effects of *t*-butyl groups.⁴⁸ The steric effect of a trimethylsilyl group is comparable to that of *t*-butyl. Thus, thermal isomerization of 1,1-bis(trimethylsilyl)ethylene should release the strain energy. 1,2-Silyl migration of **51** would yield the carbene **52**. Flash vacuum pyrolysis (FVP) were employed to study the thermal isomerization of 1,1-bis(trimethylsilyl)ethylene **51**.⁴⁹ However, this compound is thermally stable even to very high temperatures, and it only partially decomposes at 700-800°C. Methane, trimethylsilane, and vinyltrimethylsilane are the major products. Perhaps the mechanism leading to these products involves a carbene intermediate.




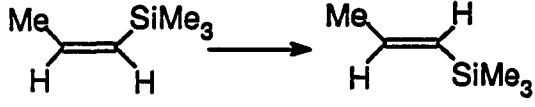
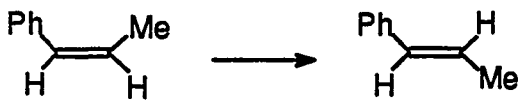




This carbene could undergo α -C-H insertion to give *E*-1,2-bis(trimethylsilyl)ethylene 53, which was separately tested in FVP and found to partially decompose at 700°C to methane, trimethylsilane, and vinyltrimethylsilane as major products. However, 53 was not detected in the reaction mixture even though it is stable enough to leave detectable amounts undecomposed under the experimental conditions. Another possibility is that the vinyltrimethylsilane came from the known decomposition of silacyclobutane 54, which was formed from intramolecular β -C-H insertion of carbene 52. The silacyclopropane 55 might be another intermediate derived from carbene 52. However, 54 and allyltrimethylsilane were not detected from the reaction mixture. They should have been detected if formed. It is most likely that high-energy radical processes instead of the carbene process dominates in the thermal decomposition of 1,1-disubstituted ethylene.

Silicon has the unique potential to assist in the heterolytic rupture of a carbon-carbon π bond - it can stabilize α -carbanions and β -carbocations and readily migrates to β -carbocations. Because of this, silicon should facilitate π -bond heterolysis and the barriers for *E-Z* isomerization of alkenes should be reduced significantly by silyl substituents.



However, this effect has not been observed in the study of thermally-induced *E-Z* isomerization of alkenes (Table I).⁴⁹ Trimethylsilyl substituents have similar activation energy and logA values to *t*-butyl substituents. The reduction in the activation energy of trimethylsilyl substituents compared to methyl substituents may be due only to steric effects.

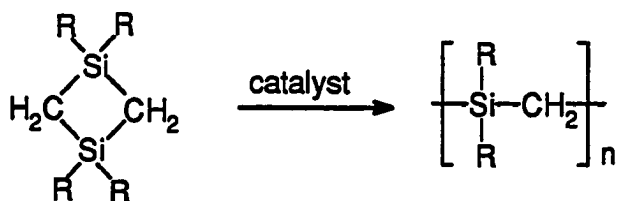
Table I. Thermally-induced *cis-trans* isomerization

	Ea (kcal/mol)	logA
	62.3 ± 0.8	13.5
	56.0 ± 0.3	13.0
	60.2 ± 0.7	15.1
	53.0 ± 0.3	14.3
	54.9 ± 0.2	14.8
	52.7 ± 0.4	13.9
	54.4	Ref. 50

All known examples of a thermal 1,2-shift along a C=C double bond to form a carbene intermediate come from molecules in which the double bond is already extremely twisted (bridgehead double bond) or in a molecule with significant ring strain. The strain enthalpies for three-, four-, five-, and six- membered silacycles are reported to be 41.4, 24.7, 4.5, and 4.0 kcal/mol, respectively.⁵¹ The strain energy of ~17 kcal/mol relieved by expanding a three- to a four-membered ring is close to that relieved by expansion of a four- to a five-membered ring, ~ 20 kcal/mol.

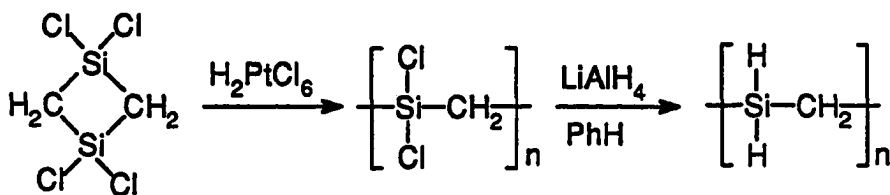
Ring opening polymerization of derivatives of 1,3-disilacyclobutane.

Ring opening polymerization of various derivatives of 1,3-disilacyclobutane to prepare polycarbosilanes as polymer precursors for silicon carbide has been well documented.⁵²⁻⁵⁴

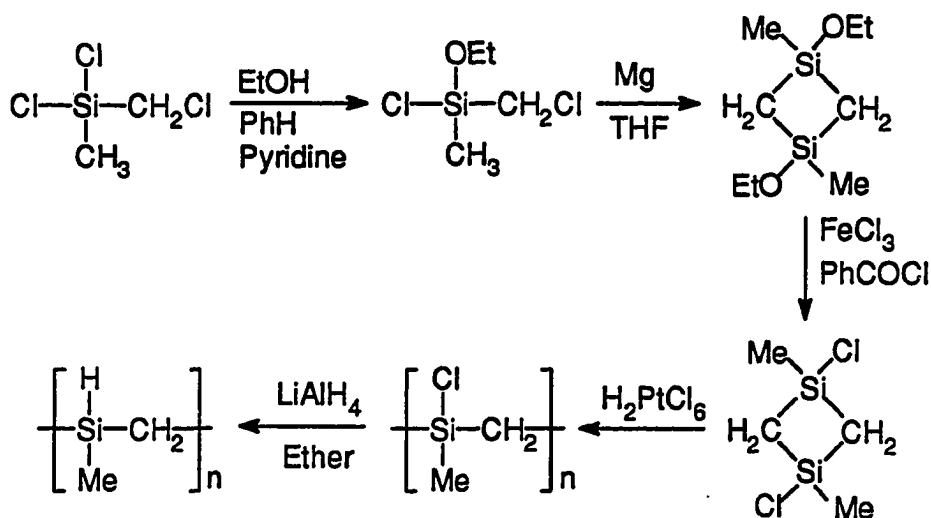


Smith patented the ring opening polymerization of 1,3-disilacyclobutane (R = H) using catalytic H_2PtCl_6 (CPA) to give linear poly(silaethylene) with an 85% ceramic yield at 900°C.⁵⁵ However, with no basic characterization reported about his polymer, the formation of linear poly(silaethylene) was questioned because the Si-H bond is also activated by the CPA catalyst.⁵⁴ An attempt to repeat this work also failed.⁵⁶

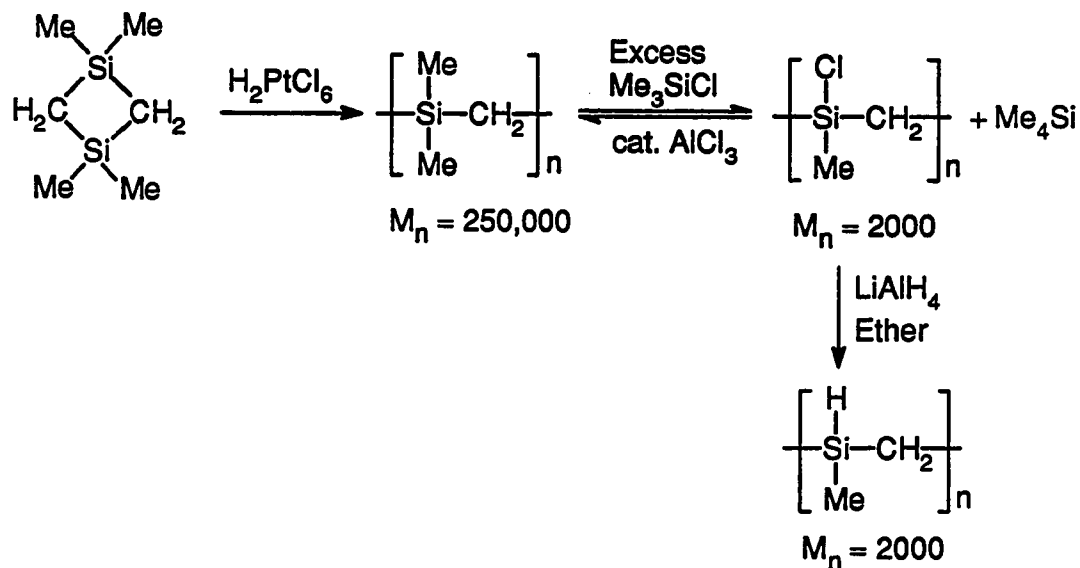
Interrante *et al.* reported the synthesis of poly(silaethylene) from the ring opening polymerization of 1,1,3,3-tetrachloro-1,3-disilacyclobutane followed by LiAlH_4 reduction.⁵⁶ The poly(silaethylene) synthesized with a molecular weight $M_n = 12,300$ was well characterized by NMR (^1H , ^{13}C , ^{29}Si). A high ceramic yield (theoretical 90.9%, observed 87%) was observed and weight loss was complete at 600°C. Poly(silaethylene) has similar properties to polyethylene except it has a lower melting point.



Wu and Interrante also reported the ring opening polymerization of 1,1,3,3-tetramethyl-1,3-disilacyclobutane catalyzed by CPA to give poly(dimethylsilaethylene) with molecular weight $M_n = 260,000$.⁵⁴ However, this polymer decomposes rapidly when heated above 450°C giving a negligible ceramic yield. A similar ring opening polymerization of 1,3-dichloro-1,3-dimethyl-1,3-disilacyclobutane catalyzed by CPA followed by LiAlH₄ reduction gives poly(silapropylene) with molecular weight $M_n = 35,000$. After thermal processing at 400°C, the ceramic yield of poly(silapropylene) can be improved from 20% to 66%.

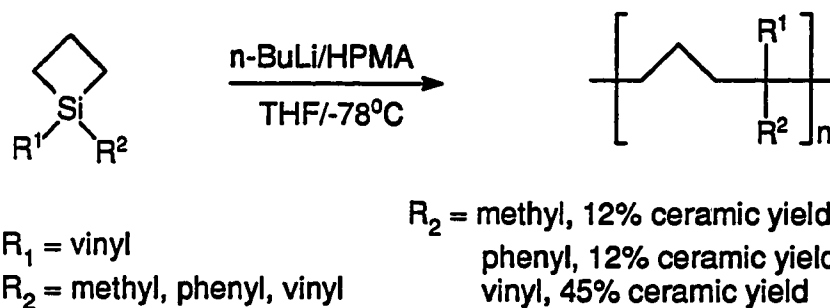


Dunoguès *et al.* have studied the modification of poly(dimethylsilaethylene) arising from ring opening polymerization.⁵⁷⁻⁵⁹ After chlorination, the polymers were then reduced to poly(silapropylene) by LiAlH₄. There is also a significant decrease in molecular weight due to chain breaking under conditions for chlorination. Although the poly(silapropylene) obtained by this route gives very low ceramic yield (~5%), the chlorination does introduce the functionality necessary for further modification of the polymers.



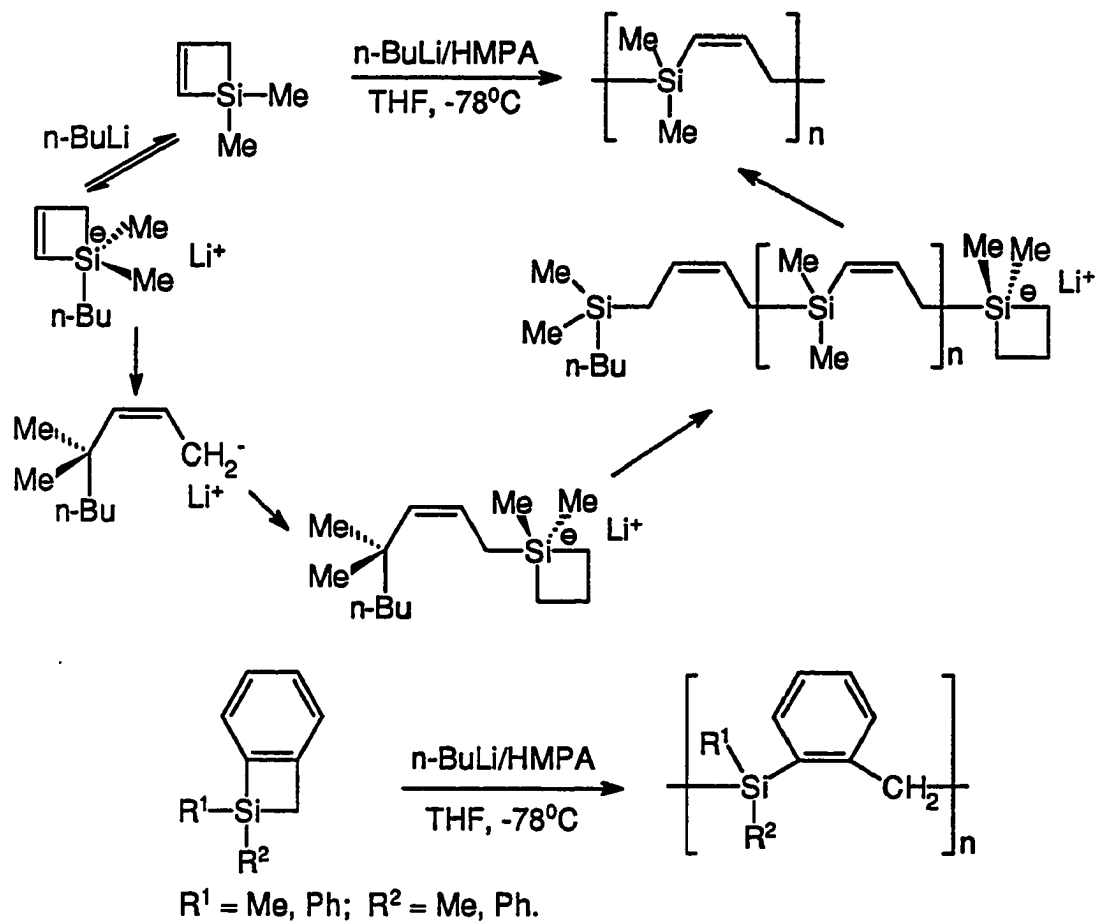
Ring opening polymerization of silacyclobutanes and silacyclobutenes.

The ring opening polymerization of 1,1-dimethyl-1-silacyclobutane under anionic,⁶⁰ thermal,⁶¹ and CPA catalysis⁶² conditions have been reported. Liao and Weber studied the anionic ring opening polymerization of other silacyclobutanes and the thermal properties of these polymers.⁶³



Theurig and Weber also studied the anionic ring opening polymerization of silacyclobutene and 2,3-benzo-1-silacyclobutene.^{64, 65} The polymerization of silacyclobutene is stereoselective and gives polymers with predominantly 1-sila-Z-but-2-ene repeating units. The mechanism for this polymerization is shown below where the first step is the formation of a pentacoordinate anionic silicon intermediate. Ring opening of this intermediate leads to Z-allyl anion which reacts with another monomer to form a new pentacoordinate anionic silicon

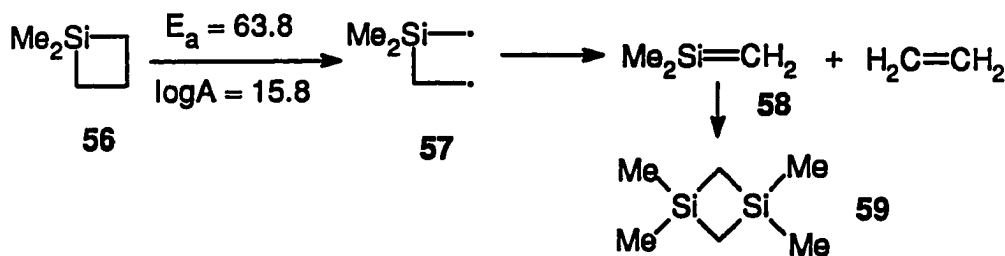
intermediate. The ring opening and reaction of *Z*-allyl anions with monomer repeats to form a polymer chain with predominantly *cis* structure. Poly(1,1-dimethyl-1-sila-*Z*-but-2-ene) from this reaction decomposes completely when heated to 430°C. Similar anionic ring opening polymerization of 2,3-benzo-1-silacyclobutene, following a similar mechanism, gives poly(2,3-benzo-1-silabutenes) with good thermal stability.



Results and Discussion

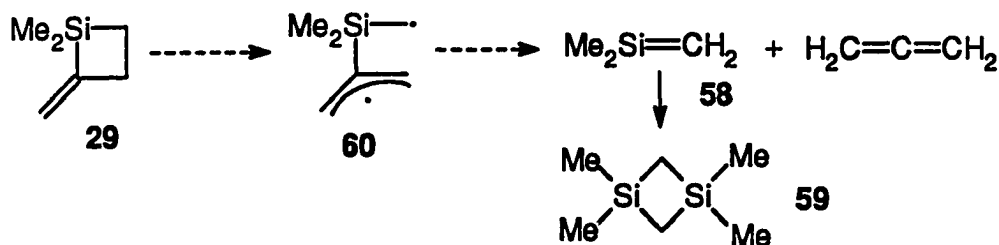
Reexamination of the thermal rearrangements of 1,1-dimethyl-2-methylene-1-silacyclobutane (29).

Silacyclobutanes are known to decompose by the initial homolytic cleavage of one of the carbon-carbon bonds.^{66,67} Thermal decomposition of **56** to **58** is believed to proceed via diradical intermediate **57** with an activation energy of 63.8 kcal/mol and a log A of 15.8 (Scheme 1). The observed 1,3-disilacyclobutane, **59**, came from the dimerization of silene **58**.



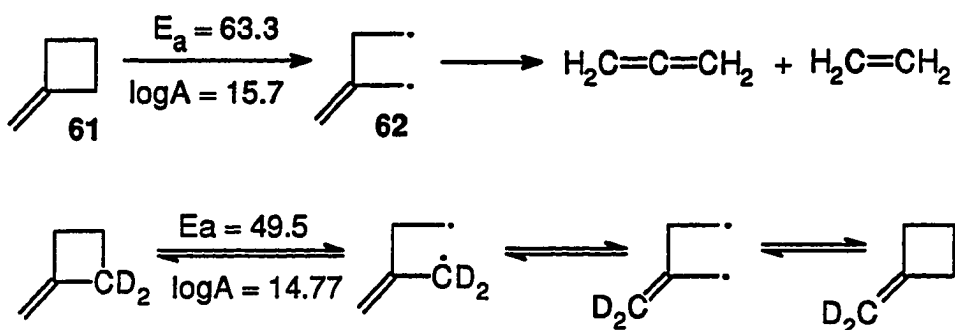
Scheme 1. Thermal decomposition of 1,1-dimethyl-1-silacyclobutane.

Intermediate **60** from the initial cleavage of the allyl-carbon bond in **29** should be stabilized either by the allylic stabilization⁶⁸ or the β -silyl effect (Scheme 2).⁶⁹ It is interesting to note that 1,3-disilacyclobutane and allene, which are the expected products from diradical intermediate **60**, were not observed.⁴³



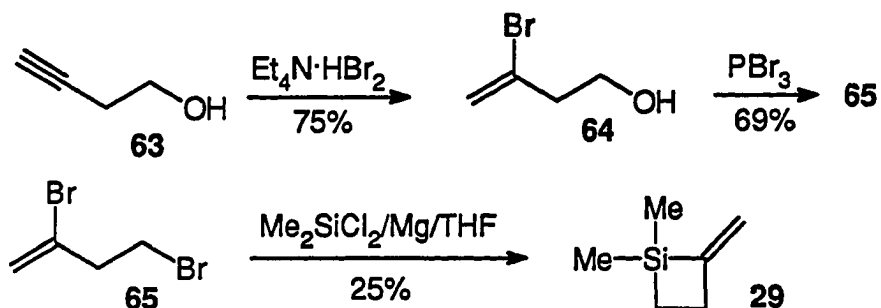
Scheme 2. The diradical process for thermal decomposition of compound **29**.

The thermal chemistry of the analogous methylenecyclobutane **61** is different from that of **29**. No ring expansion products were observed for the thermal reaction of **61**. The classical decomposition via diradical **62** is operating to produce allene and ethylene with $E_a = 63.3$ kcal/mol ($\log A = 15.7$),⁷⁰ while E_a for the isomerization of deuterated methylenecyclobutane is only 49.5 kcal/mol ($\log A = 14.77$)⁷¹ (Scheme 3).



Scheme 3. Thermal rearrangements of methylenecyclobutane.

In order to study the gas phase kinetics of the isomerization from **29** to **30** and **31**, an attempt was made to synthesize compound **29** following Conlin's procedure⁴³ using FVP. However, the yield was < 1%. Therefore, compound **29** was synthesized according to the following route (Scheme 4):

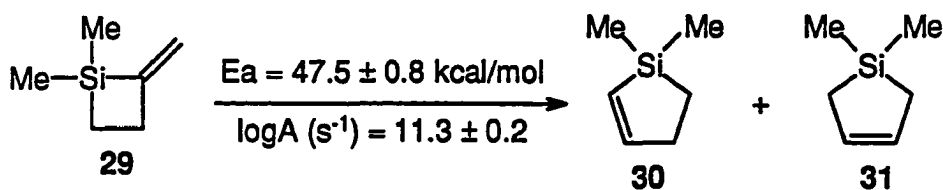


Scheme 4. Synthesis of 1,1-dimethyl-2-methylene-1-silacyclobutane (**29**).

3-Bromo-3-buten-1-ol **64** was synthesized in 75% yield from 3-butyn-1-ol **63**.⁷² Further bromination⁷³ afforded 1,3-dibromo-3-butene **65** in 69% yield. When 1:1 mixture of **65** and

dimethyldichlorosilane was added to magnesium in THF, compound **29** was obtained in 25% yield. Compound **29** synthesized according to this route was contaminated by compound **30** (**29** : **30** = 8 : 1) presumably because *Z*-1,4-dibromo-1-butene is a minor product in the synthesis of compound **65**. Compound **29** was purified by preparative GC.

Thus, a kinetic investigation of the thermal isomerization of **29** to **30** and **31** was undertaken using a pulsed, stirred-flow reactor (SFR) modeled after the system described by Davidson.⁷⁴ Thermal isomerization of **29** was carried out over a temperature range of 530-590°C where the rate of formation of **31** was followed. On the basis of 13 rate determinations in this temperature range, the Arrhenius plot (Figure 2) gave the first-order rate constant for the formation of **31**. The Arrhenius parameters are in accord with a concerted unimolecular process. The negative value of the activation entropy $\Delta S^\ddagger = -10.7$ eu at 559°C suggested a cyclic, concerted transition state, as opposed to a homolytic or heterolytic dissociation mechanism (Scheme 5).



Scheme 5. Kinetics study for the thermal isomerization from **29** to **31**.

Deuterium labeled compound **29(D)** was synthesized by the route shown above using $\text{Et}_4\text{N}\cdot\text{DBr}_2$ for hydrobromination. If the diradical intermediate **60** was formed, even it did not go on to give dimethylsilaethylene and allene, deuterium scrambling will occur to form the observable **29'** as a product. Indeed, this is exactly what was observed (Scheme 6). The chemical shifts for $^1\text{H-NMR}$ of compounds **29**, **30**, **31** are shown below (Scheme 7). As shown in Figure 3, the $^2\text{H-NMR}$ spectrum of the FVP products revealed that compound **29'** was formed before any significant amount of ring expansion products **30** and **31** were observed. This observation clearly demonstrates that the diradical intermediates were formed faster than the carbene intermediates!

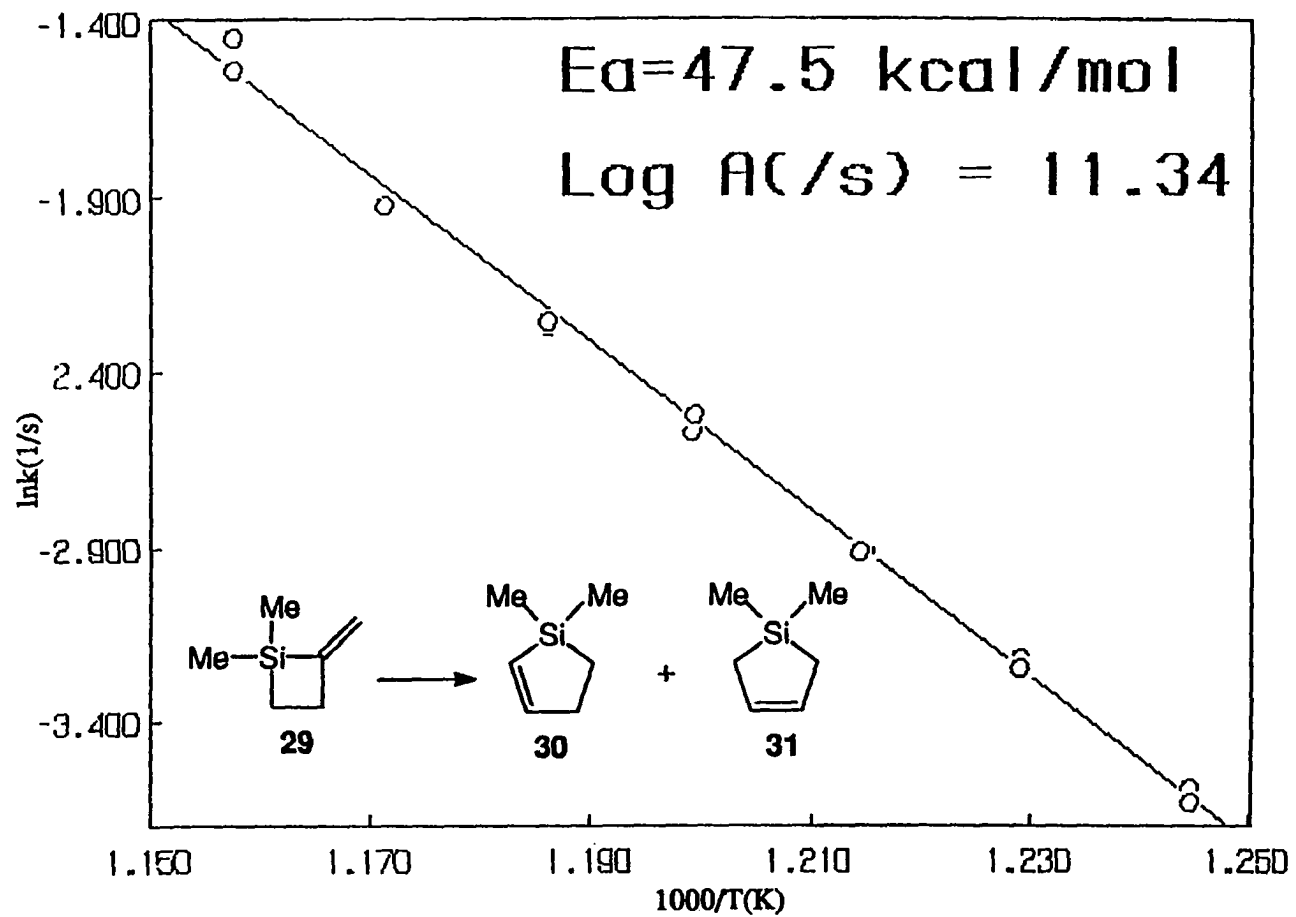
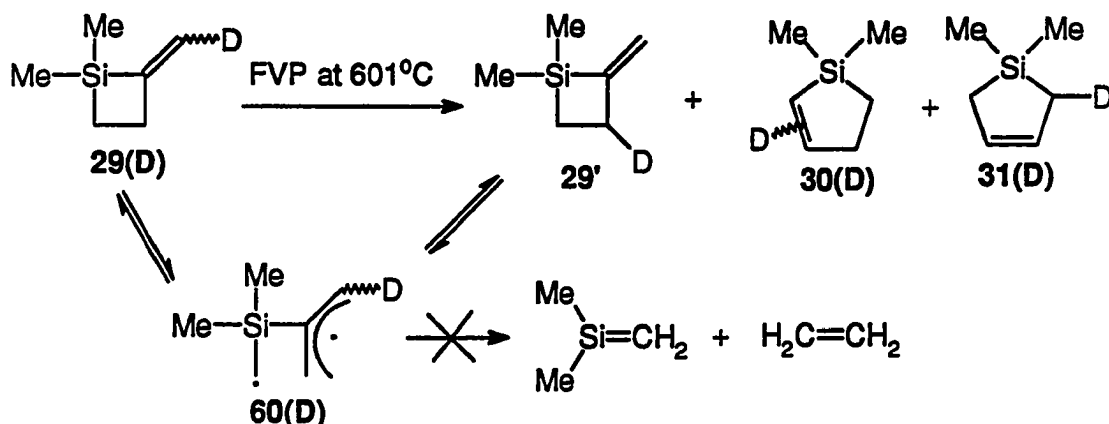
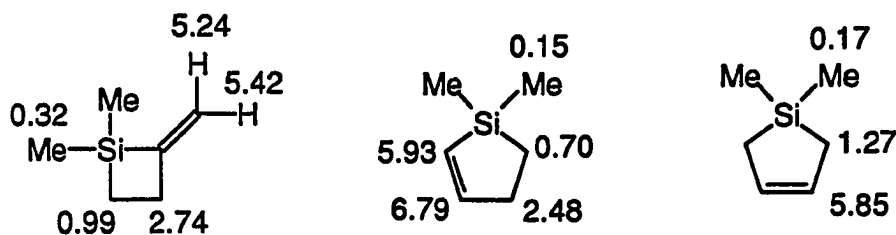


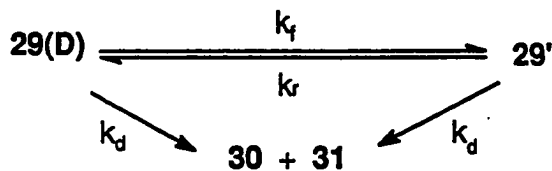
Figure 2. Arrhenius plot of the isomerization from 29 to 30 and 31.



Scheme 6. Thermal rearrangements of compound 29(D).

Scheme 7. Chemical shifts in $^1\text{H-NMR}$ of compounds 29, 30, 31.

A kinetic study of the thermal isomerization from 29(D) to 29' was undertaken using the SFR system described previously. The reaction was carried out over a temperature range of 460-530°C. The products and unreacted starting material were trapped in cooled NMR tubes (using liquid N_2) and their quantity was measured by $^2\text{H-NMR}$. A rate expression was derived by adopting Davidson's model⁷⁵ (Scheme 8):



Scheme 8. Kinetic scheme for thermal rearrangements of 29(D).

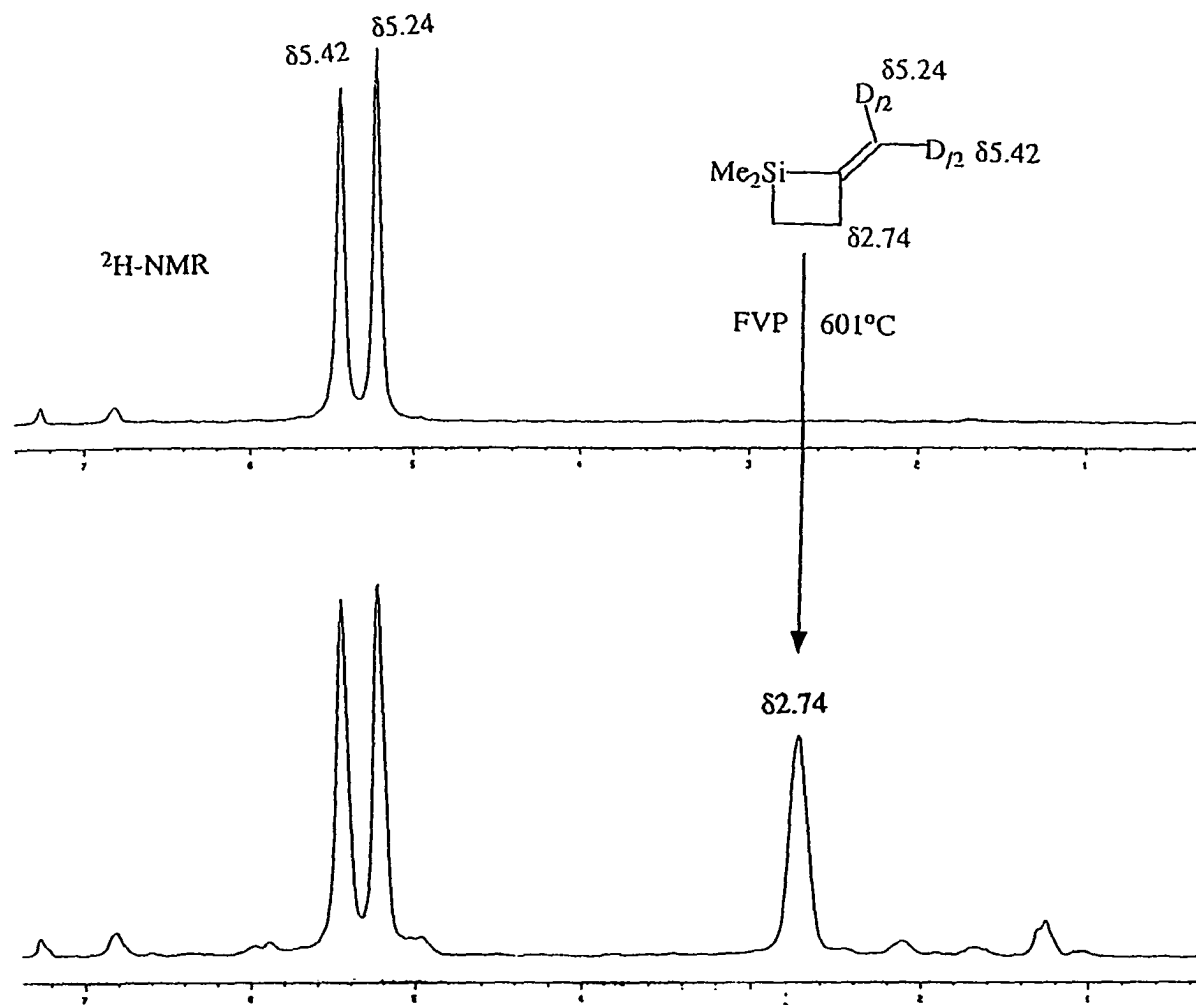


Figure 3. $^2\text{H-NMR}$ spectra for isomerization of 29(D) to 29'.

Mass balance for the product 29':

Formation - Loss = 0

$$k_f v [29(D)] - k_r v [29'] - k_d v [29'] - u [29'] = 0 \quad (I)$$

Where v = volume of reactor, u = volumetric flow rate.

Since $k_f = k_r$

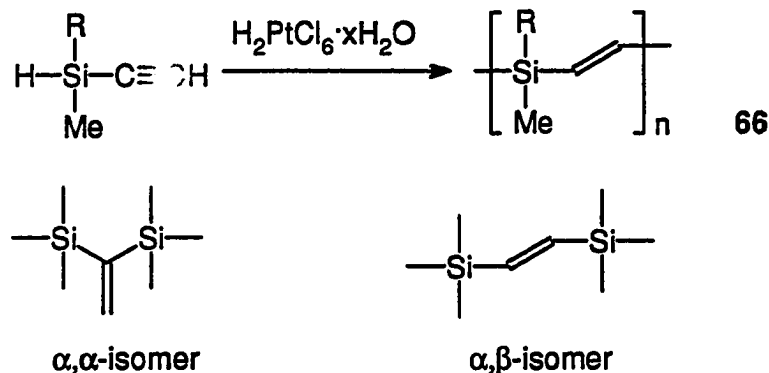
$$\text{Hence,} \quad k_f = [29'](u + k_d v) / v([29(D)] - [29']) \quad (II)$$

Once the experimental quantities of 29(D), 29', and k_d have been measured, k_f were obtained from rate expression (II). On the basis of 13 rate constants of the formation of 29' in this temperature range, the Arrhenius plot (Figure 4) gave a straight line, with Arrhenius parameters of $\log A/(s) = 13.56$ and $E_a = 50.85$ kcal/mol.

Even though the rearrangement from compound 29 to the ring expansion products (the carbene process) has a lower activation energy, it is the larger $\log A$ factor for the deuterium scrambling (the diradical process) that dominates. With this we now have a complete picture for the thermal behavior of compound 29 (Figure 5).

Synthesis of 1,1,3,3-tetramethyl-2,4-dimethylene-1,3-disilacyclobutane.

Recently, Pang *et al.* reported the efficient synthesis of silylene-vinylene preceramic polymers (66) by the CPA catalyzed hydrosilylation of ethynylsilanes (Scheme 9).⁷⁶ These poly(silylene vinylene)s have a good ceramic yield and low decomposition temperatures. Both ²⁹Si and ¹³C-NMR spectra are consistent only with the anticipated α,β -isomer structure.



Scheme 9. Synthesis of poly(silylene vinylene) with α,β -isomer structure.

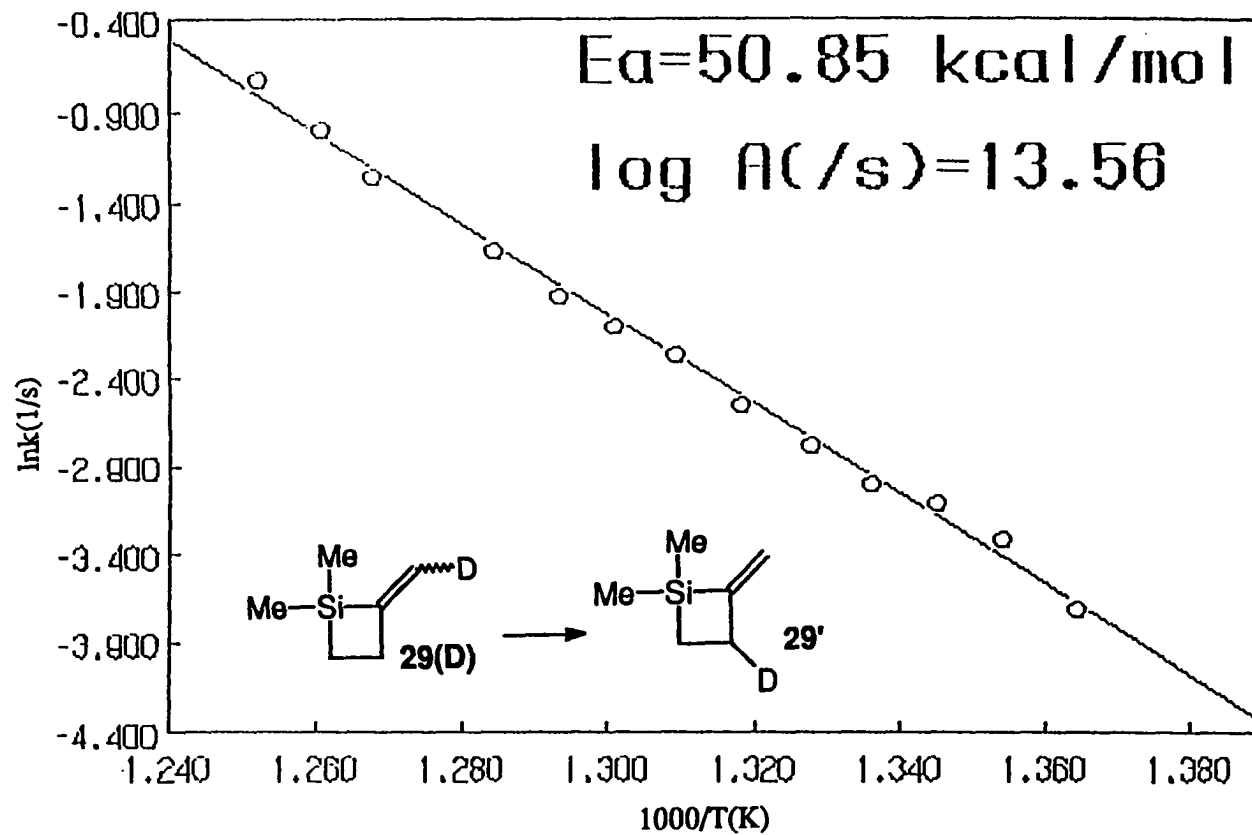


Figure 4. Arrhenius plot of the isomerization from 29(D) to 29'.

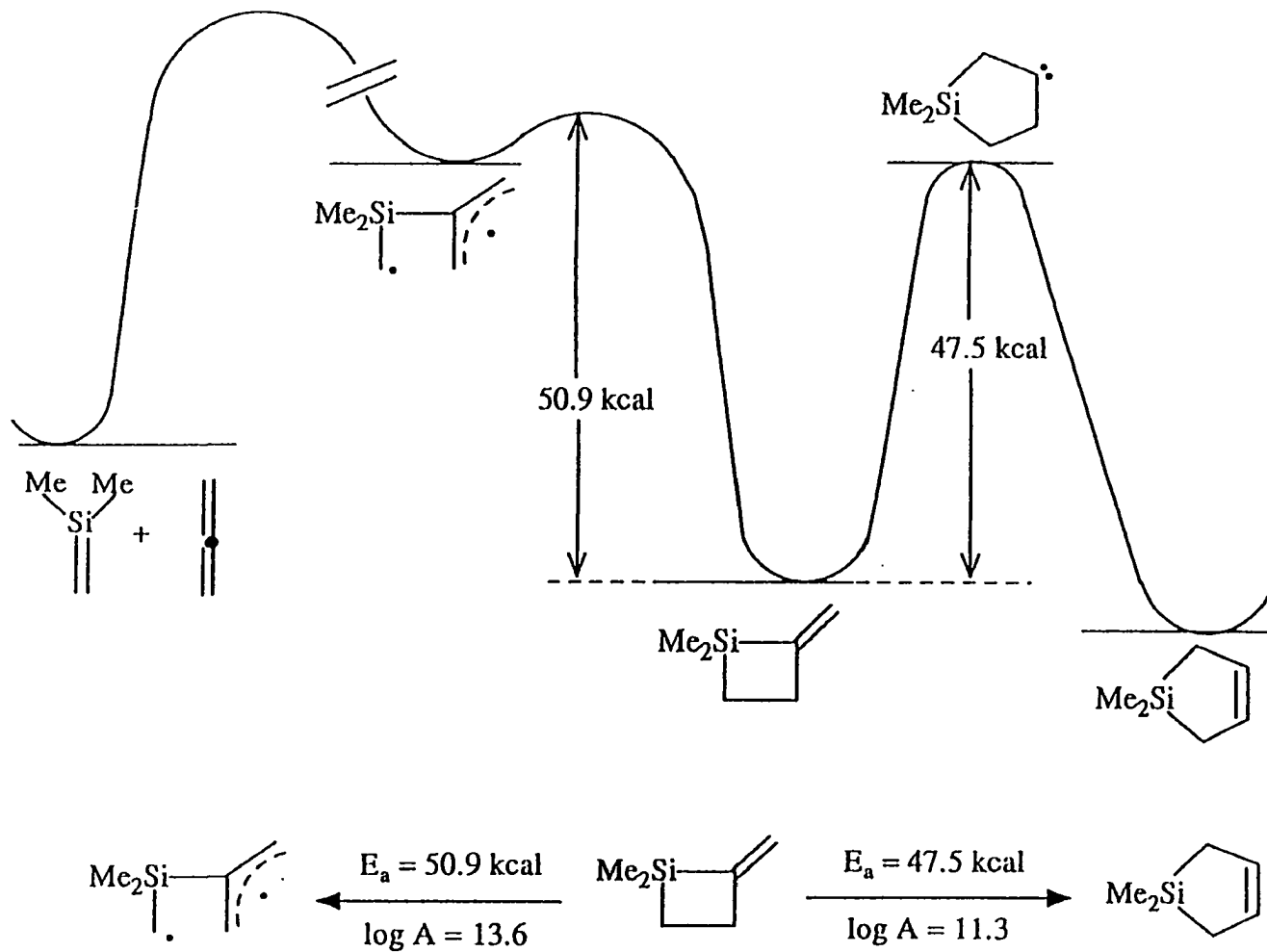
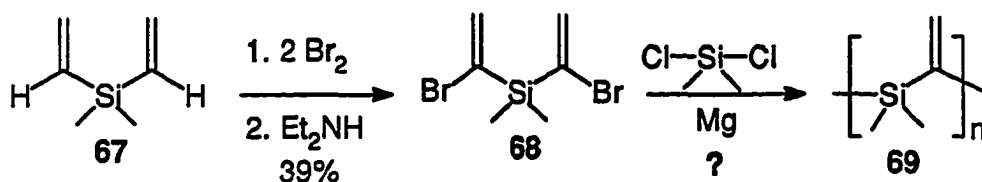
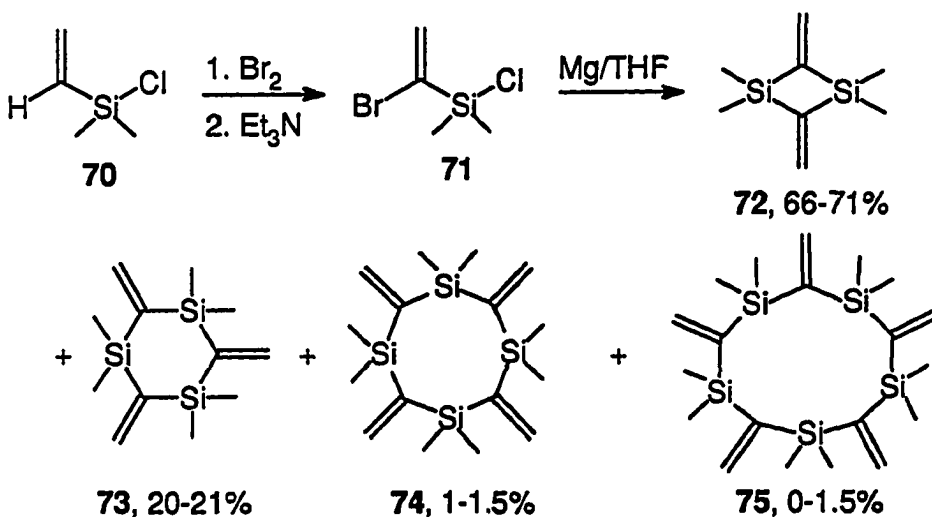


Figure 5. Energy diagram for the thermal rearrangements of compound 29.

Our initial attempt to synthesize silylene-vinylene polymers with an α , α -isomer structure (69) is shown in Scheme 10. Bromination of divinyl dimethylsilane (67) followed by dehydrobromination gives bis(α -bromovinyl)dimethylsilane (68) in 39% isolated yield.^{77,78} Reaction of 68 with magnesium to form the di-Grignard reagent, and subsequent quenching with dimethyldichlorosilane gave very low conversion to oligomers and dimer 72. A variety of conditions were employed to activate the magnesium, however, even the best activated "Rieke magnesium"⁷⁹ only produced 10% conversion to the di-Grignard reagent. Dropwise addition of a 1:1 mixture of dibromide 68 and dimethyldichlorosilane to magnesium in THF afforded cyclic dimer 72 in 18% yield.



Scheme 10. First attempted synthesis of polymer 69.

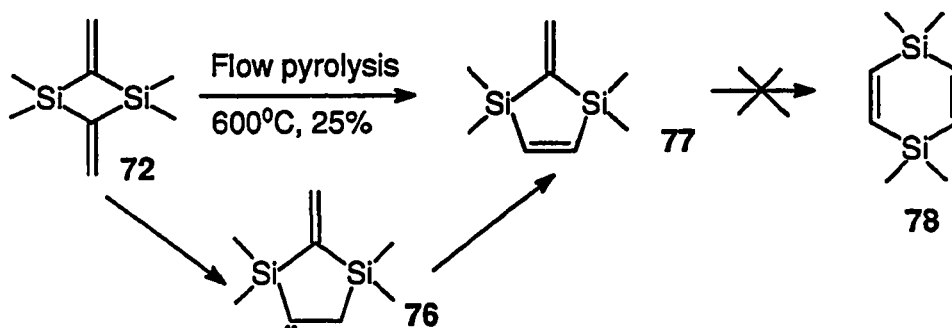


Scheme 11. Synthesis of vinylene silylene cyclics from a single precursor.

An alternative route employing a single precursor (**71**) also afforded cyclic products. Reaction of α -bromovinyl dimethylchlorosilane **71** which was obtained in 58.4% yield from vinyl dimethylchlorosilane **70** (Scheme 11)^{77, 78} with magnesium afforded cyclic dimer and trimer (**72** and **73**) with trace amounts of the cyclic tetramer and pentamer (**74** and **75**). No precipitate was observed when the product solution was dropped into methanol. While compound **75** was only characterized by GC-IR-MS, cyclics **72**, **73**, and **74** were isolated by preparative GC and fully characterized. The synthesis of these cyclics are reported for the first time here even though 2,4-bis(diphenylmethylene)-1,1,3,3-tetramethyl-1,3-disilacyclobutane from the dimerization of silaallene was reported earlier.⁸⁰

Thermal rearrangements of compound **72** and its all carbon analog.

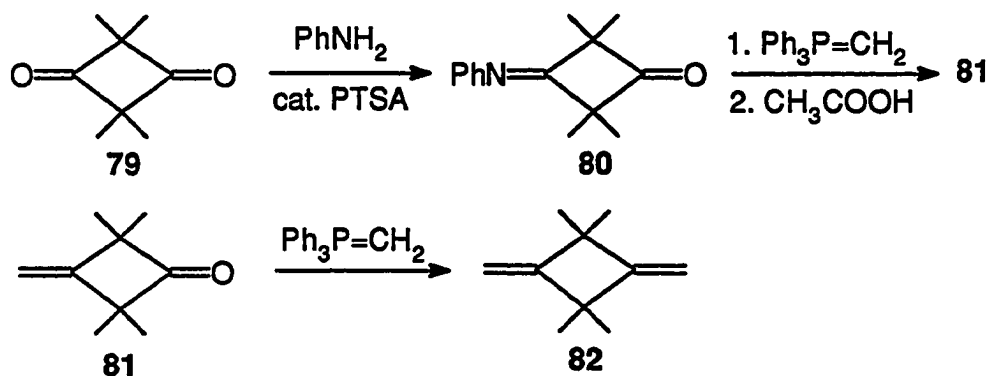
It is immediately realized that compound **72** is a good candidate to study the olefin to carbene isomerization without the possible complication of competition from the diradical process. When compound **72** was pyrolyzed in nitrogen flow at 600°C, 1,1,3,3-tetramethyl-2-methylene-1,3-disilacyclopentene **77** was obtained in 25% yield as the only product. Even at higher temperature, no cyclohexadiene **78**, which represents the ring expansion product from **77**, was observed. 1,1,3,3-Tetramethyl-1,3-disilacyclobutane, an analog of **72**, is thermally stable to much higher temperatures.⁸¹ The ring expansion of **72** can only be rationalized by vinylic silicon-carbon migration forming the carbene intermediate, **76** (Scheme 12).



Scheme 12. Thermal rearrangements of 1,1,3,3-tetramethyl-2,4-dimethylene-1,3-disilacyclobutane (**72**).

Thus, a kinetic investigation of the thermal isomerization of **72** to **77** was undertaken with use of a pulsed, stirred-flow reactor (SFR). Thermal isomerization of **72** was carried out over a temperature range of 520-600°C where the rate of formation of **77** was followed. Based on 23 rate determinations in this temperature range, the Arrhenius plot (Figure 6) gave the first-order rate constant for the formation of **77**. The plot showed that: $\log A$ (/sec) = 12.48 ± 0.33 , E_a (kcal/mol) = 54.09 ± 1.26 .

In order to answer the question of whether silicon is essential in generating carbenes from the carbon-carbon double bonds, the all carbon analog of compound **72**, **82**, was synthesized from tetramethyl-1,3-cyclobutanedione (**79**) according to literature procedures (Scheme 13).⁸²⁻⁸⁴ It is worth of pointing out that the direct reaction of compound **79** with Wittig reagents only leads to ring opening products.⁸⁵



Scheme 13. Synthesis of 1,1,3,3-tetramethyl-2,4-dimethylenecyclobutane (**82**).

When **82** was pyrolyzed under the same conditions, the decomposition of **82** started at 550°C but there was no isomerization observed up to 700°C.

Clearly and without question, two key factors contribute to the thermal olefin-to-carbene isomerization in these molecules: the ring strain energy and the superb migratory characteristics of silyl groups.^{86a} In order to gain insight into the difference in the thermal behavior of silicon and carbon analogs, we have performed the following theoretical study.

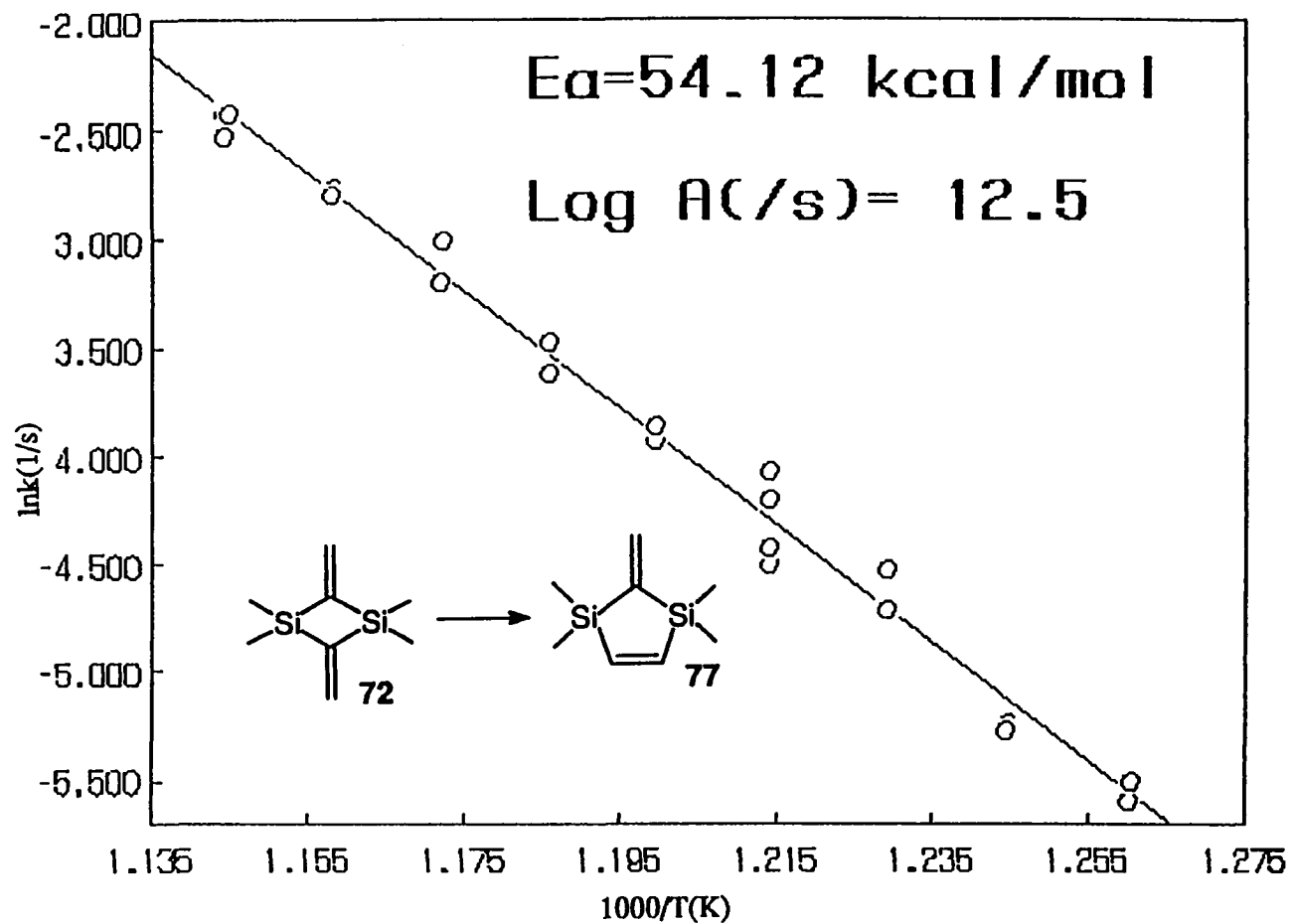
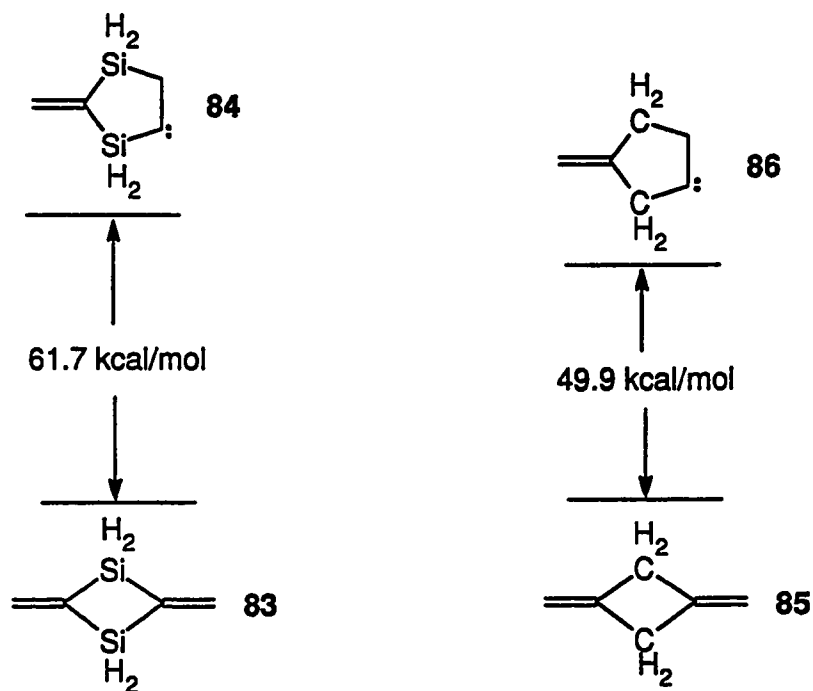


Figure 6. Arrhenius plot of the isomerization from 72 to 77.

Theoretical investigation of the thermal behavior of compounds 72 and 82.

We have observed the differences in thermal behavior between compounds 72 and 82 in our experimental studies. Are these differences due to energy differences between the two rings and their related carbenes? To answer this question, we have performed the following theoretical study on the parent Si- and C-ring systems (83 and 85).

First, the energy differences between the four membered ring starting materials and the five-membered ring carbene intermediates were calculated. The geometries were optimized at HF level with 6-31G(d) basis sets and the energies were calculated at the MP2 level with HF ZPE correction scaled by 0.89. The energy difference between the four membered-ring and the five-membered ring carbene was calculated to be 61.7 kcal/mol for the Si-ring system (83 and 84), 49.9 kcal/mol for the C-ring system (85 and 86) (Scheme 14). Based on the above calculations, the olefin to carbene isomerization should favor the C-ring system which is not observed experimentally!

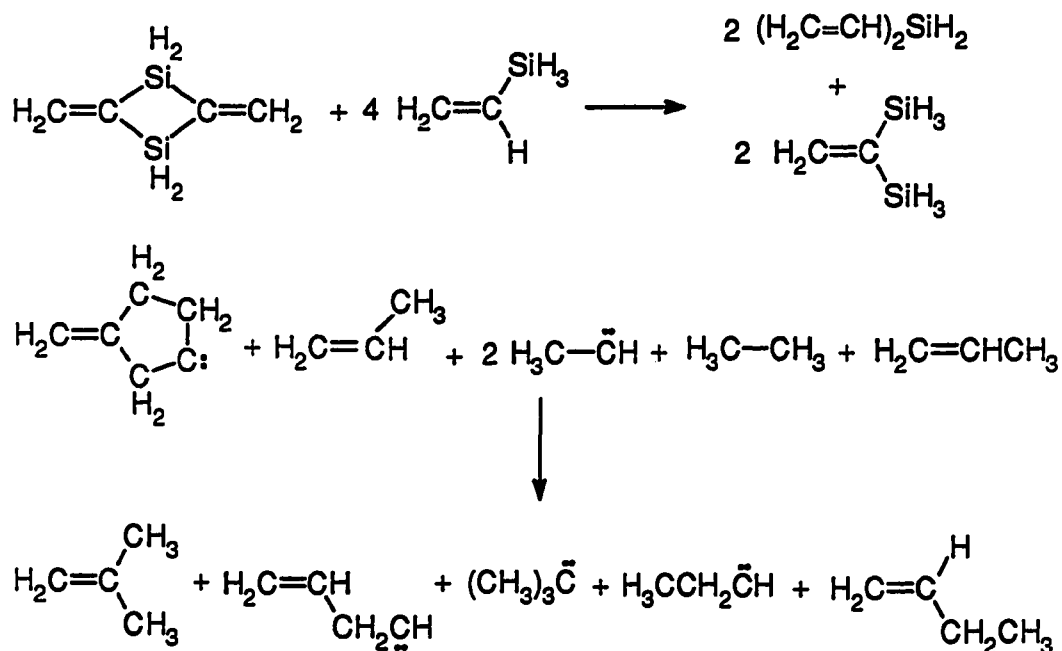


Scheme 14. Energy differences between the four-membered rings and carbene intermediates.

We know ring strain plays a very important role in these isomerization process.

Therefore, we calculated the ring strain energy differences in these two ring systems by using homodesmotic reactions in which the number of each group and type of bond is conserved.

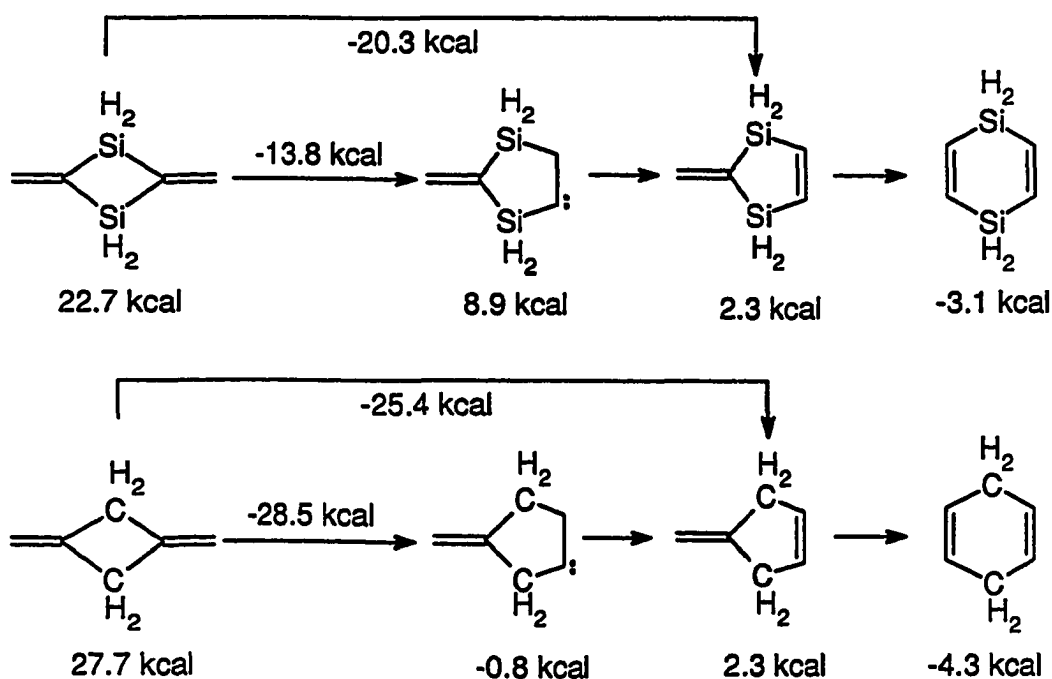
Two examples of homodesmotic reactions are shown in Scheme 15:



Scheme 15. Calculation of ring strains using homodesmotic reactions.

The geometries of all the ring systems were optimized at HF level with the 6-31G(d) basis sets and the energies were calculated at MP2 level with HF ZPE scaled by 0.89. The calculated ring strain energies for Si- and C-ring systems including the four-membered rings, five-membered ring carbene intermediates, cyclopentenes and cyclohexadienes are shown in Scheme 16. The relief in ring strain energy from four-membered ring to five-membered ring carbene is 13.8 kcal/mol for Si-ring system and 28.5 kcal/mol for C-ring system. The relief in ring strain energy from the four-membered ring to the product, cyclopentene, is 20.3 kcal/mol for the Si-system and 25.4 kcal/mol for the C-system. For either the four-membered rings to carbene intermediates or to ring expansion products, cyclopentenes, the experimentally unobserved ring expansion for the C-ring system should be favored! Also from these

calculations, we can see the driving force for further ring expansion from cyclopentene to cyclohexadiene is very small.



Scheme 16. Ring strain energies of Si- and C-ring systems.

Calculations of energy differences between the four-membered rings and carbene intermediates (Scheme 14) and relief in strain energies (Scheme 16) both predicted that the experimentally unobserved ring expansion process for the C-ring system should be favored. To explain this contradiction, calculations on the transition states and the carbene intermediates for this process were performed at MP2/6-31G(d)//HF/6-31G(d) + 0.89 ZPE (HF) level. The optimized geometries for carbene intermediates are shown in Figure 7. We can see the huge conformation difference between Si-ring carbene and C-ring carbene due to β -silicon effects.^{86b} The energy diagram for transition states and carbenes for these two ring-systems are shown in Figure 8 and the optimized geometries for the transition states are shown in Figure 9.

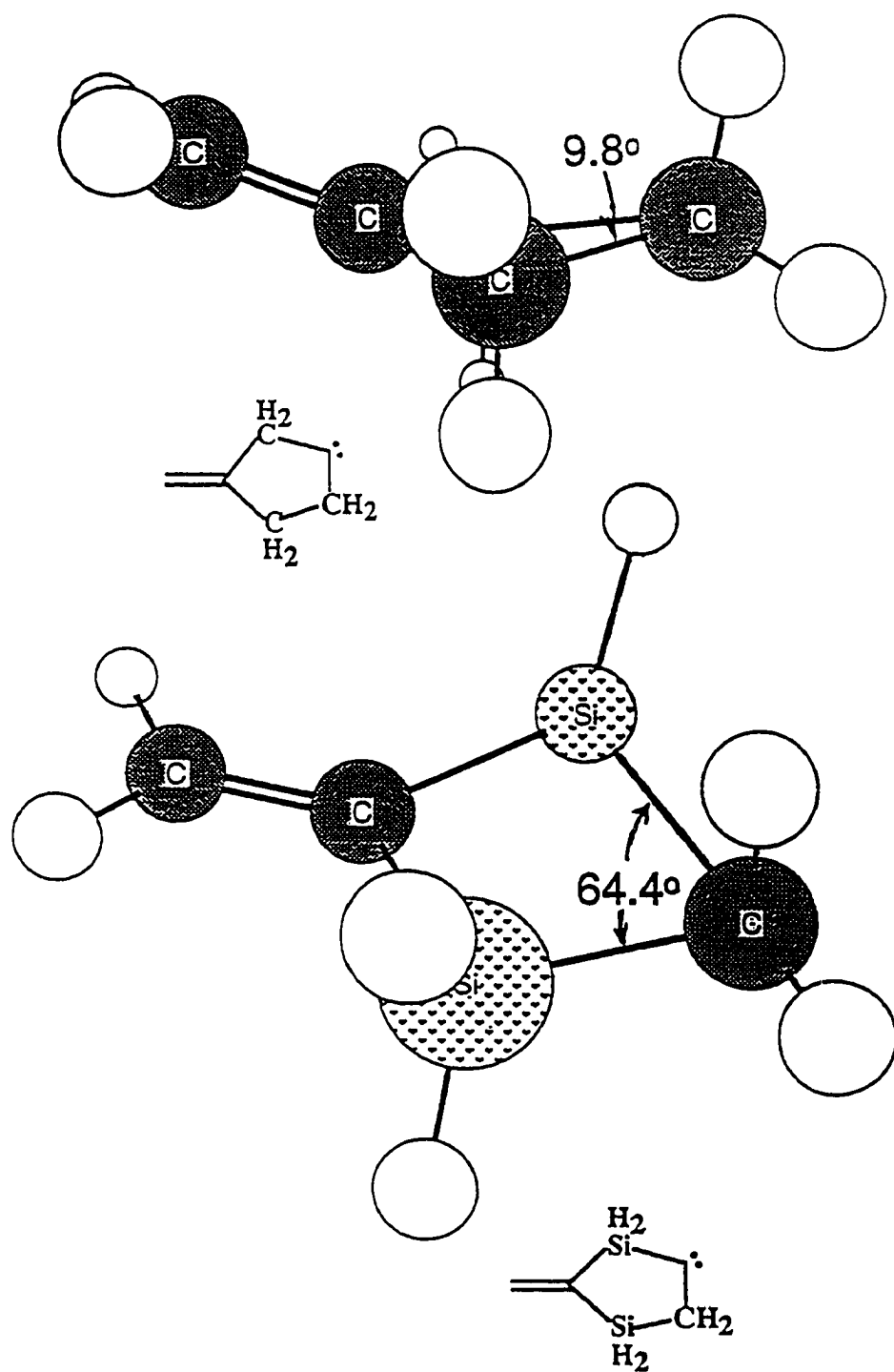


Figure 7. Optimized geometries for carbene intermediates.

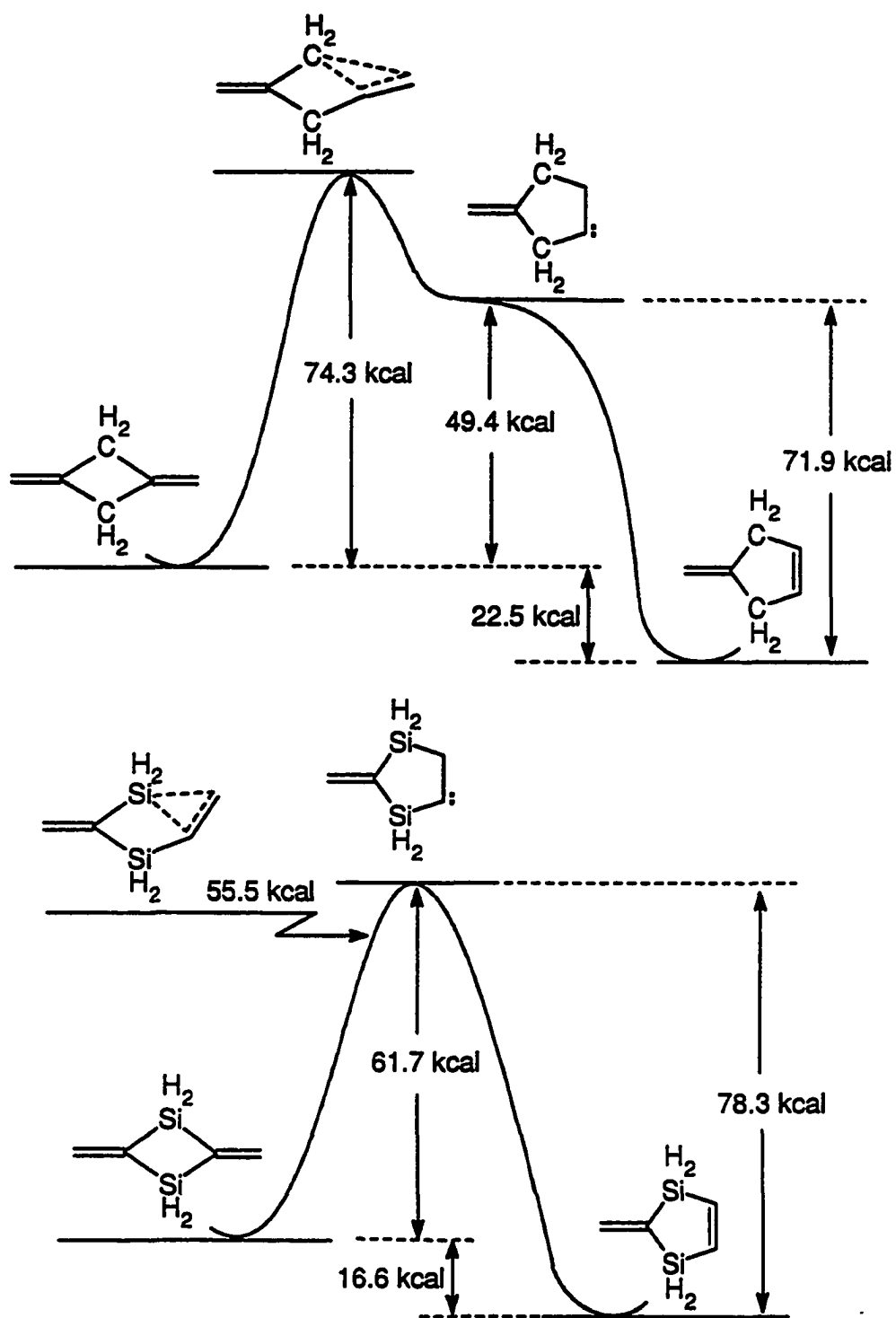


Figure 8. Energy diagram for thermal rearrangements from olefin to carbene.

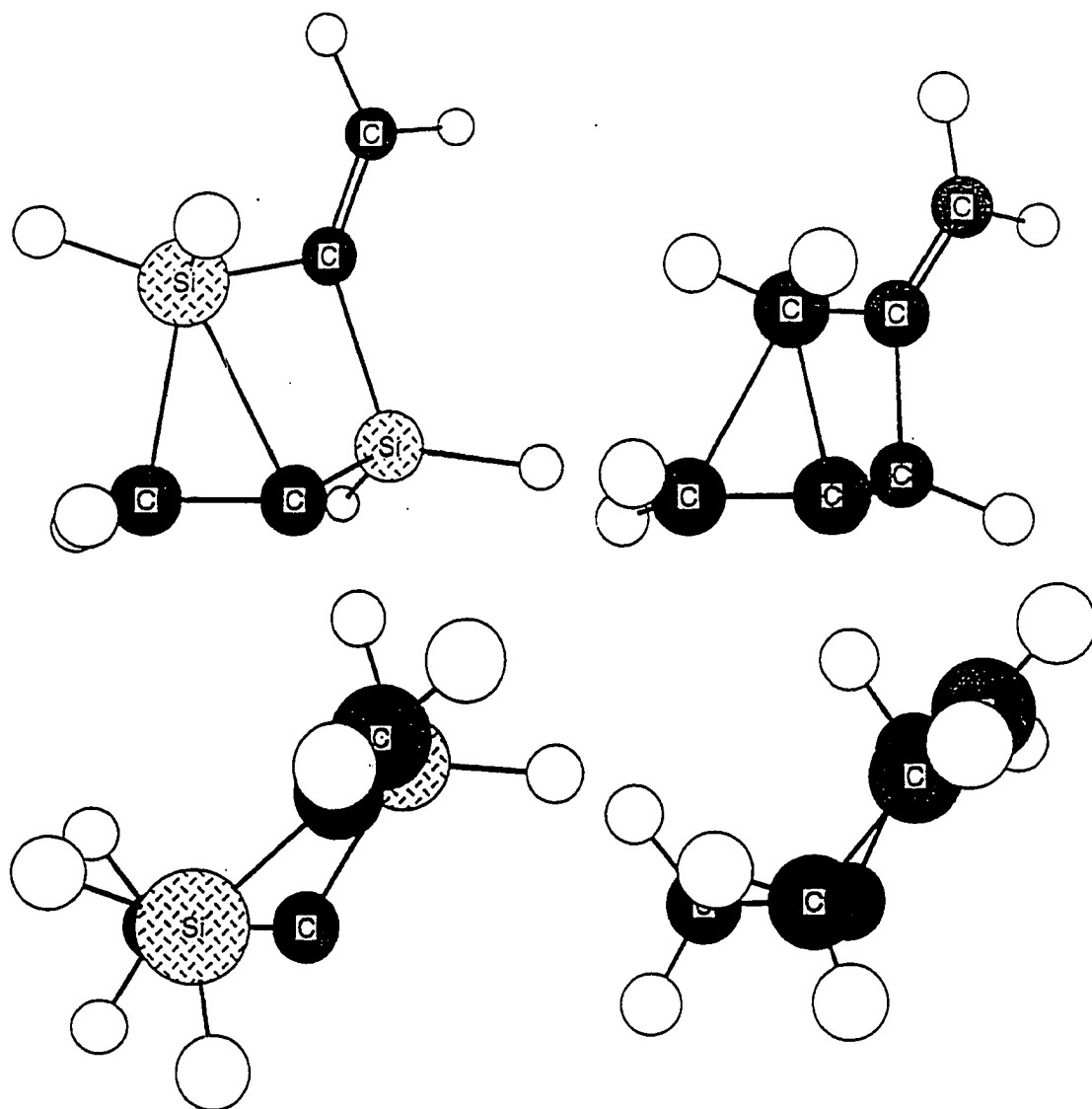


Figure 9. Optimized geometries for transition states.

From Figure 8, we can see that C-ring system has an early transition state. This can also be seen in Figure 9 where the transition state has a conformation very close to the starting four-membered ring. The calculated activation energy for olefin to carbene is 74.3 kcal/mol.

In contrast, the Si-ring system has a late transition state and the five-membered ring carbene is the actual transition state. The transition state has a conformation much closer to the five-membered ring product (Figure 9). Different from the C-ring system, the calculated activation energy (which is the energy difference between the four-membered ring and the five-membered ring carbene) is 61.7 kcal/mol.

To understand the olefin-to-carbene process better, we have also looked at model compounds. First the α -substituent effect on relative energies was studied. As we can see from Table I, for H migration on an olefin to form a carbene, as the calculation level becomes higher, the carbene is essentially the same in energy as the transition state for α -H, the carbene is about 2 kcal/mol higher in energy than the transition state for α -silyl, and finally the carbene is about 5 kcal/mol lower in energy than the transition state for α -methyl. This means there will be no barrier for the carbene-to-olefin process for α -H and α -silyl, but there will be \sim 5 kcal/mol barrier for carbene-to-olefin process for α -methyl.

Next, the migrating effect on relative energies was studied. As we can see from Table II, as the calculation level becomes higher, the energy for carbene is the same as the transition state for H-migration, \sim 5 kcal/mol higher than the transition state for silyl migration, and \sim 6 kcal/mol lower than the transition state for methyl migrating. There is no barrier for H or silyl migration from a carbene to form an olefin where a significant barrier for methyl migration from a carbene to form an olefin exists. The optimized geometries for methyl and silyl migration transition states in Figure 10 shows a late transition state for silyl migration and an early transition state for methyl migration.

Table I. α -substituent effect on relative energies (kcal/mol).

$\begin{array}{c} \text{H} \\ \\ \text{HC}=\text{CH}_2 \end{array} \longrightarrow \begin{array}{c} \text{H} \\ \diagup \quad \diagdown \\ \text{HC} \cdots \text{CH}_2 \end{array} \longrightarrow \begin{array}{c} \text{H} \\ \\ \text{H}\ddot{\text{C}}-\text{CH}_2 \end{array}$		
HF/6-31(d)	79.0	66.2
MP2/6-31G(d)	79.6	80.3
MP4/6-311G(d,p)	75.0	74.9
<hr/>		
$\begin{array}{c} \text{H} \\ \\ \text{C}=\text{CH}_2 \\ \\ \text{H}_3\text{Si} \end{array} \longrightarrow \begin{array}{c} \text{H} \\ \diagup \quad \diagdown \\ \text{C} \cdots \text{CH}_2 \\ \\ \text{H}_3\text{Si} \end{array} \longrightarrow \begin{array}{c} \text{H} \\ \\ \text{H}_3\text{Si}-\ddot{\text{C}}-\text{CH}_2 \end{array}$		
HF/6-31(d)	84.5	74.0
MP2/6-31G(d)	77.8	81.8
MP4/6-311G(d,p)	74.9	76.9
<hr/>		
$\begin{array}{c} \text{H} \\ \\ \text{C}=\text{CH}_2 \\ \\ \text{H}_3\text{C} \end{array} \longrightarrow \begin{array}{c} \text{H} \\ \diagup \quad \diagdown \\ \text{C} \cdots \text{CH}_2 \\ \\ \text{H}_3\text{C} \end{array} \longrightarrow \begin{array}{c} \text{H} \\ \\ \text{H}_3\text{C}-\ddot{\text{C}}-\text{CH}_2 \end{array}$		
HF/6-31(d)	78.8	60.4
MP2/6-31G(d)	77.8	72.8
MP4/6-311G(d,p)	72.8	67.7

Table II. Migrating group effect on relative energies (kcal/mol).

$\begin{array}{c} \text{H} \\ \\ \text{HC}=\text{CH}_2 \end{array} \longrightarrow \begin{array}{c} \text{H} \\ \diagup \quad \diagdown \\ \text{HC} \cdots \text{CH}_2 \end{array} \longrightarrow \begin{array}{c} \text{H} \\ \\ \text{H}\ddot{\text{C}}-\text{CH}_2 \end{array}$		
HF/6-31(d)	79.0	66.2
MP2/6-31G(d)	79.6	80.3
MP4/6-311G(d,p)	75.0	74.9
<hr/>		
$\begin{array}{c} \text{H}_3\text{Si} \\ \\ \text{HC}=\text{CH}_2 \end{array} \longrightarrow \begin{array}{c} \text{H}_3 \\ \\ \text{Si} \\ \diagup \quad \diagdown \\ \text{HC} \cdots \text{CH}_2 \end{array} \longrightarrow \begin{array}{c} \text{SiH}_3 \\ \\ \text{H}\ddot{\text{C}}-\text{CH}_2 \end{array}$		
HF/6-31(d)	74.1	68.5
MP2/6-31G(d)	68.5	71.1
MP4/6-311G(d,p)	63.4	68.1
<hr/>		
$\begin{array}{c} \text{H}_3\text{C} \\ \\ \text{HC}=\text{CH}_2 \end{array} \longrightarrow \begin{array}{c} \text{H}_3 \\ \\ \text{C} \\ \diagup \quad \diagdown \\ \text{HC} \cdots \text{CH}_2 \end{array} \longrightarrow \begin{array}{c} \text{CH}_3 \\ \\ \text{H}\ddot{\text{C}}-\text{CH}_2 \end{array}$		
HF/6-31(d)	91.3	70.7
MP2/6-31G(d)	88.6	84.8
MP4/6-311G(d,p)	84.9	78.8

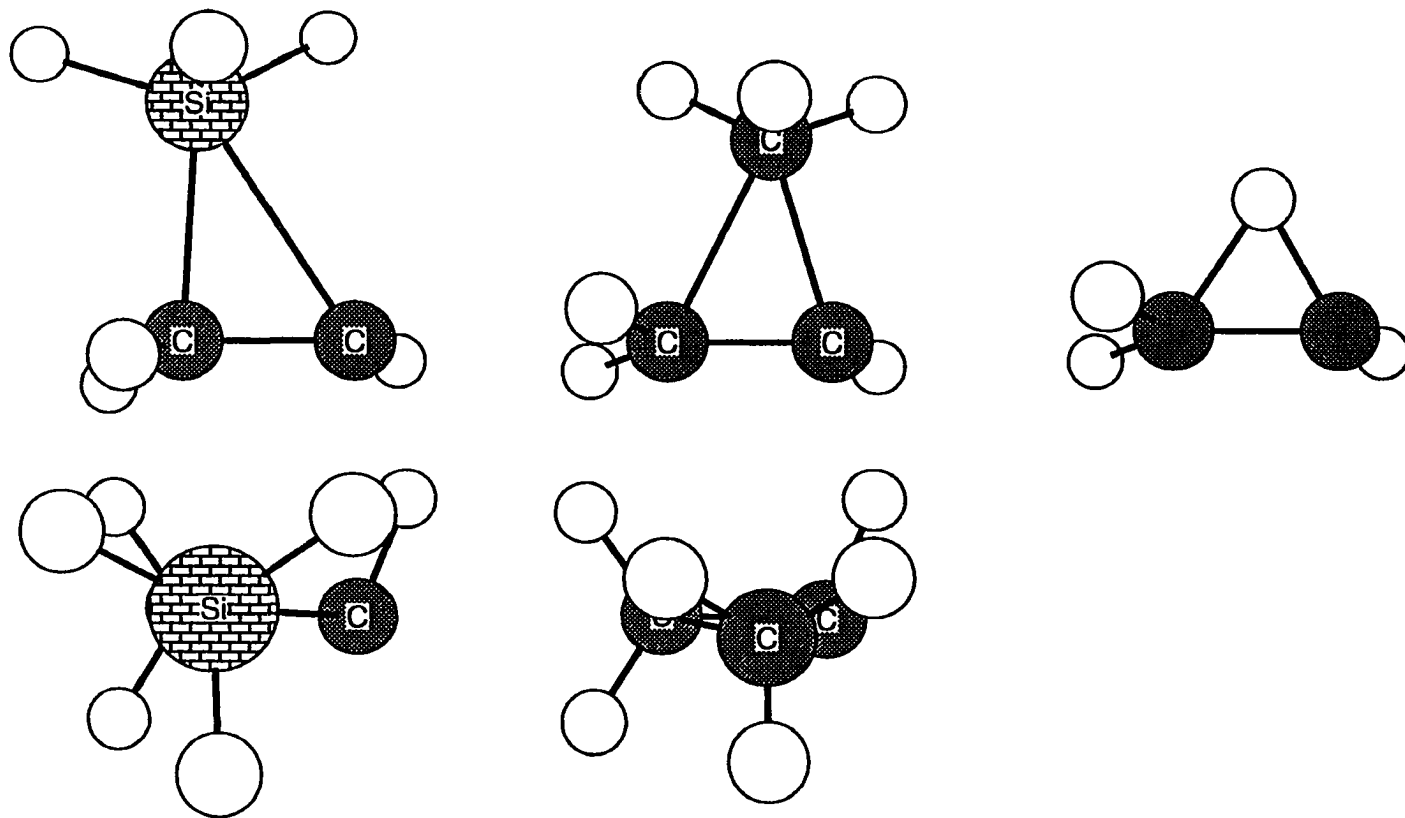
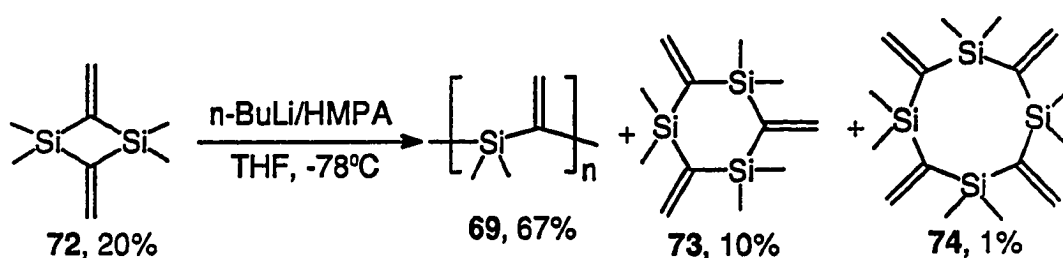


Figure 10. Optimized geometries for transition states for silyl, methyl, and hydrogen migration.

Anionic ring opening polymerization of compound 72.

Anionic ring opening polymerizations of silacyclobutane and silacyclobutene have been reported.^{60, 63-65} Following similar literature procedures,⁶³⁻⁶⁵ the anionic polymerization of dimer **72** catalyzed by *n*-butyllithium and HMPA in THF at -78°C produced poly(dimethylsilylene vinylene) **69** with an α,α -isomer structure in 67% yield. However, when the polymers formed were precipitated from methanol, cyclization products **73** and **74** were found in the methanol solution in ~10% and ~1% respectively. About 20% of unpolymerized **72** was also observed (Scheme 17).



Scheme 17. Anionic ring opening polymerization of compound **72**.

The mechanism for polymerization is shown in Scheme 18. The first step is compound **72** reacting with *n*-butyllithium to form a pentacoordinate silicon anion. Ring opening of this intermediate forms a vinylic anion which is stabilized by α -silyl. The vinylic anion reacts with another monomer **72** to form a new pentacoordinate silicon anion which is followed by ring opening to form a vinylic anion. As these processes were repeated, linear polymers with vinylic anions as end groups were formed. The formation of compounds **73** and **74** and unreacted **72** is explained by “back-biting” which competes with the linear propagation process. Similar behavior was observed by Weber⁸⁷ in the anionic ring opening polymerization of silacyclopentenes.

The molecular weight (by GPC) of the silylene-vinylene polymer **69** was: $M_w = 1.74 \times 10^4$, PDI = 2.46. Polymer **69** was also characterized by NMR (¹H, ¹³C, ²⁹Si), DSC, and TGA (Figure 11-15). While NMR spectra shows a very clean polymer formed, polymer **69** has a DSC diagram with two endothermic peaks at 54°C and 94°C. TGA shows that the thermal

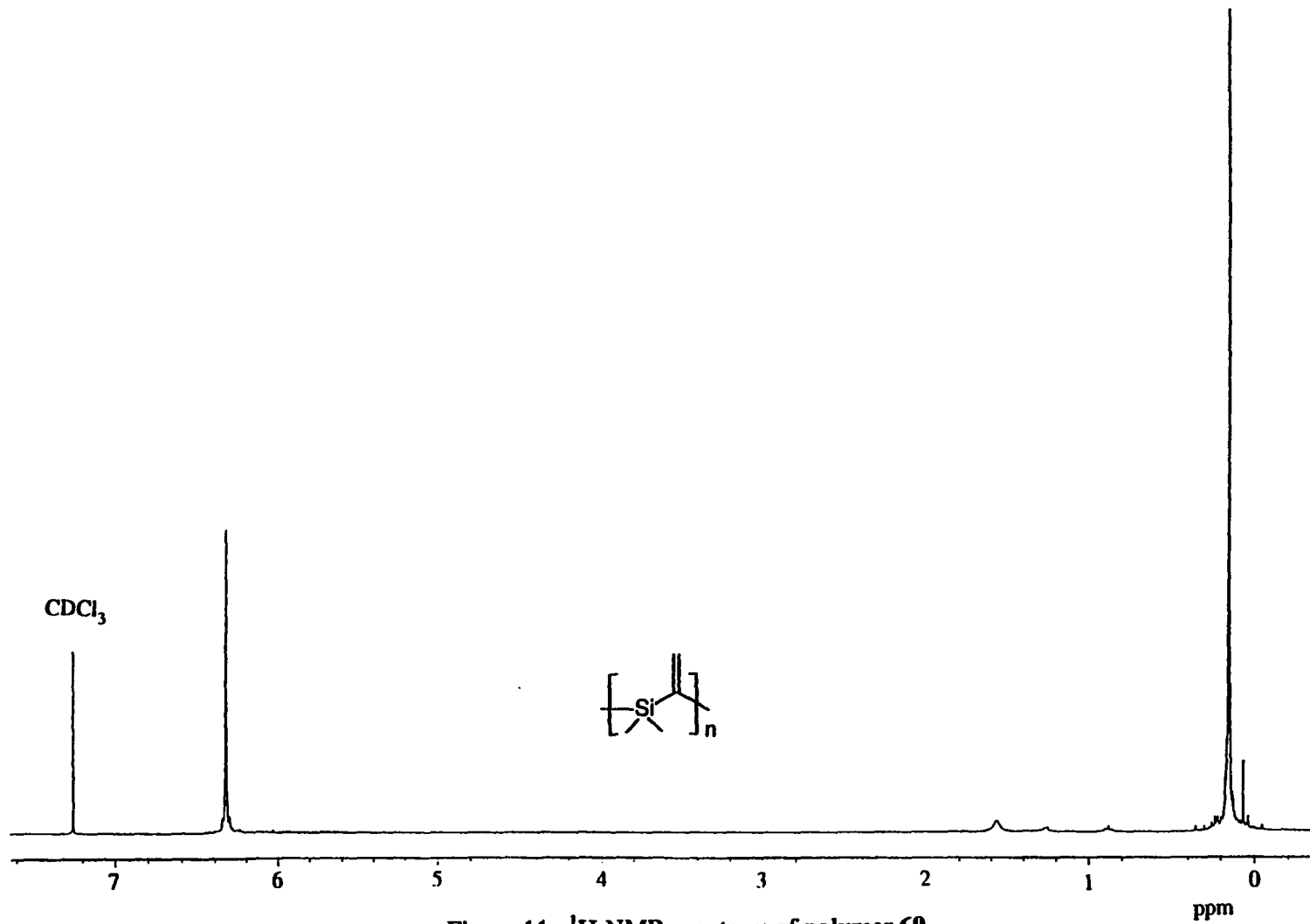


Figure 11. ¹H-NMR spectrum of polymer 69.

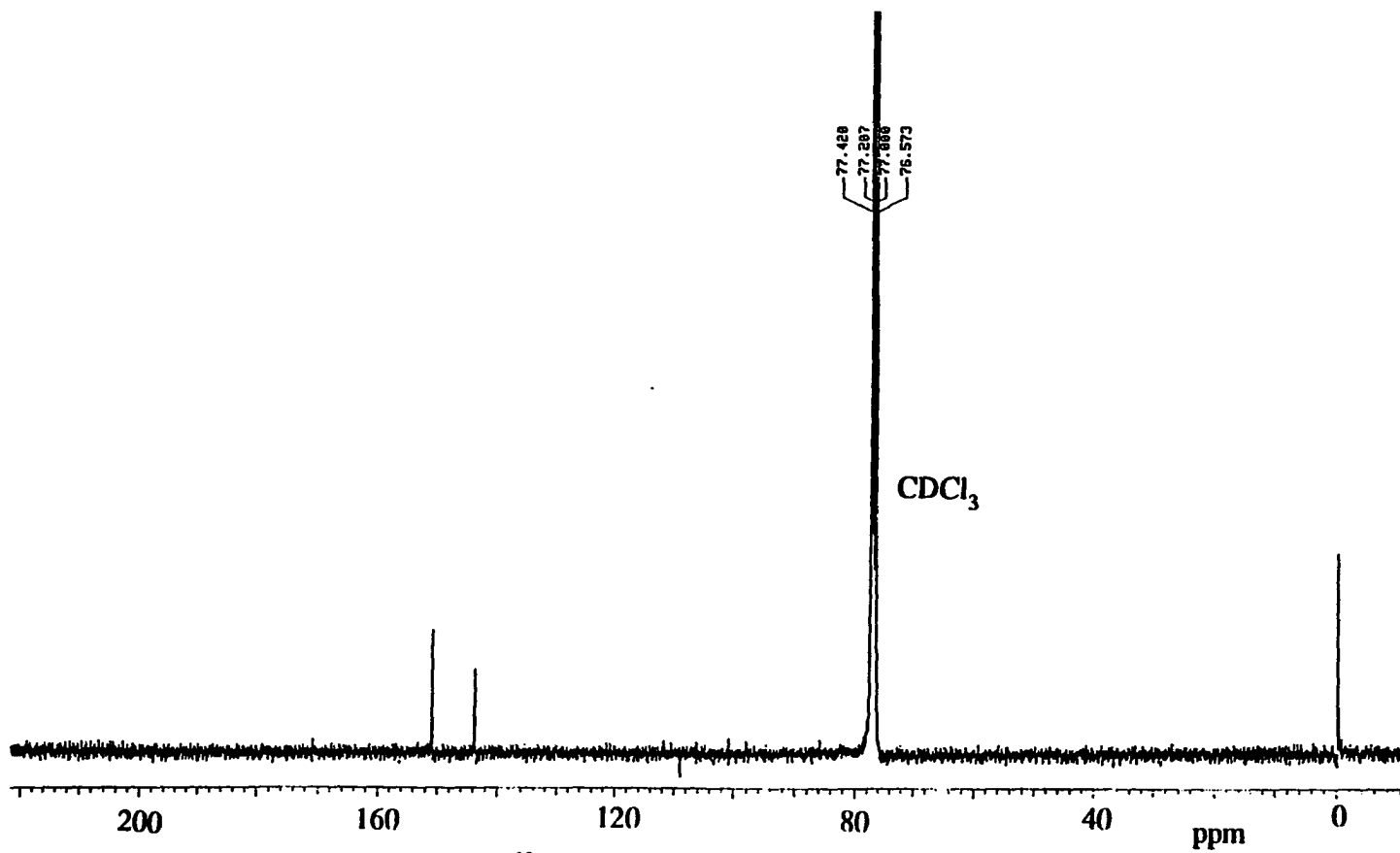


Figure 12. ^{13}C -NMR spectrum of polymer 69.

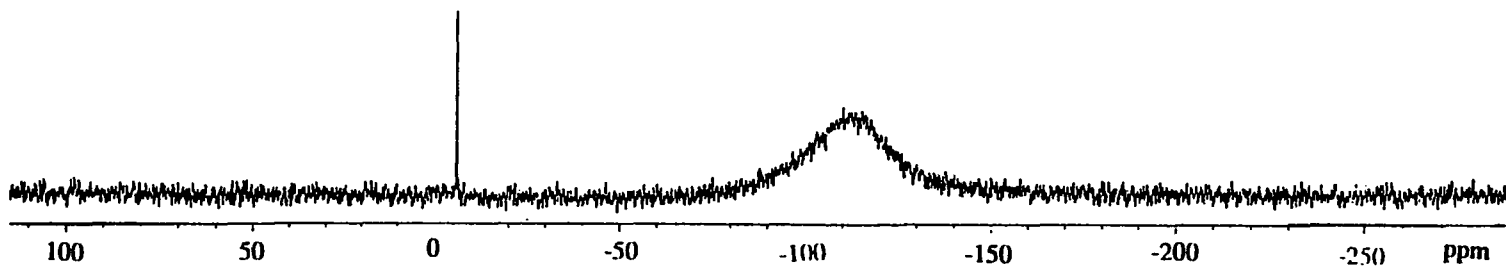


Figure 13. ^{29}Si -NMR spectrum of polymer 69.

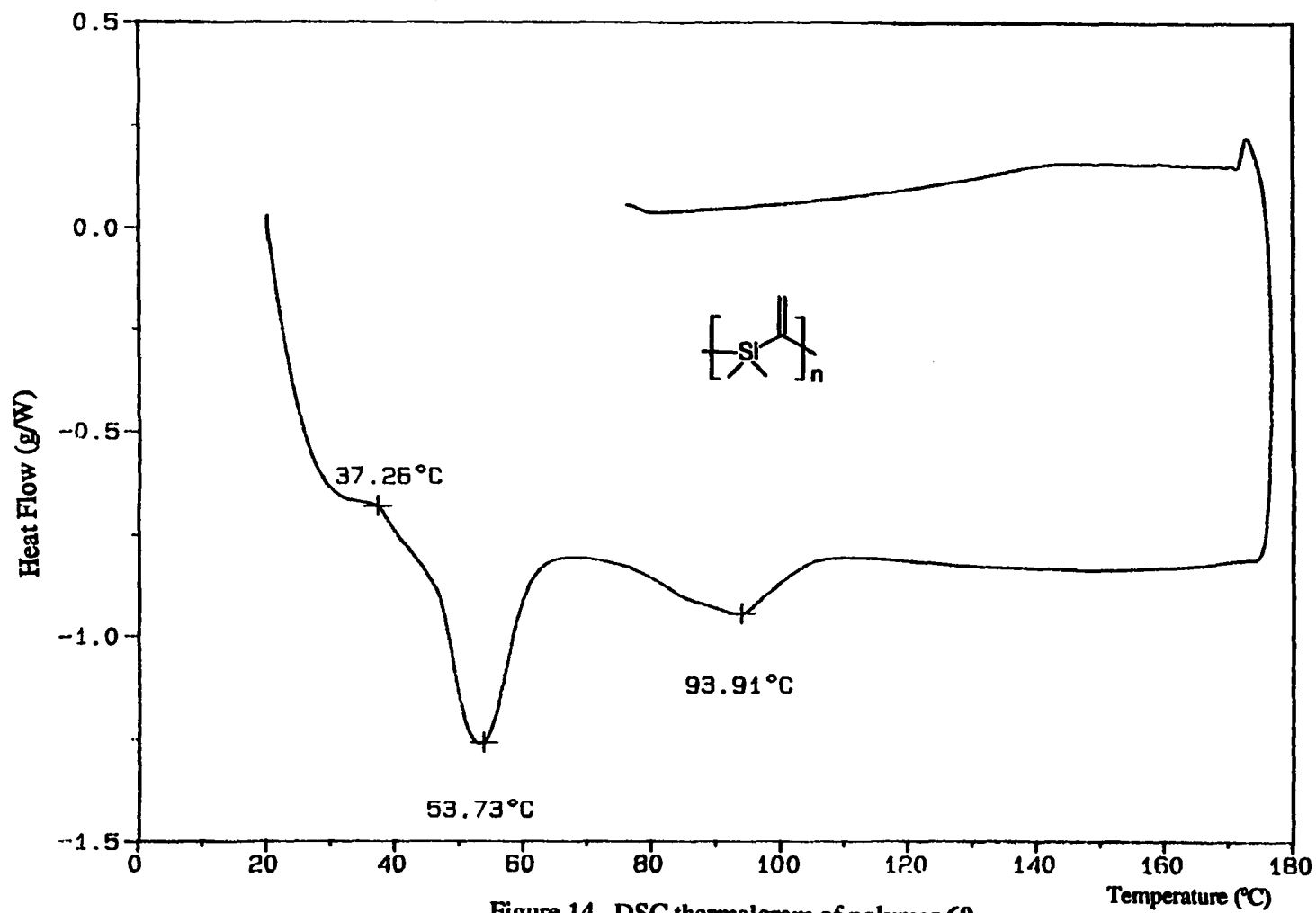
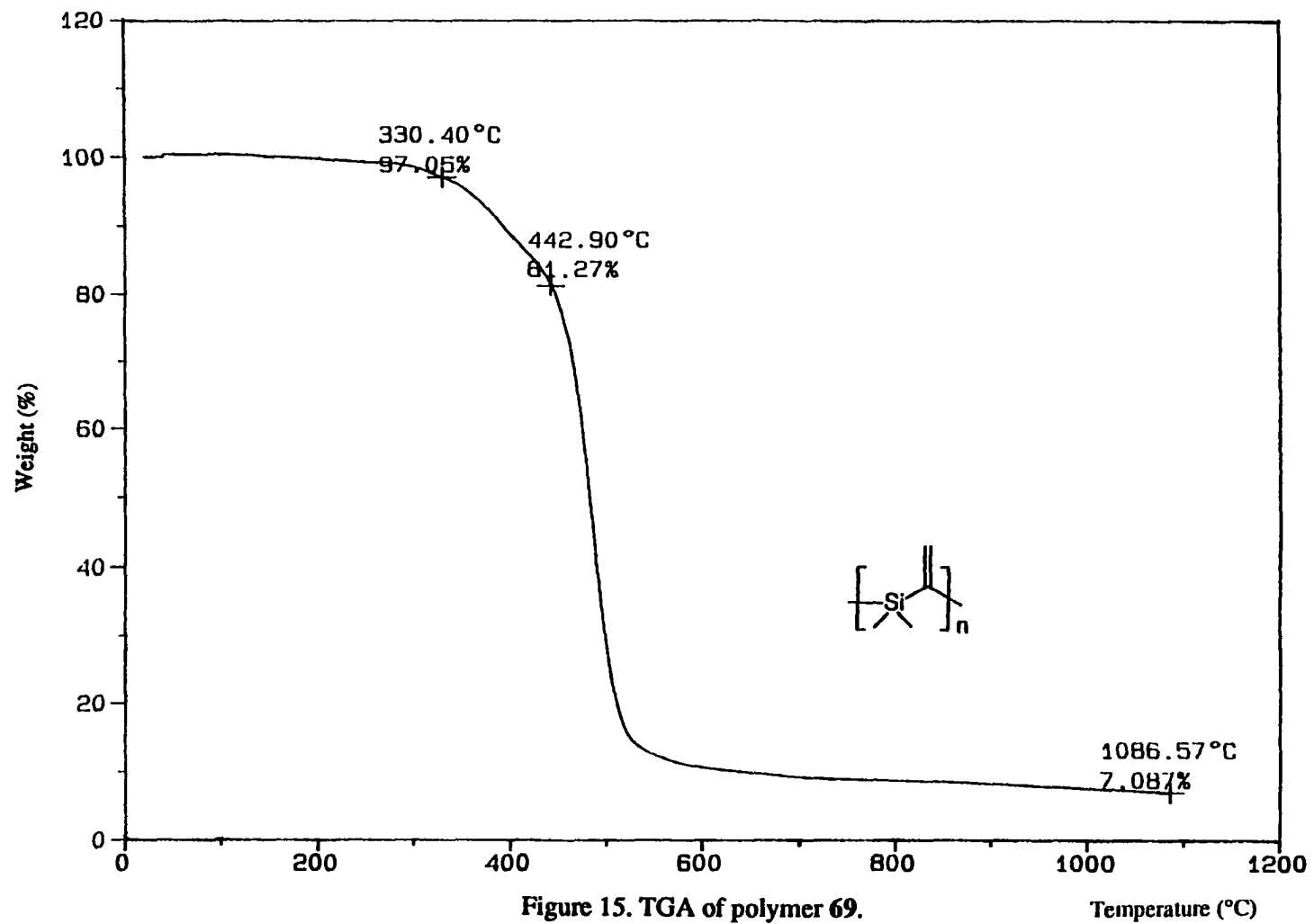
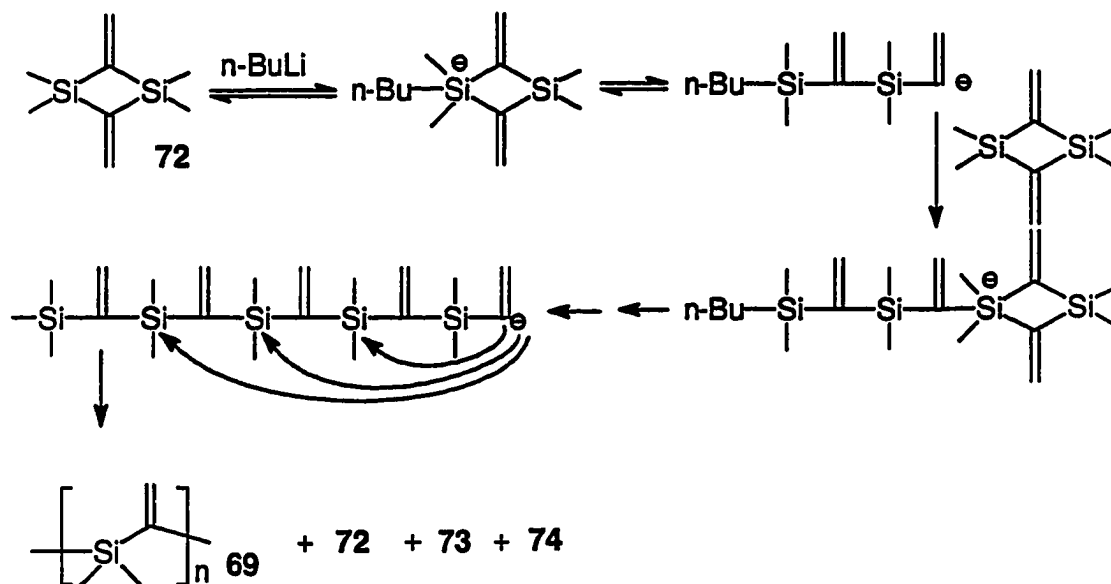


Figure 14. DSC thermalgram of polymer 69.



degradation of polymer **69** starts at ca. 330°C and the maximum rates of decomposition are between 440°C and 500°C with very low char yield (7%).



Scheme 18. Mechanism for the anionic ring opening polymerization of **72**.

Ring opening polymerization of compound **72** catalyzed by CPA.

Ring opening polymerization of silacyclobutane catalyzed by chloroplatinic acid (CPA) has been reported.⁶² Ring opening polymerization of **72** by catalytic CPA gave only a trace amount of polymer **69** while the dimer of **72**, **74**, was produced in 70% yield. The X-ray structure of dimer **9** is shown in Figure 16. The distance between 2,4-vinyls is 3.52 Å. The facile $\pi 2 + \pi 2 + \pi 2$ cycloaddition reaction of the all carbon analog of **74** with TCNE⁸⁸ was not observed even under refluxing when compound **74** was mixed with TCNE. This is presumably because of the larger separation of the vinylene groups in the silicon system.

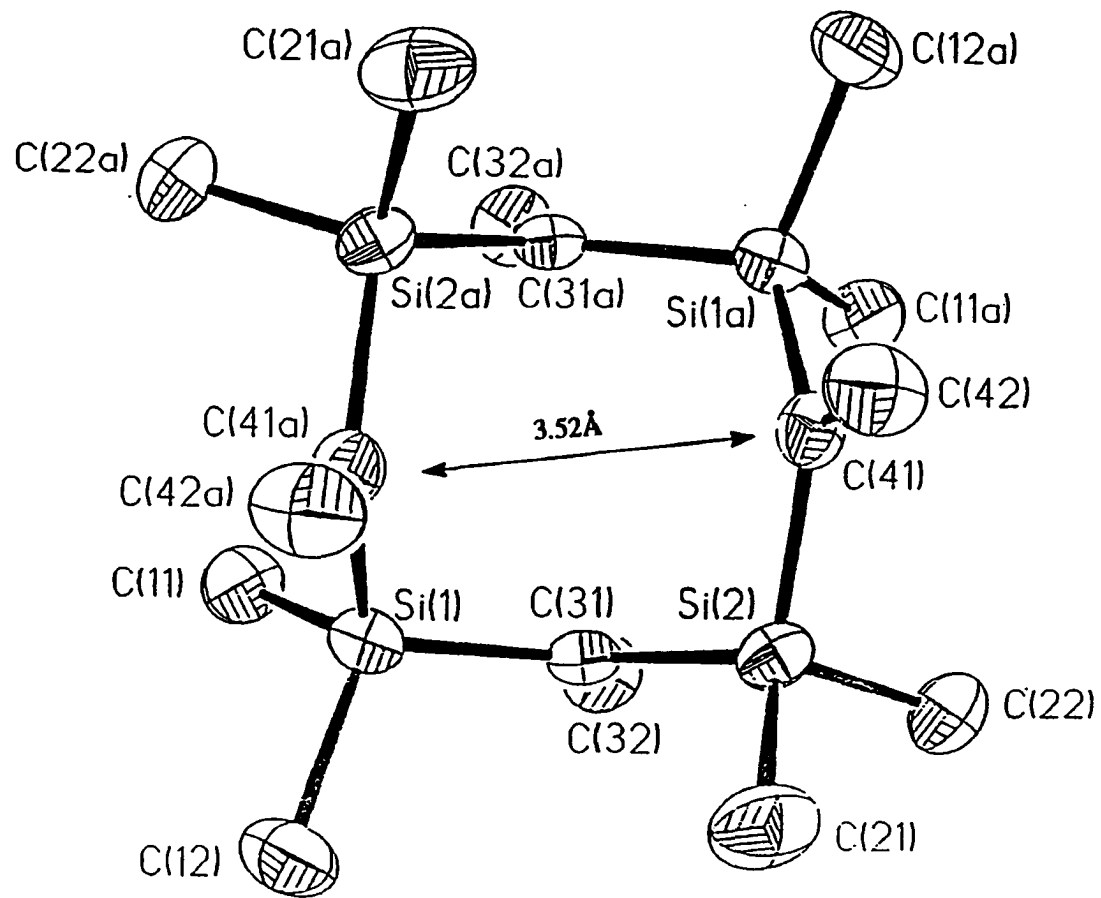


Figure 16. ORTP drawing of compound 74.

Electronic structures of silylene and vinylene cyclics and polymers.

The UV absorption spectra of compounds **72**, **73**, **74**, polymer **69**, and some model compounds are listed in Table III. Only when there are at least two silicon atoms attached to the olefin is $\lambda_{\max 2}$ observed.⁸⁹ While $\lambda_{\max 1}$ clearly corresponds to π to π^* absorption, analogs $\lambda_{\max 2}$ can be explained by π to σ^* absorption.^{90,91} Compared to the linear analogs or larger cyclics, compound **72** has ~25 nm bathochromic shift for the first band (π to π^*) and ~50 nm bathochromic shift for the second band (π to σ^*). A similar bathochromic shift for the carbon analog of **72**, **82**, (11 nm for the π to π^* absorption) is also observed. The significant bathochromic shift of compound **72** and **82** compared to their linear analogs and larger cyclics undoubtedly originates from their significant ring strains.

Table III. UV-absorption of silylene and vinylene cyclics, polymer, and related compounds.

Alkenes	$\lambda_{\max 1}$ (nm)	ϵ_1 ($\times 10^{-4}$)	$\lambda_{\max 2}$ (nm)	ϵ_2
72	212	2.85	298	330
73	197	1.69	250	1070
74	197	1.99	246	856
polymer 69	198	0.39	245	125
$\text{Me}_3\text{Si}-\text{CH}=\text{CH}_2$	194	0.19	-----	-----
$\text{Me}_3\text{Si}-\text{C}(\text{CH}_3)=\text{CH}_2$	194	0.37	-----	-----
$(\text{Me}_3\text{Si})_2-\text{C}=\text{CH}_2$	196	0.63	236	300
$(\text{CH}_3)_2-\text{C}=\text{CH}_2$ ⁹²	184	1.00	-----	-----
82	195	0.16	-----	-----

Conclusions

The thermal rearrangements of 1,1-dimethyl-2-methylene-1-silacyclobutane were reexamined and the kinetics for the rearrangements were studied. It was found by deuterium labeling experiments that the equilibrium between the diradical and the starting material happens before the isomerization to the carbene. However, the diradical does not go on to give decomposition products. A kinetic study found that for the diradical process: $E_a = 50.9$ kcal/mol, $\log A$ (1/s) = 13.6. It was also found that for the carbene process: $E_a = 47.5$ kcal/mol, $\log A$ (1/s) = 11.3.

1,1,3,3-tetramethyl-2,4-dimethylene-1,3-disilacyclobutane and the analogous larger cyclics were synthesized for the first time. It was found that this compound isomerizes to 1,1,3,3-tetramethyl-2-methylene-1,3-disilacyclopentene thermally with Arrhenius parameters $E_a = 54.12$ kcal/mol, $\log A$ (1/s) = 12.5. The same isomerization process was not observed in thermolysis of the carbon analog of the four-membered ring. Theoretical calculations of the transition states gave satisfactory explanations for the difference in thermal behavior between the Si- and C-analogs.^{94a}

Anionic ring opening polymerization of 1,1,3,3-tetramethyl-2,4-dimethylene-1,3-disilacyclobutane gives poly(silylene vinylene) with an α,α -isomeric structure as the major product. The polymer was characterized by NMR, DSC, and TGA. Ring opening polymerization of this four-membered ring catalyzed by CPA gives mainly a eight-membered ring, the dimer of the four-membered ring.^{94b}

Experimental

^1H and ^{13}C -NMR spectra were acquired on a Varian VXR-300 spectrometer. In order to assure the quantitative features of the ^{13}C -NMR and ^{29}Si -NMR spectra, the relaxation agent chromium(III) acetylacetonate was used in CDCl_3 with relaxation delay of 5 seconds. TMS was used as the external standard for ^{29}Si -NMR. Preparative GC separations were performed on a Varian Model 920 instrument and a Vorex PSGC model. Flash vacuum pyrolysis (FVP) was carried out by slow distillation of compounds through a heated, seasoned, horizontal quartz pyrolysis tube (16 mm i.d., 200 mm long) packed with quartz chips; product was collected in a trap cooled with liquid N_2 . Pressures were measured by an ion gauge placed behind the liquid N_2 trap and were typically an order of magnitude lower than in the reaction zone. The stirred flow reactor (SFR) system uses He flow to sweep the material through the reactor into a Varian 6000 GC (FID) and has the option of diverting the separated products into a VG SC-300 quadrupole mass spectrometer for mass analysis. Routine mass and IR spectra were obtained on a Hewlett Packard 5970 GC-IR-MS spectrometer. Flow pyrolysis experiments were performed by dripping the starting material into a vertical quartz tube packed with quartz chips under argon flow. The pyrolysate was collected in a trap at -78°C . ^2H -NMR was collected at 46 MHz using a 63° pulse with 4032 data points and a 1000 Hz spectral width. Field stability was obtained using a ^1H lock.

Polymer molecular weights were determined by gel permeation chromatography (GPC) with 6 Microstyragel columns in series of 500 Å, 2×10^3 Å, 2×10^4 Å, 2×10^5 Å. THF was used as eluent at a flow rate of 1 mL/min. The system was calibrated by polystyrene standards. GPC analyses were performed on a Perkin-Elmer series 601 LC equipped with Beckman solvent delivery system, a Walter Associate R401 refractive index detector and a Viscotek viscometer. Differential scanning calorimetry (DSC) analyses were performed on a Du Pont 910 Differential Scanning Calorimeter. Thermogravimetric analysis (TGA) was performed on a Du Pont 951 TGA under helium. UV spectra were obtained on a Hewlett Packard 8452A UV-VIS spectrometer.

The solvents were distilled from lithium aluminum hydride right before use. Other reagents were commercially available and were used as received.

FVP Example. In a typical FVP, a known quantity of a compound (100-500 mg) is slowly distilled off through the pyrolysis tube at 400-800°C (5×10^{-4} Torr) and is collected in a trap cooled by liquid N₂. After addition of an n-decane as an internal standard to the collected products, the products are characterized by GC-IR-MS and NMR.

Synthesis of 3-bromo-3-buten-1-ol (64)⁷². Hydrogen bromide gas was produced by adding PBr₃ (10.46 mL, 110 mmol) dropwise to water (5.94 mL, 330 mmol). The HBr produced was bubbled through tetraethylammonium bromide (63.00 g, 300 mmol) in 300 mL methylene chloride at 0°C. After the bubbling was finished, the methylene chloride solution was weighed and it was found that 20.25 g of HBr (250 mmol) was absorbed by the Et₄NBr solution. 3-Butyn-1-ol (63, 18.90 mL, 120 mmol) was then injected into the above solution. The reaction mixture was sealed and heated at 40°C for 5 hours.

After cooling the reaction mixture to 0°C, ether (600 mL) was added. The precipitate of Et₄NBr was filtered out and 28.39 g of compound 64 (75% yield) was obtained by vacuum distillation (b.p. 69-70°C/11mmHg). GCMS *m/z* 152(21, M+2), 150(21, M), 122(97), 120(100), 53(17); GC-FTIR $\nu(\text{cm}^{-1})$ 3662(m, OH), 2948(s), 1626(s), 1387(m), 1125(s), 1048(vs), 891(s); ¹H-NMR (300 MHz, CDCl₃) δ 2.27(s, 1H), 2.64(triple doublet, *J*₁ = 6 Hz, *J*₂ = 0.9 Hz, 2H), 3.78(t, *J* = 6 Hz, 2H), 5.51(d, *J* = 1.8 Hz, 1H), 5.68(m, 1H).

Synthesis of 1,3-dibromo-3-butene (65). A 100 mL round bottom flask equipped with an addition funnel and magnetic stirrer was charged with compound 64 (28.39 g, 188 mmol). The flask was cooled to -10°C by a salt/ice bath. 5.70 mL of PBr₃ was added dropwise. After the PBr₃ addition, the reaction mixture was raised to room temperature and stirred overnight. The reaction mixture was then distilled (b.p. 72-73°C/18 mmHg) to a round bottom flask with 10 mL water in it. The product was washed twice with cooled

concentrated sulfuric acid and dried over potassium carbonate. Vacuum distillation gave 26.42 g of compound **26** (69% yield). GCMS m/z 216(9, M+4), 214(17, M+2), 212(9, M), 135(52), 133(55), 53(100); GC-FTIR $\nu(\text{cm}^{-1})$ 3110(w), 2980(m), 1627(s), 1432(m), 1315(m), 1277(m), 1177(vs), 1102(m), 895(vs), 819(w); $^1\text{H-NMR}$ (300 MHz, CDCl_3) δ 2.94(t, $J = 6.9$ Hz, 2H), 3.55(t, $J = 6.9$ Hz, 2H), 5.56(d, $J = 1.8$ Hz, 1H), 5.71(d, $J = 1.8$ Hz, 1H); $^{13}\text{C-NMR}$ (75.429 MHz, CDCl_3) δ 29.50(1C), 43.87(1C), 119.35(1C), 129.73(1C).

Synthesis of 1,1-dimethyl-2-methylene-1-silacyclobutane (29). A 250 mL 2-neck round bottom flask equipped with addition funnel, condenser and magnetic stirrer was charged with magnesium (1.02 g, 42 mmol) and 80 mL dry THF. 1,2-Dibromoethane (0.2 mL) was added to the reaction mixture to activate the magnesium. The mixture of compound **65** (2.23 g, 10.4 mmol), dimethyldichlorosilane (1.26 mL, 10.4 mmol) and THF (10 mL) was added dropwise to the above reaction mixture to keep the reaction under a mild reflux. The reaction was then refluxed for another hour. After cooling to room temperature, the reaction mixture was poured into a cold mixture of 300 mL pentane and 50 mL 2.0 M hydrochloric acid. Most of the THF was washed away by repetitive washing with acidic water. After drying over sodium sulfate, most of the pentane was removed by distillation over a 30 cm long fractionating column. Compound **29** synthesized according to this route was contaminated by compound **30** (**29** : **30** = 8 : 1) presumably because *Z*-1,4-dibromo-1-butene is a minor product in the synthesis of compound **65**. 0.29 g of compound **4** (25% yield) was obtained after purification by preparative GC with Varex PSGC 10-40 model with 6 feet long column (3/8" i.d.) packed with 20% SE-30-CW packing materials. For compound **29**: GCMS m/z 113(1.2, M+1), 112(12, M), 97(57, M-Me), 85(12), 84(100), 83(12), 72(23), 71(14), 69(14), 59(17), 58(69), 53(12); GC-FTIR $\nu(\text{cm}^{-1})$ 3045(m), 2963(s), 2914(s), 1832(w), 1415(m), 1256(s), 913(s), 862(vs), 814(s); $^1\text{H-NMR}$ (300 MHz, CDCl_3) δ 0.32(s, 6H), 0.99(t, $J = 8.7$ Hz, 2H), 2.74(m, 2H), 5.19(double triplet, $J_1 = 6.0$ Hz, $J_2 = 2.1$ Hz, 1H), 5.42(q, $J = 2.1$ Hz, 1H); $^{13}\text{C-NMR}$ (75.429 MHz, CDCl_3) δ -0.81(2C), 10.19(1C), 31.95(1C), 118.24(1C), 158.50(1C). (NMR

spectral data are different from Conlin's because these are obtained from a CDCl_3 solution and Conlin's are from a neat sample).

For compound 30: GCMS m/z 113(1.7, M+1), 112(14, M), 98(10), 97(100), 95(28), 71(8), 69(9), 58(8), 53(6); GC-FTIR $\nu(\text{cm}^{-1})$ 2957(s), 2911(s), 1566(m), 1445(w), 1322(w), 1258(s), 1139(w), 1097(w), 979(w), 848(vs), 794(s). The NMR spectral data was obtained by subtracting that of compound 29 from the spectra of the mixture of compounds 29 and 30. $^1\text{H-NMR}$ (300 MHz, CDCl_3) δ 0.15(s, 6H), 0.70(t, $J = 6.9$ Hz, 2H), 2.48(m, 2H), 5.93(double triplet, $J_1 = 9.9$ Hz, $J_2 = 2.1$ Hz, 1H), 6.79(double triplet, $J_1 = 10.2$ Hz, $J_2 = 2.7$ Hz, 1H); $^{13}\text{C-NMR}$ (75.429 MHz, CDCl_3) δ -1.29(2C), 8.29(1C), 31.64(1C), 129.90(1C), 152.71(1C).

For compound 31: GCMS m/z 113(3.5, M+1), 112(31, M), 98(10), 97(100), 95(26), 71(11), 59(11), 58(24); GC-FTIR $\nu(\text{cm}^{-1})$ 3028(s), 2916(m), 2904(s), 1605(w), 1405(w), 1260(m), 1100(s), 944(w), 846(vs); $^1\text{H-NMR}$ (300 MHz, CDCl_3) δ 0.17(s, 6H), 1.27(d, $J = 1.2$ Hz, 4H), 5.85 (t, $J = 1.2$ Hz, 2H).

Synthesis of compound 29(D). The OH group was changed to the OD group first. 3-Butyn-1-ol (20.0 mL, 263 mmol) and D_2O (23.75 mL, 1.315 mol) were charged into a 100 mL round bottom flask equipped with magnetic stirrer and septum. The mixture was stirred at room temperature for 5 hours. Methylene chloride (50 mL) was added to extract the product. The aqueous layer was extracted by another two portions of methylene chloride (25 mL). The combined methylene chloride layer was dried over sodium sulfate and used directly for the next step.

Instead of H_2O , D_2O was used to react with PBr_3 to give DBr to combine with Et_3NBr . The procedure from this point is exactly the same as that for the synthesis of compound 29. According to both $^1\text{H-NMR}$ and $^2\text{H-NMR}$, in compound 29(D) synthesized, deuterium is present in the two different positions in 2-methylene group at ca. one-to-one ratio.

Synthesis of bis(α -bromovinyl)dimethylsilane (68). An oven-dried 100 mL, three-necked round bottom flask, equipped with mechanical stirrer and addition funnel was charged with dimethyldivinylsilane (4.89 g, 40 mmol) under argon flow. After the flask was cooled to -78°C by a dry-ice/isopropanol mixture, bromine (4.10 mL, 80 mmol) was added dropwise under vigorous stirring. After the addition was finished, the reaction mixture was stirred for another 10 minutes and the red color of bromine almost disappeared completely. Diethylamine (17.0 mL, 165 mmol) was then added cautiously. After this addition, the reaction was raised to room temperature and stirred for another 5 hours. The salts precipitated out were filtered and washed with ether. The filtrate was washed with dilute HCl acid three times, water twice, and then dried over sodium sulfate. Vacuum distillation gave 3.88 g (39% yield) compound 68 (b. p. 56-58°C/10 mmHg). GCMS *m/z* 257(7), 255(13), 253(6, M-Me), 231(9), 229(18), 227(9), 205(48), 203(100), 201(49), 139(74), 137(74), 109(25), 107(18), 53(22), 52(85); GC-FTIR $\nu(\text{cm}^{-1})$ 3081(w), 2974(w), 2911(w), 1839(w), 1592(w), 1396(m), 1326(w), 1261(s), 1088(w), 918(s), 835(vs), 789(s); $^1\text{H-NMR}$ (300 MHz, CDCl_3) δ 0.40(s, 6H), 6.37(d, $J = 2.1$ Hz, 2H), 6.44(d, $J = 1.8$ Hz, 2H); $^{13}\text{C-NMR}$ (75.429 MHz, CDCl_3) δ -4.08(2C), 132.59(2C), 132.72(2C).

Reaction of compound 68 and dichlorodimethylsilane with magnesium. An oven-dried 50 mL three-neck round bottom flask equipped with a magnetic stirrer, condenser and septum was charged with magnesium (0.292 g, 12 mmol) and dry THF (10 mL). Dibromoethane (0.1 mL) was added to activate the magnesium. After the reaction started, a mixture of compound 68 (1.4 g, 5 mmol) and of dichlorodimethylsilane (0.645 g, 5 mmol) in THF (5 mL) was added dropwise to keep the reaction solution refluxing. The reaction was refluxed for another 3 hours after the addition. Then the reaction mixture was poured into a cooled mixture of 20 mL hexanes and 20 mL of 2.0 M HCl. The organic layer was washed with dilute HCl one more time, and then washed with water twice and dried over sodium sulfate. One drop of the product solution was dropped into methanol, no precipitate was observed which indicates that no polymeric products with significant molecular weights were formed. According to GC,

GC-MS, the reaction is not clean and compound **72** accounts for the ~18% yield (calculated against the internal standard).

Synthesis of α -bromovinyl dimethylchlorosilane (71**).** An oven-dried 250 mL three-neck round bottom flask equipped with a mechanical stirrer, addition funnel and septum was charged with vinyl dimethylchlorosilane (13.4 mL, 100 mmol) under slow argon flow. After cooling the flask to -78°C , Br_2 (5.6 mL, 108 mmol) was added dropwise under mechanical stirring. After the addition, the reaction mixture was warmed up to room temperature for 15 minutes. Then it was cooled to 0°C by an ice bath and triethylamine (93 mL, 600 mmol) was added cautiously. The reaction mixture was stirred for another 2 hours at room temperature after the addition. The salts formed were filtered out under an argon atmosphere and were washed twice by anhydrous ether. 11.65 g of compound **71** (yield 58.4%) was distilled out from the filtrate (b.p. $64\text{--}65^{\circ}\text{C}/35$ mmHg). GCMS m/z 202(9.0, M+4), 200(32, M+2), 198(23, M), 185(35), 183(25), 161(27), 159(100), 157(73), 95(14), 93(39), 65(19), 63(30); GC-FTIR $\nu(\text{cm}^{-1})$ 2979(w), 1594(w), 1400(m), 1264(s), 922(s), 827(vs); $^1\text{H-NMR}$ (300 MHz, CDCl_3) δ 0.56(s, 6H), 6.38(d, $J = 1.8$ Hz, 1H), 6.47 (d, $J = 2.1$ Hz, 1H); $^{13}\text{C-NMR}$ (75.429 MHz, CDCl_3) δ 0.43(2C), 131.8 (1C), 131.9(1C).

Synthesis of compounds **72, **73**, and **74**.** An oven-dried 50 mL three-necked round bottom flask equipped with a magnetic stirrer, condenser and septum was charged with magnesium (0.292 g, 12 mmol). After stirring under argon flow for half an hour, Dry THF(10 mL) was injected. Dibromoethane (0.1 mL) was added to activate the magnesium. After the reaction started, compound **71** (2.06 g, 10.3 mmol) was added dropwise to keep the reaction solution under reflux. The reaction was refluxed for another 3 hours after the addition. Then the reaction mixture was poured to cooled mixture of 20 mL hexanes and 20 mL 2.0 M HCl acid. The organic layer was washed with dilute HCl acid one more time, then washed with water twice and dried over sodium sulfate. One drop of the product solution was dropped in methanol; there was no precipitate observed indicating that no polymeric products with

significant molecular weights were formed. The solvents were removed by distillation over a ca. 30 cm long column. According to analytical GC, the cyclization oligomers yields were obtained in different experiments: compound **72** 66-71%, compound **73** 20-21%, compound **74** 1-1.5%, compound **75** 0-1.5%. These products were separated by preparative-GC on a 9 foot long column (1/8" i.d.) packed with 20% SE-30-CW packing materials.

Characterization of compound 72. GCMS m/z 169(19, M+1), 168(100, M), 154(17), 153 (95, M-Me), 127(23), 125(15), 113(18), 83(33), 73(25), 59(19); HRMS calculated for $C_8H_{16}Si_2$ m/z 168.07908, measured m/z 168.0789 (Kratos MS 50); GC-FTIR $\nu(\text{cm}^{-1})$ 3000(w), 2935(w), 1601(w), 1426(w), 1250(m), 1118(w), 960(w), 840(vs), 791(s); $^1\text{H-NMR}$ (300 MHz, CDCl_3) δ 0.24(s, 12H), 6.37(s, 4H); $^{13}\text{C-NMR}$ (75.429 MHz, CDCl_3) δ -1.12(4C), 137.95(2C, with 2H attached), 161.69 (2C, with no H attached); $^{29}\text{Si-NMR}$ (59.591 MHz, CDCl_3) δ -6.85; UV (nm, hexanes) $\lambda_{\text{max}}(\epsilon)$ 212(2.85×10^4), 298(330).

Characterization of compound 73. GCMS m/z 253(1.9, M+1), 252(6.9, M), 239(13), 238(27), 237(100, M-Me), 73(13); HRMS calculated for $C_{12}H_{24}Si_3$ m/z 252.1186, measured m/z 252.1189 (Kratos MS 50); GC-FTIR $\nu(\text{cm}^{-1})$ 3009(w), 2963(w), 2932(w), 1572(vw), 1416(w), 1255(m), 1145(w), 962(w), 847(s), 787(m); $^1\text{H-NMR}$ (300 MHz, CDCl_3) δ 0.16(s, 18H), 6.33(s, 6H); $^{13}\text{C-NMR}$ (75.429 MHz, CDCl_3) δ -2.34(6C), 138.94(3C), 153.32(3C); $^{29}\text{Si-NMR}$ (59.591 MHz, CDCl_3) δ -9.04; UV (nm, hexanes) $\lambda_{\text{max}}(\epsilon)$ 197(1.69×10^4), 250(1070).

Characterization of compound 74. mp 159-160°C. GCMS m/z 338(13, M+2), 337(22, M+1), 336(64, M), 323(18), 322(33), 321(95, M-Me), 277(25), 265(11), 264(30), 263(93), 262(45), 261(26), 249(18), 248(31), 247(73), 237(17), 235(16), 234(13), 233(53), 223(17), 189(13), 83(22), 73(100), 53(26); HRMS calculated for $C_{16}H_{32}Si_4$ m/z 336.15812, measured m/z 336.15835 (Kratos MS 50); GC-FTIR $\nu(\text{cm}^{-1})$ 3001(w), 2960(w), 2933(w), 1612(w), 1433(w), 1256(m), 961(w), 926(w), 841(vs); $^1\text{H-NMR}$ (300 MHz, CDCl_3) δ 0.12(s, 24H),

6.30(s, 8H); ^{13}C -NMR (75.429 MHz, CDCl_3) δ -2.10(8C), 140.54(2C), 152.00(2C); ^{29}Si -NMR (59.591 MHz, CDCl_3) δ -7.61; UV (nm, hexanes) $\lambda_{\text{max}}(\epsilon)$ 197(1.99 x 10⁴), 245(856).

Characterization of compound 75. GCMS m/z 421(13, M+1), 420(30, M), 405(10, M-Me), 348(17), 347(44), 331(13), 317(14), 273(14), 261(13), 247(19), 237(17), 225(11), 213(11), 212(12), 211(11), 199(13), 198(20), 197(83), 83(17), 73(100), 59(24); GC-FTIR $\nu(\text{cm}^{-1})$ 2958(m), 2932(m), 1612(w), 1431(w), 1255(m), 985(m), 959(m), 922(m), 837(s), 787(s).

Characterization of compound 77. GCMS m/z 170(3, M+2), 169(6.2, M+1), 168(35, M), 154(17), 153(100, M-Me), 127(20), 113(11), 83(16), 73(16), 59(17); GC-FTIR $\nu(\text{cm}^{-1})$ 2996(m), 2960(m), 1598(w), 1441(w), 1308(w), 1255(m), 1132(w), 960(w), 845(vs), 794(s). NMR spectra are from the subtraction of compound 72 from the spectra of pyrolysate. ^1H -NMR (300 MHz, CDCl_3) δ 0.15(s, 12H), 6.43(s, 2H), 7.14 (s, 2H); ^{13}C -NMR (75.429 MHz, CDCl_3) δ -1.88(4C), 137.98(1C), 152.12(1C), 154.36 (2C); ^{29}Si -NMR (59.591 MHz, CDCl_3) δ -4.03.

Synthesis of Compound 82.⁹³ Based on the literature procedure⁸²⁻⁸⁴, an oven-dried 100 mL round bottom flask equipped with a magnetic stirrer and Dean-Stark trap, 2,2,4,4-tetramethylcyclobutane-1,3-dione (14.0g, 100 mmol), aniline (9.18 mL, 100 mmol) were charged with *p*-toluenesulfonic acid monohydrate (0.125 g) and of benzene (50 mL). The mixture was stirred under reflux for 6 hours while the water formed was removed by azeotropic distillation. After removal of benzene at atmospheric pressure, the products were separated by vacuum distillation. 12.9 g of 2,2,4,4-tetramethyl-3-phenyliminocyclobutanone (80, 60% yield) was obtained (b.p. 100°C/1mmHg). GCMS m/z 216(2, M+1), 215(13, M), 146(12), 145(100), 144(31), 130(31), 104(11), 77(30); GC-FTIR $\nu(\text{cm}^{-1})$ 3075(w), 2975(s), 2935(m), 2876(w), 1808(m), 1308(w), 1697(vs), 1595(m), 1486(m), 1462(m), 1370(w), 1266(w), 1049(m), 897(w), 837(w).

An oven-dried 500 mL two-neck round bottom flask equipped with a magnetic stirrer, addition funnel and argon flow system was charged with potassium *tert*-butoxide (8.96 g, 80 mmol), *tert*-butanol (50 mL), and dry ether (200 mL). After the potassium *tert*-butoxide was dissolved, methyltriphenylphosphonium bromide (28.56 g, 80 mmol) was added at once and stirred at room temperature for one hour before compound **80** (8.56 g, 40 mmol) was added to the yellow mixture. The reaction was stirred overnight. After filtration to remove the triphenylphosphine oxide, the filtrate was diluted with water and the water layer was extracted by ether (40 mL x 2). Ether was removed by rotary evaporation from the combined organic layer. Characterization of 2,2,4,4-tetramethyl-3-phenylimino-1-methylenecyclobutane: GCMS *m/z* 214(5, M+1), 213(33, M), 198 (33, M-Me), 145 (55), 144(27), 130(26), 118(26), 117(100), 104(27), 95(60), 81(14), 77(67), 67(26), 55(12), 53(15); GC-FTIR $\nu(\text{cm}^{-1})$ 3072(m), 2971(vs), 2931(s), 2873(m), 1781(w), 1724(s), 1657(s), 1594(m), 1485(m), 1367(w), 1222(m), 1170(w), 1113(w), 1028(m), 888(m).

The crude imine was stirred and refluxed with 100 mL 50% acetic acid for about one hour. Then the reaction was cooled, quenched by sodium bicarbonate and extracted by ether for three times. After extraction, the combined ether layer was washed with dilute HCl acid, sodium bicarbonate solution and saturated sodium chloride solution, then dried over sodium sulfate. Ether was removed by rotary evaporation and 3.31 g of 2,2,4,4-tetramethyl-3-methylene-cyclobutanone (**81** 60% yield) was obtained. GCMS *m/z* 138(1.5, M), 110 (76, M-CO), 95(100), 70(26), 67(85), 55(29), 53(28); GC-FTIR $\nu(\text{cm}^{-1})$ 3071(w), 2972(s), 2876(m), 1805(vs), 1673(m), 1457(m), 999(m), 892(m).

An oven-dried 100 mL two-neck round bottom flask equipped with a magnetic stirrer, addition funnel and argon flow system was charged with potassium *tert*-butoxide (2.24 g, 20 mmol), *tert*-butanol (12 mL) and dry ether (50 mL). After the potassium *tert*-butoxide was dissolved, methyltriphenylphosphonium bromide (7.14 g, 20 mmol) was added at once and stirred at room temperature for one hour before compound **81** (1.27 g, 9.2 mmol) was added

to the yellow mixture. The reaction mixture was stirred at room temperature for 6 hours. After filtration to remove the triphenylphosphine oxide, the filtrate was diluted with water and the water layer was extracted by pentane (15 mL x 3). The combined pentane layer was washed with dilute HCl acid and water, and then dried over sodium sulfate. After removing pentane by distillation, crude compound **82** (1.0 g, 80% yield) was obtained. Compound **82** was purified to more than 99.5% pure by preparative-GC on a 9 foot long column (1/8" i.d.) packed with 20% SE-30-CW packing materials. Spectral data for compound **82**: m.p. 68-69°C (literature 66-68°C⁸²). GCMS *m/z* 136(9.0, M), 122(12), 121(100, M-Me), 107(11), 106(11), 105(35), 93(44), 91(45), 79(49), 77(31), 67(24), 65(12), 55(12), 53 (23); HRMS calculated for C₁₀H₁₆ *m/z* 136.12520, measured *m/z* 136.12610 (Kratos MS 50); HRMS calculated for C₉H₁₃ (M-Me) *m/z* 121.10173, measured *m/z* 121.10187 (Kratos MS 50); GC-FTIR $\nu(\text{cm}^{-1})$ 3039(s), 2933(s), 1492(m); ¹H-NMR (300 MHz, CDCl₃) δ 1.23(s, 12H), 4.84(s, 4H); ¹³C-NMR (75.429 MHz, CDCl₃) δ 27.56(4C), 47.90(2C), 100.39(2C), 168.05(2C); UV (nm, hexanes) $\lambda_{\text{max}}(\epsilon)$ 195(1.6 x 10³).

Anionic ring opening polymerization of compound **72**. A 25 ml oven-dried round bottom flask equipped with magnetic stirrer and septum was charged with compound **72** (0.62 g, 3.7 mmol), dry THF (20 mL), and 5 drops of HMPA (distilled over sodium right before use). The flask was filled with argon by the freezing and thawing technique (three times). After the reaction was cooled to -78°C, n-butyllithium solution (80 μL in hexanes) was injected quickly, the color of the solution turned red then yellow. After the reaction was stirred for 2 hours at -78°C, saturated ammonium chloride solution (10 mL) was added slowly. After 10 mL of hexanes was added, the organic layer was washed with water twice and dried over sodium sulfate. The polymer was then precipitated out in 50 mL of methanol. After vacuum drying, polymer **69** (0.42 g) was obtained, while ~20% compound **72**, ~11% compound **73** and ~1% compound **74** were detected by GC (according to the internal standard). GPC: $M_w = 1.72 \times 10^4$, $M_n = 7.01 \times 10^3$, PDI = 2.46; ¹H-NMR (300 MHz, CDCl₃) δ 0.15(s, 6H), 6.33(s, 2H); ¹³C-NMR (75.429 MHz, CDCl₃) δ -0.23(2C),

143.70(1C), 150.83(1C); $^{29}\text{Si-NMR}$ (59.591 MHz, CDCl_3) δ -6.19(1Si); UV (nm, hexanes) $\lambda_{\text{max}}(\epsilon)$ 198(3.9×10^3), 245(125), ϵ is calculated based on the concentration of repeating units (M); DSC shows two endothermic peaks at 54°C and 94°C; TGA shows the thermal degradation of the polymer starts at -330°C and the maximum rates of decomposition are between 440°C and 500°C with only 7% char yield.

Attempted ring opening polymerization of compound 72 catalyzed by CPA. A oven-dried 5 mL test tube equipped with magnetic stirrer and septum was charged with compound 72 (0.2 g) and a small particle of chloroplatinic acid under argon flow. It was then heated in a oil bath at 90-100°C for 1.5 hours. After dissolving of the product in 5 mL of THF, the THF solution was added to 20 mL of methanol and only a trace amount of polymer was observed. After flashing through a silica gel column, 0.14 g of compound 74 was isolated as colorless crystals, with a m.p. of 159-160°C.

III. THE FIRST SYNTHESIS AND STUDY OF CUMULENE-CONTAINING POLYMERS

Literature Survey

Introduction to nonlinear optical (NLO) effects in organic materials.

In photonics, photons are used to acquire, process, store, and transmit information in analogy to the role of electrons in electronics. The development of highly active nonlinear optical (NLO) materials is critical for frequency conversion, light modulation, and optical switching in the design of optics.⁹⁵ Organic materials offer the following advantages: low cost, ease of fabrication and integration into devices, tailorability, high laser damage thresholds, low dielectric constants, fast nonlinear optical response times.⁹⁶

The very basic nonlinear optical effects in organic molecular system are shown in the following. The dipole moment induced in an atom or molecule by an external field E can be written as

$$(\mu - \mu_0) = \alpha \cdot E + \beta \cdot EE + \gamma \cdot EEE + \dots \dots$$


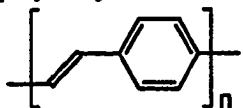
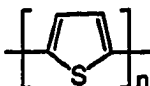
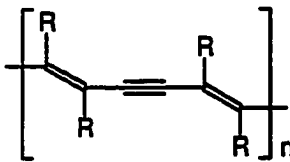
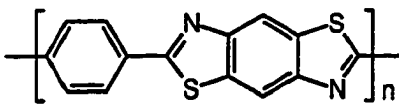
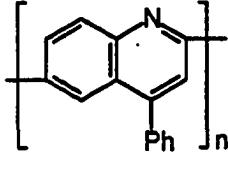
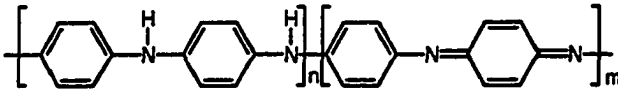
α , β , and γ are often referred to as the polarizability, first hyperpolarizability, and second hyperpolarizability respectively. Similarly, the polarization induced at the bulk or macroscopic level by an external field E can be expressed as

$$P = \chi^{(1)} \cdot E + \chi^{(2)} \cdot EE + \chi^{(3)} \cdot EEE + \dots \dots$$

where the coefficients $\chi^{(1)}$, $\chi^{(2)}$, and $\chi^{(3)}$ correspond to linear susceptibility, first nonlinear susceptibility, and second nonlinear susceptibility. While β and γ corresponds to the second-order and the third-order nonlinear optical response at microscopic level, $\chi^{(2)}$ and $\chi^{(3)}$ corresponds to the second-order and the third-order nonlinear optical response at the bulk (macroscopic) level respectively.

Organic polymeric materials with π -conjugated systems such as polyacetylene,⁹⁷ poly(phenylene vinylene) (PPV),⁹⁸ polythiophene,⁹⁹ polydiacetylene¹⁰⁰ and some other conjugated polymers have shown to exhibit very large nonlinear optical response (Table I).

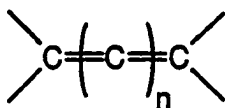
Table I. Selected organic polymers that exhibit third-order nonlinearities.^{95b}

Polymer	Nonresonant $\chi^{(3)}$ (esu) [wavelength]	Resonant $\chi^{(3)}$ (esu) [wavelength]	Measurement method	Ref.
 polyacetylene	1.0×10^{-10} [950nm]	1.1×10^{-9} [620nm]	THG spectroscopy	97
 poly(phenylene vinylene) (PPV)		4.0×10^{-10} [602nm]	DFWM	98
 polythiophene		4.0×10^{-10} [602nm]	DFWM	99
 (4-BCMU, red form) R = $(\text{CH}_2)_4\text{O}_2\text{CNHCH}_2\text{CO}(\text{CH}_2)_3\text{CH}_3$ polydiacetylene	4.0×10^{-10} [602nm]		DFWM	100
 (PBZT) poly(phenylenebenzobisthiazole)	4.5×10^{-10} [602nm]		DFWM	101
 polyquinoline (PPO)	2.3×10^{-12} [2.38 μm]	1.1×10^{-11} [1.2 μm]	THG spectroscopy	102
 polyaniline (emeraldine base)		3.7×10^{-11} [1.83 μm]	THG spectroscopy	103

* THG, third harmonic generation; DFWM, degenerate four-wave mixing.

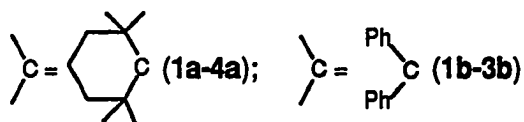
Cumulene molecules and their structural features.

A special class of conjugated organic molecules are cumulenes, compounds with two sp^2 -hybridized carbons separated by n sp -hybridized carbons with $n+1$ double bonds ($n \geq 1$).^{104a}



Within the cumulene backbone, two extended π -systems occupy two orthogonal planes. Most of the C=C bonds in cumulenes are shorter than a "standard" C=C bond (1.34Å) and the odd number C=C bonds are slighter longer than the even number C=C bonds as shown in Table II.¹⁰⁵⁻¹⁰⁸ The x-ray structures are in good agreement with the theoretical prediction.¹⁰⁹

Table II. Bond length (Å) of the double bonds in cumulenes from X-ray structures.¹⁰⁵⁻¹⁰⁸



	Compounds	x	y	z
1a		1.305		
2a		1.328	1.256	
3a		1.315	1.276	
4a		1.329	1.259	1.299
1b		1.310		
2b		1.348	1.260	
3b		1.327	1.271	

When n is an odd number, the two end planes of the cumulene molecule are orthogonal to each other. When n is an even number, the molecule should be planar even though it may not be so because of steric interactions between the substituents. For example, in compound **2b**, the four phenyl rings make dihedral angles of 30, 28, 29, 42°, respectively, with the plane through the butatriene system.¹⁰⁵

Correlated *ab initio* electronic calculation of cumulene geometry revealed that cumulenes are bent rather than linear.¹¹⁰ Bend angles as much as 9° were calculated for pentatetraene and hexapentaene (Fig. 1a). The calculated results do not agree with reported X-ray diffraction results (Fig. 1b).¹⁰⁵⁻¹⁰⁸ According to X-ray structural studies, acyclic cumulenes from allene to hexapentaene are almost linear. No bend angles larger than 4° were observed.

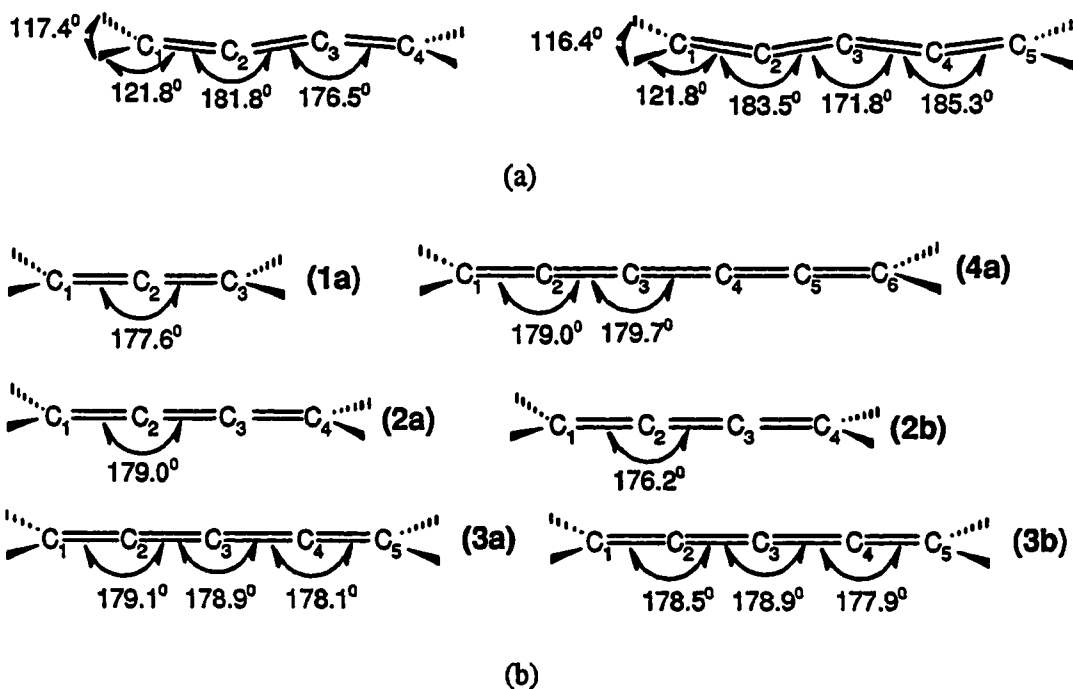
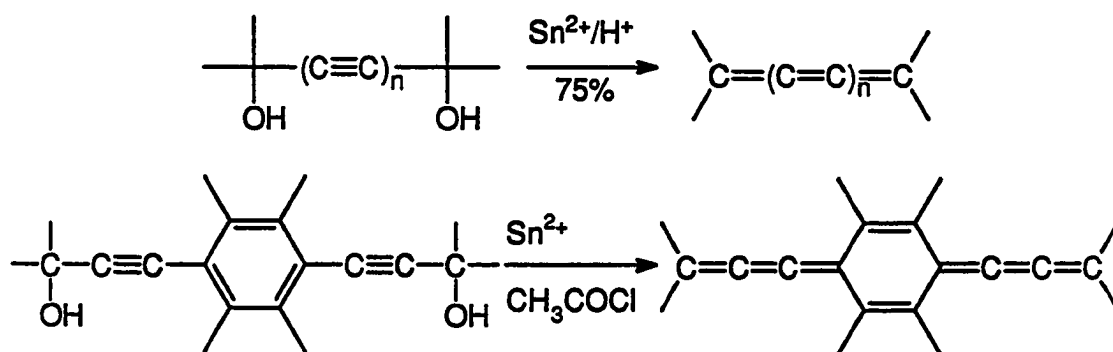


Figure 1. Geometries of cumulenes: (a) MP2/6-31G optimized geometries of butatriene and pentatetraene; (b) X-ray structures of allene, butatrienes, pentatetraenes and hexapentaene.

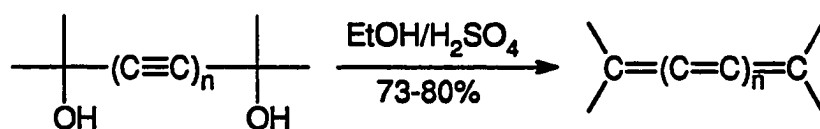
Synthesis of cumulene molecules.

Synthesis of cumulenes has been extensively reviewed.¹⁰⁴ The common synthetic approaches to cumulenes are listed here (the synthesis of allenes and heterocumulenes are not included).

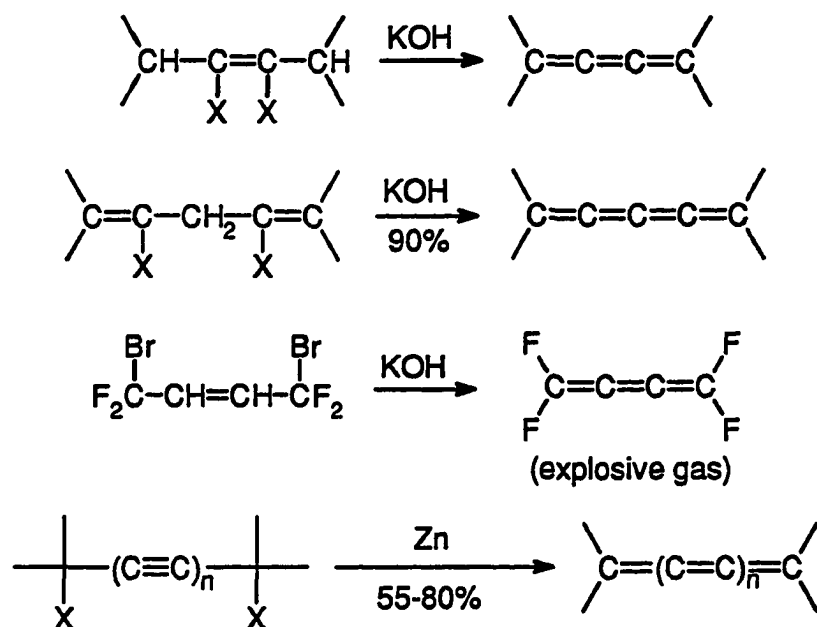
1. Reductive elimination from diols.^{104, 111-114} This is the simplest and the most widely used method for preparation of cumulenes. However, only cumulenes with an even number of carbon atoms (odd number of double bonds) are obtained by this route. Tin (II) chloride is usually used as the reducing agent. The diol precursors are usually obtained from the reactions of acetylenic Grignard or lithium reagents with the corresponding ketones or aldehydes.



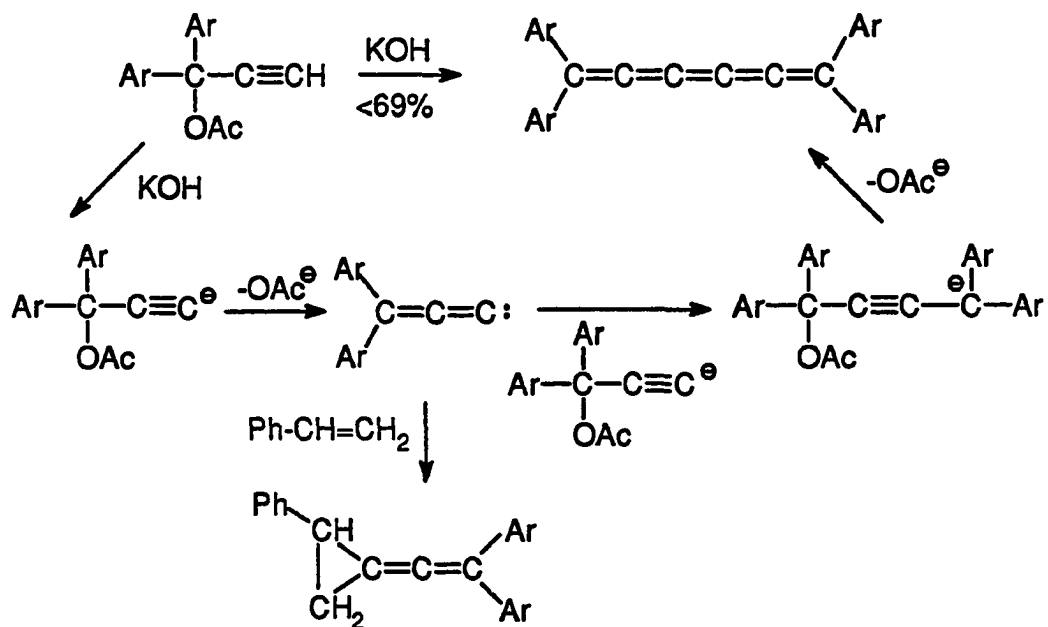
It was also reported that the diol precursor was converted to cumulene upon heating in sulfuric acid/ethanol solution.¹¹⁵ The reducing agent here was proposed to be the SO₂ produced upon heating ethanol with H₂SO₄.



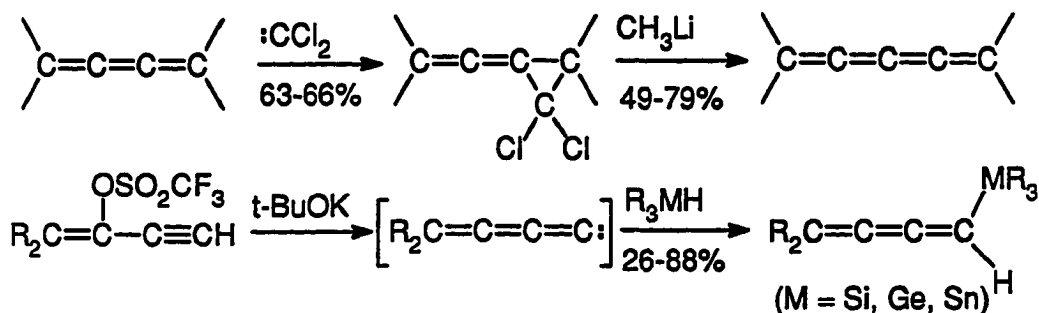
2. Elimination from halides.¹⁰⁴ Elimination of HX under basic conditions or X₂ by zinc from the corresponding dihalides afforded cumulenes in excellent yield. Tetrafluorobutatriene, an explosive gas, where the corresponding diol precursor is not available, was obtained by this route.^{104a}



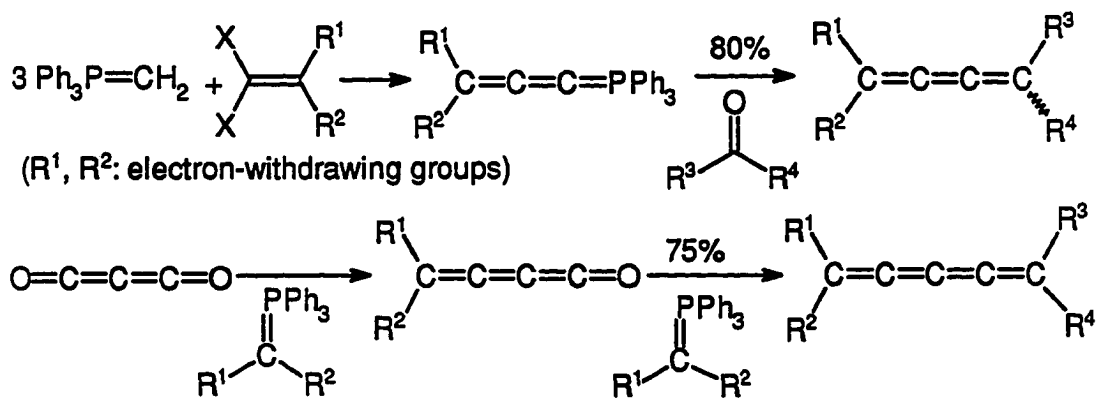
3. Self-condensation of diarylpropynols.^{104a} Hexapentaenes were obtained by self-condensation of diarylpropynols. However, the yield of cumulenes from this route is typically low. A carbene intermediate was proposed based on the trapping product by styrene.



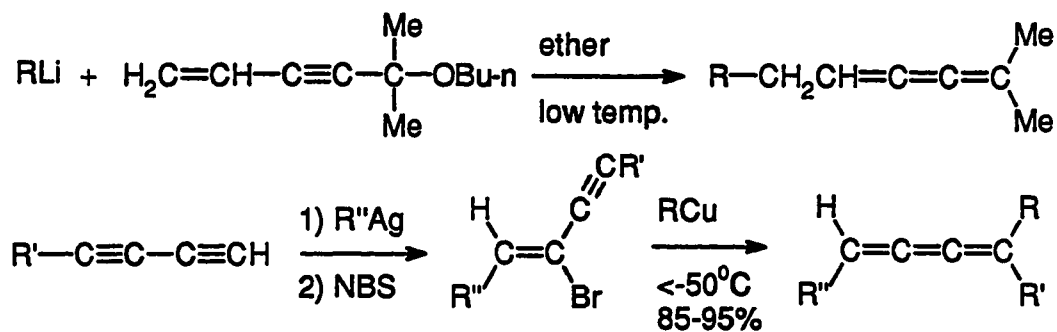
4. Carbene insertion. The length of cumulene segment can be increased by one carbon atom through the carbene insertion route.^{104, 108, 116} This route is usually used to synthesize cumulenes with an odd number of carbon atoms from the easily obtained cumulenes with an even number of carbons. Silicon, germanium, and tin-functionalized cumulenes have been synthesized by carbene insertion.¹¹⁷



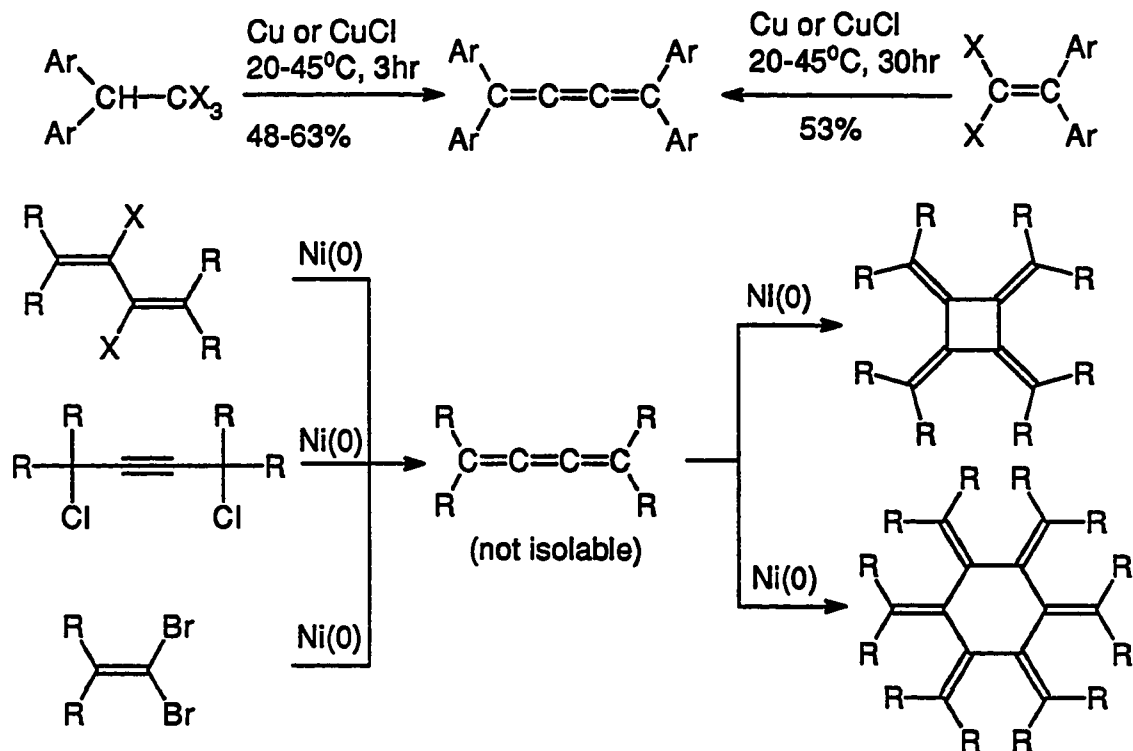
5. Wittig reaction. Wittig reactions are used for the synthesis of cumulenes in two different approaches. The first approach is to synthesize a cumulenic Wittig reagent and then couple with the corresponding ketone to give the desired cumulenes.¹¹⁸ In the second approach, carbon suboxide is reacted with two equivalents of Wittig reagents sequentially to give the cumulenic products.^{119, 120}



6. S_N' process.^{104c, 121} Cumulenes are also obtained from S_N' reaction under appropriate reaction conditions. Two different S_N' reaction examples are given below.

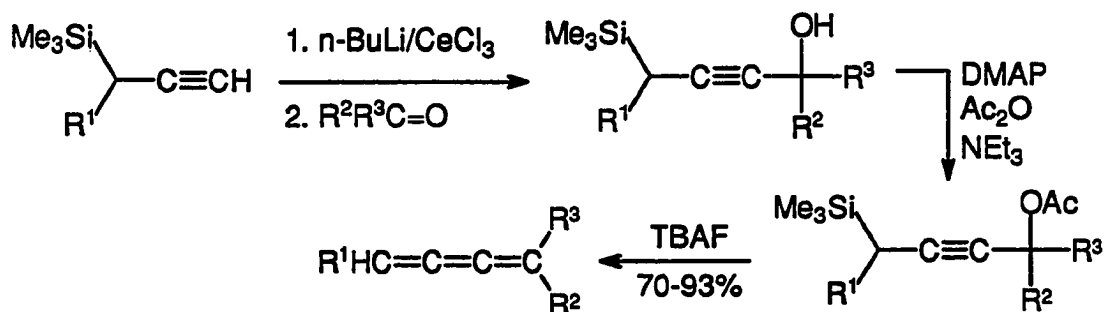


7. Catalytic coupling.^{122, 123} Catalytic coupling of halides with transition metal catalysts is another route to cumulenes. Cumulenes obtained from the reductions or coupling reactions of the corresponding halides by nickel (0) catalysts, which can not be isolated, oligomerize to give [4] and [6] radialenes.

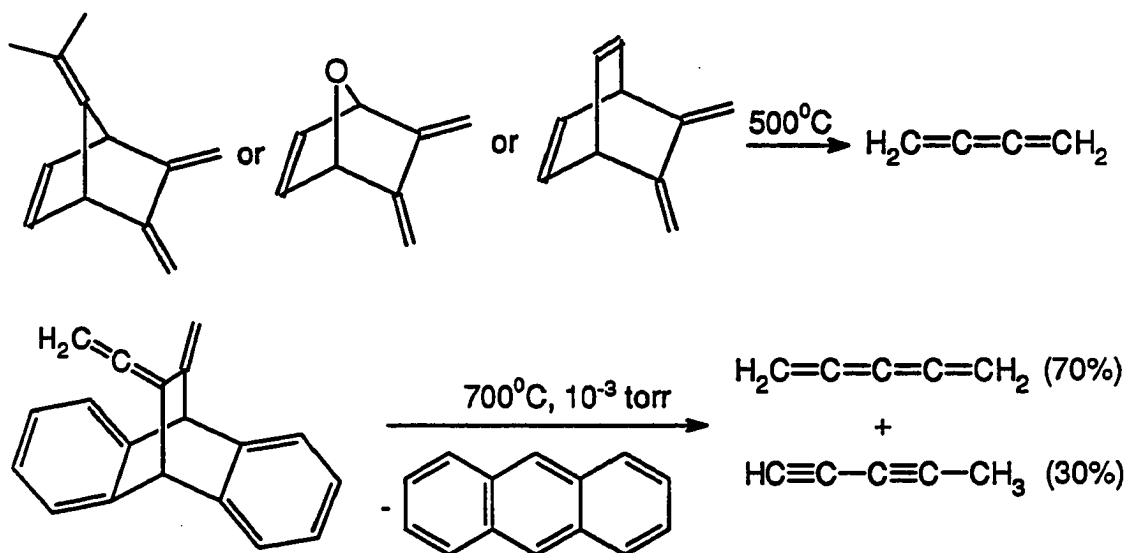


8. Fluoride-induced elimination.¹²⁴ Silyl prop-2-ynilic alcohols were obtained from the reaction of silyl prop-2-ynilic cerium reagents with the corresponding ketones or aldehydes. Conversion of the alcohols into the corresponding acetates in 4-(dimethylamino)pyridine

(DMAP) followed by tetrabutylammonium fluoride (TBAF)-induced 1,4-elimination gave alkyl or aryl substituted butatrienes in excellent yields.

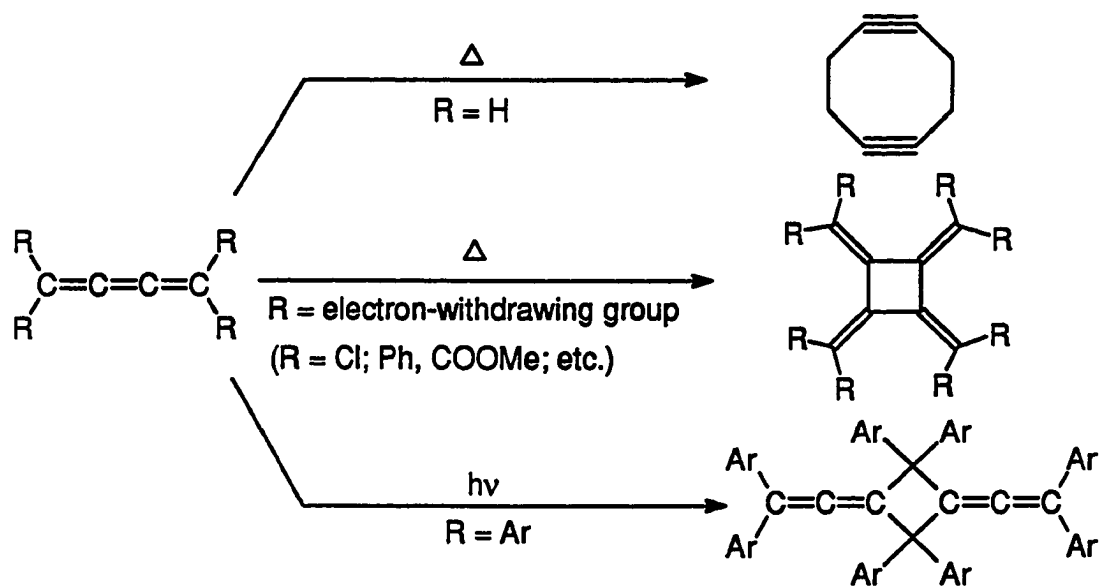


9. Thermolysis.^{125, 126} Cumulenes are also produced thermally in a *retro*-Diels-Alder fashion.



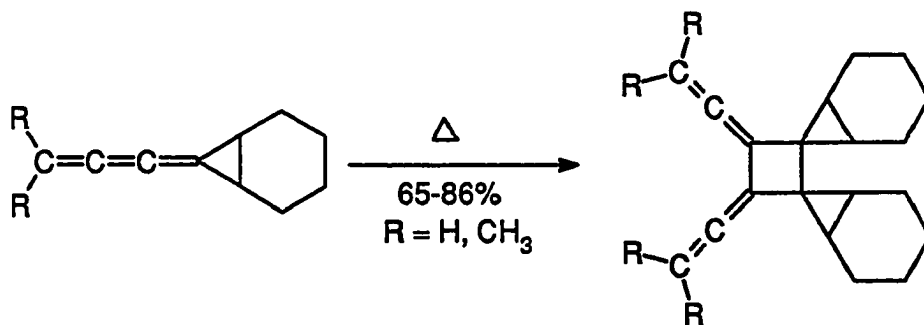
Chemistry and stability of cumulenes.

Cumulenes have a high degree of unsaturation. Many reactions characteristic to unsaturated organic compounds such as *cis-trans* isomerization, hydrogenation (partial or complete), halogenation, and oxidation can readily happen with cumulenes.^{104a} If at least one hydrogen is present as a substituent, then a cumulene can isomerize to an en-yne form under basic conditions.

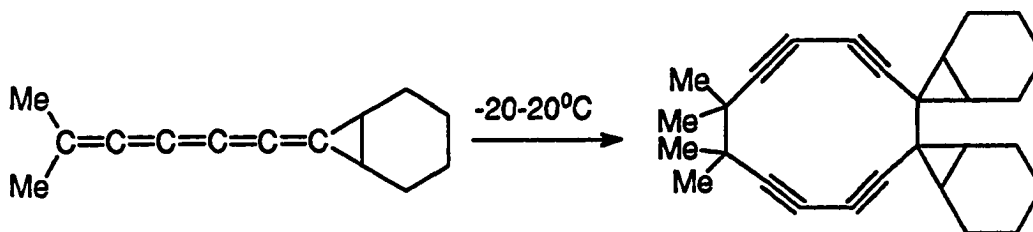
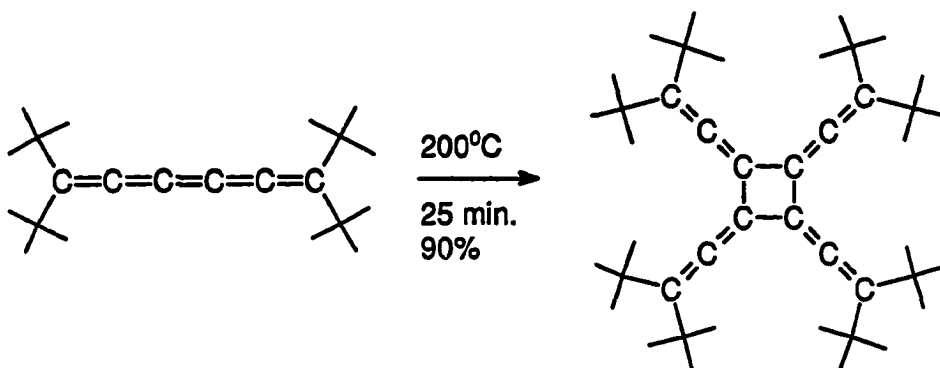
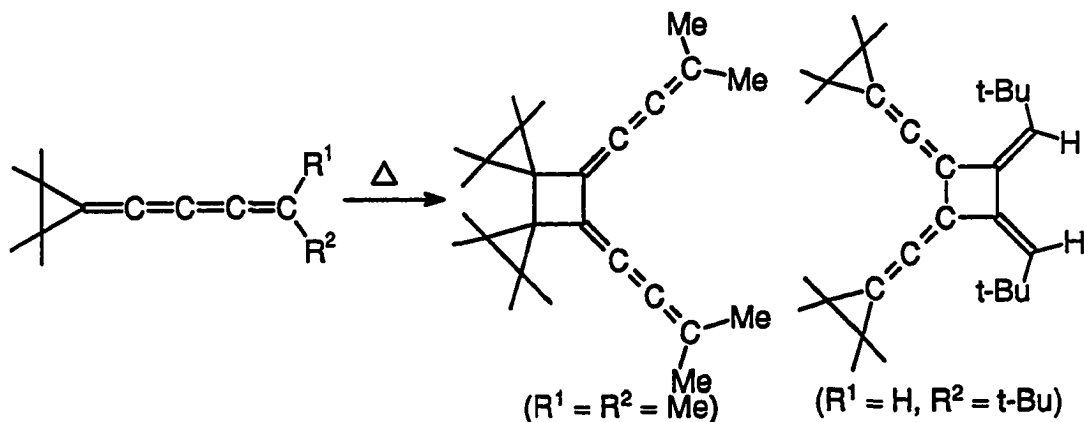


Thermal dimerization of cumulenes is a very important synthetic route to radialenes.¹²⁷ However, butatriene itself does not dimerize thermally. Instead, a trace amount of cyclooctadiene, a [4+4] product, was isolated from the polymeric products and characterized by X-ray diffraction.¹²⁸ Butatrienes with electron-withdrawing substituents dimerize in a [2+2] fashion to give [4] radialenes thermally.¹²⁹⁻¹³¹ The product of solid-state photodimerization of tetraphenylbutatriene was reported first as [4] radialene¹³² but was later proved to be a [2+2] head-to-tail dimer of the end double bond.¹³³

Butatrienes with alkyl substituents dimerize via 2 + 2 cycloadditions of the end double bonds in a head to head fashion.¹³⁴



The substituents of higher-order cumulenes such as pentatetraene and hexapentaene affect the products of thermal dimerization as shown below by three examples.¹³⁴⁻¹³⁷ There has been no satisfactory explanation for this divergent behavior.

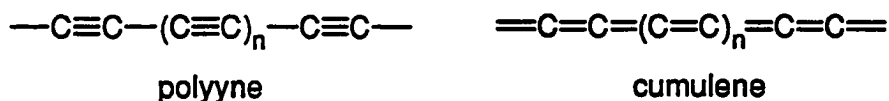


Butatriene itself is extremely labile. The stability increases as the number of aryl or alkyl substituents increases. 1,4-Distyrylbutatriene was obtained only by very careful isolation.^{104a} Tetraaryl or tetra(*t*-butyl) substituted butatrienes, pentatetraenes, and hexapentaenes are stable crystals with high melting points. Substituted octaheptaenes and decanonaenes could not be

isolated in a pure state due to their instability while octaheptaenes are relatively stable in solution.^{104a}

Polyynes (carbynes).

An infinite linear carbon chain, as a polymeric carbon allotrope,¹³⁸ could have two forms: an *acetylenic* form or a *cumulenic* form. The acetylenic form was predicted to be the preferred form over the cumulenic form according to *ab initio* Hartree-Fock level calculation.^{139, 140} Polyynes are expected to be one-dimensional conductors, and calculations predicted an unusual variety of soliton and polaron states.¹⁴¹

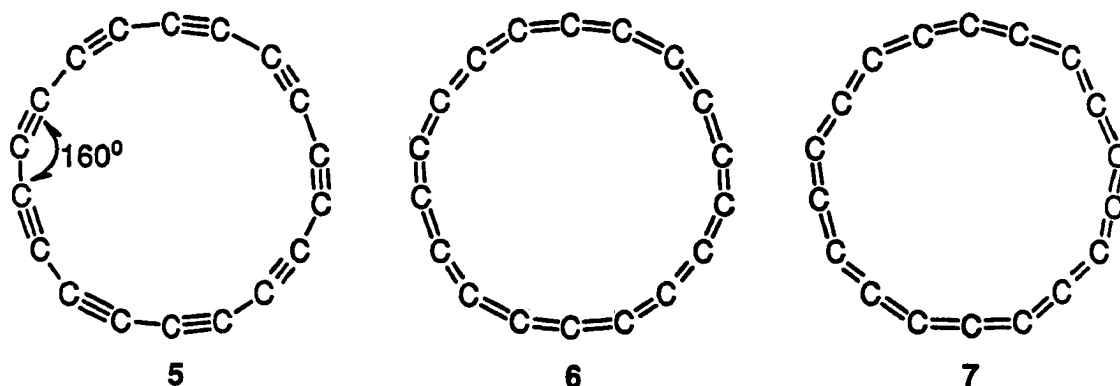


Reports on preparation of the polyynes are controversial: materials obtained by oxidative coupling of acetylenes, dehydrochlorination of poly(vinylidene chloride) (CHCl)_x,¹⁴² or contact heating of pyrolytic graphite at temperatures of 2700-3000K led only to ill-defined materials with poorly reproducible structural characteristics.^{143, 144} However, in a stepwise fashion, based on selective desilylation and oxidative coupling of acetylenes, Walton was able to prepare oligomers with up to 16 conjugated acetylene units protected by two triethylsilyl groups at the end.¹⁴⁵

A monocyclic structure is preferred for the neutral C_n when n ≥ 10 according to extended Hückel¹⁴⁶ and semiempirical MNDO study.^{147, 148} *Ab initio* calculations also shows that the acetylenic diradicals are more stable than the cumulenic dicarbenes and cyclic alkynes for C_n where n = 4, 6, 8.¹⁴⁹



Cyclic polyynes, such as C_{18} , **5**, have been targets for both synthetic¹³⁸ and theoretical study. *Ab initio* calculations also predicted that the monocyclic form is preferred over the linear form for C_{18} .¹⁵⁰ Results of SCF calculations with a 3-21G or larger basis set suggest that the cyclic acetylenic D_{9h} structure (**5**) is more stable than the cumulenic structures D_{18h} (**6**) and D_{9h} (**7**) while optimization at the MP2 level including valence electron correlations predicted that **6** is favored over **5** and **7**.^{150, 151} Even though theoretical calculation¹⁵⁰ predicted a relative stable ground state geometry for **5** with alternating C-C (1.36Å) and C≡C (1.20Å) bonds and a 160° C-C≡C angle, generation of **5** from well-defined precursors has only produced time-of-flight mass spectroscopic evidence.^{138, 150}

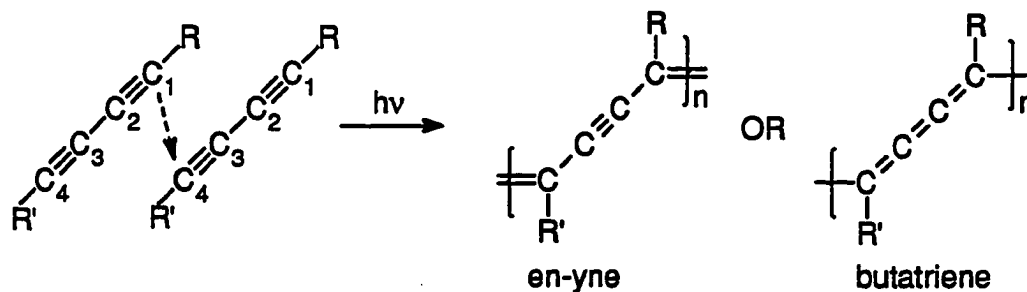


Polydiacetylenes (polyen-yne)s.

Crystals of substituted diacetylenes can be polymerized photochemically (by UV, X-ray, or γ -ray quanta) or thermally to give polydiacetylenes.¹⁵² Single crystal polydiacetylene was obtained with nearly the same dimensions as the monomer in an ideal polymerization of the bis(*p*-toluene sulphonate) ester of 2,4-hexadiyne-1,6-diol. Several polydiacetylene X-ray crystal structures are available. Polydiacetylenes represent the only kind of polymers that are single crystals.

Polydiacetylenes could exist in two different forms: the en-yne form or the butatriene form as shown in the following. There is no credible evidence for the butatriene form from the crystallographic^{152a} and solid state ¹³C-NMR studies.¹⁵³ *Ab initio* calculation of the

ground state of the infinite polydiacetylene chain predicted that the en-yne form is favored over the butatriene form by 12 kcal/mol per C_4H_2 unit.¹⁵⁴



Sixl proposed that the butatriene form was formed from the diradical reactive end while the en-yne form was from the carbene reactive end.^{152a} Evidences for oligomeric butatriene came from the low temperature optical spectroscopy of the growing chain. Sixl proposed that the oligomeric butatriene was formed through the energetically favored diradical reactive ends. In longer chains, the higher energy carbene intermediate was compensated by the more stable en-yne form product and became the only reactive ends. Trace amount of butatriene type of defects were also proposed in the solid state ^{13}C -NMR study of the bromination poly(1,6-dicarbazol-2,4-hexadiyne).¹⁵⁵

Theoretical calculation of polarizabilities and second hyperpolarizabilities of cumulenes.

Polyacetylene is the most widely studied conjugated polymer since it has been shown that its conductivity can be improved to 1.5×10^5 s/cm upon doping.¹⁵⁶ It also represents the largest $\chi^{(3)}$ (on the order of 10^{-9} esu) among the organic polymers studied. Theoretical calculation at the *ab initio* level predicted that the longitudinal polarizability of polyacetylenes depends on the chain length L as $L^{1.541-1.663}$. Saturation effects on longitudinal linear polarizability α after 15-20 double bonds (50Å) and second hyperpolarizability γ after 10-15 double bonds were also predicted.^{157, 158} According to these calculations, the smaller the bond length alternation in the polymer chain, the larger hyperpolarizability the polymers should have.

Even though no cumulene oligomers or polymers had ever been made, *ab initio* calculations of longitudinal polarizabilities have shown that cumulenes should possess high polarizability and thus are promising candidates for NLO materials.¹⁵⁷⁻¹⁵⁹ *Ab initio* calculation results of longitudinal linear polarizability α_{zz} of polyacetylenes (also referred to as polyenes), polyynes, polydiacetylenes (also referred as polyen-ynes), and cumulenes are listed in Table III.¹⁵⁷ According to these calculations, cumulenes possess the largest longitudinal linear polarizability values compared to polyenes, polyynes, polyallenes, and polyen-ynes for the same chain length. This was attributed to the smaller bond length alternation in the cumulene systems.

Table III. Comparison of the longitudinal linear polarizability (α_{zz}) (au).^{157a}

	# of carbons	2	4	6	8
Moieties					
-C=C-		17.48	47.85	100.50	174.56
-C≡C-				91.12	
-C=C-C≡C-C=C-				85.30	
-C=C=C-				86.80	
-C=C=C=C=C=C-				174.29	

Linear polarizability and second hyperpolarizability tensors of the polyene, polyyne, and cumulenes computed by *ab initio* SCF theory with augmented 3-21G basis sets were reported by Prasad's group in 1989.¹⁵⁹ According to the results in Table IV and V, cumulenes should have larger linear polarizability and second hyperpolarizability than polyenes which have the largest experimentally measured third-order nonlinearity. Polyynes have a smaller linear polarizability and second hyperpolarizability than polyenes.

Table IV. Longitudinal linear polarizability tensors (au) of polyenes, polyynes, and cumulenes computed by using split-valence orbital basis set.

	# of carbons	2	4	6	8
Moieties					
<i>trans</i> -C=C-		28.23	72.10	137.60	217.94
-C≡C-		26.49	69.17	130.62	206.52
=C=C=			101.27	227.47	422.37

Table V. Longitudinal second hyperpolarizability tensors (au) of polyenes, polyynes, and cumulenes computed by using split-valence orbital basis set.

	# of carbons	2	4	6	8
Moieties					
<i>trans</i> -C=C-		-116.1	906.0	8805.0	32200.0
-C≡C-		1.9	841.1	5600.0	19388.0
=C=C=			-1551.0	-8822.0	-36726.0

A model exact static and frequency-dependent linear polarizabilities and second hyperpolarizabilities and THG coefficients of polyenes, polyen-yenes, and cumulenes calculated within the correlated Pariser-Parr-Pople (PPP) model defined over the π -frame were performed by Albert et al (1992).¹⁶⁰ It was also found that for the same chain length, cumulenes have the largest polarizabilities and third harmonic generator (THG) coefficients. The polyen-yenes have the smallest polarizability and THG coefficients. The optical gaps for these systems were also calculated with cumulenes possessing the smallest gap at 0.75 eV, polyenes at 2.86 eV, and polyen-yenes at 4.37 eV.

Surprisingly, the calculations reported by Garito in 1994 predicted larger linear polarizability and smaller third-order nonlinear optical properties for cumulenes compared to polyenes with the same chain length (Table VI).¹⁶¹ Not only does this contradict Prasad's calculations, but also his experimental results.¹⁶² From both calculations and experimental measurements, γ_{zzzz} of cumulenes is negative in sign. However, the exact calculation method was not mentioned in the paper and this makes it difficult to compare it with Prasad's calculations.

Table VI. Linear and nonlinear susceptibilities of various systems.¹⁶¹

System	$\alpha_{zz}(-\omega, \omega)$ (10^{-24} esu) ($h\omega = 0.15\text{eV}$)	$\gamma_{zzzz}(-3\omega, \omega, \omega, \omega)$ (10^{-36} esu) ($h\omega = 0.05\text{eV}$)
<i>trans</i> -hexatriene	12.6	4.3
hexapentaene	44.4	3.6
hexatriyne	16.2	3.2
diallene	24.2	3.6

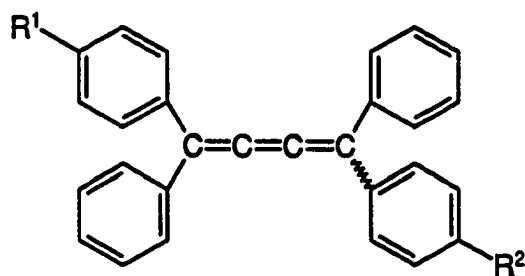
Experimental determinations of nonlinear optical properties of cumulenes.

Ermer reported the primary results of the synthesis and second-order nonlinear optical susceptibilities of a series of polar cumulenes measured by DC electric field-induced second harmonic generation (EFISH) in 1990 and 1991.^{163, 164} The first set of values reported in Table VII were from the EFISH measurements by using a laser pump at 1.064 μm wavelength. To eliminate the concerns about dispersion, $\beta\mu$ values were also measured at 1.9 μm . As shown in Table VI, while changing R^1 from hydrogen to methyl almost brings no change to the $\beta\mu$ value, changing R^1 to alkoxy significantly increases the $\beta\mu$ value.

Prasad reported the first experimental determination of the third-order nonlinear optical susceptibilities of some cumulenes in 1993.¹⁶² The effective values (Table VIII) of the second

hyperpolarizability, $\langle\gamma\rangle$, of each compound was determined using femtosecond degenerate four-wave mixing (DFWM) techniques. For most of the cumulenes (10-13, 15-18), the $\langle\gamma\rangle$ value measured is resonant enhanced value because the experiments were performed at 602nm wavelength on THF solution where most of them have strong absorption. Conjugate signals were compared with those from a reference liquid.

Table VII. Physical characteristics and EFISH results of some polar cumulenes.^{163, 164}



R ¹	R ²	m.p.(°C)	λ_{\max} (nm) ^a	$\beta\mu^b$	
				1.064 μm	1.09 μm
H	NO ₂	211-213	442 (3.24)	675	145
CH ₃	NO ₂	235-237	448 (3.47)	600	----
OCH ₃	NO ₂	250-252	459 (3.51)	850	----
O(CH ₂) ₁₁ CH ₃	NO ₂	132-135	461 (3.39)	----	280

^a λ_{\max} in 1,4-dioxane, $\text{ex}10^4$ in parentheses

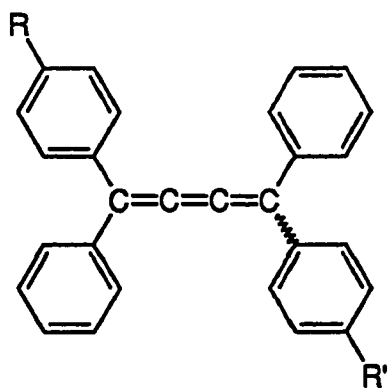
^b $\times 10^{30} \text{cm}^5 \text{D/esu}$

Extended π -electron delocalization is considered to be one of the most important structural features of an organic system that contributes to its high third-order nonlinear susceptibility. Even though the direct correlation between the observed third-order nonlinearity and the conjugation length is very complicated, some trends can still be observed from the values in Table VIII. From compound 2b, a butatriene, to 10, a pentatetraene, the absolute value of $\langle\gamma\rangle$ increases by almost one order of magnitude. Compound 17, which

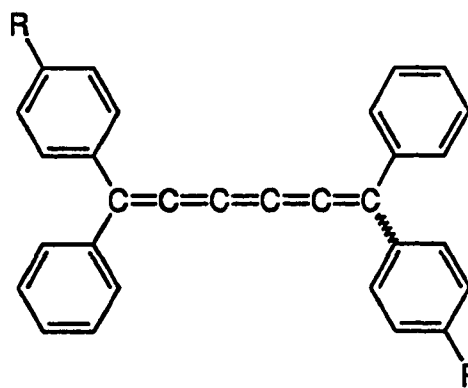
Table VIII. Optical and third-order nonlinear properties of some cumulenes.^a

compound	λ_{\max} (nm)	ϵ at 602 nm (L cm ⁻¹ mol ⁻¹)	$\langle\gamma\rangle$ (esu)
2b	417	below resolution	-3×10^{-33}
8	440	below resolution	-7×10^{-33}
9	460	below resolution	-9×10^{-34}
10	480	18	-1×10^{-32}
11	517	780	-1×10^{-33}
12	505	140	-4×10^{-33}
13	507	1200	-3×10^{-32}
14	386	below resolution	-1×10^{-36}
15	535	600	-2×10^{-32}
16	485	16	-1×10^{-33}
17	458, 576	48500	-4×10^{-31}
18		40700	-3×10^{-31}

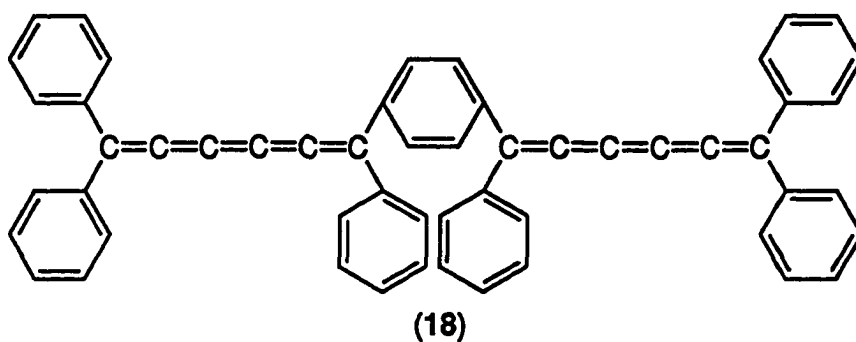
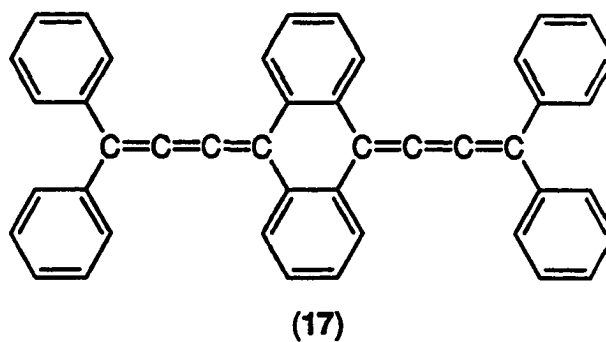
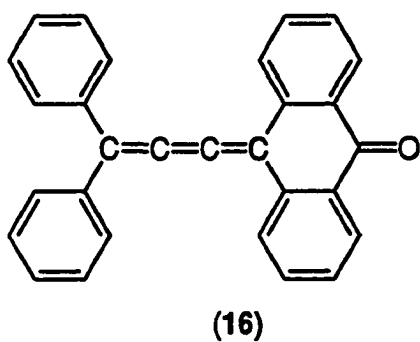
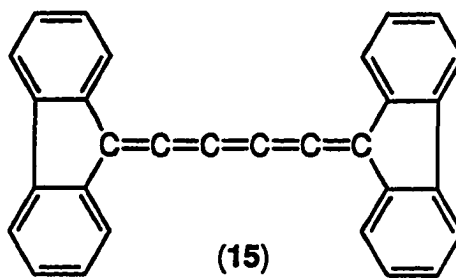
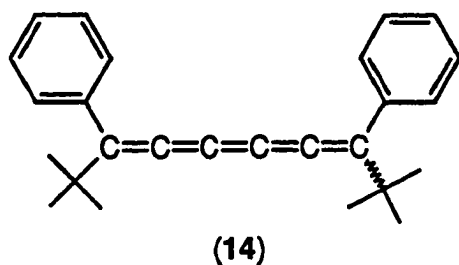
^a The estimated values are based on the assumption that for THF, the $\chi_{\text{THF}}^{(3)} = +3.7 \times 10^{-14}$ esu, $\langle\gamma\rangle_{\text{THF}} = +1.5 \times 10^{-36}$ esu.



R = R' = H (2b); R = R' = OCH₃ (8);
R = NO₂, R' = O(CH₂)₁₁CH₃ (9)



R = R' = H (10); R = R' = NO₂ (11)
R = R' = OCH₃ (12);
R = NO₂, R' = OCH₃ (13)



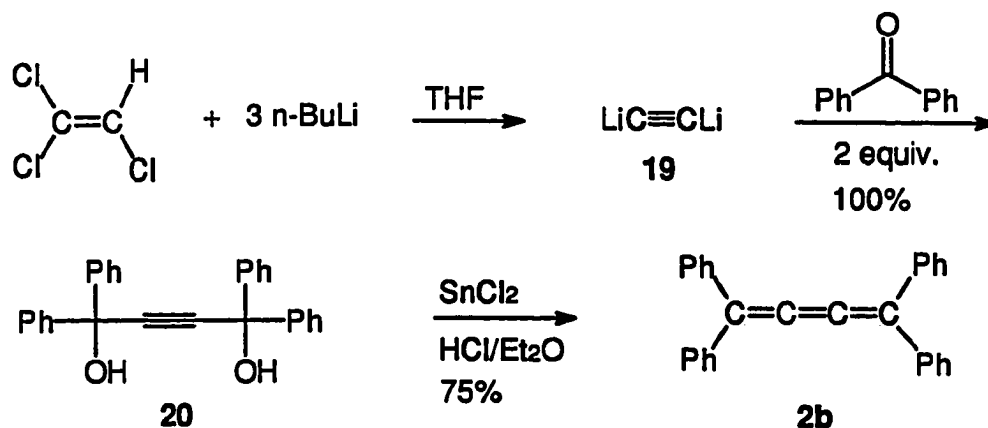
can be roughly regarded as a dimer of compound **2b**, shows two orders of magnitudes increase in the $\langle \gamma \rangle$ value as compared to **2b**. Compound **18**, a dimer of compound **10**, shows a one order increase in the $\langle \gamma \rangle$ value as compared to **10**.

A conjugated polymer with a conjugated cumulenenic system in the polymer backbone could be expected to have a small band gap and exhibit high nonlinear optical response. In this section, for the first time, the synthesis and study of cumulene-containing polymers are reported.

Results and Discussion

Synthesis and characterization of poly(*p*-phenylene-1,4-diphenyl-1,2,3-butatriene).

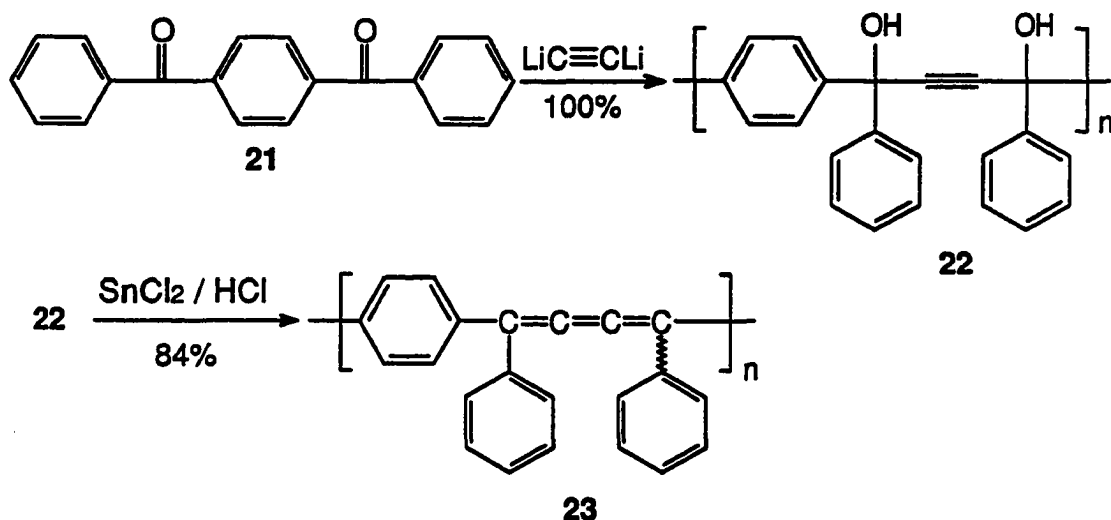
The synthetic route to cumulenes (butatrienes) employed in this work is based on dilithium acetylene (**19**) which can be quantitatively obtained from the reaction of trichloroethylene and three equivalents of *n*-butyllithium.¹⁶⁵ When the dilithium acetylene reacts with benzophenone, 1,1,4,4-tetraphenyl-2-butyne-1,4-diol (**20**) is obtained in quantitative yield. Further reduction of diol **20** by tin(II) chloride under acidic condition gives 1,1,4,4-tetraphenyl-1,2,3-butatriene (**2b**) in 75% isolated yield. This model reaction is shown in Scheme 1.



Scheme 1. Synthesis of 1,1,4,4-tetraphenyl-1,2,3-butatriene.

It is the quantitative conversion of trichloroethylene to dilithium acetylene and then also to the diol precursors that makes the synthesis of cumulene-containing conjugated polymers possible. When dilithium acetylene (**19**) reacts with commercially-available *p*-dibenzoylbenzene (**21**), polymer precursor (**22**) is obtained in quantitative yield. Actually, because of the presence of many hydroxyl groups in polymer **22**, it is very difficult to get rid of all the THF from the polymer even after drying at 67°C under vacuum (0.25 mmHg) for extended periods. Further reduction of **22** affords poly(*p*-phenylene-1,4-diphenyl-1,2,3-

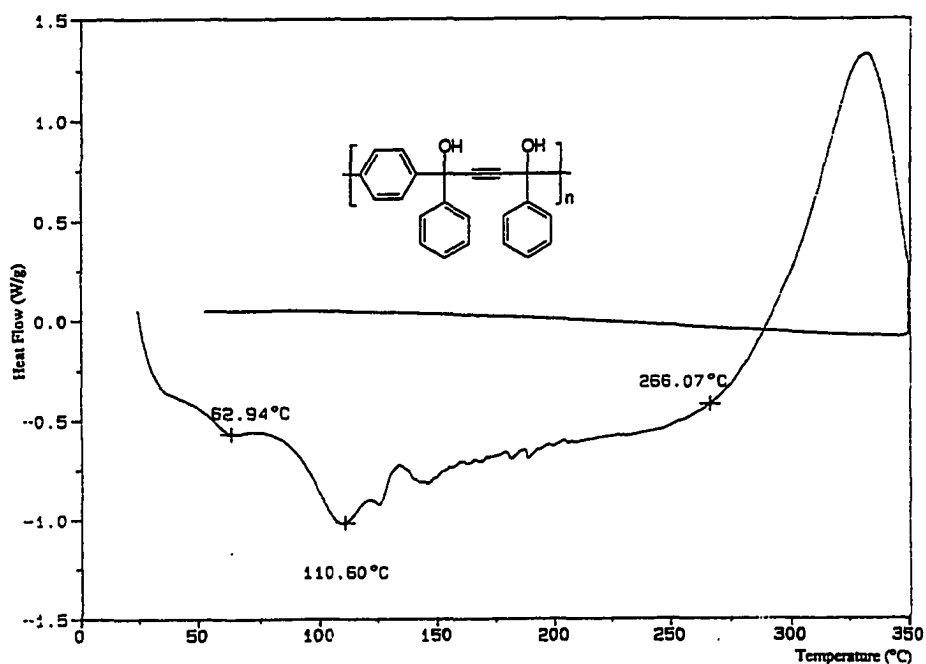
butatriene) (**23**) in 84% yield (Scheme 2). However, the polymer **23** obtained is only partially soluble in common organic solvents such as THF and toluene.



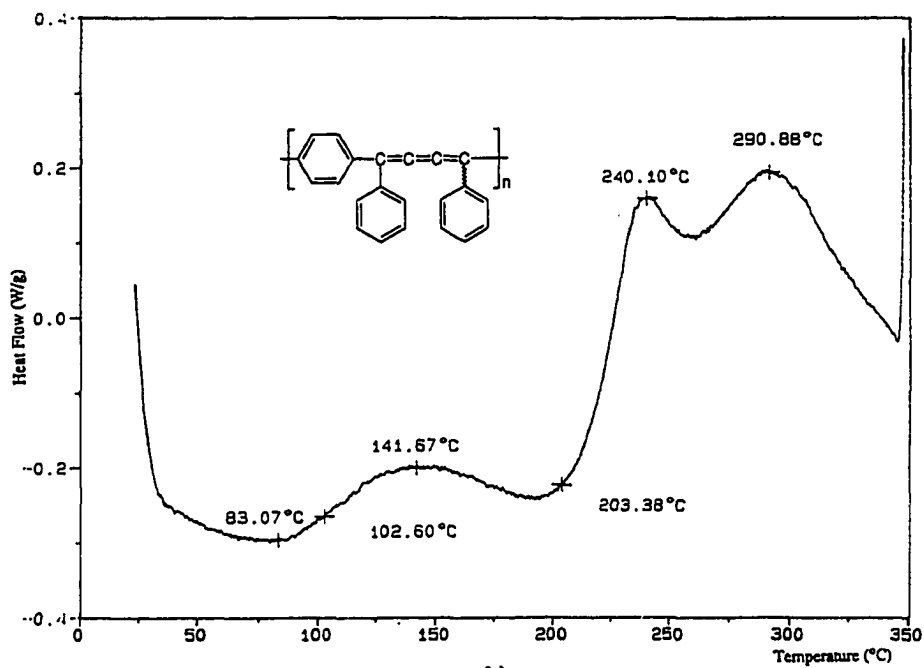
Scheme 2. Synthesis of poly(*p*-phenylene-1,4-diphenyl-1,2,3-butatriene).

Polymer precursor **22** was characterized by GPC, NMR (^1H and ^{13}C), FTIR, and DSC. The molecular weight of **22** is relatively low ($M_w = 3.62 \times 10^3$, PDI = 1.36) which is explained by the difficulty in controlling the stoichiometry of dilithium acetylene in relatively small scale reactions. The hydroxyl group absorbs at 3339 cm^{-1} in FTIR. A differential scanning calorimetry (DSC) thermogram of polymer **22** is shown in Fig. 2a where an endothermic peak is observed at $\sim 110^\circ\text{C}$ and an exothermic reaction starts at $\sim 266^\circ\text{C}$.

Because polymer **23** is only partially soluble in common organic solvents, the characterization of this polymer was largely based on comparing the solid state ^{13}C -NMR spectra of this polymer with that of the model compound, 1,1,4,4-tetraphenyl-1,2,3-butatriene, **2b**. The ^{13}C -NMR spectrum of 1,1,4,4-tetraphenyl-1,2,3-triene **2b** reveals that the β -C has the most characteristic and diagnostic resonance at about 152 ppm (Table IX).¹⁶⁶ In the solid-state ^{13}C -NMR spectra of polymer **23** (Fig. 3), the β -C at 151.17 ppm is easily identified. Polymer **23** has a weak absorption at 1944 cm^{-1} in FTIR which corresponds well with the asymmetrical butatriene stretch absorption at $\sim 2000\text{ cm}^{-1}$.^{104a} DSC analysis of



a)



b)

Figure 2. DSC thermogram of a) polymer 22 and b) polymer 23.

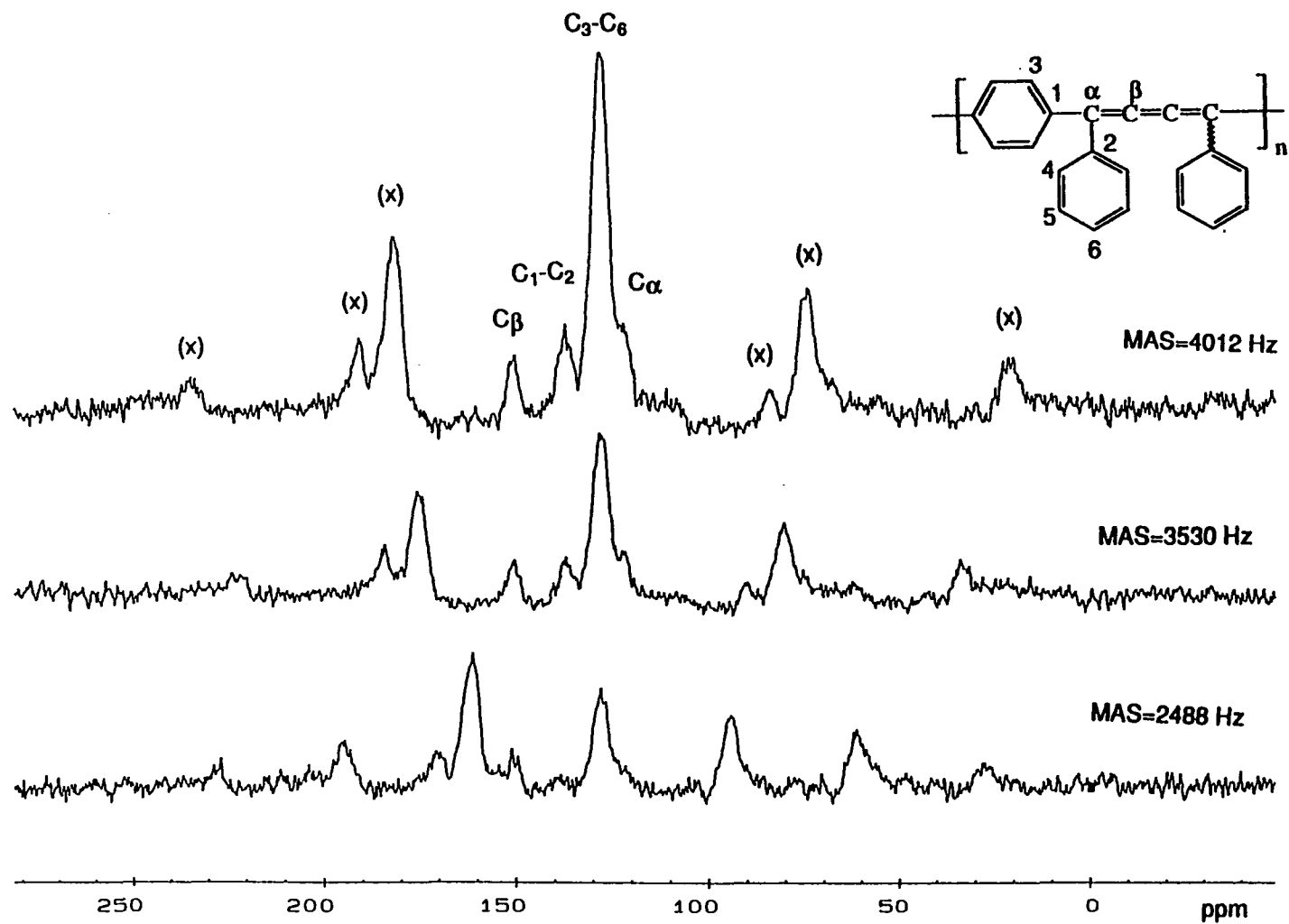


Figure 3. CPMAS ^{13}C -NMR spectra of polymer 23. ((x)-spin side bands)

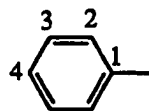
polymer **23** shows that an exothermic reaction starts at $\sim 103^\circ\text{C}$ before it melts (Fig. 2b). In contrast to the model compound **2b** which has a sharp UV-VIS absorption λ_{max} at 417 nm, the strong UV-VIS absorption of polymer **23** extended all the way from 400 nm to 550 nm and the absorption tails until 650 nm (Figure 9).

Table IX. ^{13}C -NMR chemical shifts of cumulenes and related compounds.¹⁶⁶

Compound	cumulene group ^a			Phenyl group ^b			
	δC_α	δC_β	δC_γ	δC_1	δC_2	δC_3	δC_4
$\text{Ph}_2\text{C}=\text{CPh}_2$	141.01 (123.13)			143.72	131.31	127.62	126.39
$\text{Ph}_2\text{C}=\text{C}=\text{CPh}_2$	112.53 (73.57)	208.26 (212.47)		136.28	128.38	128.52	127.33
$\text{Ph}_2\text{C}=\text{C}=\text{C}=\text{CPh}_2$	122.74 (118.00)	152.03 (171.10)		138.81	129.46	128.42	127.94
$\text{Ph}_2\text{C}=\text{C}=\text{C}=\text{C}=\text{CPh}_2$	117.77	181.61	119.25	136.22	129.15	128.53	128.21
$\text{Ph}_2\text{C}=\text{C}=\text{C}=\text{C}=\text{C}=\text{CPh}_2$	124.71	149.42	127.33	137.96	129.16	128.35	128.35
$\text{PhC}\equiv\text{CPh}$	89.69 (73.16)			123.52	131.67	128.54	128.43
$\text{PhC}\equiv\text{C}=\text{C}\equiv\text{CPh}$	81.50 (66.30)	74.37 (67.52)		121.88	132.35	128.42	129.10

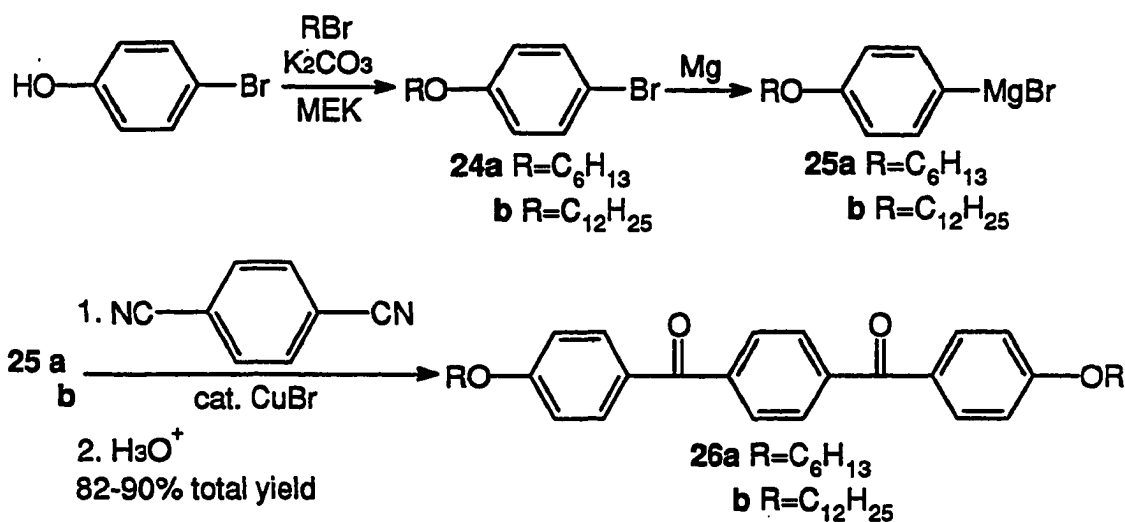
^a The carbons in cumulenes are numbered: $\text{R}_2\text{C}_\alpha=\text{C}_\beta=\text{C}_\gamma=\dots$, and the numbers in parentheses are for the systems when the substituents are hydrogen atoms.

^b The carbon atoms in the phenyl substituents are numbered:



Synthesis and characterization of poly(phenylene butatriene)s with alkoxy side chains.

In order to improve the solubility of the cumulene-containing polymers, alkoxy side chain substituted derivatives of **23** were synthesized. The almost quantitative alkylation of *p*-bromophenol¹⁶⁷ afforded the necessary *p*-alkoxybenzenes **24a** and **24b**. Reaction of Grignard reagents (**25a** and **25b**) and 1,4-dicyanobenzene with catalytic copper (I) bromide, followed by acidic work up, produced 1,4-bis(*p*-alkoxybenzoyl)benzene (**26a** and **26b**) in 82-90% total yield.¹⁶⁸

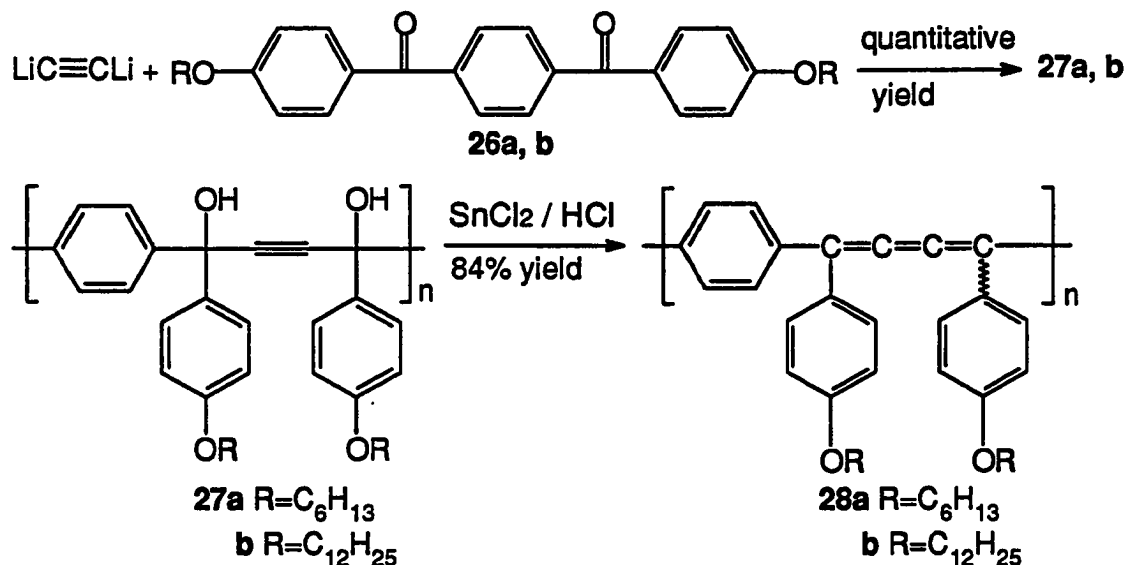


Scheme 3. Synthesis of 1,4-bis(*p*-alkoxybenzoyl)benzene.

Reaction of the diketone **26a** or **26b** with dilithium acetylene afforded the diol polymer precursors **27a** or **27b** in quantitative yield (Scheme 4). According to GPC, the molecular weight for **27a** is $M_w = 3.72 \times 10^3$, PDI = 1.40; the molecular weight for **27b** is $M_w = 4.44 \times 10^3$, PDI = 1.32. The hydroxyl groups in polymer **27a** and **27b** absorb at 3429 cm⁻¹ and 3423 cm⁻¹ in FTIR and the FTIR spectrum of polymer **27b** is shown in Fig. 4. DSC of polymer **27a** shows two small endothermic peaks at 88 and 103°C and an exothermic reaction

starts at 238°C. DSC of polymer **27b** shows two small endothermic peaks at 81 and 113°C and an exothermic reaction starts at 196°C (Fig. 5).

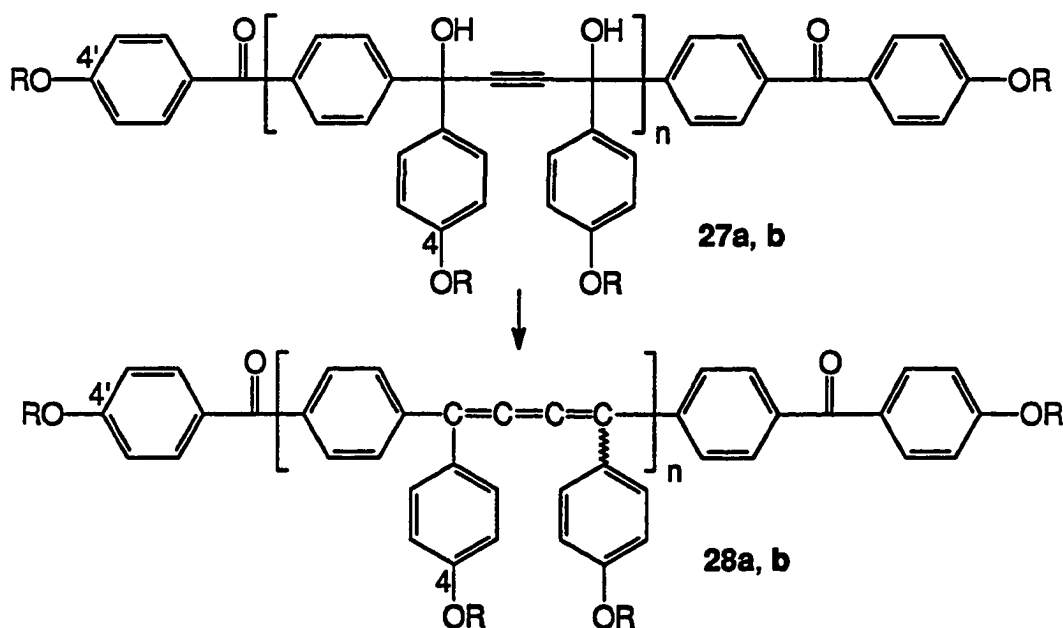
Poly(*p*-phenylene butatriene) with alkoxy side chains (**28a**, **28b**) were then obtained by reductive elimination as shown in Scheme 4. The polymers obtained were readily soluble in common organic solvents such as chloroform, THF, benzene, and toluene. While polymer **28a** forms brittle films, polymer **28b** has excellent film-forming ability. The weak butatriene absorption is at 1948 cm⁻¹ (**28a**) and 1942 cm⁻¹ (**28b**) in FTIR and the FTIR spectrum of polymer **28b** is shown in Fig. 6. DSC analysis shows that exothermic reactions start at 154°C for polymer **28a** and 125°C for polymer **28b** (Fig. 16a) before the polymers melt.



Scheme 4. Synthesis of alkoxy substituted poly(*p*-phenylene butatriene)s.

The solution ¹³C-NMR spectra of polymer **27b** and **28b** are shown in Fig. 7 and 8. From the ¹³C-NMR spectra, the end groups for polymers **27a**, **27b** and **28a**, **27b** are assigned as *p*-alkoxybenzoyl groups (Scheme 5.). The number of repeating units of the polymers can also be obtained from the ratio of the integrated C4 and C4' signals. The results from both ¹³C-NMR spectral integration and GPC are listed in Table X.

As shown in Fig. 9, different from the compound **2b** with a sharp absorption peak at 418 nm, polymers **23**, **28a**, and **28b** have similar UV-VIS absorption spectra, with a broad strong absorption band extended from 400 to 570 nm and the absorption tails until 700 nm. Compared to the above solution UV-VIS spectra, significant red shift was observed in the UV-VIS spectra of polymer film as shown in Fig. 10. None of these polymers is photoluminescent. No large domain of crystallinity was observed in X-ray powder diffraction study of polymer **28a**.



Scheme 5. End groups of polymers **27a**, **27b**, **28a**, and **28b**.

Table X. GPC and ^{13}C -NMR spectral integration results.

Polymer	22	27a	28a	27b	28b
M_w ($\times 10^{-3}$)	3.62	3.72	-----	4.44	-----
PDI	1.36	1.40	-----	1.32	-----
n (GPC)	8.53	5.19	-----	4.95	-----
n(^{13}C -NMR)	-----	9.38	5.18	6.38	4.60

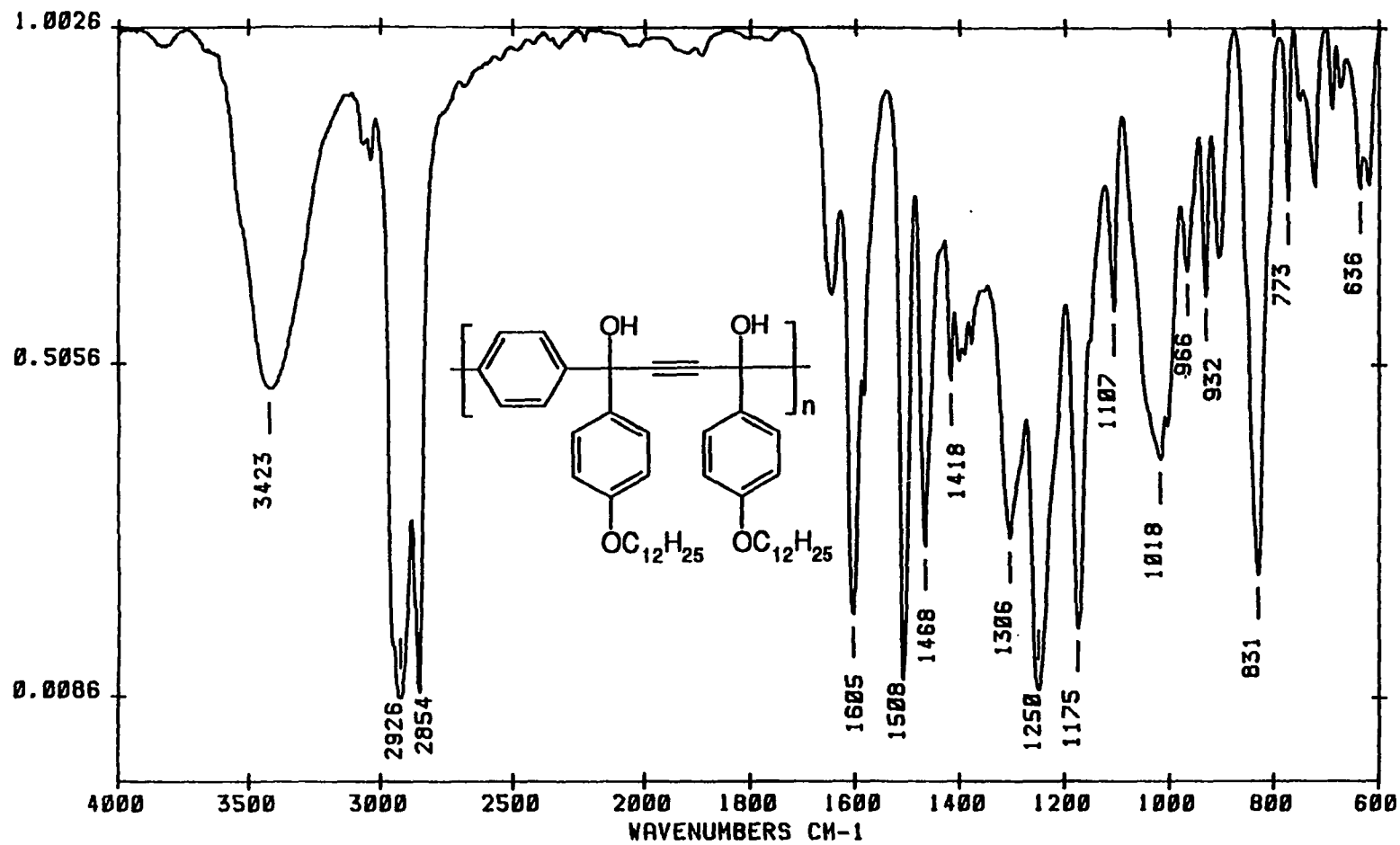


Figure 4. FTIR spectrum of polymer 27b.

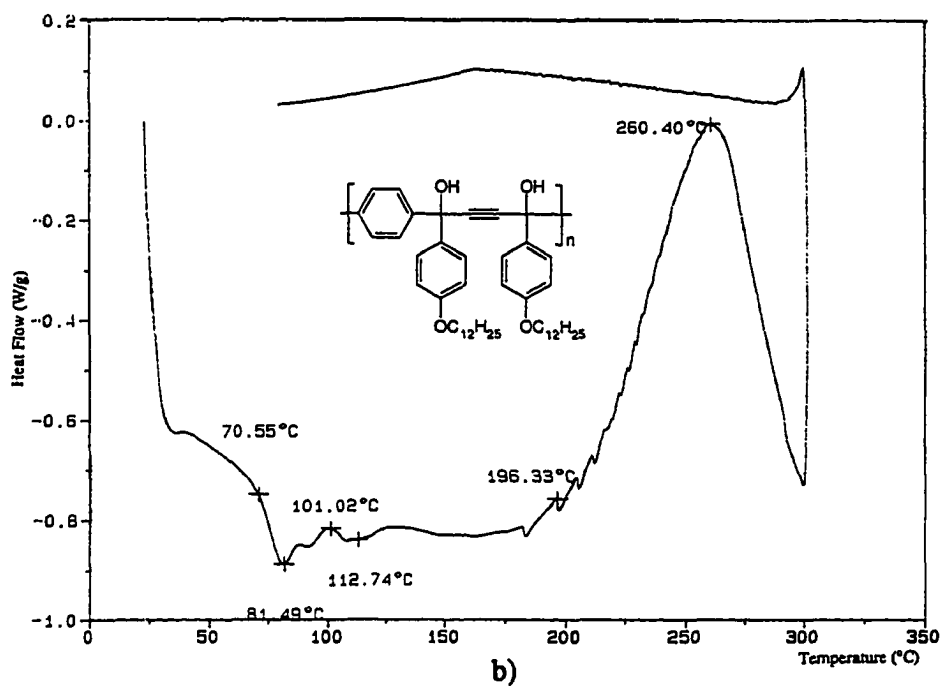
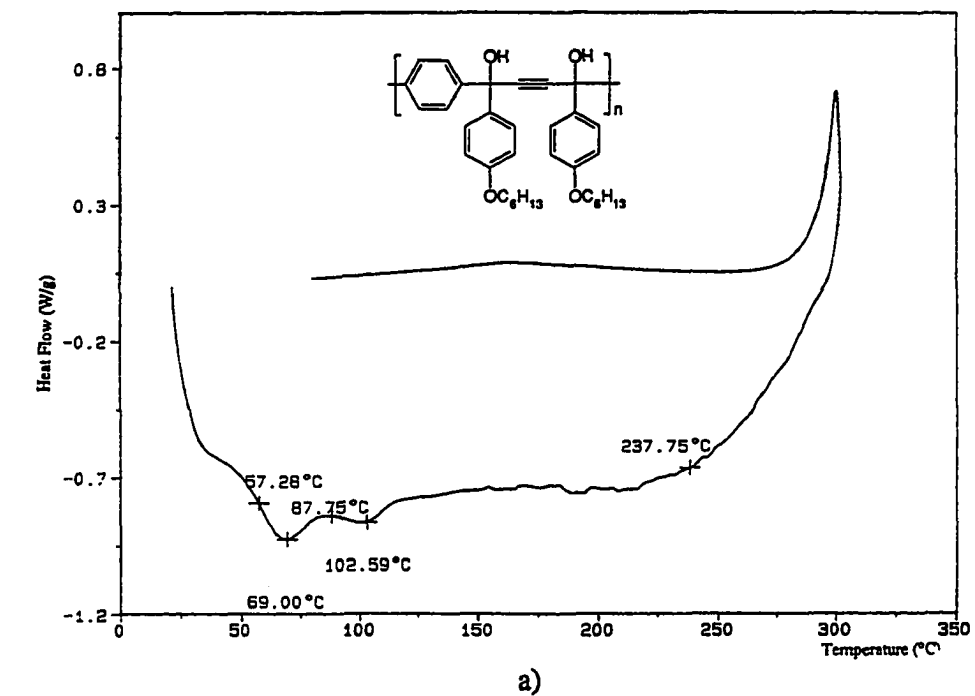


Figure 5. DSC thermogram of a) polymer 27a and b) polymer 27b.

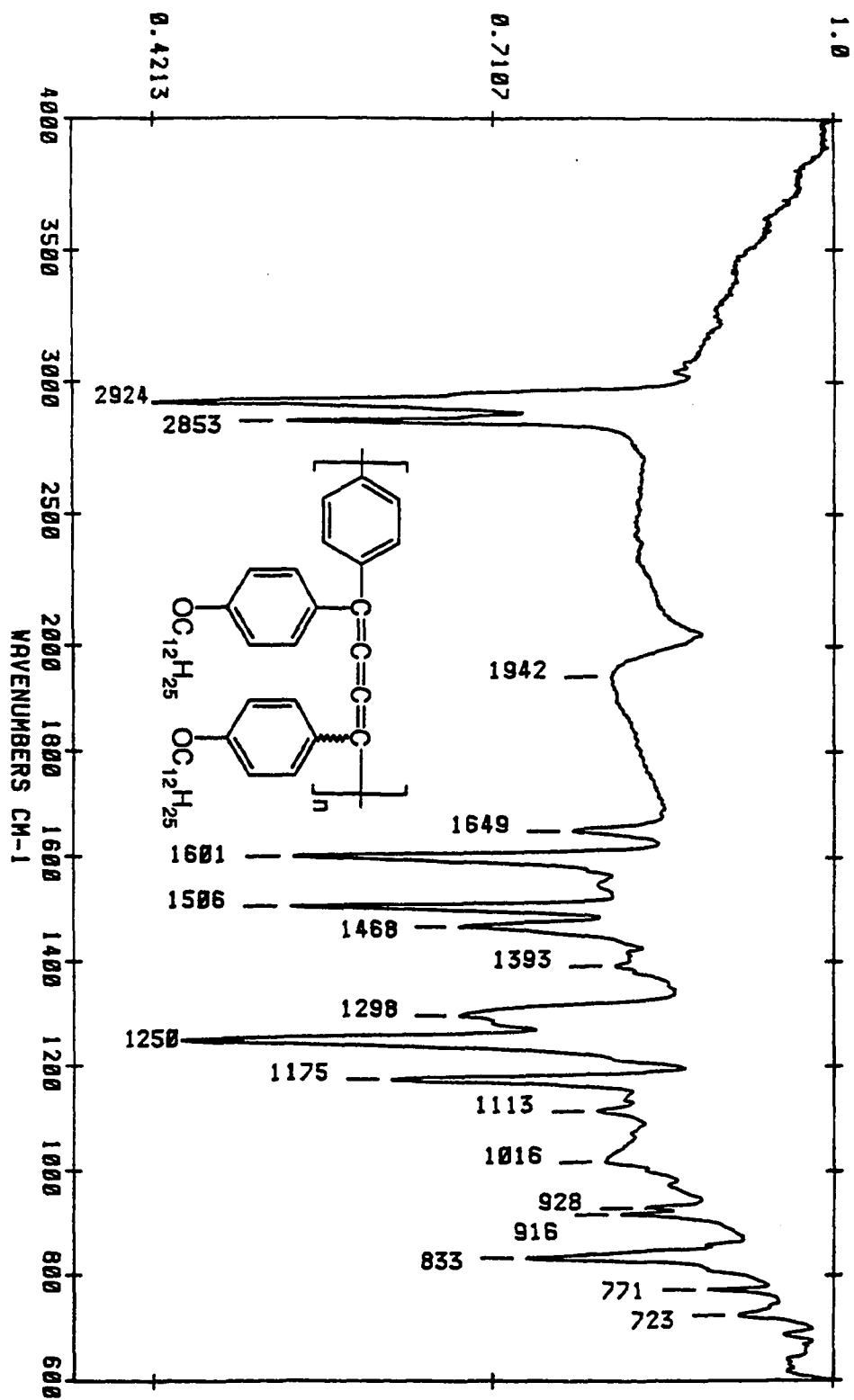


Figure 6. FTIR spectrum of polymer 28b.

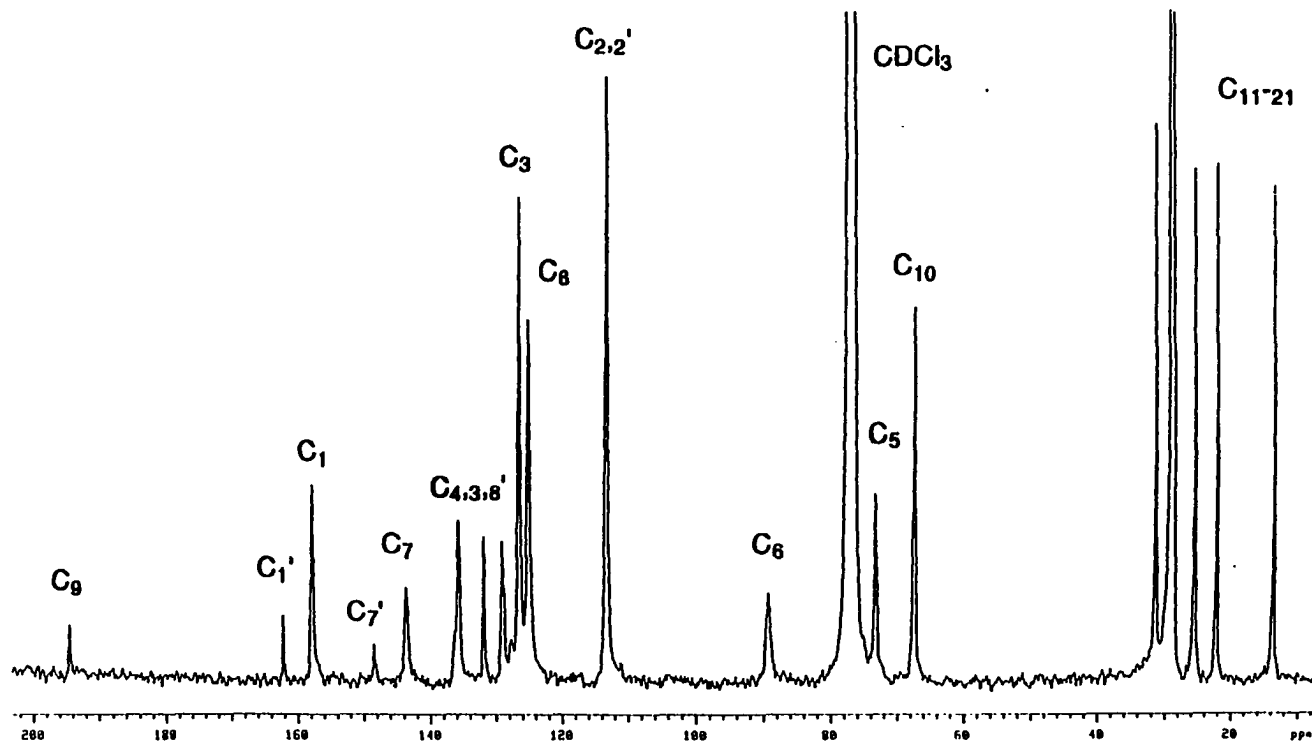
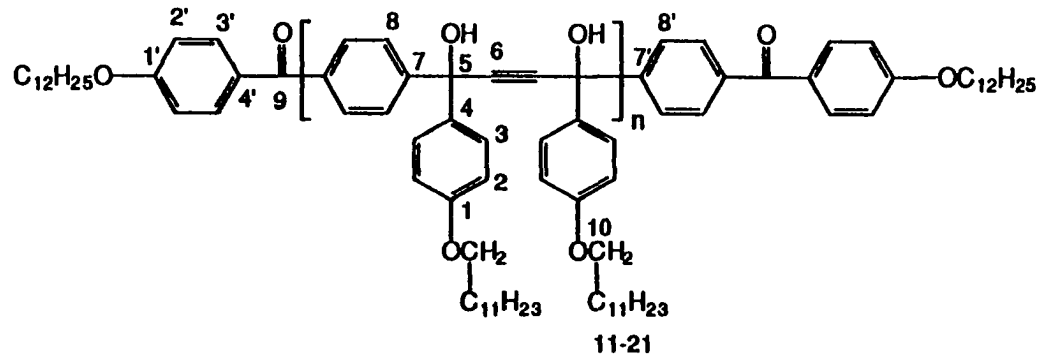


Figure 7. ¹³C-NMR spectrum of polymer 27b.

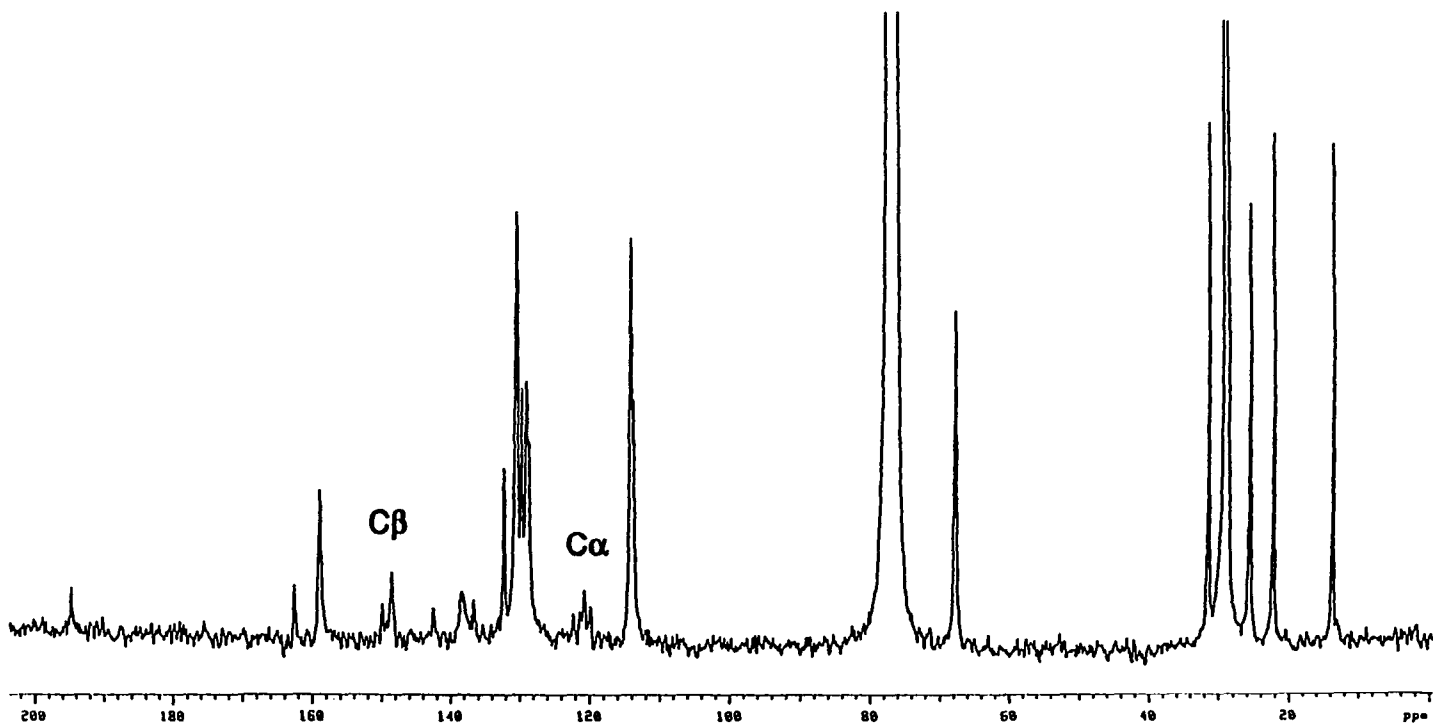
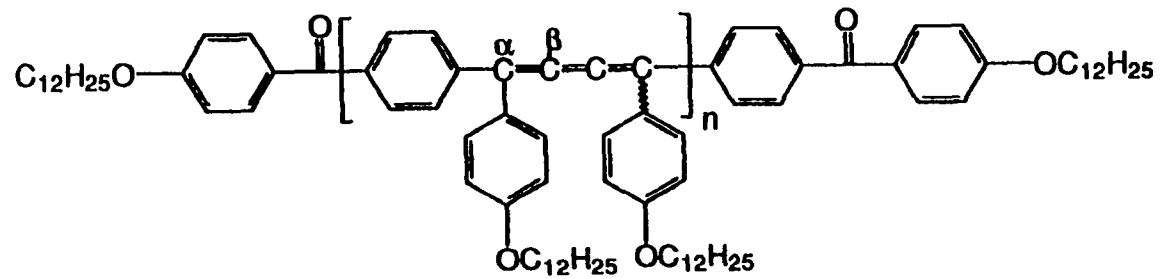


Figure 8. ^{13}C -NMR spectrum of polymer 28b.

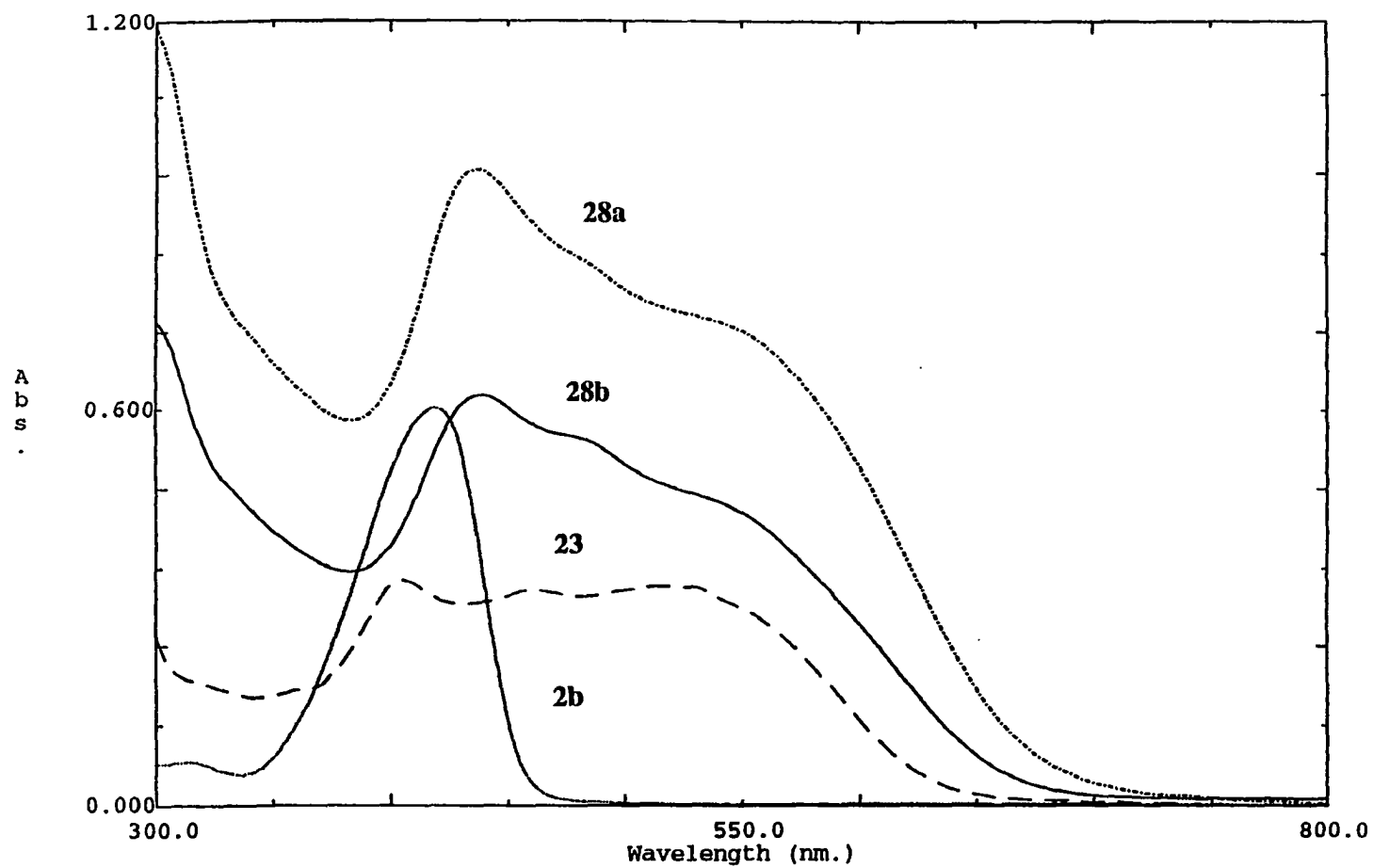


Figure 9. UV-VIS absorption spectra of 2b, 23, 28a, and 28b.

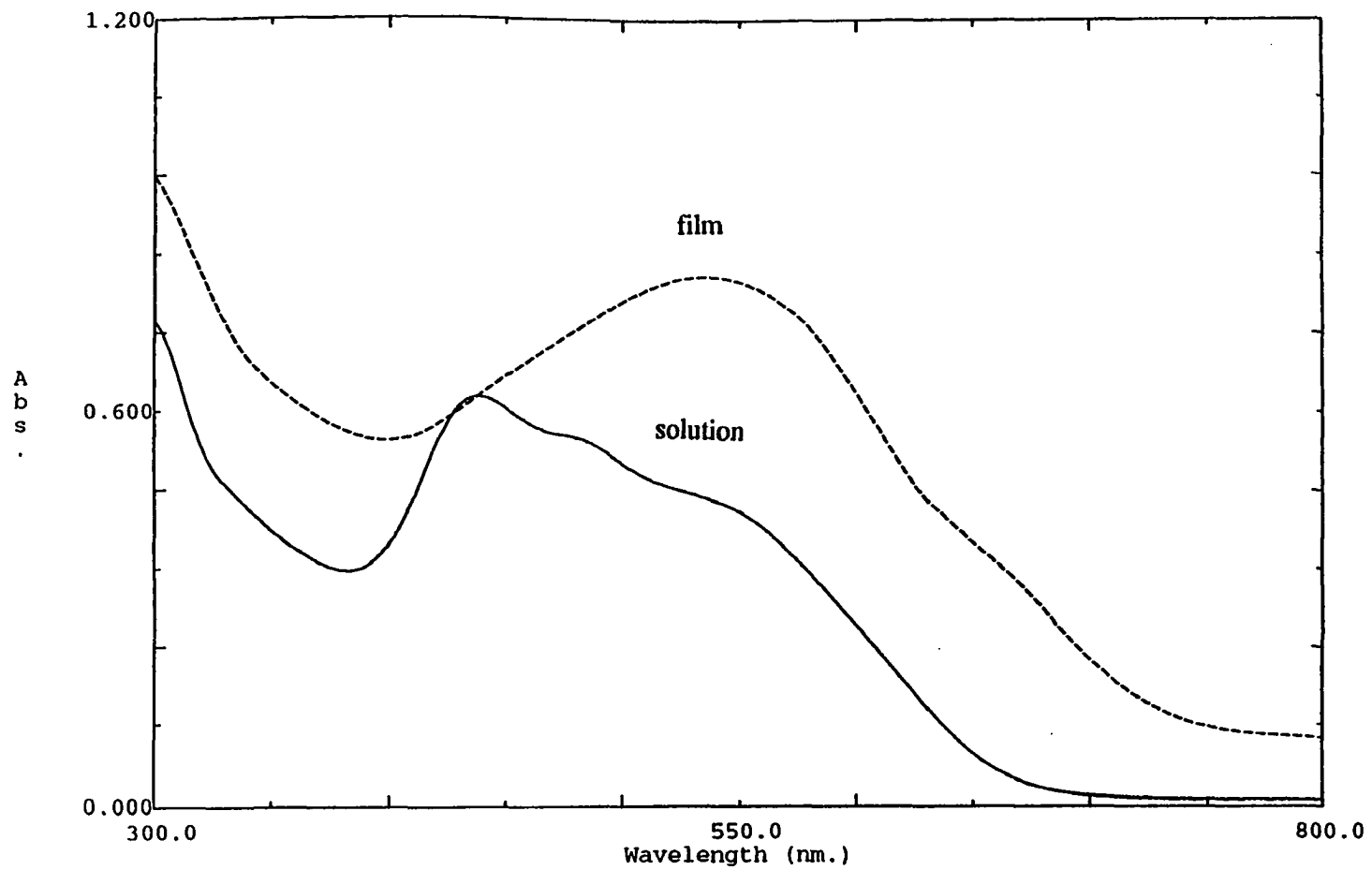


Figure 10. Solution and film UV-VIS absorption spectra of polymer 28b.

Electrical conductivity of polymer 28a and 28b.

The cumulene-containing conjugated polymers, like all organic polymers, are insulators when undoped. The conductivity of spin-coated polymer film was measured by two in-line probes. Polymer 27a has a conductivity of 10^{-7} s/cm and 28b has a conductivity of 4.1×10^{-7} s/cm. A brief exposure to an iodine atmosphere (doping), however, raises the conductivity of 28a to 1.2 s/cm and that of 28b to 0.90 s/cm. After exposure of the polymer (undoped) to air for more than three month, the doped conductivity remained as high as measured for a freshly prepared sample. Attempts to observe the charge transfer band in UV-VIS region in polymer solution and film were not successful because the UV-VIS absorption of iodine ($\lambda_{\text{max}}^{\text{THF}} = 447$ nm) superimposes the absorption of polymers 28 a and 28b.

ESR study of polymer 28a.

The dramatic conductivity increase upon iodine vapor doping is interpreted by the formation of polarons upon iodine doping (polarons are delocalized radical ions which are radical cations in this iodine-doping case). This is supported by an ESR study of polymer 28a. The undoped and I₂-doped ESR spectra of 28a were shown in Fig. 11. The ESR spin density of undoped polymer is very low, $N_S = 3.4 \times 10^{14}$ spins/g (2.7×10^{-7} spins per repeating unit), and the derivative peak-to-peak width is $\Delta H_{\text{pp}} \approx 2.7\text{G}$. It is interesting to compare the behavior of the ESR of polymer 28a to that of polydiethynylsilanes (PDES)¹⁶⁹, since these later polymers exhibit a behavior similar to that of polymer 28a: their undoped and doped conductivities are similar, and they are also essentially nonluminescent. In the undoped PDES prepared from the hydrogenated monomers, $\Delta H_{\text{pp}} \approx 10\text{G}$, and the spin density is $\sim 7.1 \times 10^5$ spins per repeat unit. However, when the PDES is prepared from the deuterated monomers, $\Delta H_{\text{pp}} \approx 3.6\text{G}$. It therefore appears that in the PDES, as well as in other π -conjugated polymers, the major source of the line width is the hyperfine coupling with protons. The narrow ESR line width of the undoped polymer 28a therefore suggests that hyperfine coupling with ¹H is very weak. This observation and conclusion are consistent with localization of the spin defects on the -C=C=C=C- segments of the polymer 28a.

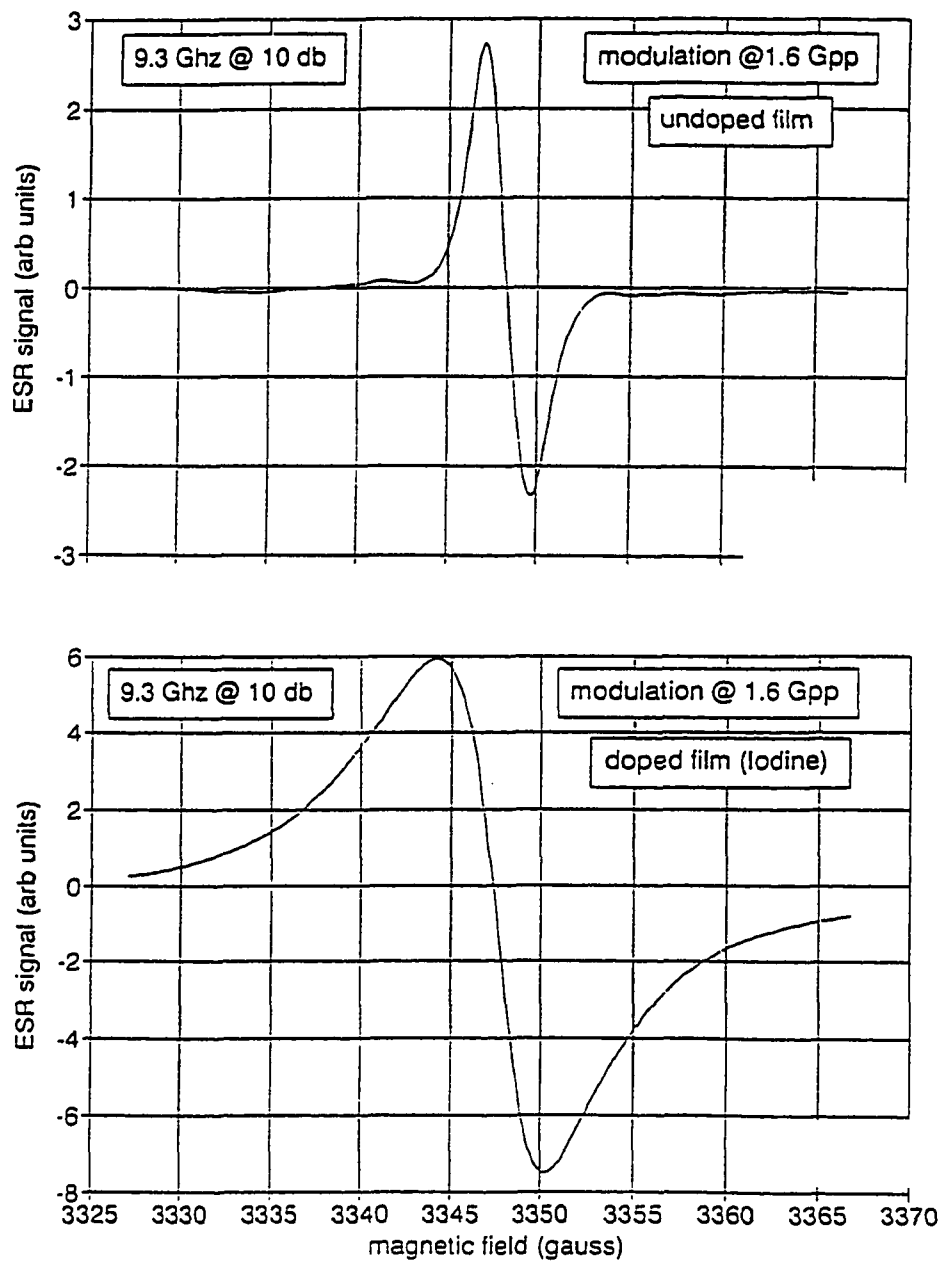


Figure 11. ESR spectra of undoped and iodine-doped film of polymer 28a.

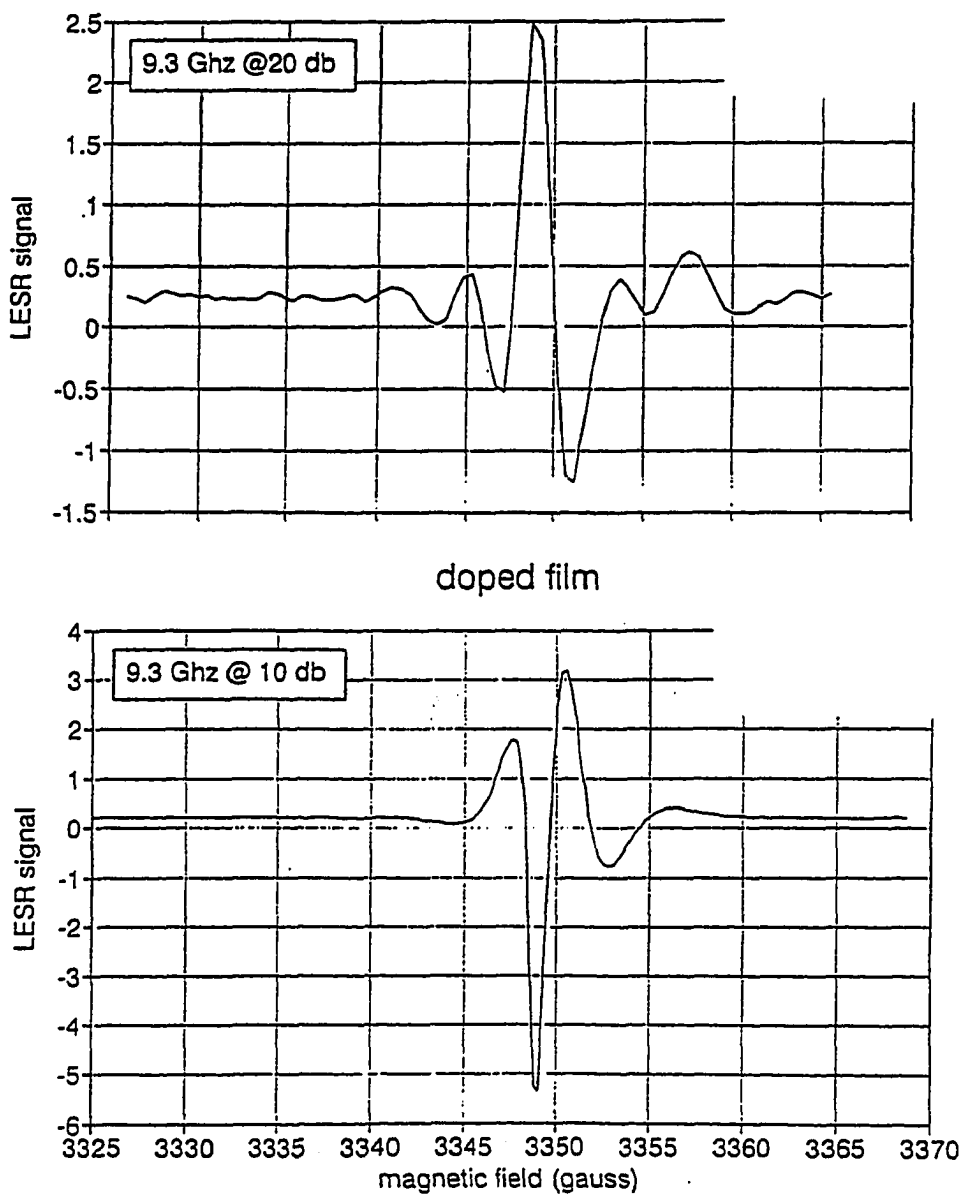


Figure 12. Light induced ESR of polymer 28a.

Upon exposure of polymer 28a to iodine vapor at room temperature, N_s increases to $\sim 1.2 \times 10^{17}$ spins/g (1×10^4 spin per repeating unit), and ΔH_{pp} increases to 5.9G. The values are also comparable with those observed in PDES: in these latter materials prepared from hydrogenated monomers, addition of iodine to PDES solutions initially decrease the ΔH_{pp} to ~ 3.4 G. However, upon heavier doping of up to 40 wt.%, ΔH_{pp} increases to ~ 7 G. It therefore appears that the behavior of the doping induced ESR of polymer 28a is similar.

Finally, polymer 28a also exhibited a light-induced ESR similar to that of the PDES as shown in Fig. 12. The strikingly similar behavior of polymer 28a suggests a similar electronic structure. The absence of photoluminescence in these polymers, similar to *trans*-polyacetylene, but in contrast to many other π -conjugated systems, such as polythiophenes and poly(*p*-phenylenevinylene)s, etc., is consistent with the hypothesis that the lowest singlet excited state is the dipole-forbidden 2^1A_g . In the luminescent polymers, it is widely believed that the lowest excited singlet state is dipole-allowed $1B_u$.¹⁷⁰

Non-linear optical susceptibilities of polymer 28b.

Z-scan technique. In a typical Z-scan experiment (Fig. 13), the transmittance of a sample ($D2/D1$) is measured through a finite aperture in the far field as the sample is moved along the propagation path (z) of a focused Gaussian beam. The sign and the magnitude of the nonlinear refraction are deduced from such a transmittance curve (Z-scan).¹⁷¹

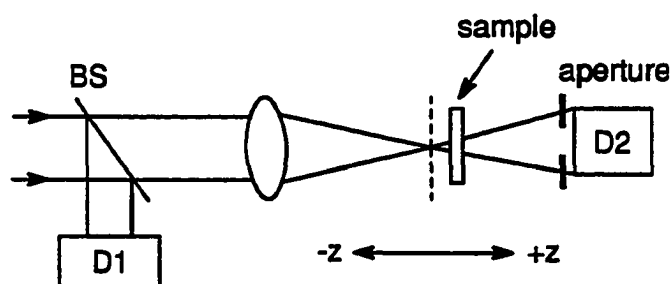


Figure 13. The Z-scan experimental apparatus.¹⁷¹

Apparatus. Nonlinear studies necessitate the use of short pulses at low repetition rates. Short pulses provide high peak powers and probe the more desirable fast nonlinear mechanisms. Slow repetition rates are required to ensure that the observed effects are not due to accumulated long-time effects which may occur when there is insufficient relaxation time between pulses. To satisfy these requirements we used a frequency doubled Nd: YAG Regenerative Amplifier with a 50 Hz repetition rate to pump a Dye Amplifier containing kiton red. This combination provided us 590 nm, 10 psec light pulses at 1 kHz repetition rate and with intensities up to 60 GW/cm².

Low intensity scans were also conducted following each high intensity scan. This was done to insure that the observations were not due to surface inhomogeneities caused by film deposition at the glass solution interface. Closed and open aperture Z scans were performed on the toluene and chloroform solvents alone to determine their contributions any measured $\chi^{(3)}$ effect. The contributions were small, on the order of 10⁻¹⁴ esu. The system was calibrated and validated by measuring the third order nonlinearity of CS₂, $\text{Re}\chi^{(3)}$, to be + 2.0 x 10⁻¹² esu.

Intensity-dependent third order nonlinear susceptibility of polymer 28b. Both the real and imaginary parts of $\chi^{(3)}$ were evaluated with the Z scan technique at 590 nm using closed and open apertures, respectively. Open aperture Z scans on polymer 28b at 590 nm with intensity between 0.16 GW/cm² and 15 GW/cm² are shown in Figures 14-16. Intensity higher than 15 GW/cm² could damage the polymer sample permanently. While a sharp Z-scan curve was obtained when the lowest intensity (0.16 GW/cm²) was applied (Fig. 14), as the intensity was increased, a dip at the top of the Z-scan curve was observed (Fig 15). When the highest intensity (15 GW/cm²) was used, the deepest dip was observed in the Z-scan curve (Fig. 16).

This is explained by the intensity-dependent saturation effect. As shown in Fig. 17, the positive third order nonlinearity due to two photon absorption (TPA), $\chi^{(3)}_{\text{TPA}}$, is independent of intensity. However, the magnitude of the negative third order nonlinearities due to saturation effects, $\chi^{(3)}_{\text{SAT}}$, increase as the intensity increases (the absolute values of $\chi^{(3)}_{\text{SAT}}$ decrease). Because of the decrease in the absolute values of $\chi^{(3)}_{\text{SAT}}$ with increasing intensity,

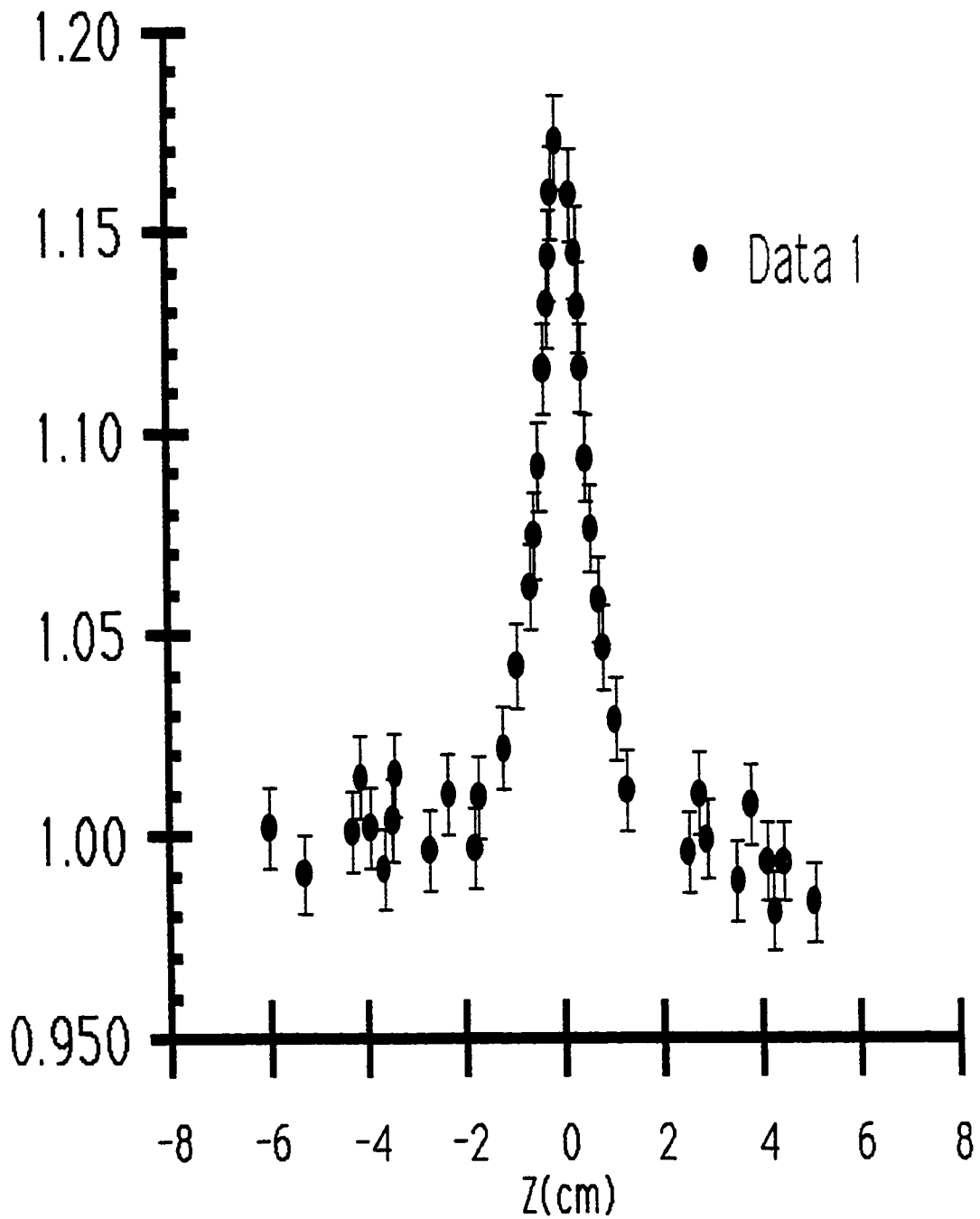


Figure 14. Open aperture Z-scan (intensity = 0.16 GW/cm^2 , lowest used).

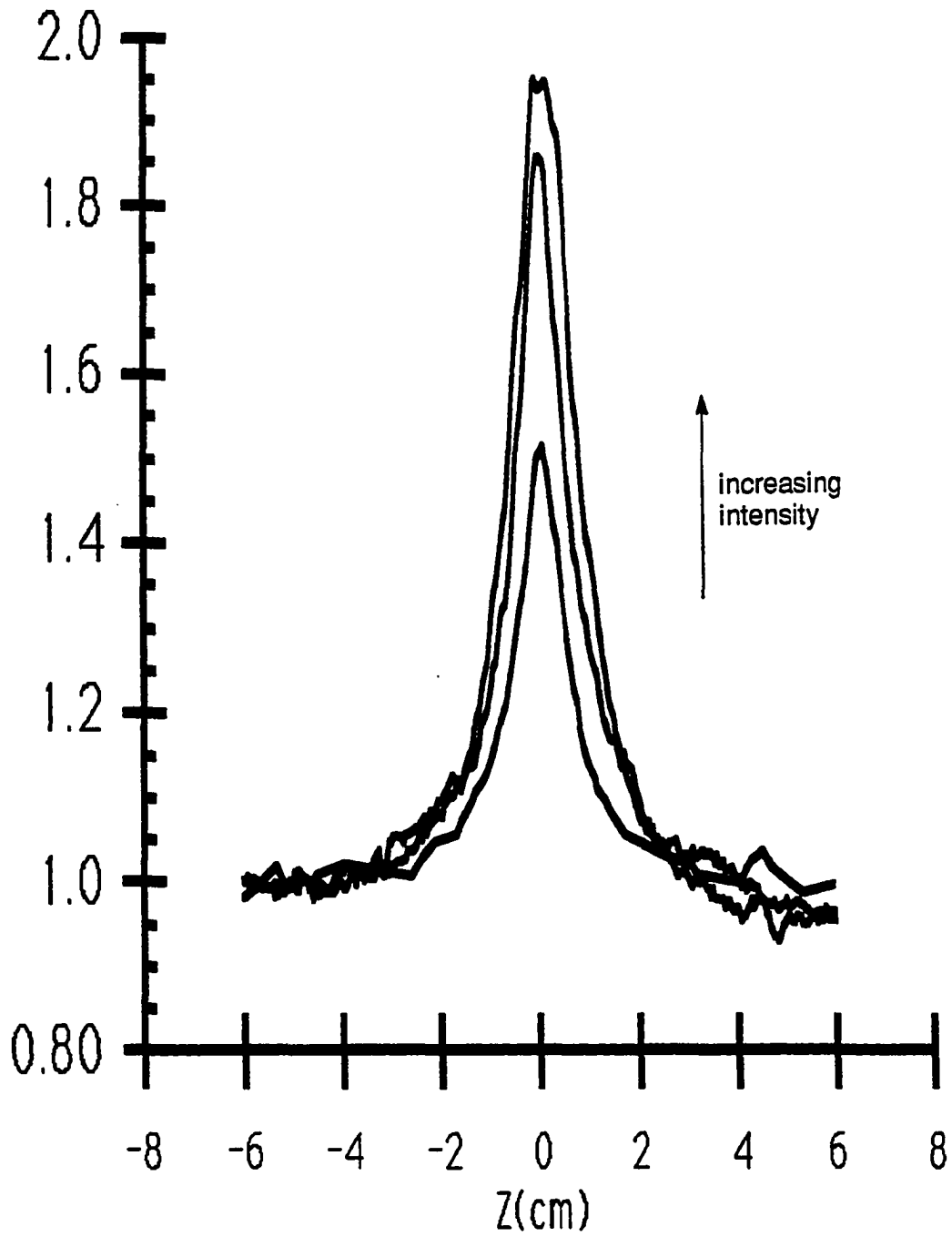


Figure 15. Open aperture Z-scan at increasing intensities.

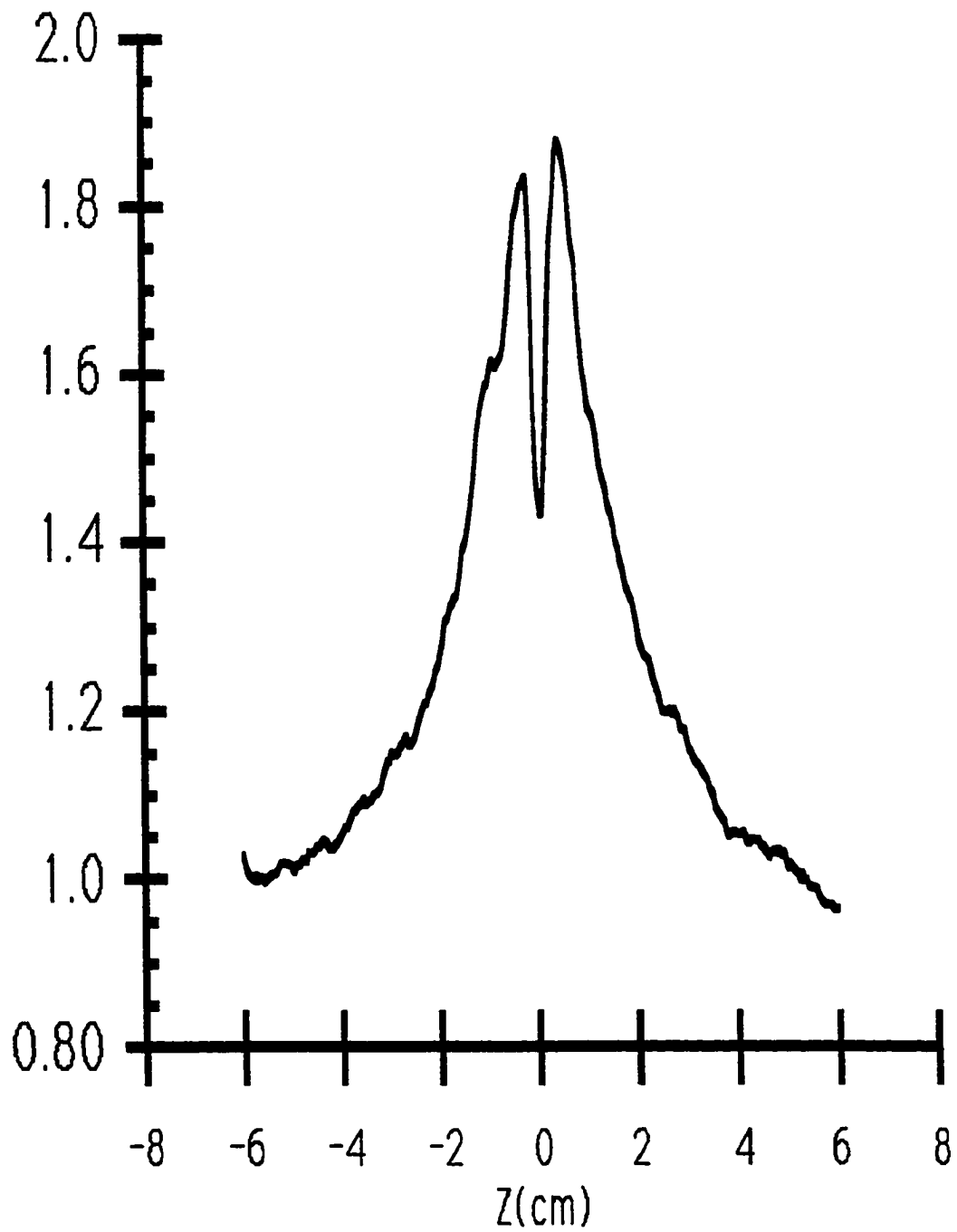


Figure 16. Open aperture Z-scan (intensity = 15.0 GW/cm², highest used).

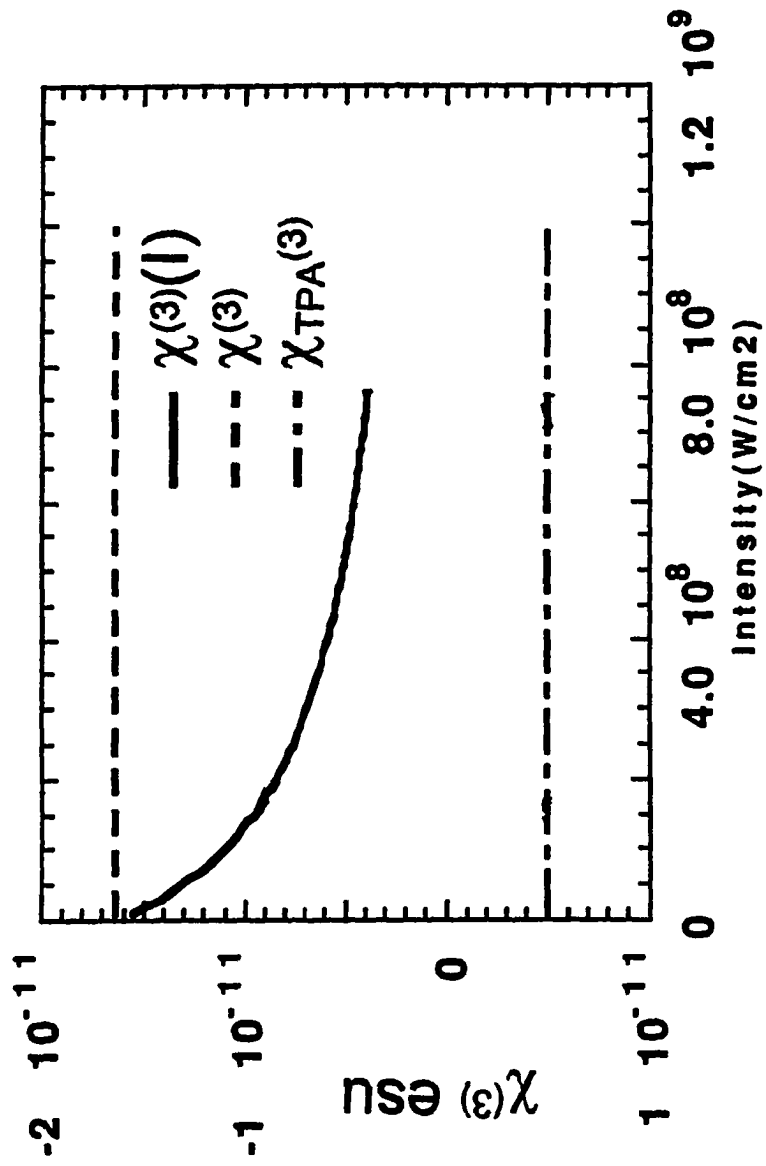


Figure 17. Intensity-dependent $\chi^{(3)}$ of polymer 28b.

two photon absorption is observed at higher intensity in the Z-scan curve which reflects the total third order nonlinearity.

This intensity-dependent saturation effect can be explained by either higher order nonlinear susceptibility terms or by saturation due to phase space-filling. Approximation by adding in higher order terms until a reasonable curve fit is obtained according to the following formula makes the problem computationally intractable and physically unrealistic.

$$\chi^{(3)}(I) = \chi^{(3)} + \chi^{(5)} I + \chi^{(7)} I^2 + \dots$$

Instead, assume one-photon saturation and $\chi^{(3)}$ due to two photon resonance, the linear susceptibility is expressed as:

$$\chi^{(1)}(I) = \frac{\chi_0^{(1)}}{\sqrt{1 + \frac{I}{I_s}}} + \chi^{(3)} I$$

Expand the above equation in Taylor series to get (where I_s is the saturation intensity):

$$\chi^{(1)}(I) = \chi_0^{(1)} - \frac{\chi_0^{(1)}}{2I_s} I + \frac{(\chi_0^{(1)})^2}{4I_s^2} I^2 - \dots + \chi^{(3)} I$$

Two terms of $\chi^{(3)}$ are evident:

$$\chi_{TOT}^{(3)} = \chi_{SAT}^{(3)} + \chi_{TPA}^{(3)}$$

where,

$$\chi_{SAT}^{(3)} = -\frac{\chi_0^{(1)}}{2I_s}$$

According to the approximation of one-photon saturation and $\chi^{(3)}$ due to two photon resonance, simulations of open aperture Z-scan curves with increasing intensity are shown in Fig. 18 and they are very well matched with the experimentally measured Z-scan curves (Fig. 14-16).

Based on the curve-fitting of the open aperture (both high concentration and low concentration) and closed aperture Z-scan curves shown in Fig. 19-21, the real and imaginary part of the third order nonlinearity of polymer 28b was measured to be:

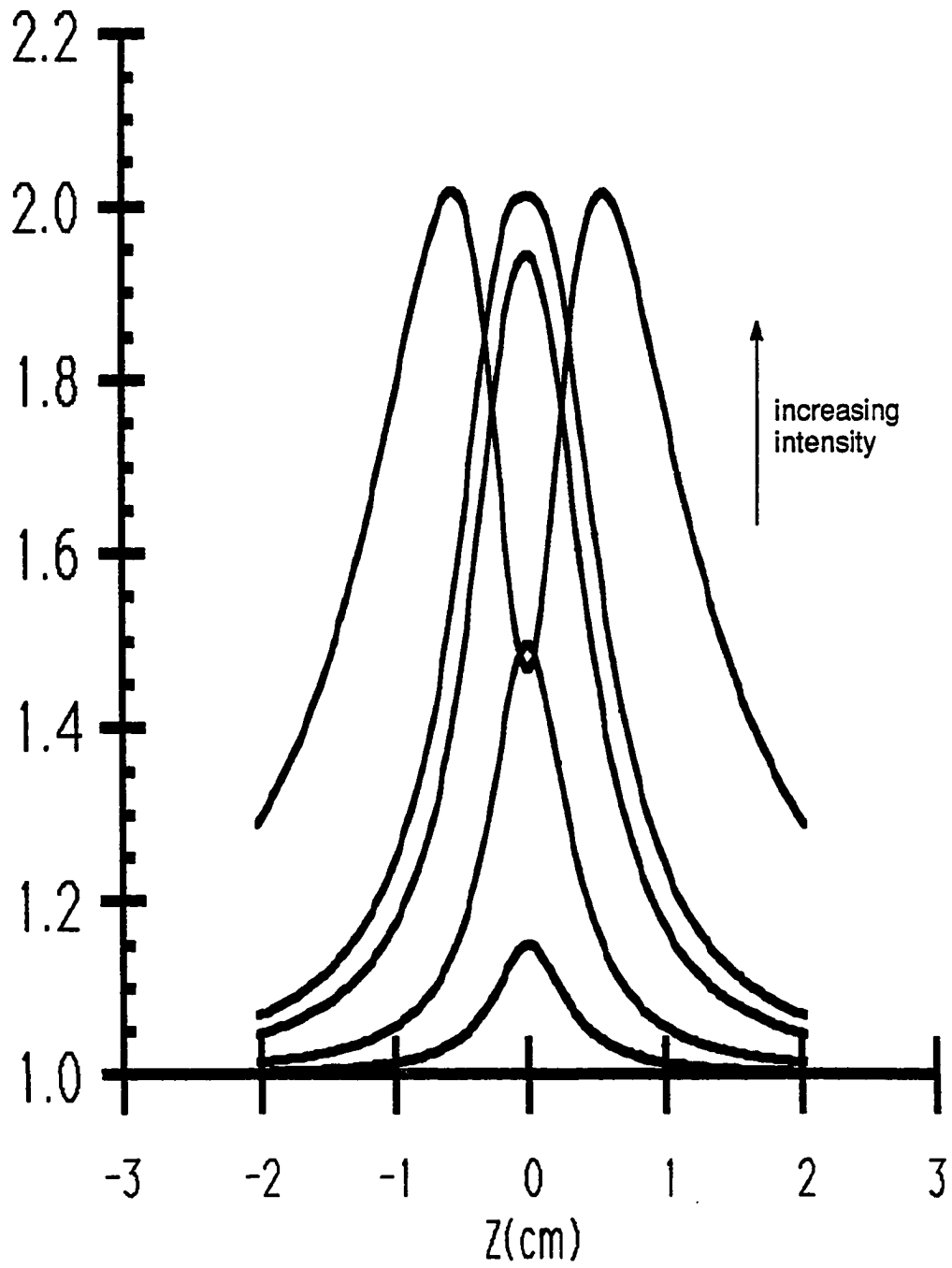


Figure 18. Open aperture simulations with increasing intensity.

$$\text{Re } \chi_{SAT}^{(3)} = -1.0 \times 10^{-11} \text{ esu},$$

$$\text{Re } \chi_{TPA}^{(3)} = -6.6 \times 10^{-12} \text{ esu},$$

$$\text{Im } \chi_{SAT}^{(3)} = -3.3 \times 10^{-12} \text{ esu},$$

$$\text{Im } \chi_{TPA}^{(3)} = +5.8 \times 10^{-12} \text{ esu},$$

$$|\chi_{TOT}^{(3)}| = 3.2 \times 10^{-11} \text{ esu}$$

The molecular second hyperpolarizabilities $\langle \gamma \rangle$ based on $\chi^{(3)}$ due to two photon resonance are calculated according to the following formula:

$$\langle \gamma \rangle = \frac{\chi_{TPA}^{(3)}}{L^4 N}$$

where N is the number density (cm^{-3}) and L is the Lorentz-Lorentz correction due to the local field. The real and imaginary part of the second hyperpolarizabilities of polymer **28b** are:

$$\langle \gamma \rangle_{\text{RE}} = -7.5 \times 10^{-30} \text{ esu},$$

$$\langle \gamma \rangle_{\text{IM}} = +6.5 \times 10^{-30} \text{ esu},$$

$$|\langle \gamma \rangle| = 1.0 \times 10^{-29} \text{ esu}$$

Z-scan technique makes it possible to distinguish the part of $\chi^{(3)}$ that is an effective nonlinearity due to saturation and the part that is due to two photon resonance. This can not be accomplished by the degenerate four-wave mixing (DFWM) technique. The second hyperpolarizability $\langle \gamma \rangle$ measured for polymer **28b** is about two orders of magnitude higher than the cumulene molecule with the highest second hyperpolarizability ($\langle \gamma \rangle = 10^{-31}$ esu) reported by Prasad.¹⁶² Compared to the corresponding model compound **2b**, the increase is four orders of magnitude. Also it is worth pointing out that with the DFWM technique, the saturation effect and the two photon resonance can not be distinguished. The second hyperpolarizability $\langle \gamma \rangle$ measured is actually higher than what it should be. Introducing the cumulene units into polymer chain is a very effective way to synthesize materials with high third order nonlinearities.

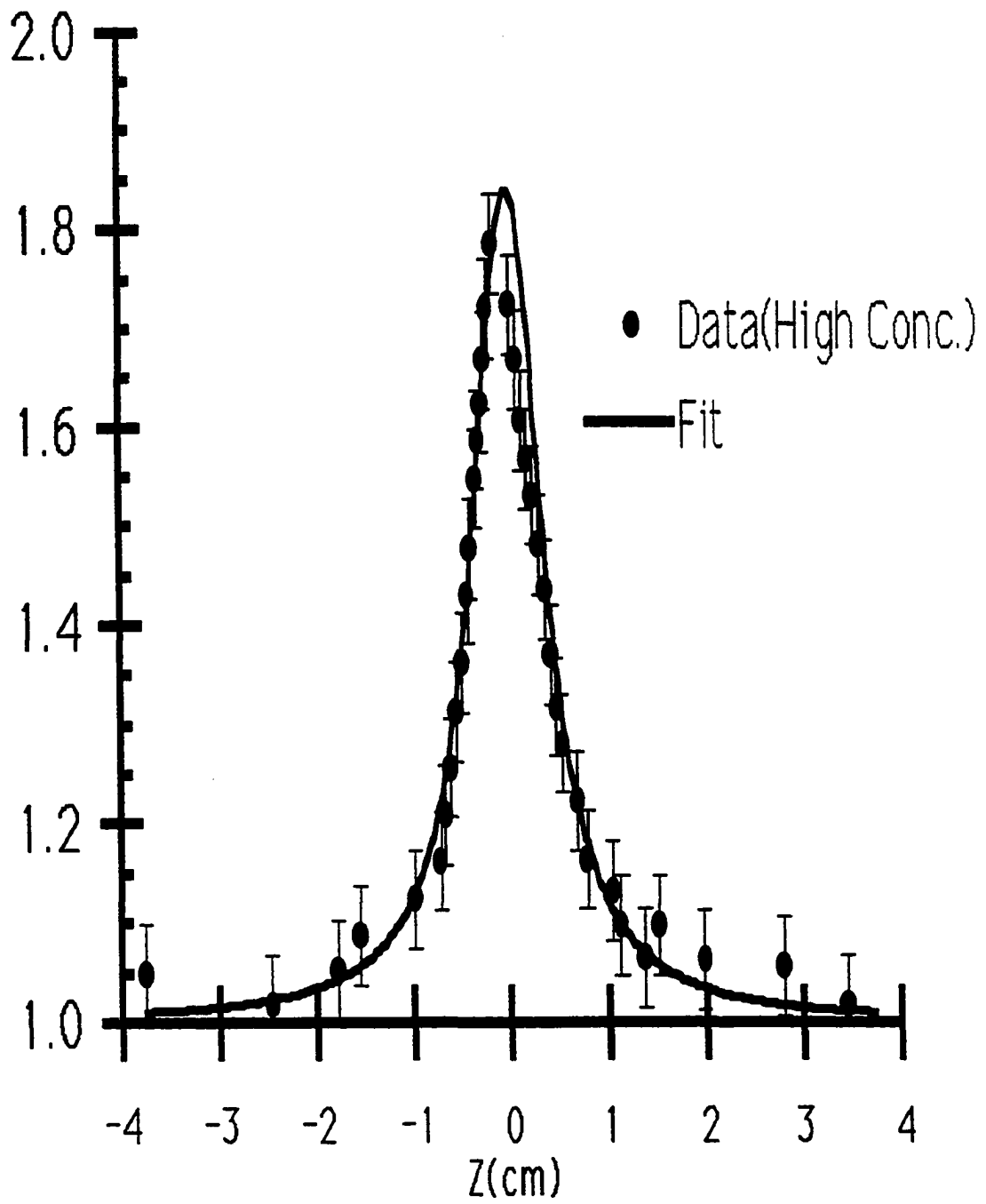


Figure 19. Open aperture Z-scan curve-fitting (high concentration).

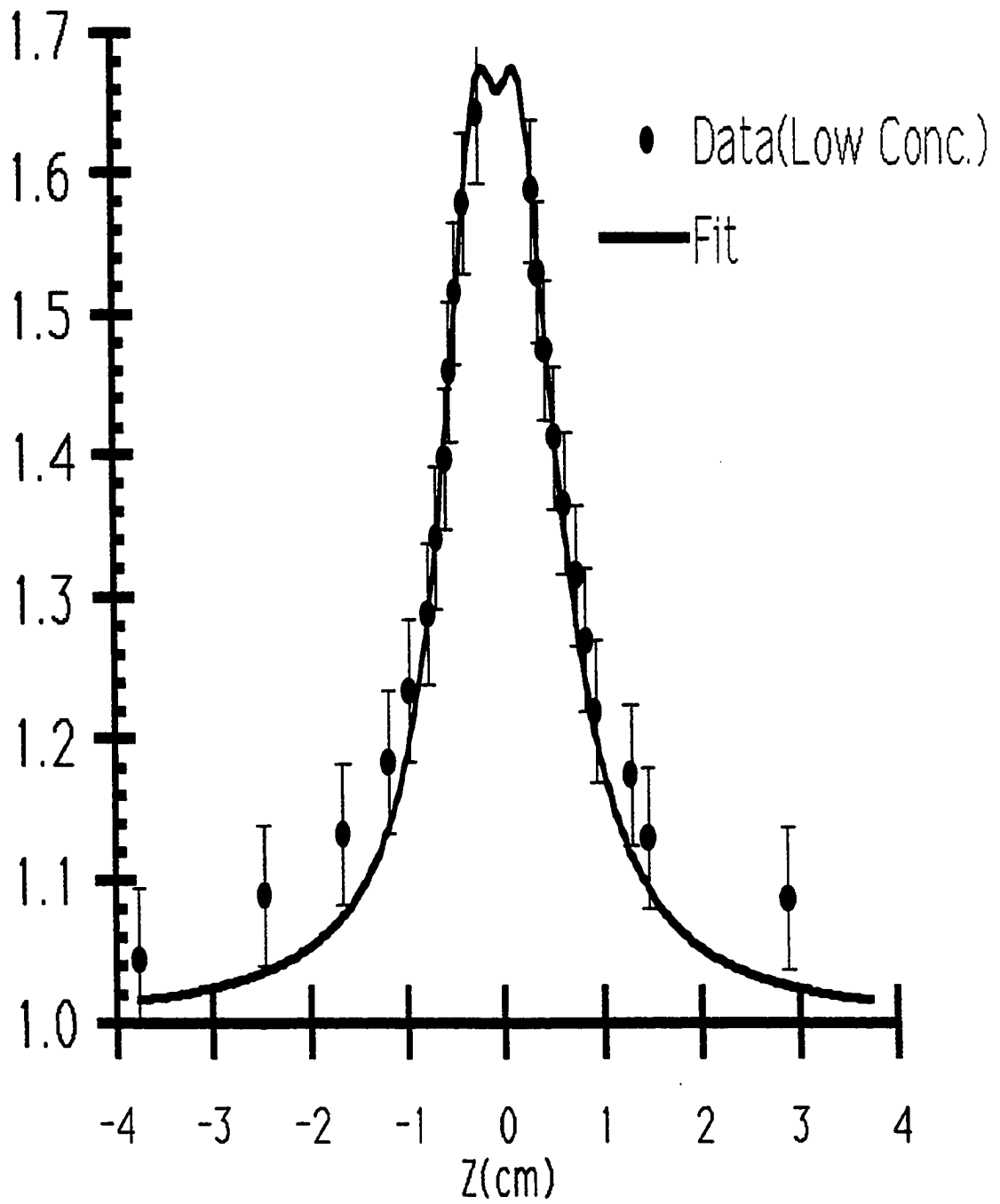


Figure 20. Open aperture Z-scan curve-fitting (low concentration).

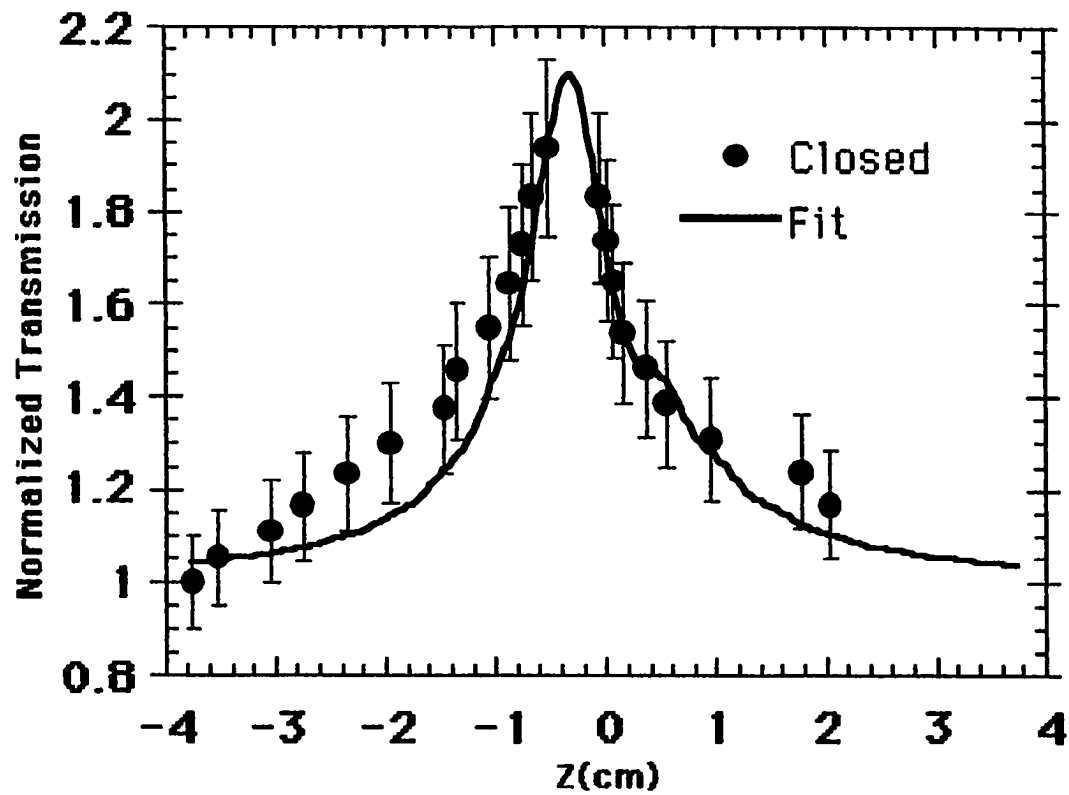


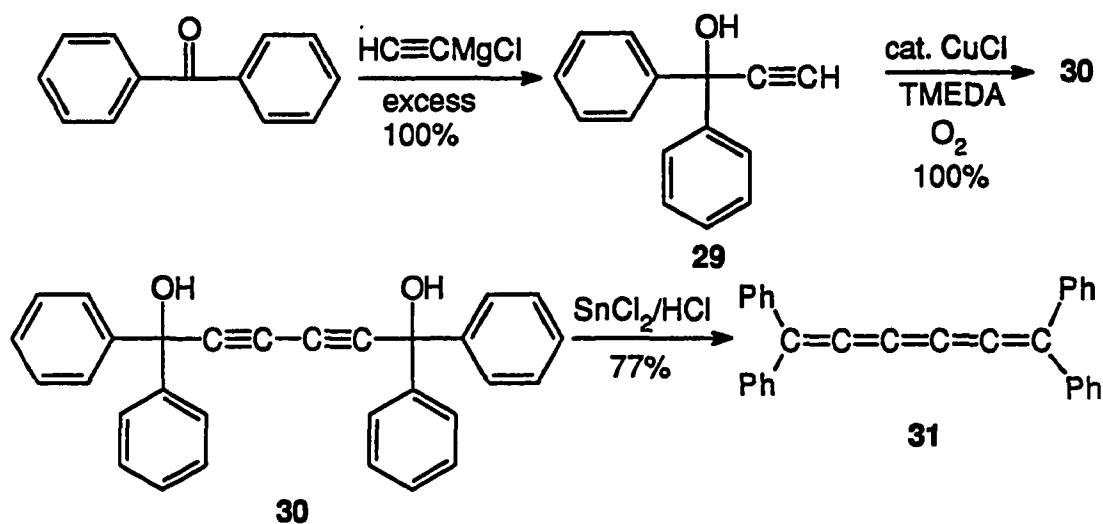
Figure 21. Closed aperture Z-scan curve fitting.

The off resonance third order nonlinearity of polymer **28b** and third order nonlinearity of other cumulene-containing polymers are in the process of being measured.

Synthesis and study of higher-order cumulene-containing conjugated polymers - poly(*p*-phenylene hexapentaene).

From the above discussions, we have seen that poly(phenylene butatriene)s are conjugated polymeric materials with promising third order nonlinear optical properties. From Prasad's report,¹⁶² we have seen that when the order of cumulene was increased from tetraphenylbutatriene to tetraphenylhexapentaene, the second order hyperpolarizability $\langle\gamma\rangle$ increased by almost one order of magnitude. The obvious question is : will introduction of higher-order cumulene units into a conjugated polymer main chain further increase the third order nonlinear optical response of the material?

The synthesis of hexapentaene-containing conjugated polymers is based on the cuprous catalyzed oxidative coupling reaction of acetylenes.¹⁷³ The model reaction is shown in Scheme 6:



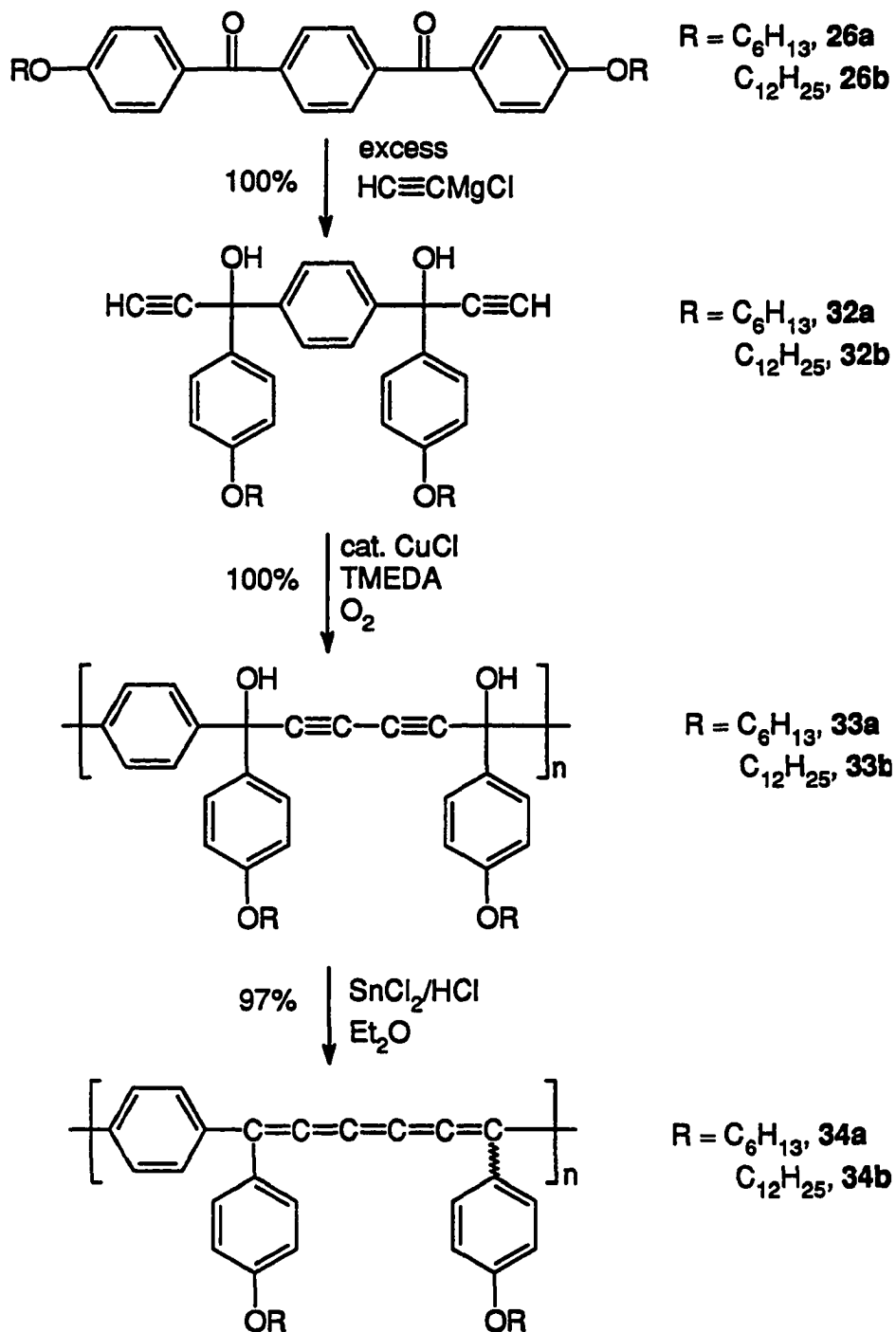
Scheme 6. Synthesis of 1,1,6,6-tetraphenyl-1,2,3,4,5-hexapentaene (**31**).

Reaction of benzophenone with ethynyl magnesium chloride affords 1,1-diphenyl-2-propyn-1-ol (**29**) in quantitative yield. Oxidative coupling of **29** with catalytic cuprous chloride/TMEDA complex gave 1,1,6,6-tetraphenyl-2,4-hexadiyne-1,6-diol (**30**) in 100% yield. 1,1,6,6-Tetraphenyl-1,2,3,4,5-hexapentaene (**31**), a red crystal, was then obtained in 77% yield from the reduction of **30**. The cuprous-catalyzed oxidative coupling reaction of acetylenes is very attractive for polymer synthesis because it is a very clean reaction, the desired product is usually obtained in quantitative yield and requires only mild reaction conditions.

Following similar synthetic route as that shown above for tetraphenylhexapentaene, hexapentaene-containing polymers were synthesized as shown in Scheme 7. First, reaction of 1,4-bis(*p*-alkoxybenzoyl)benzene **26a** or **26b** with ethynyl magnesium chloride gave diacetylene monomers **32a** or **32b**, viscous liquids with slightly yellow color, in quantitative yield. Oxidative coupling of compound **32a** or **32b** afforded polymer **33a** or **33b**, faint yellow powders, in 100% yield.

According to GPC, the molecular weights of polymers **33a** and **33b** are relatively high, for polymer **33a**: $M_w = 2.18 \times 10^4$, PDI = 2.62; for polymer **33b**: $M_w = 2.80 \times 10^4$, PDI = 3.07. Both polymer **33a** and **33b** have excellent film forming ability. In FTIR, the hydroxyl groups absorb at 3427 cm^{-1} and 3422 cm^{-1} respectively for polymers **33a** and **33b**. From the quantitative ^{13}C -NMR spectrum of polymer **33b** in Fig. 22, we can see that polymer **33b** obtained is very clean. The chemical shifts of acetylenic carbons are at 82.49 ppm and 74.03 ppm, and the chemical shift of the carbon attached to hydroxyl group is at 70.75 ppm. DSC analysis shows that polymer **33a** has a very small endothermic peak at $\sim 88^\circ\text{C}$ and an exothermic reaction starts at $\sim 168^\circ\text{C}$. Polymer **33b** has a very small endothermic peak at $\sim 106^\circ\text{C}$ and an exothermic reaction starts at $\sim 131^\circ\text{C}$ (Fig. 23).

Reduction of the polymers **33** to give polymers **34** proceeds smoothly with almost quantitative yield. However, the workup process for this reduction reaction is a little tricky. After the reduction is finished, the reaction solution is a purple homogeneous solution with no precipitated polymers. The UV-VIS absorption spectra were obtained from this solution.

Scheme 7. Synthesis of poly(*p*-phenylene hexapentaene)s.

The purple solution was then poured into methanol and black polymers precipitated out. The precipitated polymers were quickly filtered and washed with dilute hydrochloric acid and methanol and then dried under vacuum. Polymer 34b so obtained is readily soluble in common organic solvents but needs to be kept under argon or vacuum to avoid becoming an insoluble material. No matter how fast the workup procedure was performed, polymer 34a, after being precipitated out in methanol could not be redissolved in common organic solvents.

Polymer 34b with longer alkoxy side chains are more stable than polymer 34a. Even though the exact reasons for polymer 34 becoming insoluble are not known, steric hindrance from the longer alkoxy side chains preventing the interchain crosslinking of the hexapentaene units is a likely explanation for the better stability of polymer 34b.

The hexapentaene units in polymer 34a absorb 2000 cm^{-1} and hexapentaene units in polymer 34b absorb at 2002 cm^{-1} in FTIR. DSC analysis shows that an exothermic reaction starts at -150°C for polymer 34a and an exothermic reaction starts at -105°C for polymer 34b. From the DSC thermograms of butatriene-containing polymer 28b and hexapentaene-containing polymer 34b shown in Fig. 24, we can see that neither polymer melts. While a fast exothermic reaction starts for polymer 28b at -125°C , a slow exothermic reaction starts at -105°C for polymer 34b. Because polymer 34a can not be redissolved in common organic solvents, only polymer 34b was characterized by solution NMR. In tetraphenylhexapentaene, the most diagnostic carbon is the $\beta\text{-C}$ at 149.42 ppm. However, in ^{13}C -NMR spectrum of polymer 34b (Fig. 25), only a weak peak was observed at 148.59 ppm and the hexapentaene structure can not be established exclusively from the ^{13}C -NMR study. Polymer 34a and 34b have almost identical UV-VIS absorption spectra with strong absorption between 400-600 nm and the absorption tails until 800 nm, $\sim 70\text{ nm}$ red shift is observed compared to polymer 28a (Fig. 26).

Surprisingly, polymer 34b, even after doped with iodine vapor, remains a insulator. The third order nonlinear optical properties are still in the process of being measured.

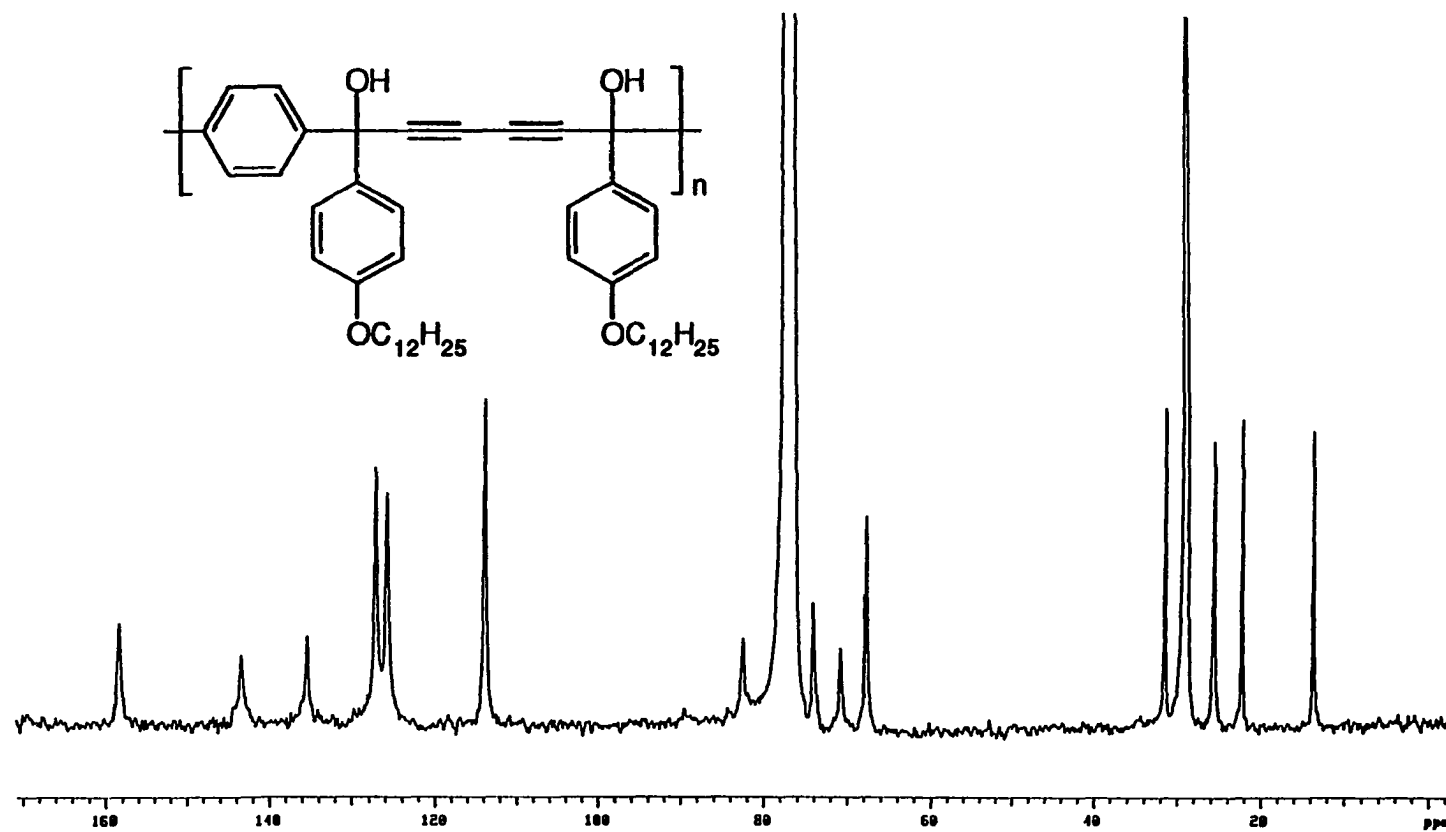
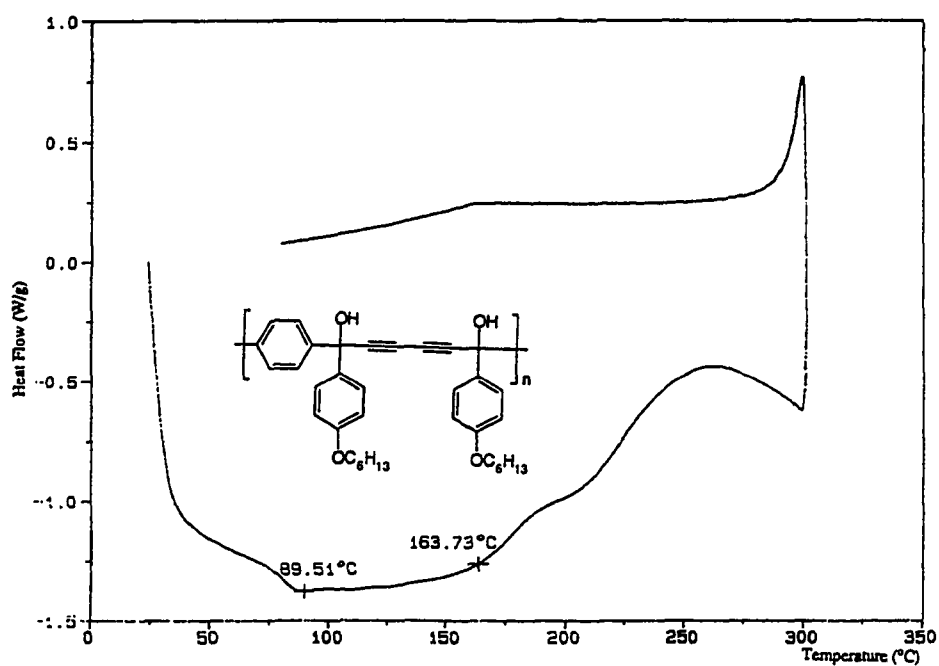
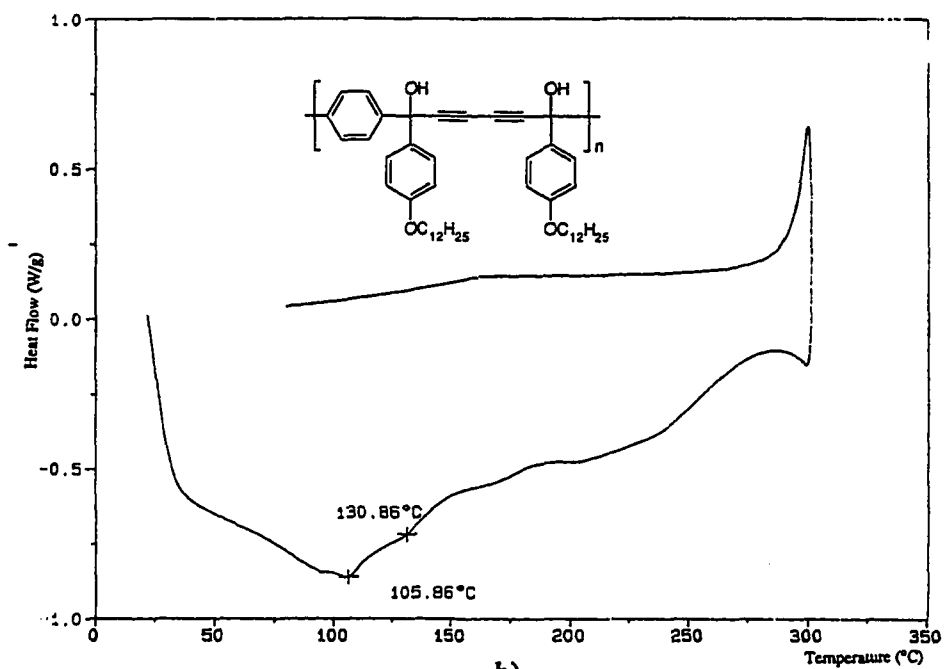


Figure 22. ^{13}C -NMR spectrum of polymer 33b.



a)



b)

Figure 23. DSC thermogram of a) polymer 33a and b) polymer 33b.

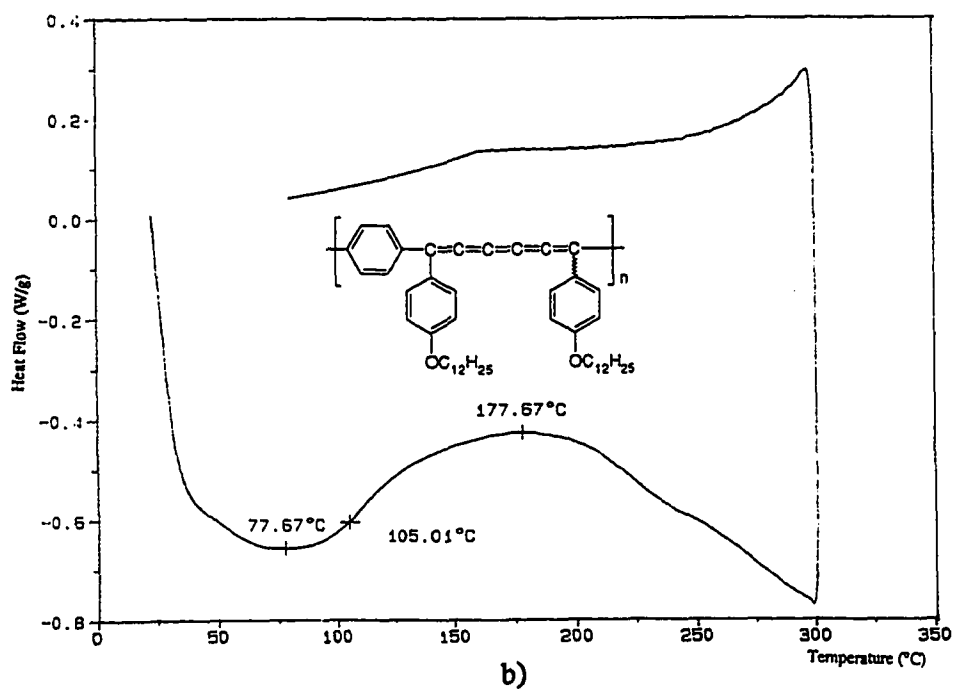
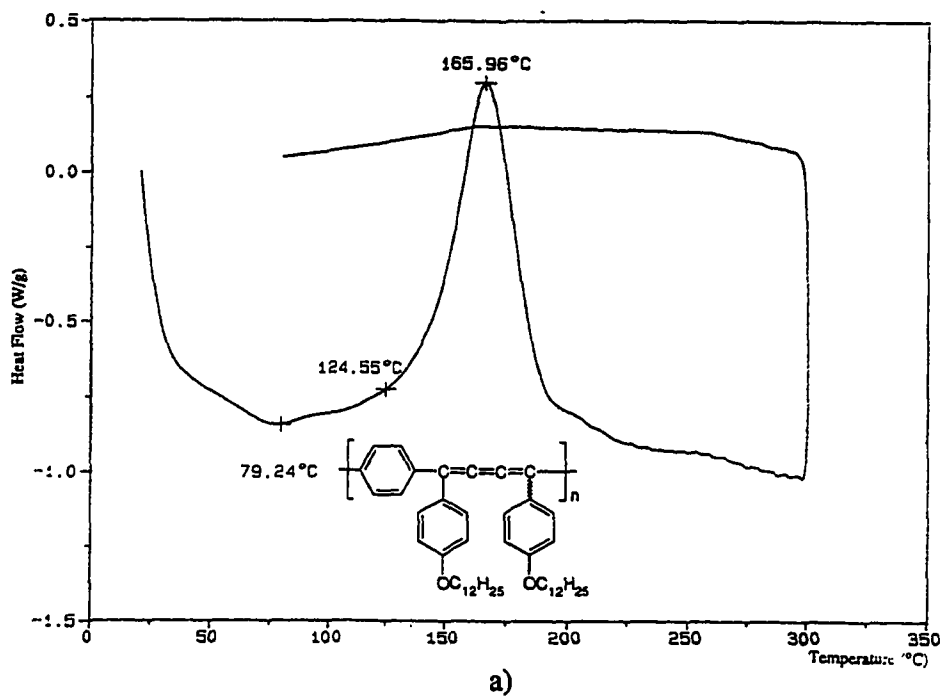


Figure 24. DSC thermogram of a) polymer 28b and b) polymer 34b.

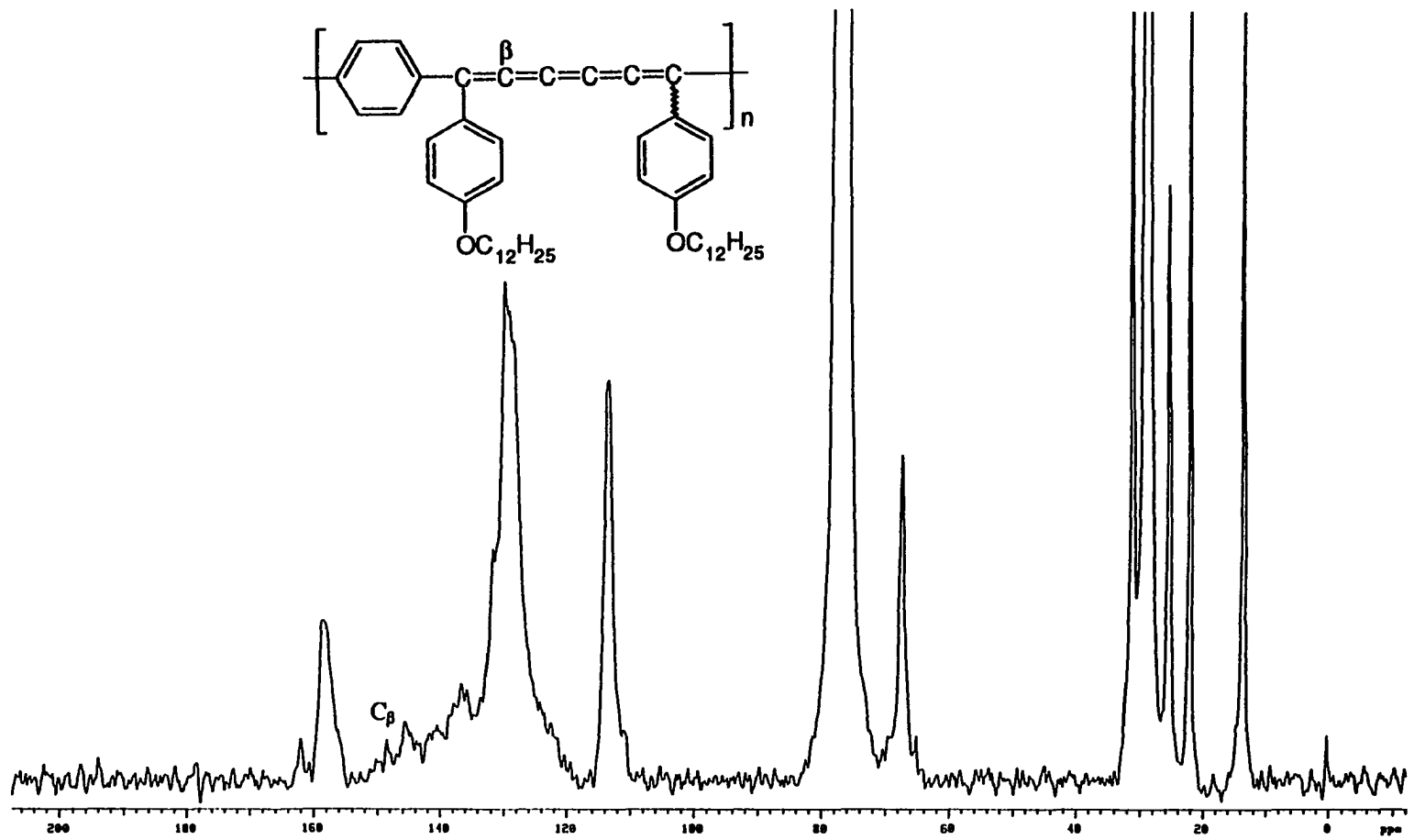


Figure 25. ^{13}C -NMR spectra of polymer 34b.

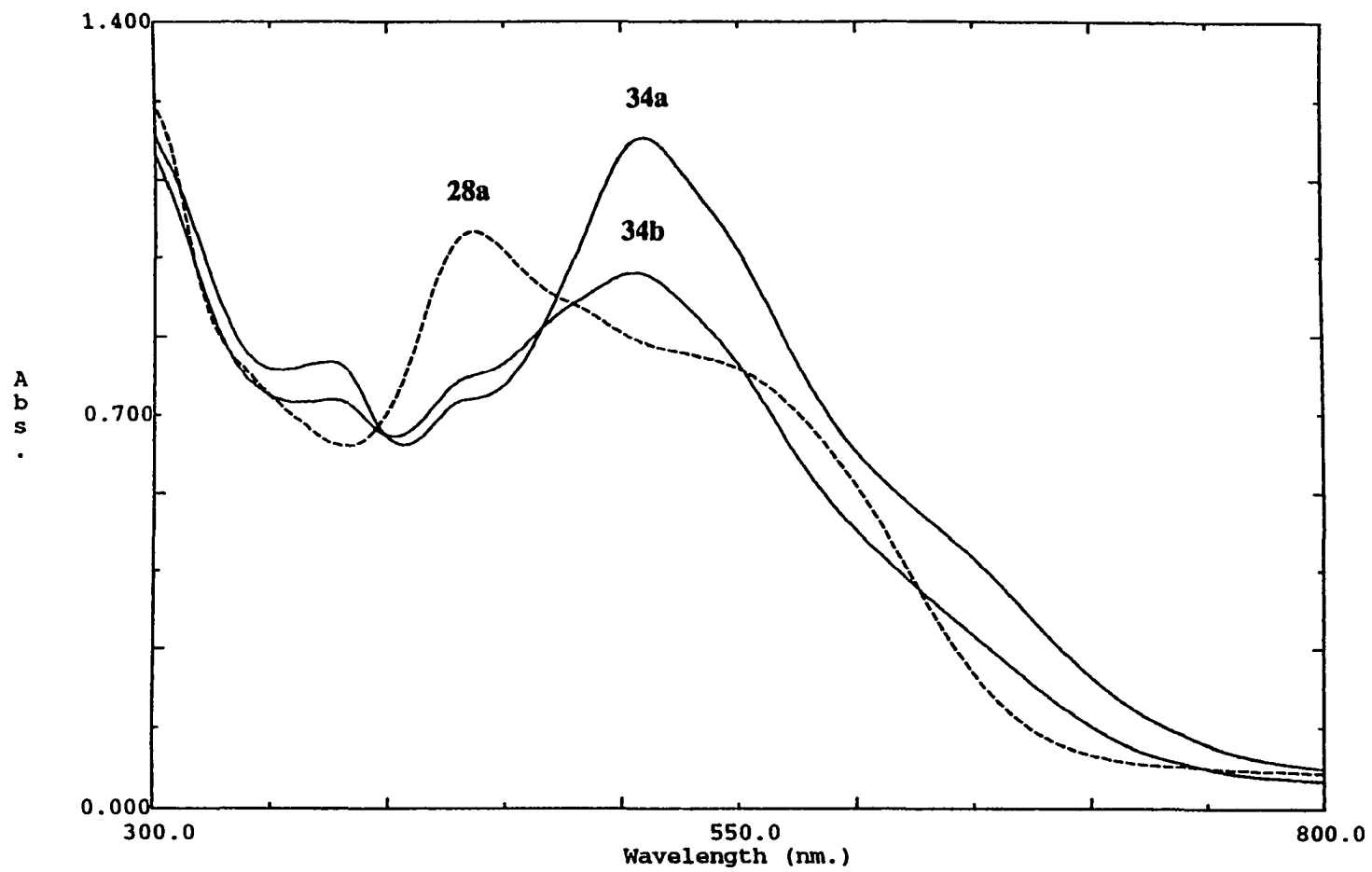
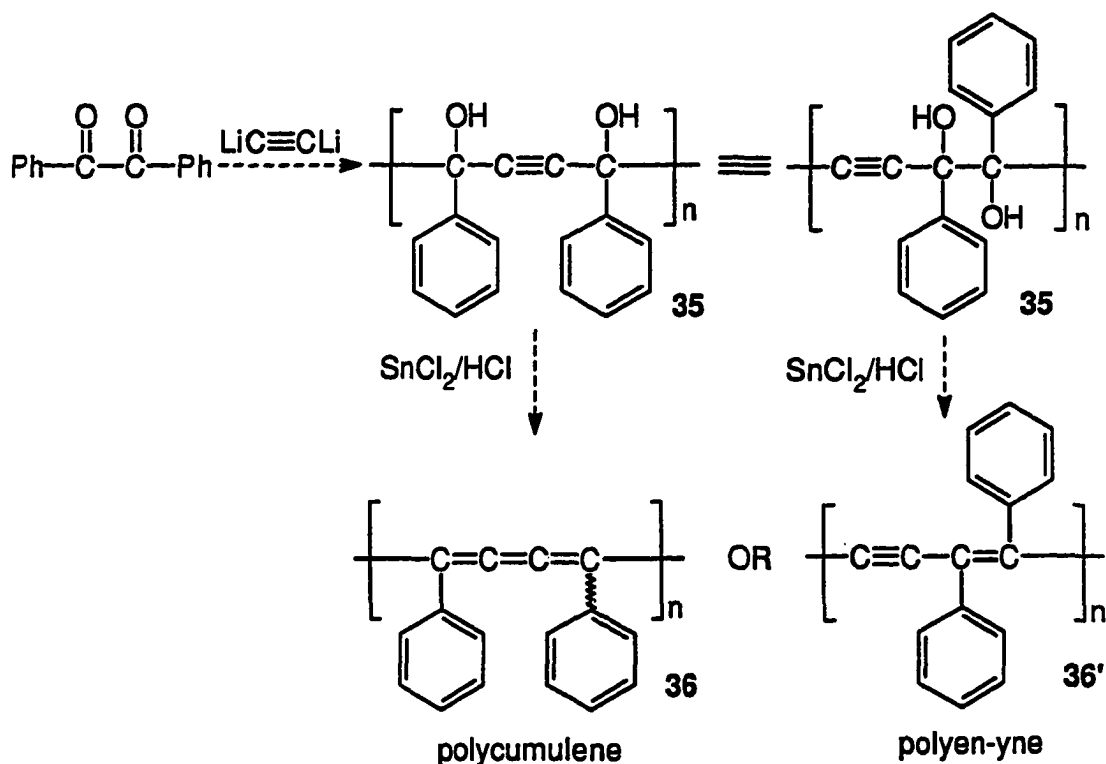


Figure 26. UV-VIS absorption spectra of polymer 28a, 34a, and 34b.

Attempted synthesis of polycumulenes.

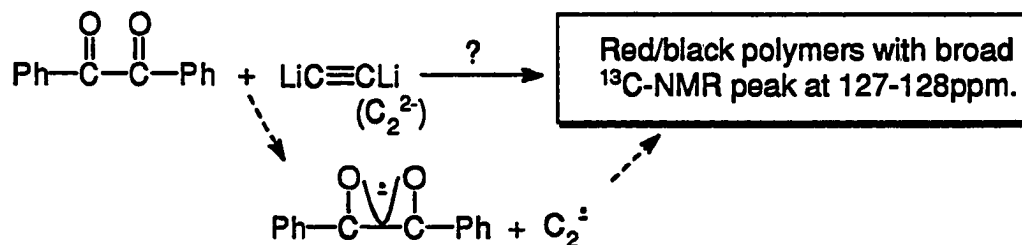
The cumulene-containing conjugated polymers discussed above contain both phenylenes and cumulenes (either butatrienes or hexapentaenes) in the polymer main chain. Can we synthesize polymers that contain only cumulene units in the polymer main chain? This is of great interest because if we could, it would give us a great opportunity to test the theoretical work reviewed in the literature survey section. Also it would give us an opportunity to compare the properties of polycumulenes with the isomeric polydiacetylenes (polyen-ynes).

The route designed is to react benzil with dilithium acetylene to give the precursor polymer **35** and further reduction of polymer **35** to give either polycumulene **36** or polyen-yne **36'** (Scheme 8.). From theoretical calculations,¹⁵⁴ it was already known that the en-yne structure is more stable than the polycumulene structure. Polymer **36** can only be expected as the kinetic product.



Scheme 8. Attempted synthesis of polycumulene from benzil.

However, the above synthetic route failed in the first step. The reaction of benzil and dilithium acetylene yield a red/black polymer with broad ^{13}C -NMR peaks at 127-128 ppm. There is no corresponding peaks observed for the acetylene carbons and the C-OH carbons under quantitative ^{13}C -NMR data collection conditions. Even though the mechanism for the formation of the uncharacterizable polymer was not clear, the anticipated first step is the charge transfer process where one electron was transferred from the dilithium acetylene to benzil, a very good electron acceptor (Scheme 9).

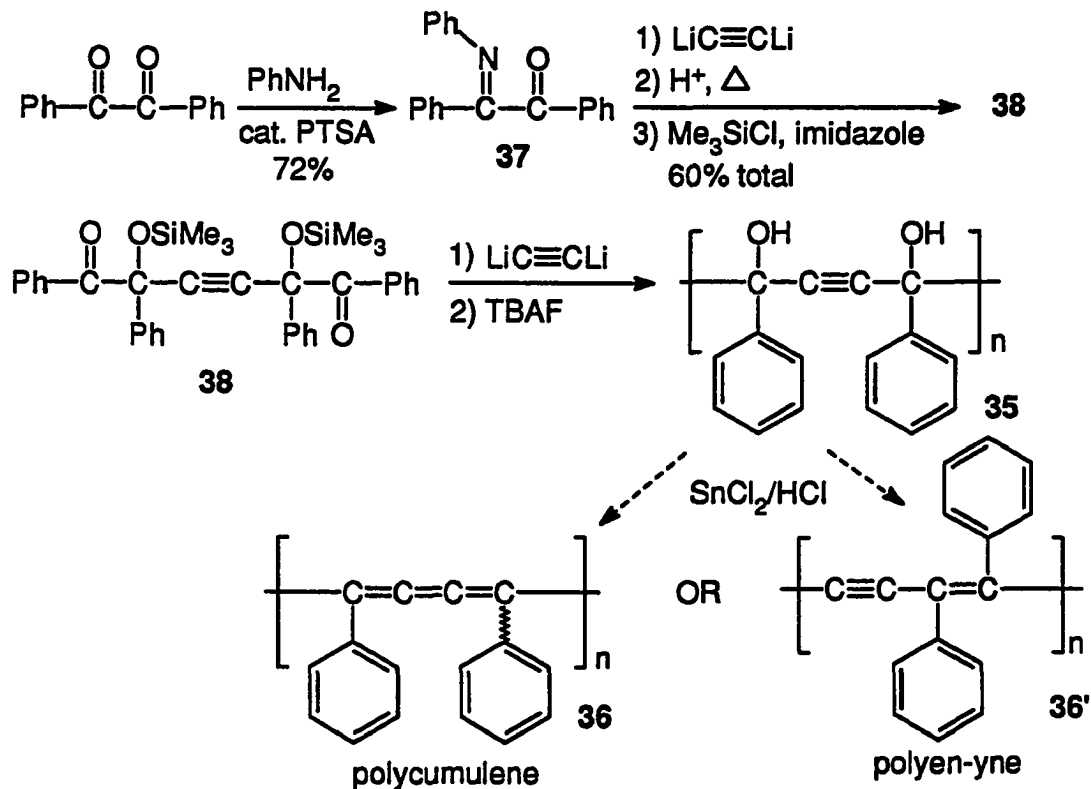


Scheme 9. Reaction of benzil and dilithium acetylene.

To avoid the problem of electron transfer, a step-wise synthesis of polycumulene was designed (Scheme 10). First, compound **37**, with one of the carbonyl groups protected as an imine,¹⁷⁴ reacts with dilithium acetylene. After deprotection of the imine group under acidic conditions and protecting the hydroxyl groups with trimethylsilyl groups, compound **38** was obtained in 60% yield after silica gel column purification. However, further reaction of compound **38** with dilithium acetylene did not give the desired polymer even before the silyl group deprotection. Under both acidic and neutral work up conditions, the polymers obtained have a very complicated ^{13}C -NMR spectra with 9 peaks in the 127-128 ppm region and 6 peaks in the 130-135 ppm region and 4 peaks in the 89-95 ppm region. Future attempts to synthesize precursor polymer **35**, will require new synthetic approaches.

Synthesis and study of cumulene-containing polymers with flexible blocks in the main chain.

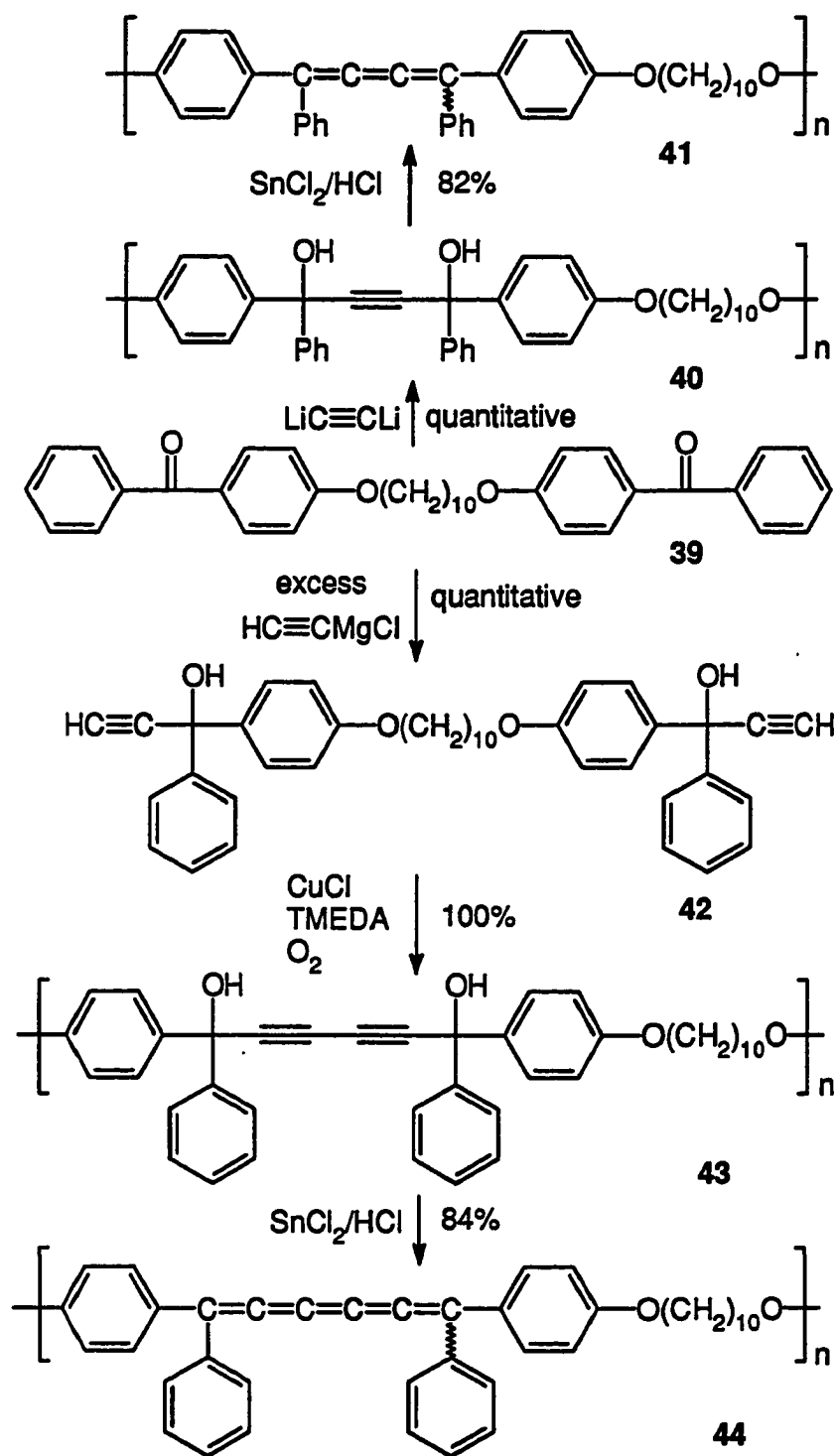
Incorporating flexible blocks into the polymer main chain is a common strategy to improve the solubility and processability of polymers containing rigid segments.¹⁷⁵ Here, the



Scheme 10. Attempted step-wise synthesis of polycumulene.

synthesis and study of alternative copolymers containing cumulene segments and flexible blocks in the polymer main chain are discussed.

The first synthetic route starts from diketone **39** which was obtained in 95% yield from the condensation of 4-hydroxybenzophenone and 1,10-dibromodecane under basic conditions (Scheme 11). Reaction of diketone **39** and dilithium acetylene afforded polymer **40** ($M_w = 22,000$, $M_w/M_n = 2.58$) in quantitative yield. Reduction of polymer **40** gave the butatriene-containing polymer **41** ($M_w = 18,700$, $M_w/M_n = 2.22$) in 82% yield. The ^{13}C -NMR spectrum of polymer **41** is shown in Fig. 27. Both polymers **40** and **41** have excellent film-forming ability. DSC analysis shows that polymer **40** has an endothermic peak at 58°C and an exothermic reaction starts at 196°C , while polymer **41** shows two endothermic peaks at 89°C and 161°C (Fig. 28). However, attempt to observe the liquid crystalline phase for polymer **41**



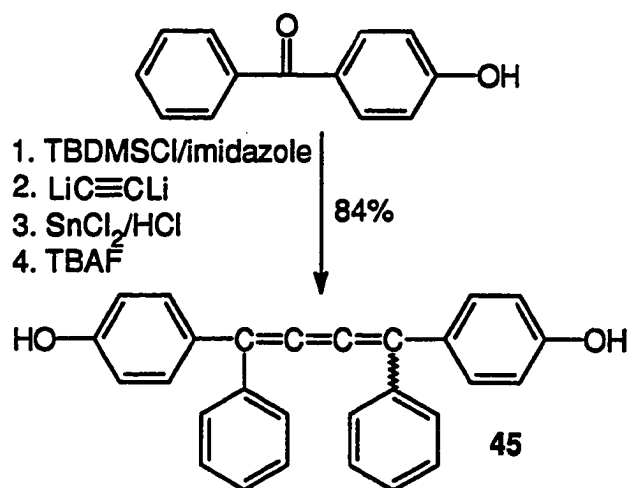
Scheme 11. Synthesis of cumulene-containing polymers with flexible blocks in the main chain from diketone 39.

with cross polarized microscopy failed because the entire polymer body did not melt and the two endothermic peaks observed on DSC was suspected to come from only part of the polymer.

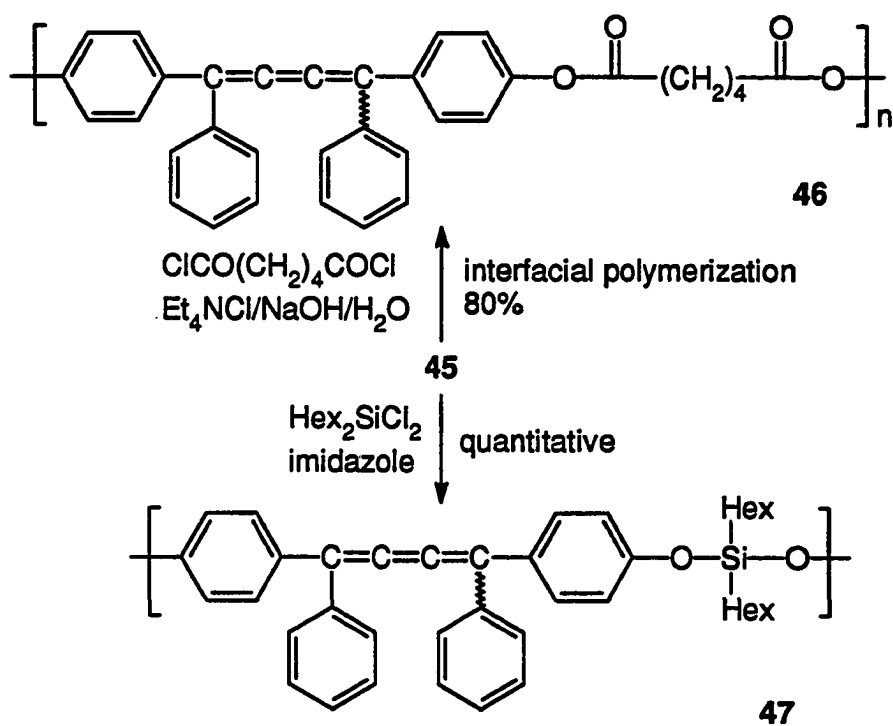
A higher order cumulene (hexapentane) containing polymer was also synthesized from diketone **39**. Cuprous-catalyzed oxidative coupling of diacetylene **42** afforded diol polymer **43** ($M_w = 13,000$, $M_w/M_n = 2.58$) in quantitative yield. When polymer **43** was reduced, surprisingly, most of polymer **44** precipitated out from the THF/ether solution as an elastomeric material. This elastomer could not be dissolved in THF. The structure of polymer **44** was thus confirmed largely by solid state ^{13}C -NMR spectra (Fig. 29). DSC analysis showed that polymer **43** melts at 72°C followed by an exothermic reaction at 194°C while polymer **44** melts at 86°C followed immediately by an exothermic reaction (Fig. 30). The UV absorption spectra of polymers **41** and **44** are shown in Fig. 31.

Our second synthetic route involved bisphenolcumulene **45** which was synthesized from 4-hydroxybenzophenone in four steps and 84% total yield (Scheme 12). After the hydroxyl groups in 4-hydroxybenzophenone were protected with silyl groups, the compound was reacted with the dilithium acetylene to give the diol precursor. After converting the diol precursor to cumulenes by SnCl_2/HCl , the silyl group was removed by tetrabutylammonium fluoride (TBAF). Bisphenol cumulene **45** was obtained as a yellow crystal but turned into deeper color if left in air for too long.

The chemistry of bisphenol A, long as a very important building block in polymer synthesis, can be applied to bisphenolcumulene **45**. Two examples are shown in Scheme 13 where in one an ester linkage was introduced by interfacial polymerization¹⁷⁶, and in the other a siloxane linkage was introduced. The ^{13}C -NMR and ^{29}Si -NMR spectra of polymer **47** and the ^{13}C -NMR spectrum of polymer **46** are shown in Figs. 32-34. DSC of polymer **46** has two endothermic peaks at 142°C and 161°C (Fig. 35) while no melting was actually observed from polymer **46** with cross polarized microscope. Polymer **47** does not soften or melt before an exothermic reaction begins at 191°C . The UV absorption spectra of bisphenolcumulene **45** and polymers **46** and **47** are shown in Fig. 36.



Scheme 12. Synthesis of bisphenolcumulene 45.



Scheme 13. Synthesis of cumulene-containing polymers with flexible blocks in the main chain from bisphenol cumulene 45.

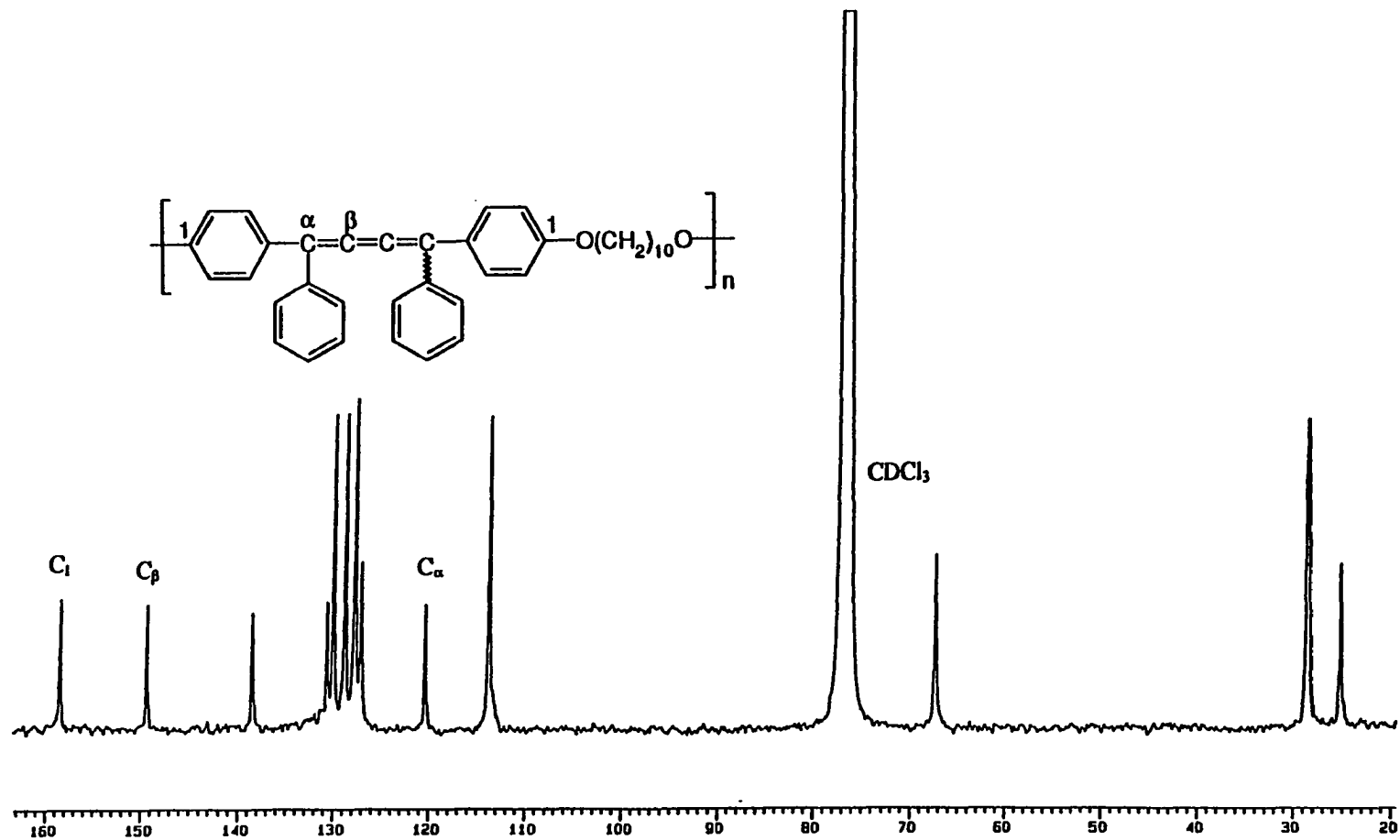


Figure 27. ¹³C-NMR spectrum of polymer 41.

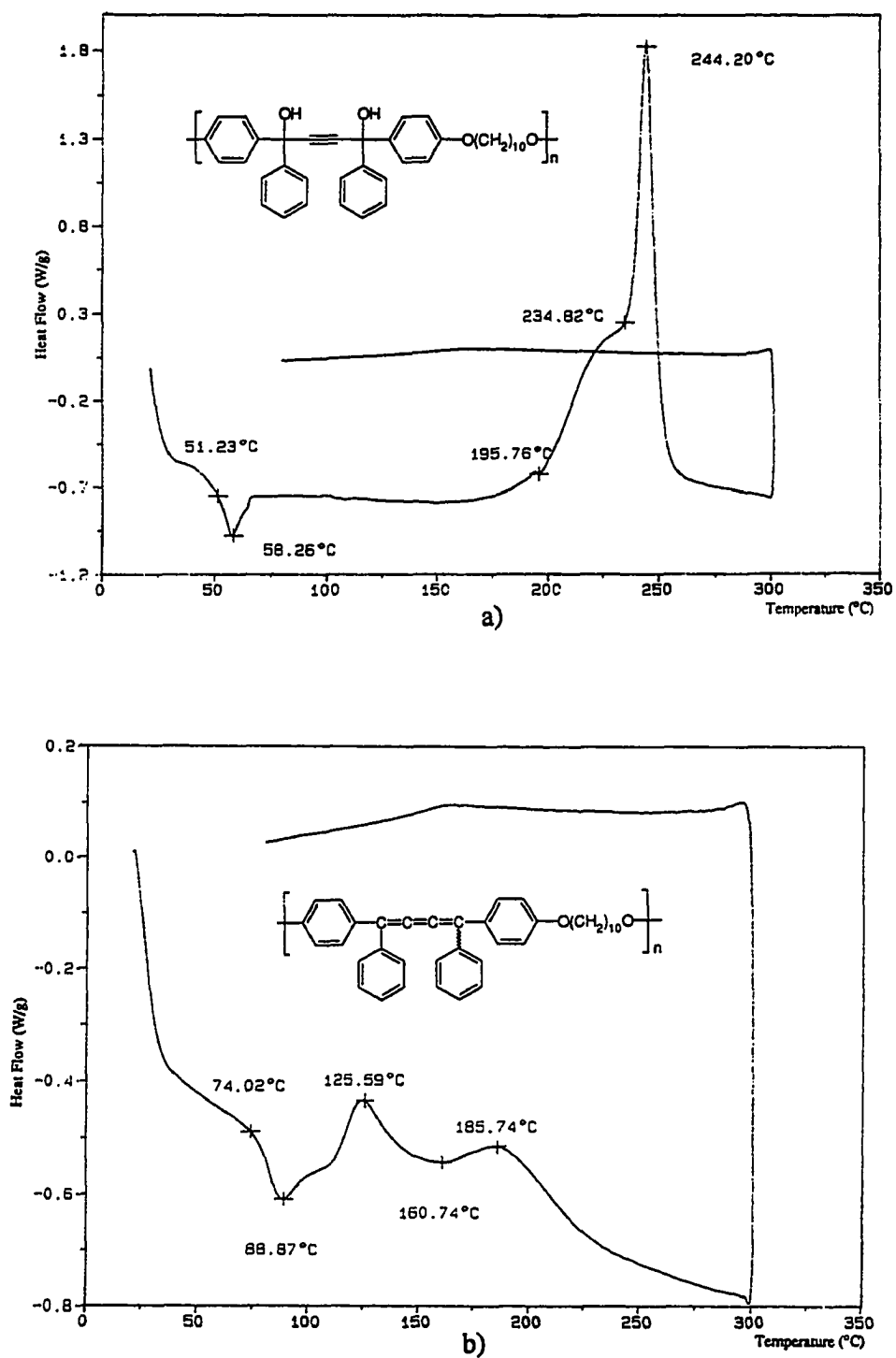


Figure 28. DSC thermogram of a) polymer 40 and b) polymer 41.

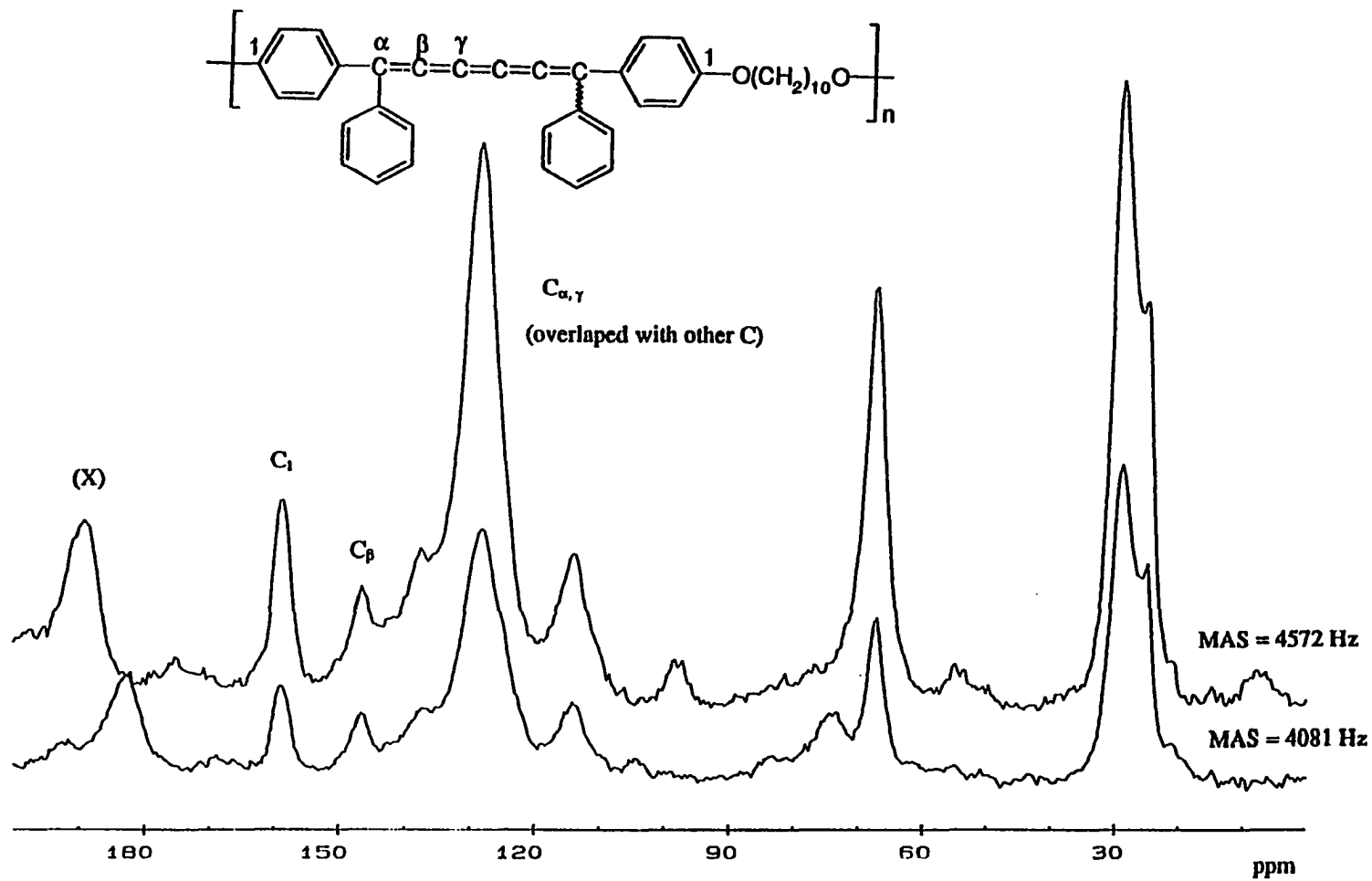


Figure 29. CPMAS ^{13}C -NMR spectra of polymer 44.

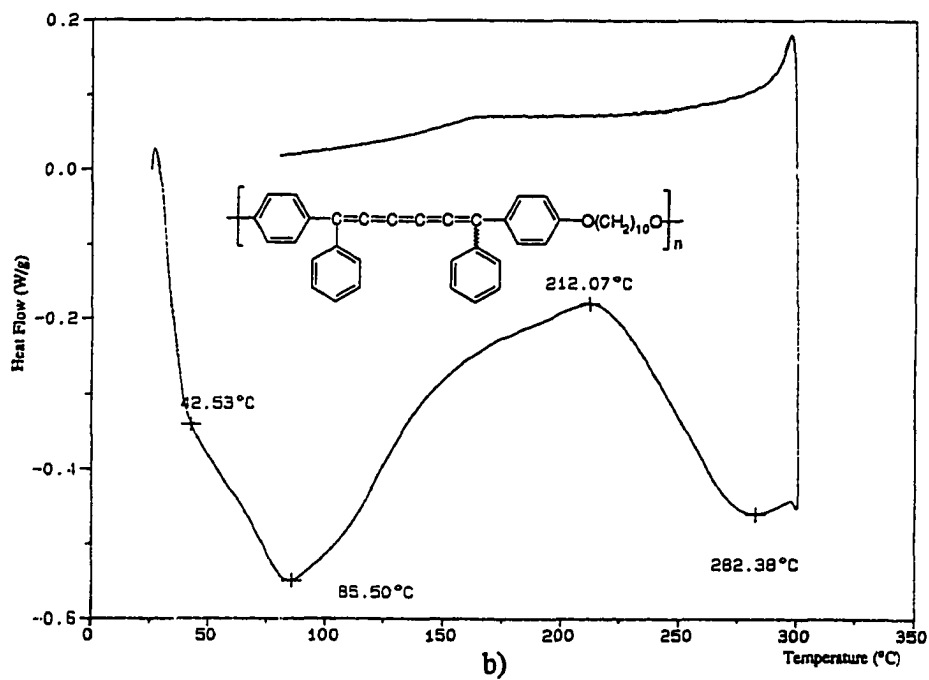
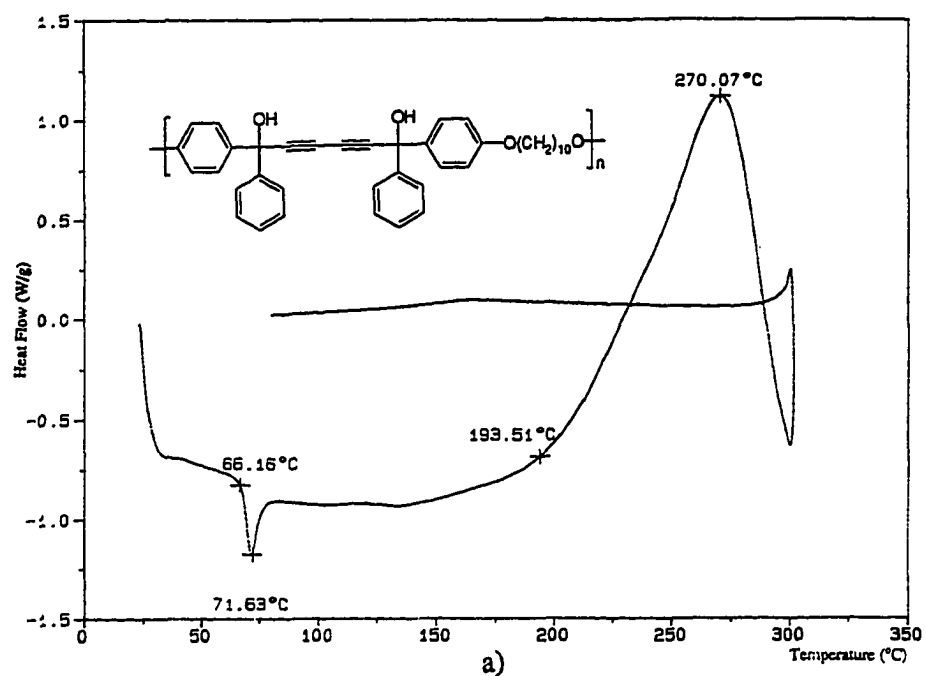


Figure 30. DSC thermogram of a) polymer 43 and b) polymer 44.

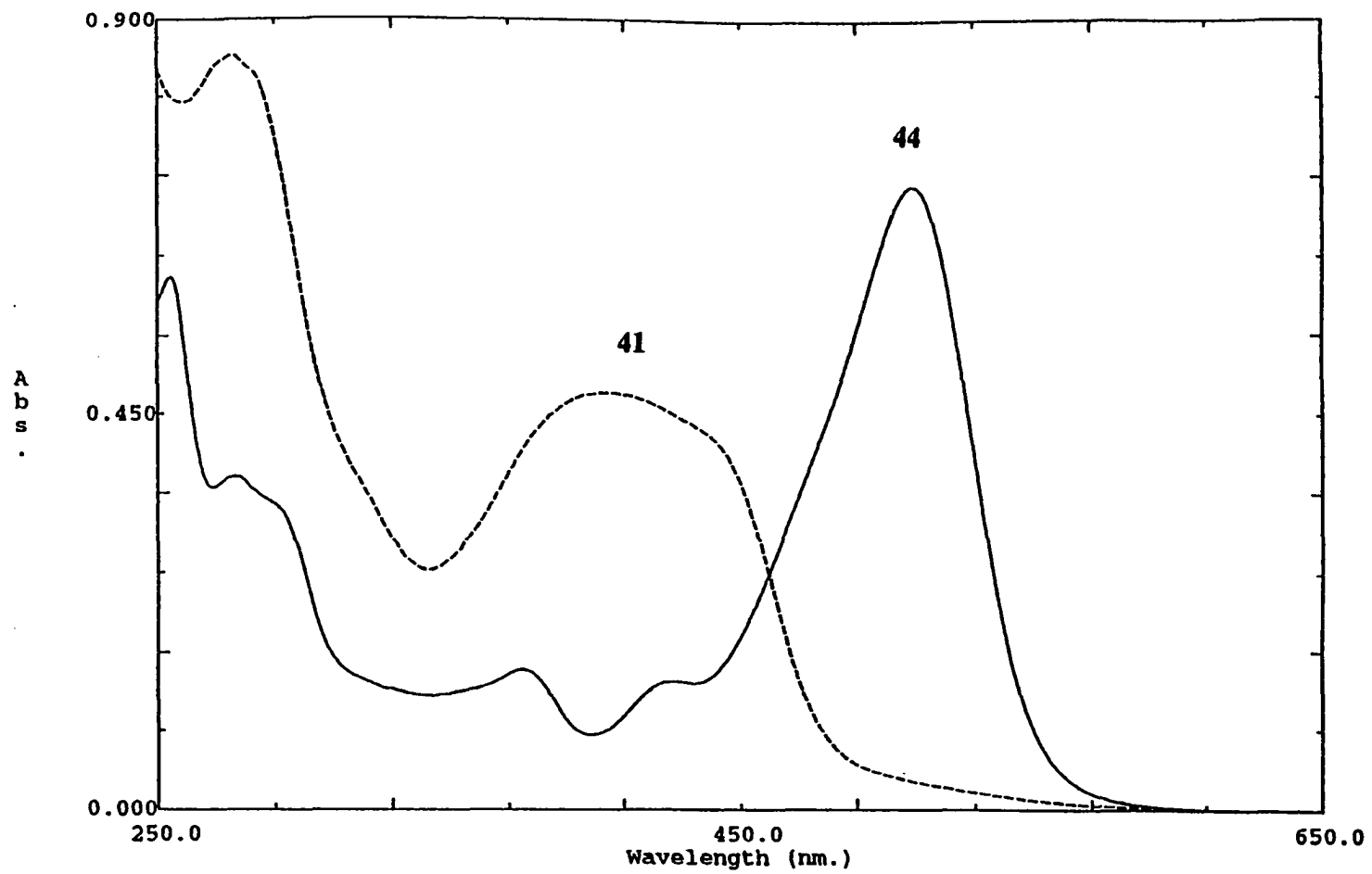


Figure 31. UV-VIS absorption spectra of polymer 41 and 44.

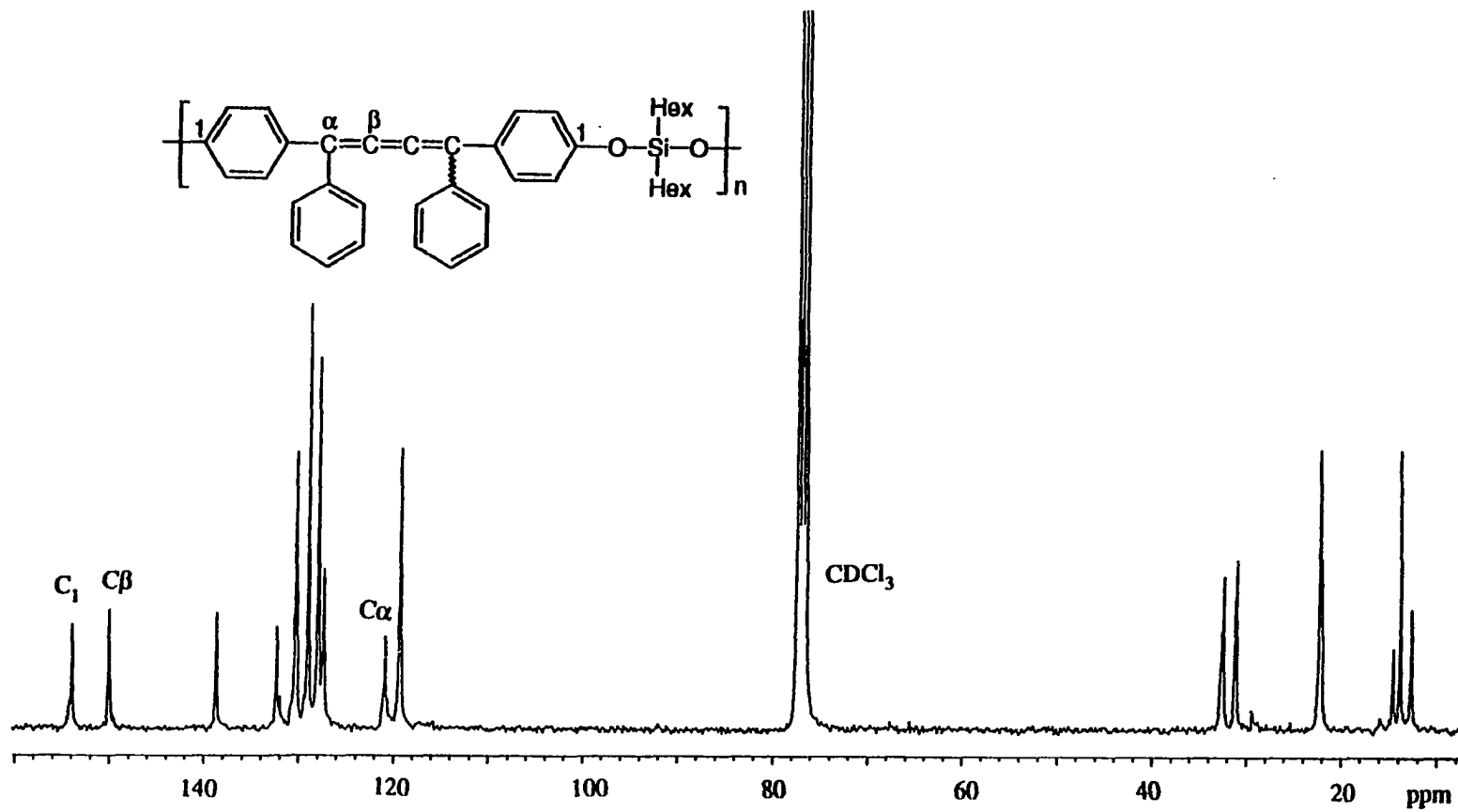


Figure 32. ^{13}C -NMR spectrum of polymer 47.

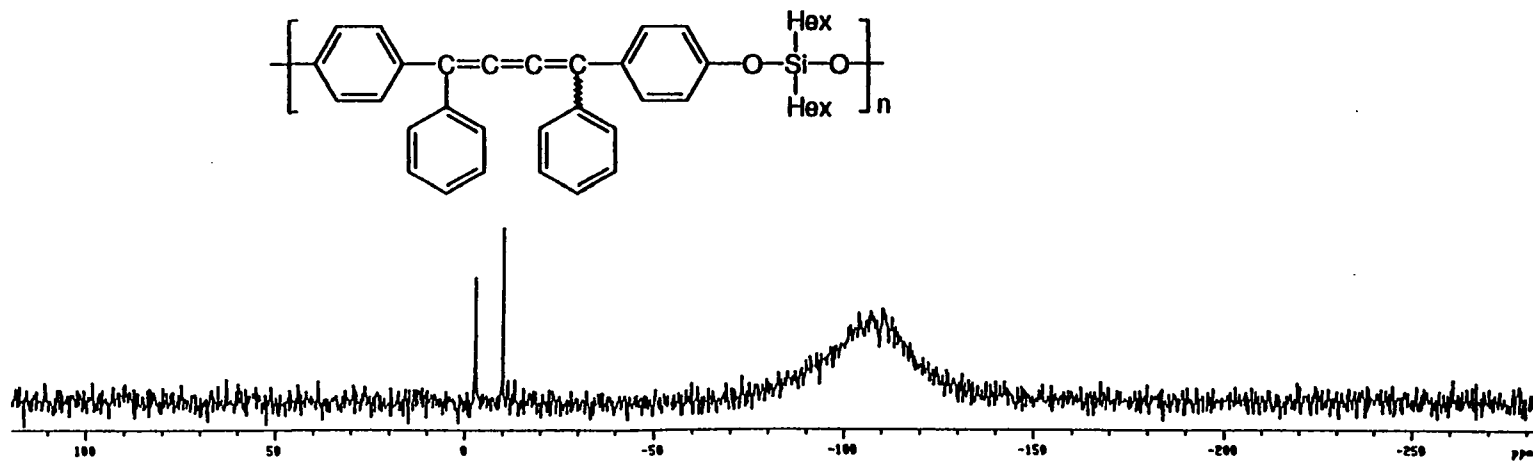


Figure 33. ^{29}Si -NMR spectrum of polymer 47.

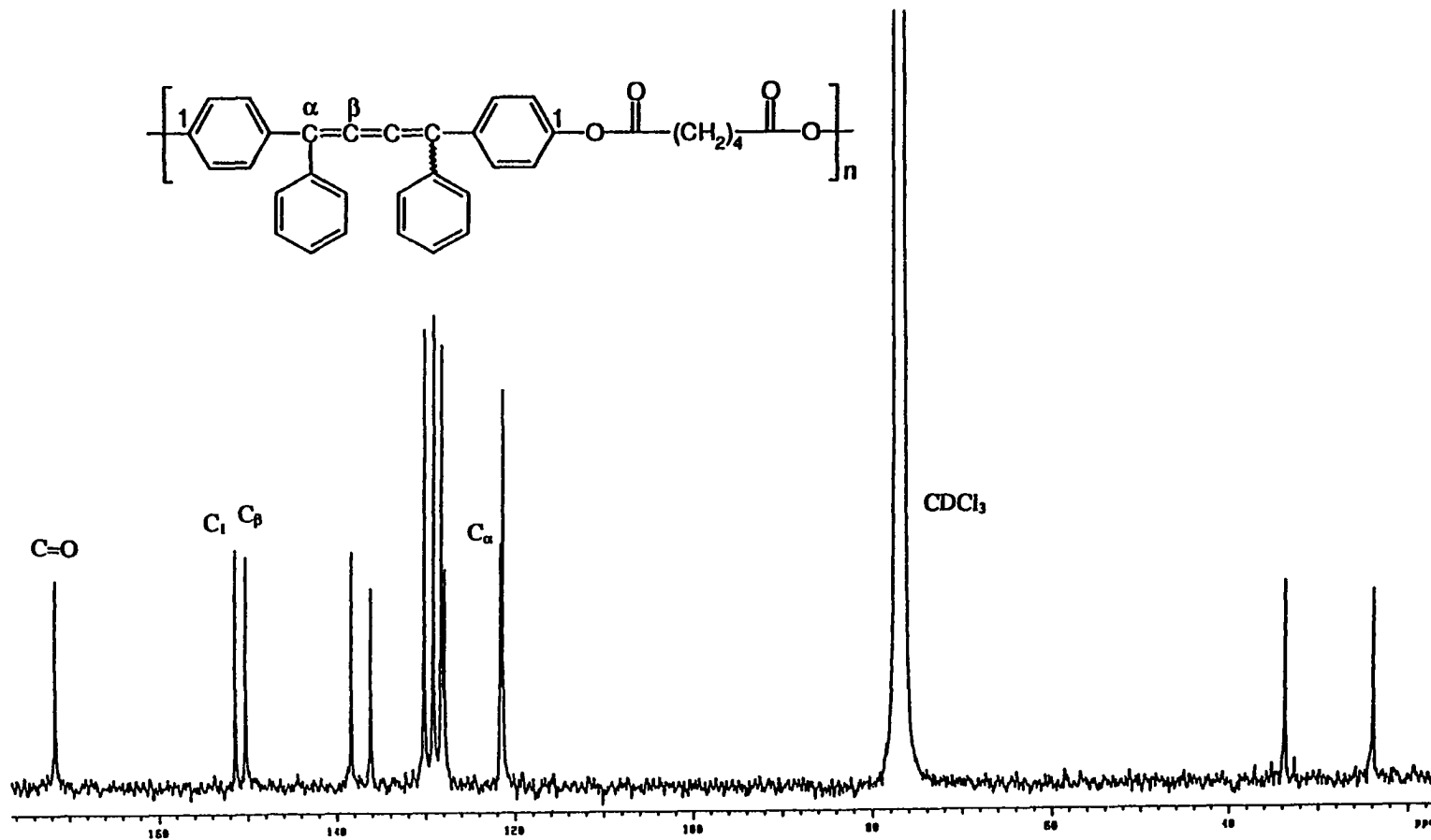


Figure 34. ^{13}C -NMR spectrum of polymer 46.

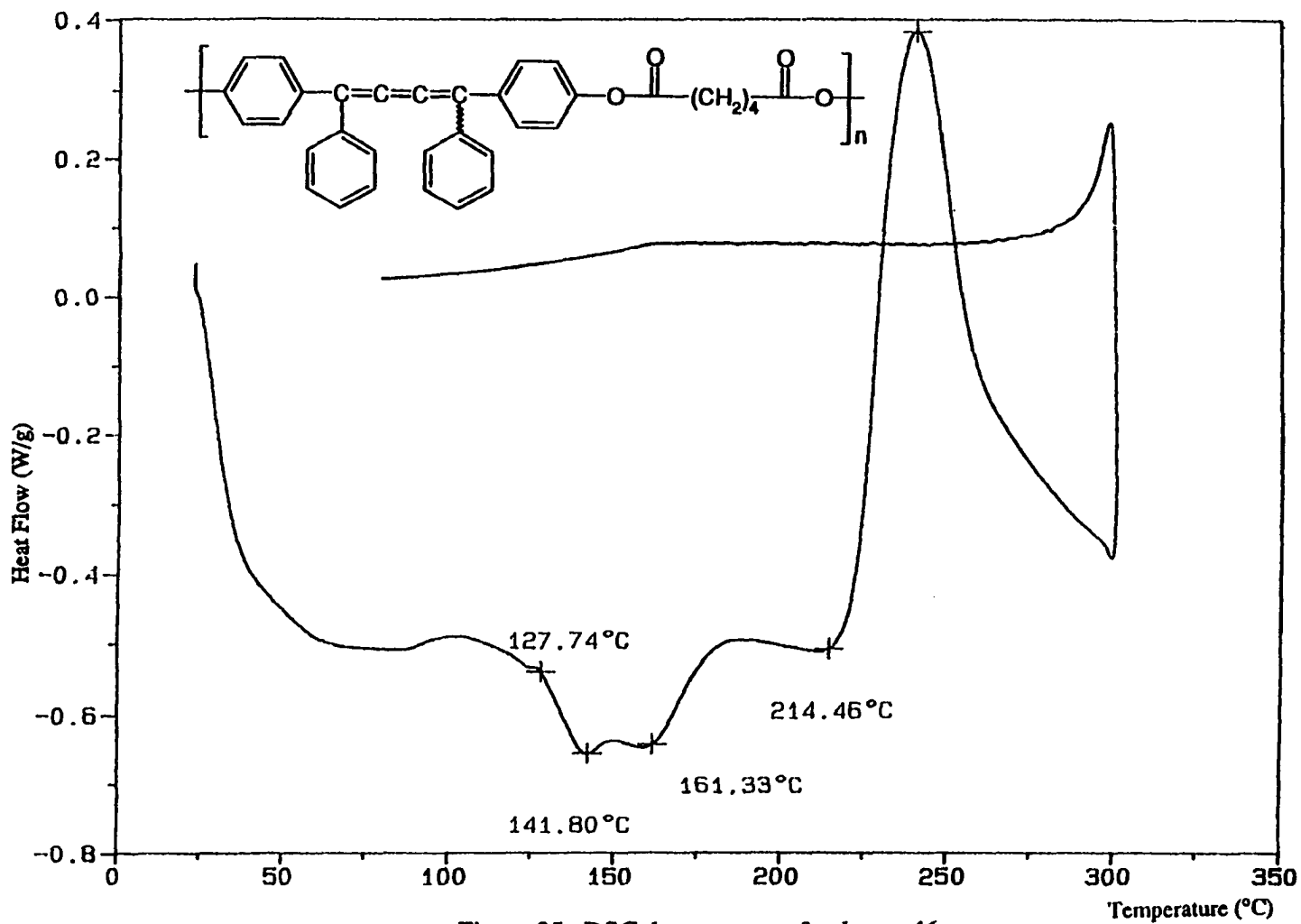


Figure 35. DSC thermogram of polymer 46.

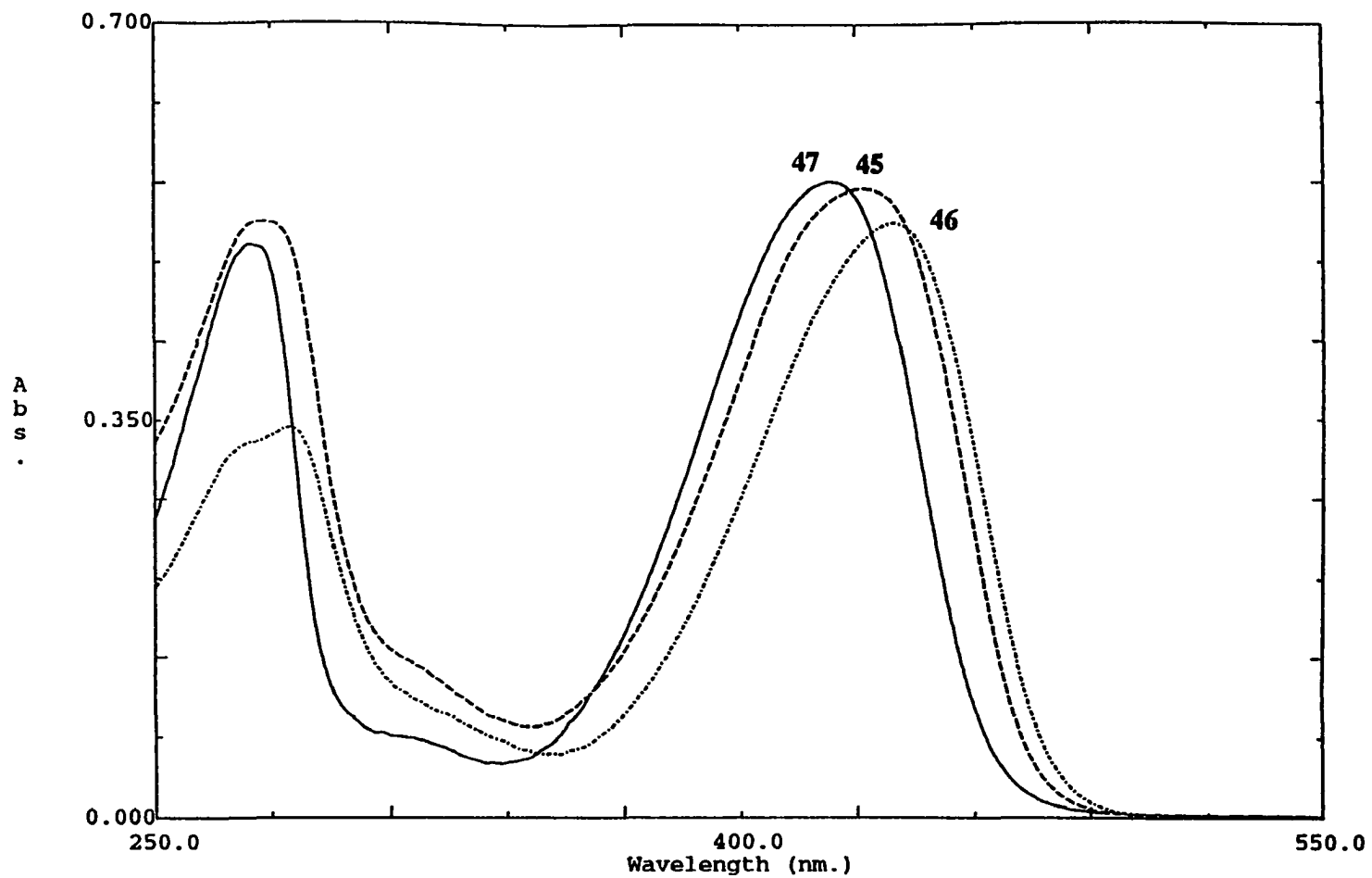
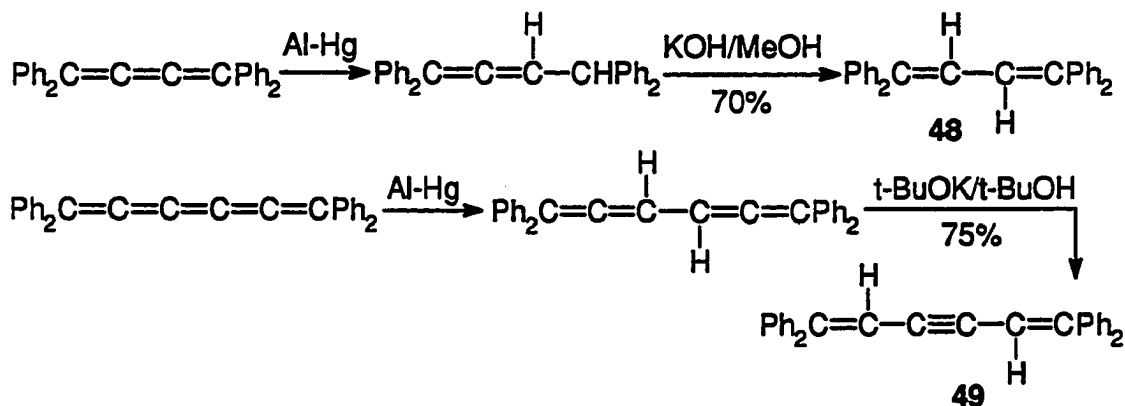


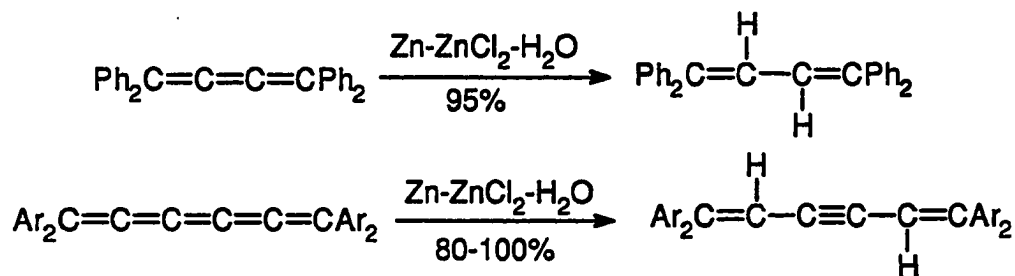
Figure 36. UV-VIS absorption spectra of 45, 46, 47.

Synthesis and comparative study of butatriene- and butadiene-containing polymers.

Butatrienes can be partially hydrogenated to give allenes if treated with aluminum amalgam in aqueous THF. The allenes obtained can be further isomerized to butadienes (**48**) if heated in KOH/MeOH solution for several hours. Under similar conditions, hexapentaenes can also be transformed to diallenes and then to en-yne-ene structures (**49**).¹⁷⁷

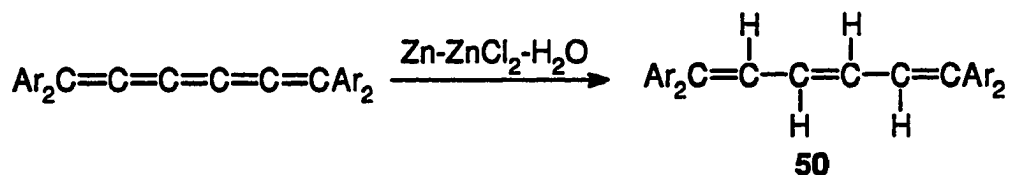


Kishigami reported that the above two-step transformation can be accomplished in one step under milder conditions by using the Zn-ZnCl₂-H₂O reduction system.¹⁷⁸ For butatriene, the reaction was accomplished by refluxing the butatriene with zinc and zinc chloride in aqueous THF solution for several hours. For hexapentaene, the mixture was just stirred at room temperature for 10 minutes.



Different from the literature where the reduction of hexapentaene is finished in 10 minutes¹⁷⁸, in our hands, the red color of hexapentaene solution did not disappear after 2 hours of stirring at room temperature. So the reaction was stirred overnight and turned yellow. Hexatriene **50**, not **49**, was obtained almost in quantitative yield. The difference

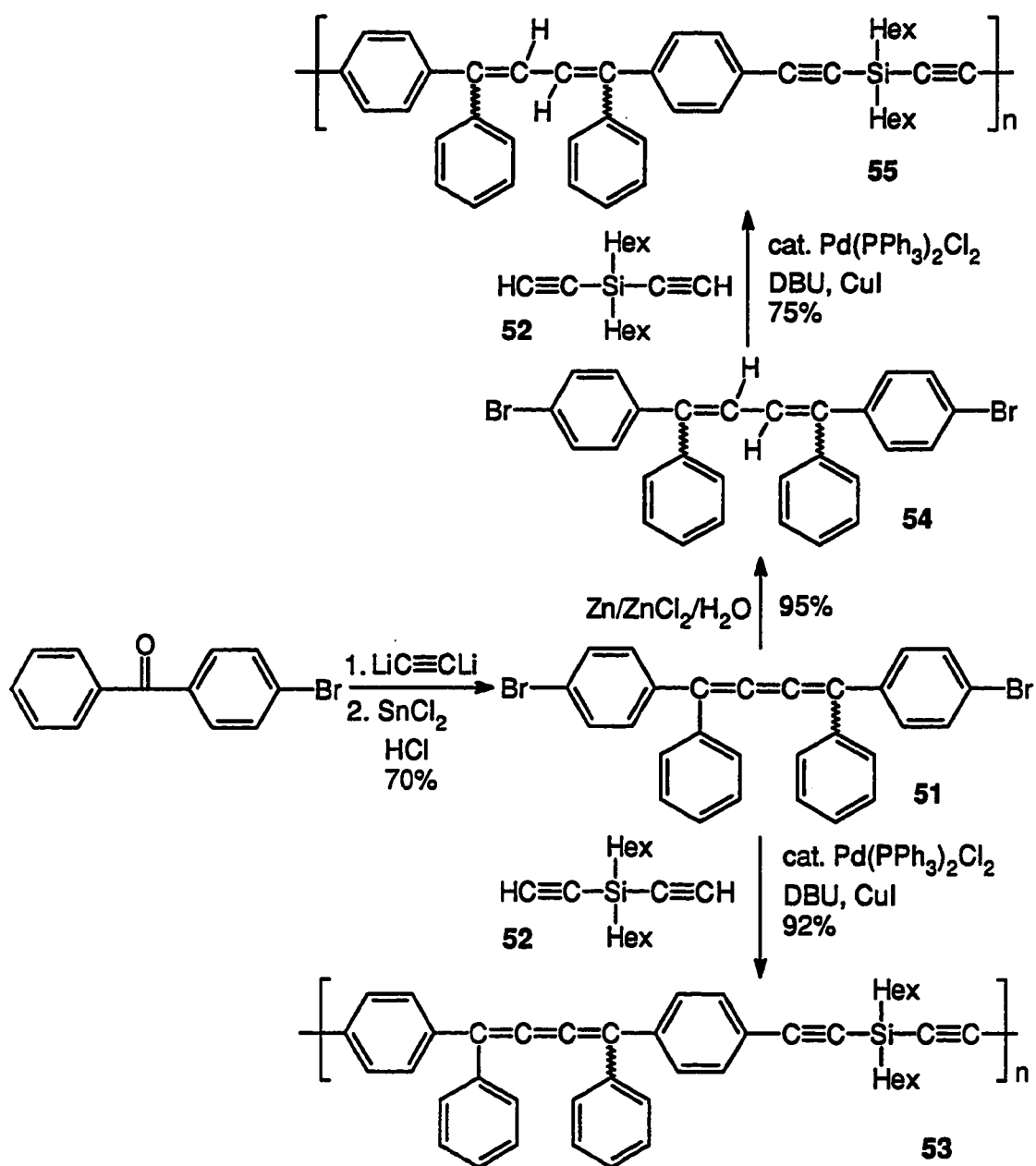
between our observation and Kishigami's could arise from the differences between the particle sizes of zinc powder applied.



Tetraphenylbutatriene and tetraphenylhexapentaene are not photoluminescent while their partially hydrogenated forms, tetraphenylbutadiene and tetraphenylhexatriene, are strongly photoluminescent. One of the most recent interests in conjugated polymers which are photoluminescent is building polymer-based electroluminescent devices.¹⁷⁹ Thus it was of interest to see if any of the cumulene-containing polymers can be partially hydrogenated to give polymers that are photoluminescent. However, attempt to partially hydrogenate polymers **28a**, **34b** and **41** by using the Zn-ZnCl₂-H₂O system all failed even after extended periods of reflux and the recovered polymers were largely unchanged.

Apparently, partial hydrogenation of cumulenes is much easier done in the small molecules. An attempt to partially hydrogenate bisphenolcumulene **45** also failed, presumably because the hydroxyl groups are efficient radical trappers. 1,4-Bis(*p*-bromophenyl)-1,4-diphenyl-1,2,3-butatriene (**51**), synthesized from *p*-bromobenzophenone in two steps in 70% yield, was partially hydrogenated to give 1,4-bis(*p*-bromophenyl)-1,4-diphenyl-1,3-butadiene (**54**) in 95% yield. Compound **54** presumably contains a mixture of *cis* and *trans* isomers. Condensation of the dibromides **51** or **54** with diethynyldihexylsilane (**52**) based on palladium catalyzed coupling reactions gave corresponding butatriene and butadiene containing polymers (**53** and **55**).¹⁸⁰

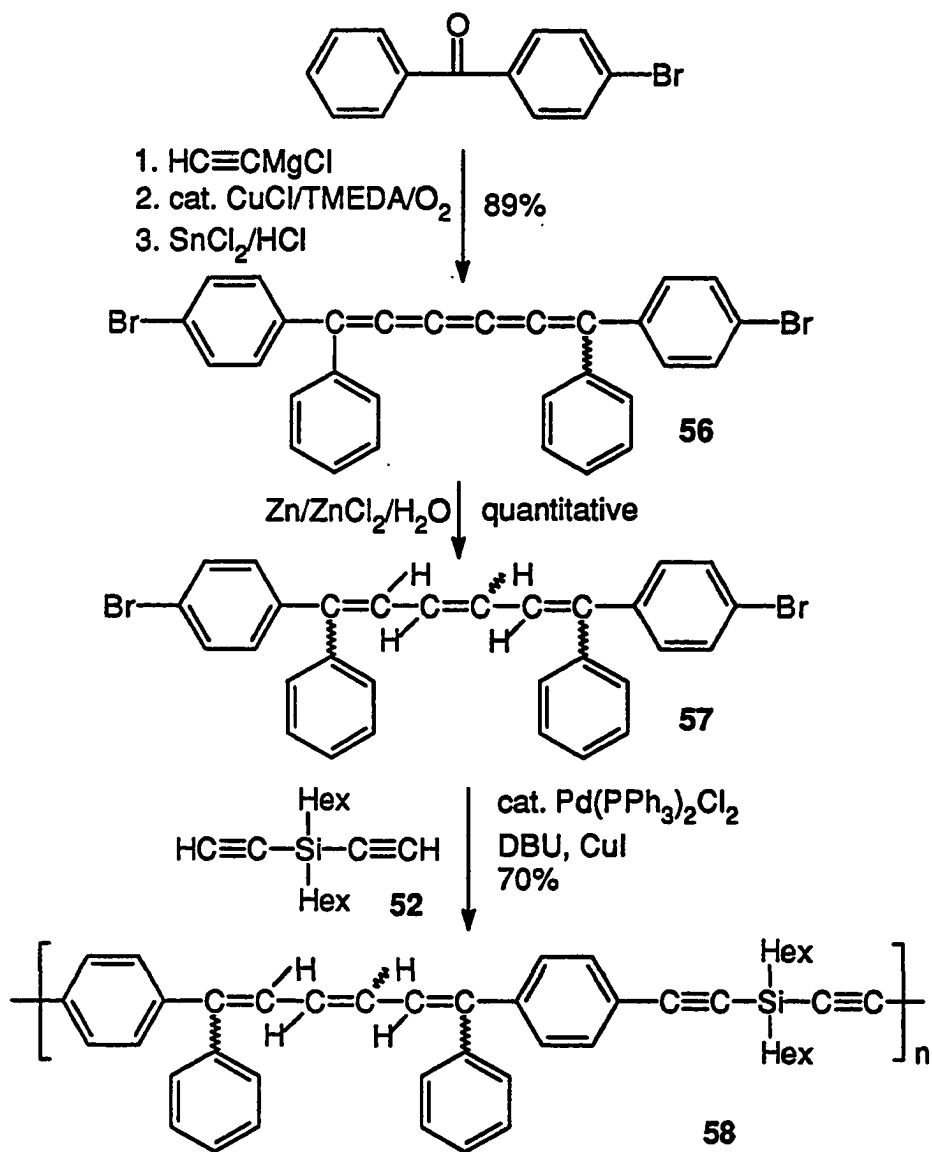
Polymer **53** has relatively high molecular weight: $M_w = 1.77 \times 10^4$, PDI = 2.53 while polymer **55** has relatively lower molecular weight: $M_w = 6.90 \times 10^3$, and PDI = 1.79. The ¹³C-NMR spectra of polymer **53** and **55** were shown in Fig. 37 and 38. DSC study shows that while polymer **55** does not soften or melt before an exothermic reaction starts at 165°C,



Scheme 13. Synthesis of butatriene and butadiene containing polymers.

polymer **53** softens at 142°C and an exothermic reaction starts at 185°C (Fig. 39). The UV-VIS absorption spectra of polymer **53**, polymer **55**, compound **2b**, and compound **48** were

shown in Fig. 40, from which we can see that about 73 nm and 83 nm blue shift were observed from butatrienes to butadienes in small molecules and polymers respectively. Most importantly, as shown in Fig. 41, while polymer **53** with the butatriene structure is not luminescent at all, polymer **55** is strongly luminescent. Polymer **55** is also electroluminescent, however, LED devices made from polymer **55** only had a very short lifetime.



Scheme 14. Synthesis of monomers for hexapentaene and hexatriene containing polymers.

1,6-Bis(*p*-bromophenyl)-1,6-diphenyl-1,2,3,4,5-hexapentaene (**56**) was synthesized from *p*-bromobenzophenone in three steps in 89% yield. It was successfully reduced to the corresponding hexatriene **57** in almost quantitative yield by using the Zn-ZnCl₂-H₂O system. However, attempt to polymerize 1,2,3,4,5-hexapentaene **56** with diethynyldihexylsilane (**52**) failed. The obtained polymer can not be redissolved and the characteristic peak of hexapentaene β-C at ~149 ppm was not observed in the solid state ¹³C-NMR spectra of obtained polymer. Crosslinking of the hexapentaene catalyzed by the palladium catalyst could have happened.

Palladium catalyzed polymerization of 1,3,5-hexatriene (**57**) with diethynyldihexylsilane (**52**) was successful. However, polymer **58** obtained has a poor solubility in common organic solvents such as THF and CCl₃. The ¹³C-NMR spectrum of polymer **58** is complicated and there are many peaks in the acetylene carbon area because of the *Z-E* isomers of the triene units (Fig. 42). Polymer **58** (λ_{max} = 397 nm) has an ca. 25 nm red shift in the UV-VIS absorption compared to the model compound **50** (λ_{max} = 372 nm) as shown in Fig. 42. Polymer **58** and the model compound **50** are both photoluminescent (Fig. 43) and polymer **58** is being studied as a material for LED devices. DSC analysis shows that polymer **58**, similar to polymer **55**, does not soften or melt before an exothermic reaction starts at 173°C.

Theoretical investigation of 1,2,3-butatriene and 1,3-butadiene-containing polymers (**53** and **55**).

In the past decades, 'bond alternation' theory has become popular for interpreting why some polymer are luminescence and some are not.^{170, 181} While polysilanes are luminescent, they do not have any bond alternation. Even for the poly(*p*-phenylene vinylene) (PPV), it's difficult to define the alternate parameter "δ", because it has three different bonds at ground state for a perfect polymer. Actually, bond alternation theory is an attempt at using some phenomena to explain other phenomena. As shown in the above discussion, 1,2,3-butatriene-containing polymer **53** is not photoluminescent, but the reduced form, 1,3-butadiene-containing polymer **55** is. The only difference between the two polymers is that one of the

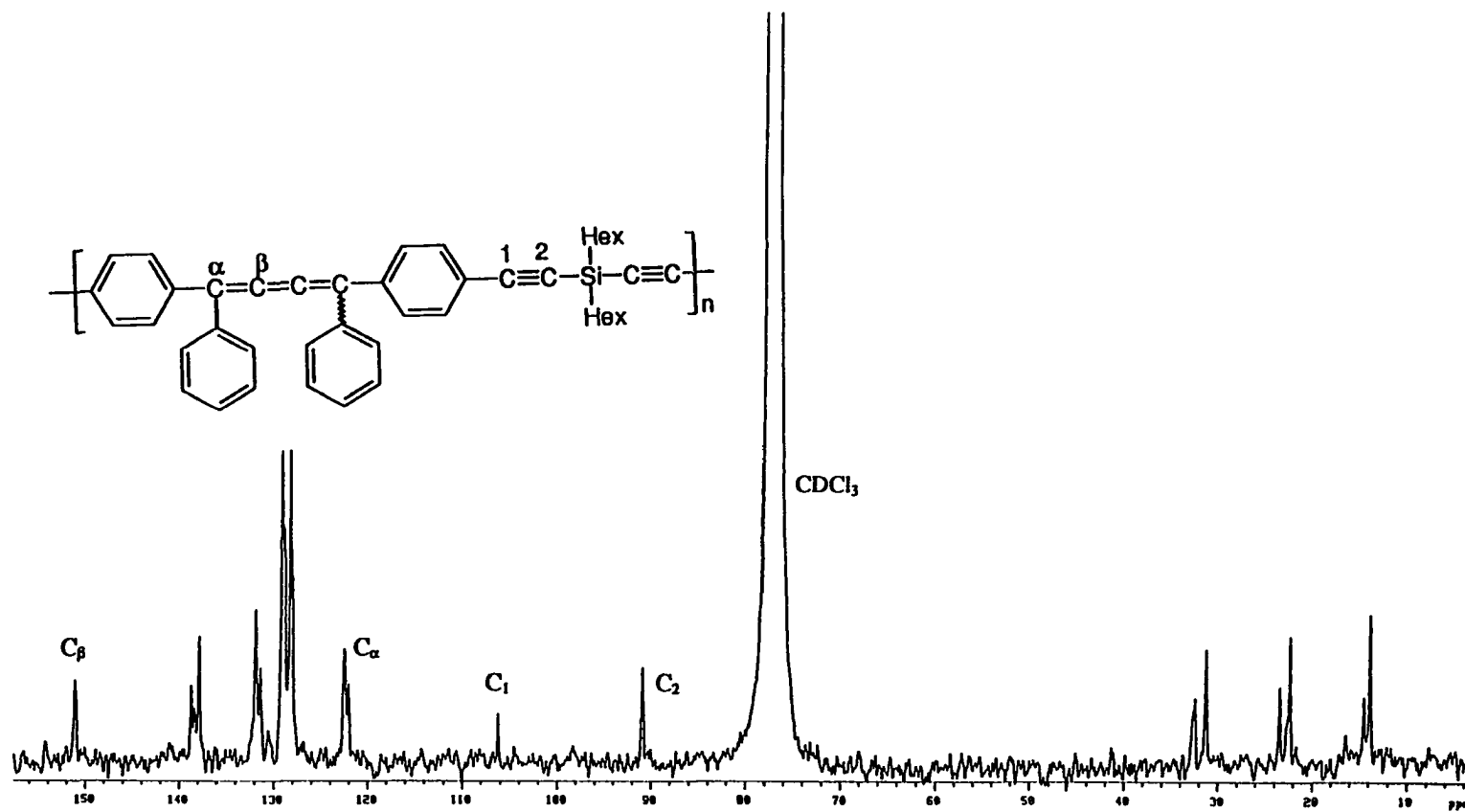


Figure 37. ¹³C-NMR spectrum of polymer 53.

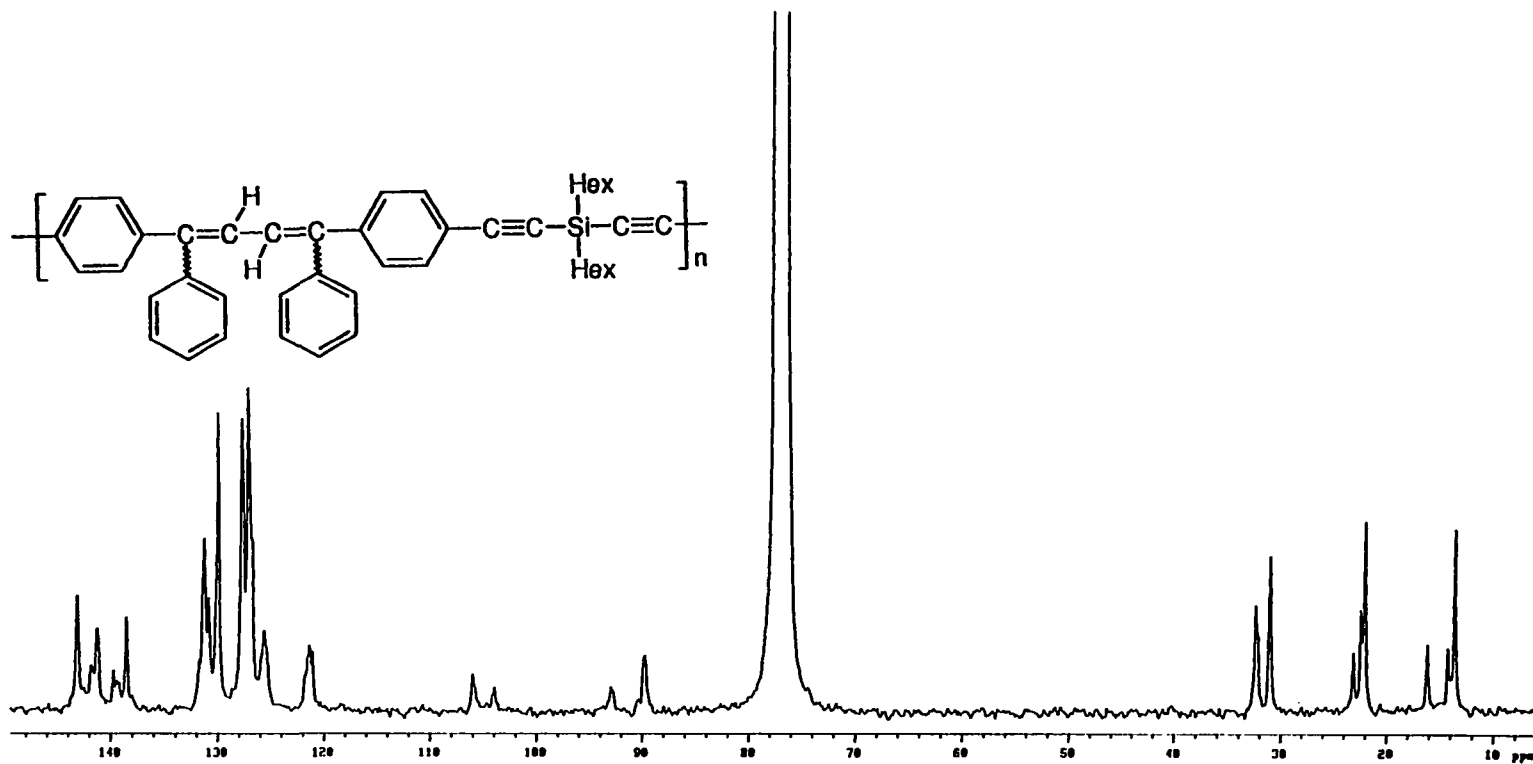


Figure 38. ^{13}C -NMR spectrum of polymer 55.

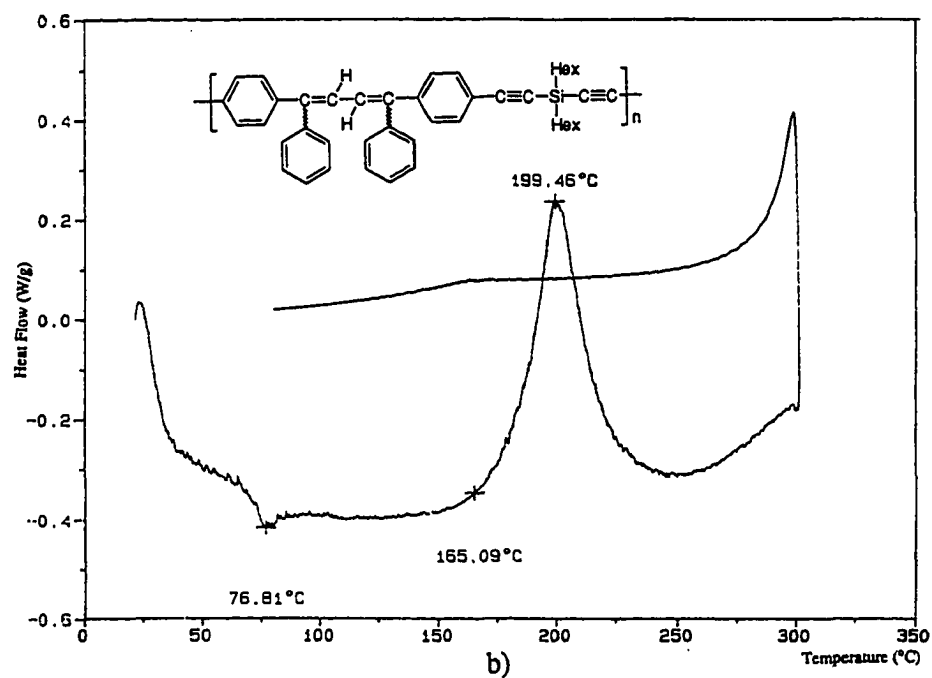
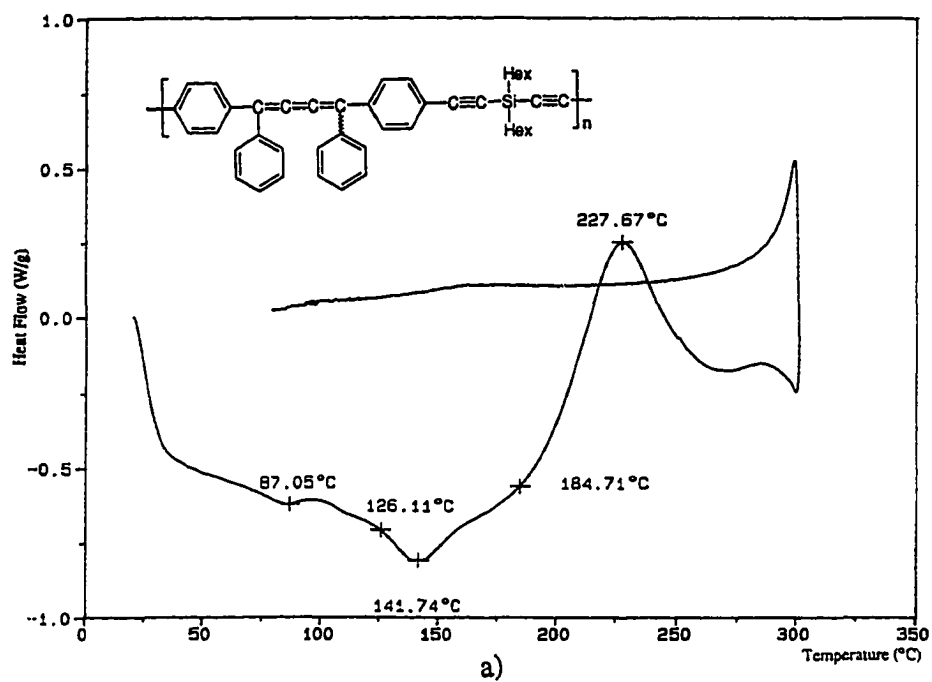


Figure 39. DSC thermogram of a) polymer 53 and b) polymer 55.

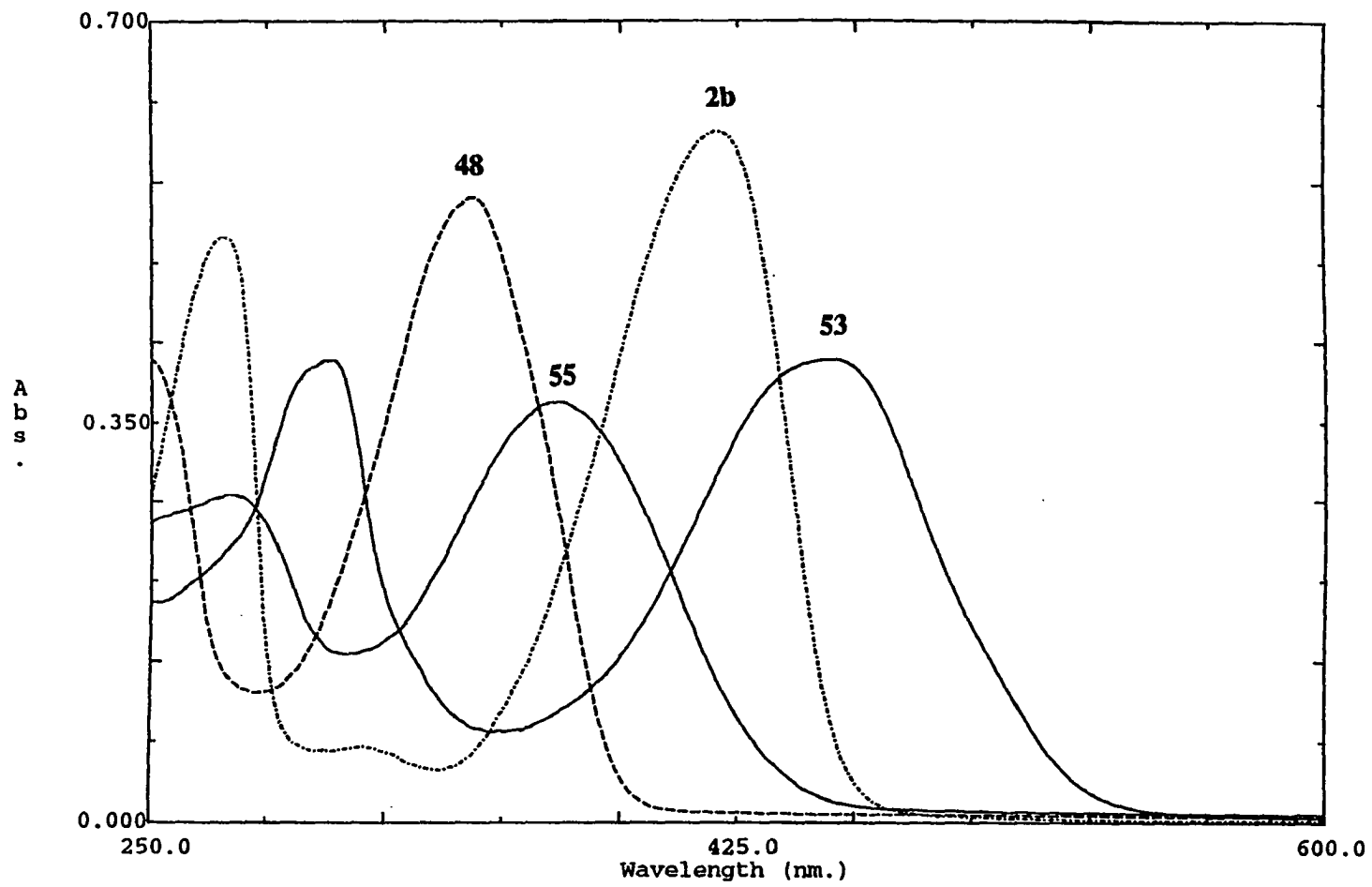


Figure 40. UV-VIS absorption spectra of 2b, 48, 53, 55.

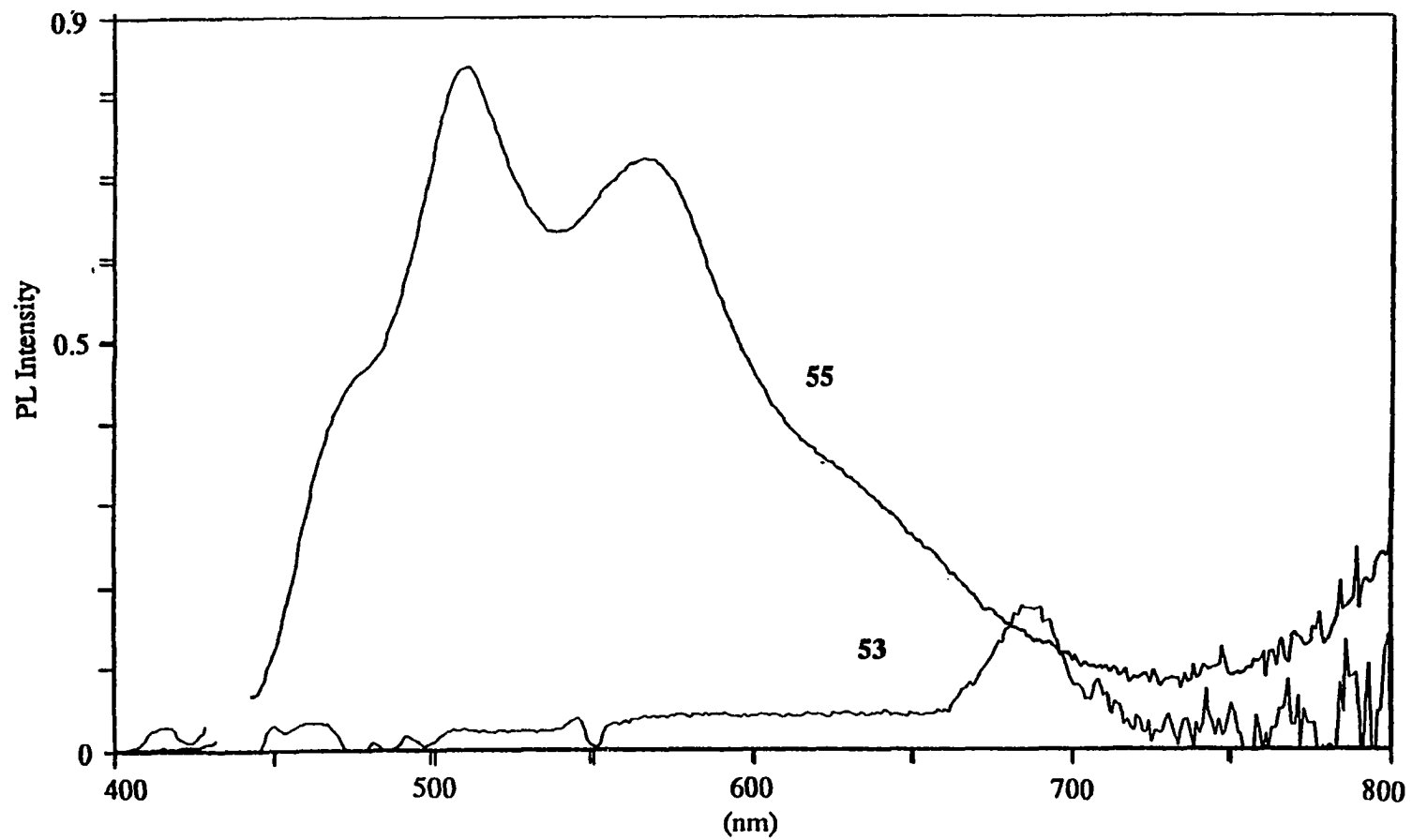


Figure 41. Photoluminescence spectra of polymer 53 and 55 (excited at 353 nm).

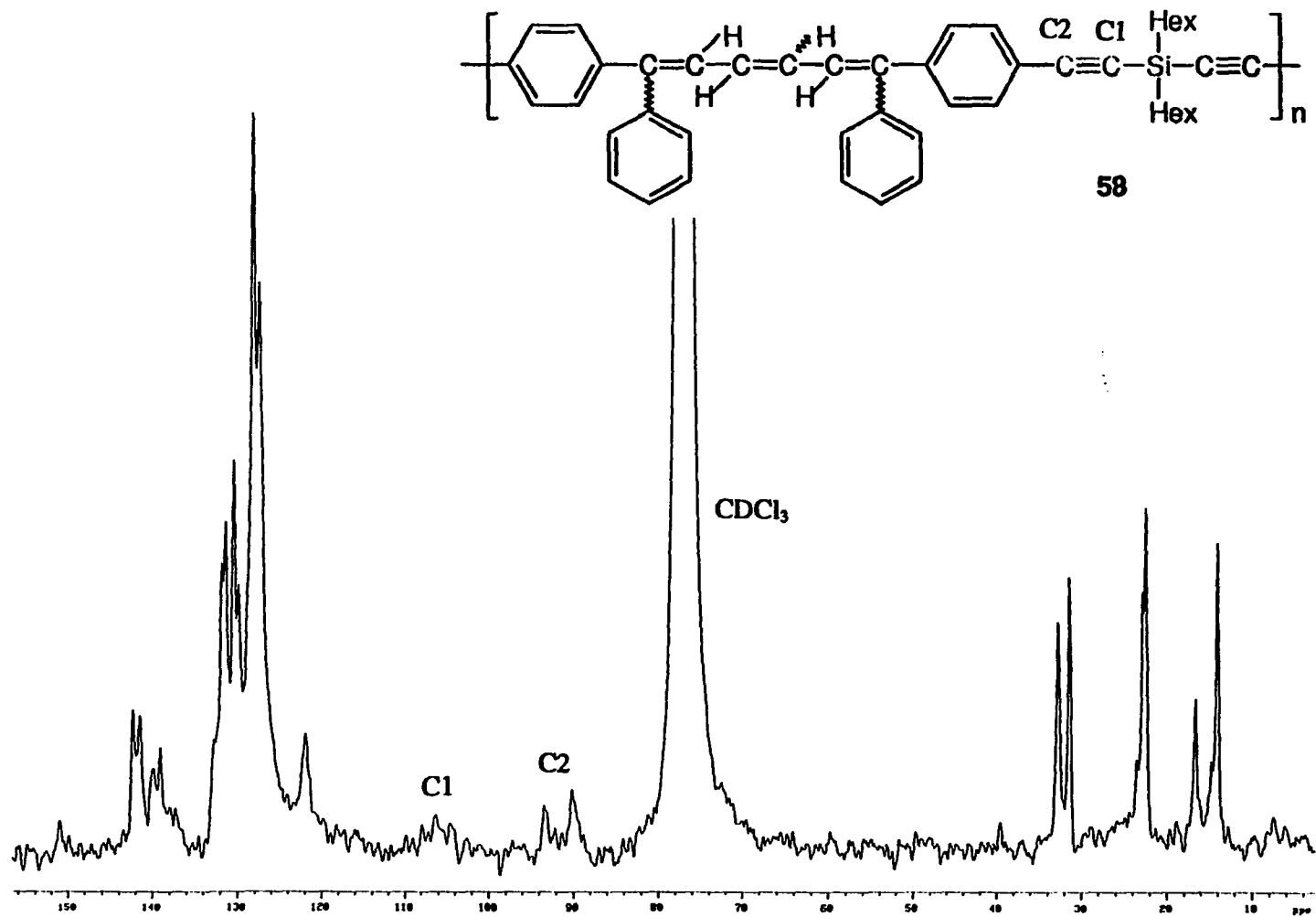


Figure 42. ¹³C-NMR spectrum of polymer 58.

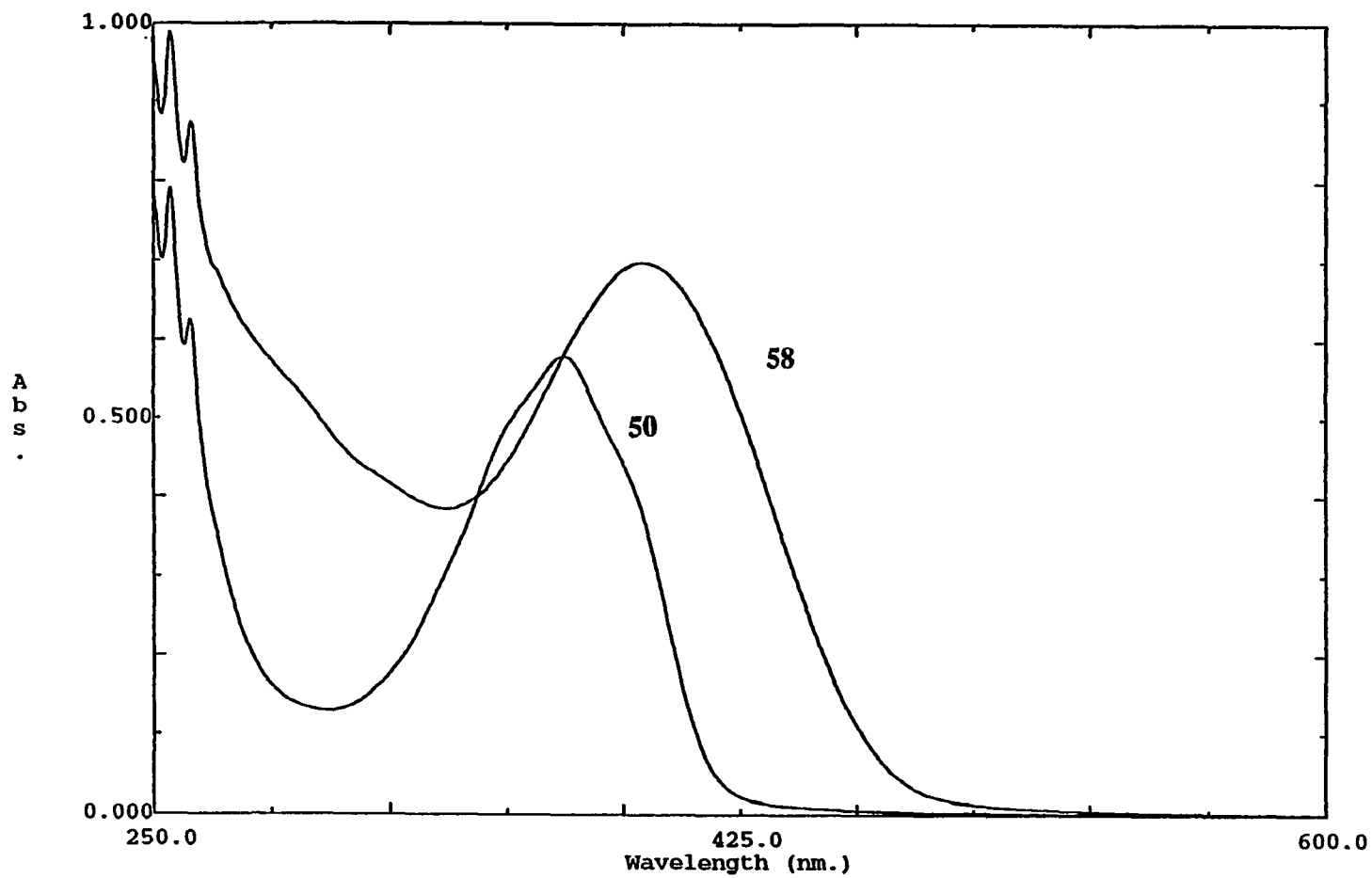


Figure 43. UV-VIS absorption spectra of 50 and polymer 58.

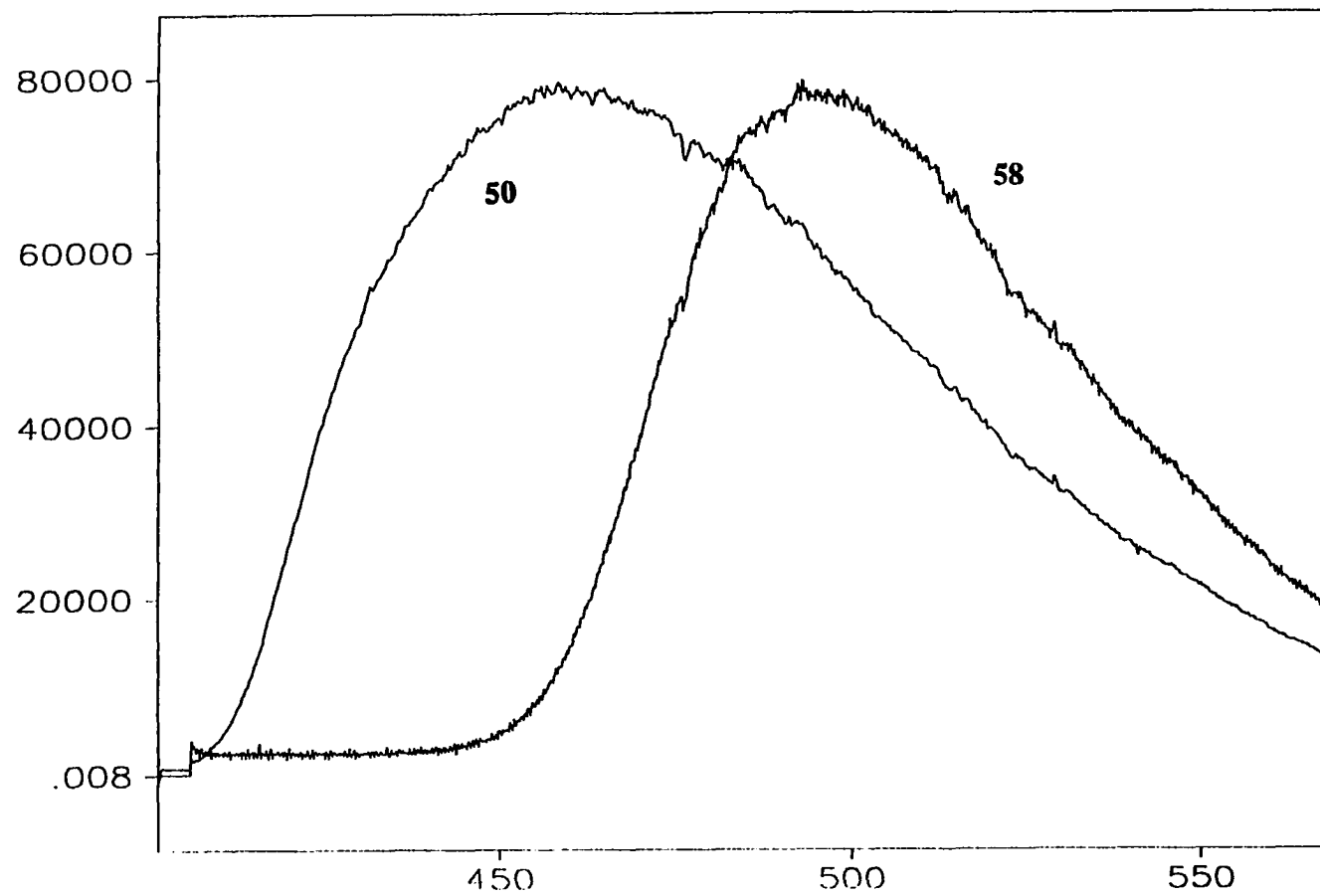


Figure 44. Photoluminescence spectra of 50 and polymer 58 (excited at 308 nm).

double bonds is replaced by a single bond. If looking only at the butadiene and butatriene parts, the bond alternation theory is apparently correct, as **55** (two double bonds are separated by a single bond) is alternative and **53** (three double bonds are directly connected) is not. However in 1,1,4,4-tetraphenyl-1,2,3-butatriene (**2b**), the double bonds are significantly different with the central one (1.260Å) being much shorter than the other two (1.348Å) (Table II). Thus, the bonds are alternative. Actually, in butadiene, the double bond (1.38Å) is longer than normal double bond, and the single bond (1.47Å) is shorter than normal single bond. Of course in their entireties both polymers are bond alternative, since both have three different bonds: the phenyl bonds, the single bonds, and the double bonds. Thus, it is necessary to find a fundamental structural theory that will explain the different properties of these two polymers.

When a molecule absorbs a photon, its electron is excited into a higher energy level (orbital). If no photochemical reaction happens, there are two ways for the molecule to release the energy, one is by the light emission, like photoluminescence, the other is by the thermal emission. Vibrational-rotational relaxation is very fast (10^{-14} - 10^{-12} s, ps order), in contrast to electron transition (fluorescence, 10^{-9} - 10^{-7} s, ns order) (Fig. 45). During the fast relaxation (heat release) to reach the zeroth vibrational level of the electron excited state, many processes such as cross coupling with other states may occur. Molecules that are not photoluminescent are due to their transferring from one excited state to the other which may relax to ground state or may be transition forbidden, finally losing energy through thermal emission.

The situation we encountered in polymer **53** is just like this. AM1/CI and *ab initio* at the MCSCF/SOCI (3-21G) level were carried out for butatriene as a model. The results are shown in Figure 46. The first allowed transition goes to a state with 1B_u geometry. However, after it is excited into the 1B_u state, the molecule immediately is trying to twist to release the energy. Because the symmetry is reduced to C_{2v} , the state become 1B . This state crosses with two states, 3B and 1A , and cross coupling will transfer the energy to these states, which do not result in luminescence.

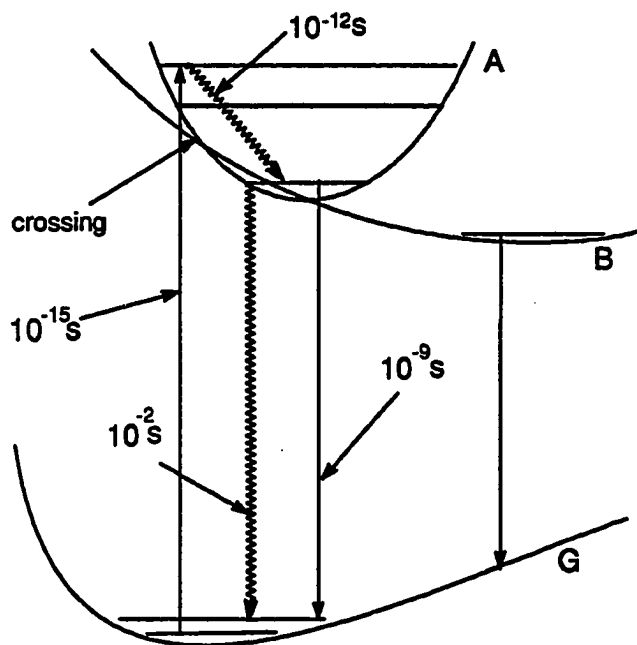


Figure 45. Schematic diagram for energy transfer process.

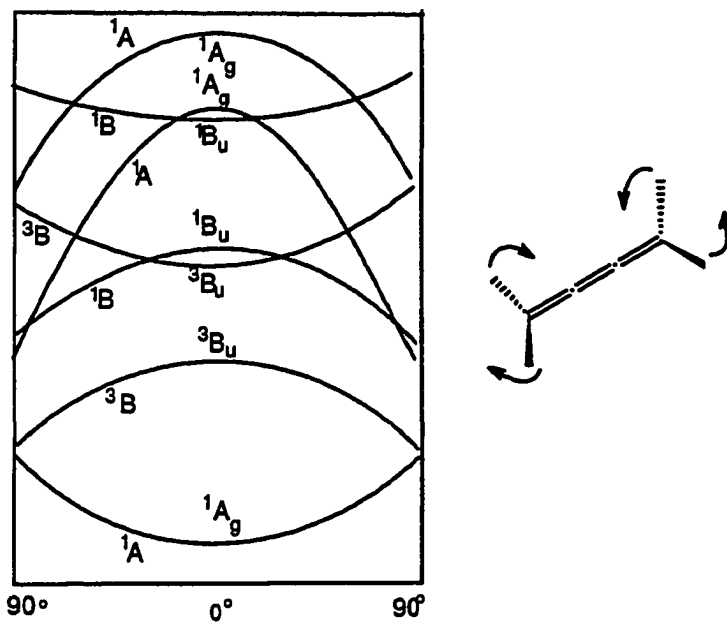


Figure 46. Energy diagram for butatriene at SOCI/MCSCF level.

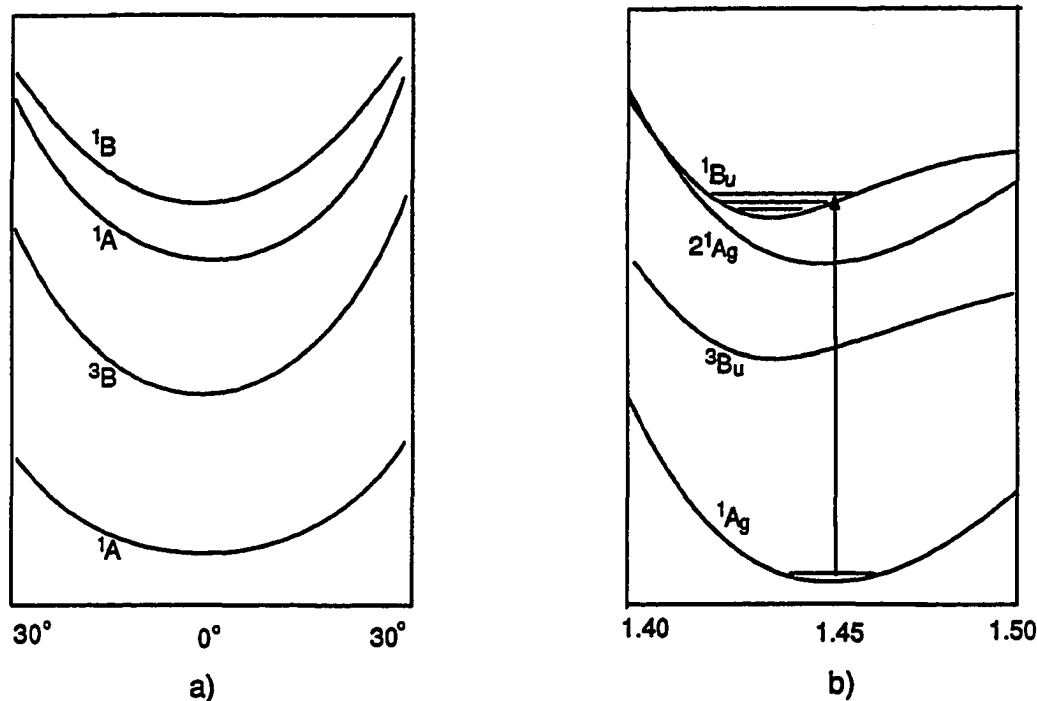


Figure 47. a) The potential energy surface for scissoring vibration for butadiene;
 b) The potential energy surface vs the single bond length of butadiene.

For polymer 55, butadiene is used as a model compound for the calculations. However, for the butadiene, these scissoring vibrations do not release energy from the excited state, nor do they afford the state crossing, and the results are shown in Figure 47a.

From Figure 47b, we can see that the excited butadiene molecule at 1B_u state will release energy by reducing the length of the single bond first. Because it does not cross with any other states during this process, it will then emit light. Here, we should mention that in the butadiene polymer, the 1B_u state has lower energy than $2{}^1A_g$ does.

In the summary, during the energy releasing process, the vibrational process is 10^3 times faster than light emission, and may cause the molecule transfer to other states in which light can not be emitted. That is what happens in this case. Excited molecules always find a way to release their surplus energy. The way in which the surplus energy is released is dependent upon the molecular structures.

Calculation details. In the AM1/CI calculations, 1,1,4,4-tetraphenyl-1,2,3-butatriene and 1,1,4,4-tetraphenyl-1,3-butadiene were used as model molecules.

In the *ab initio* calculations, 1,3-butatriene and 1,2,3-butadiene were used as the model molecules. The 3-21G basis set was chosen. First, the geometries were optimized at HF level. Then, the MCSCF calculations (6 active orbitals and 6 active electrons) were carried out to get the optimized wavefunctions. Finally, the second order configuration interaction (SOC) calculations (11,526-23,139 configurations) were performed to obtain the ground and excited state energies. All calculations were carried by GAMESS.

Conclusions

Cumulene-containing polymers were synthesized for the first time. To improve the solubility and processability of the polymers, alkoxy side chains¹⁸³ or flexible blocks (ester, siloxane, or alkoxy blocks)¹⁸⁴ as main chain segments were introduced. All the polymers synthesized were characterized by FTIR, NMR (¹H, ¹³C, and ²⁹Si), GPC, UV-VIS, and DSC.

Poly(*p*-phenylene butatriene)s were synthesized via condensations of dilithium acetylene and *p*-dibenzoylbenzene. Upon exposure to I₂ vapor, the conductivity of these polymers increased from $\sim 10^{-7}$ s/cm to ~ 1 s/cm. The ESR spectra of undoped and doped (by I₂ vapor) polymers were obtained. Intensity-dependent third order nonlinear response of poly(*p*-phenylene butatriene)s is observed by Z-scan technique. The high third order nonlinear optical response $\text{Re}\chi^{(3)}$ and second hyperpolarizability measured by Z-scan technique are 3.2×10^{-11} and 1.0×10^{-29} esu.¹⁸⁵

Poly(*p*-phenylene hexapentaene)s were synthesized by cuprous catalyzed oxidative coupling reaction of acetylenes. While a 70 nm red shift was observed compared to the butatriene-containing conjugated polymers, the conductivity of these polymers can not be increased by iodine doping. Third order nonlinearities of these polymers are still in the process of being measured.

An interesting comparison were made to 1,2,3-butatriene and 1,3-butadiene-containing polymers. While none of the cumulene-containing polymers were photoluminescent, 1,3-butadiene-containing polymers are strongly photoluminescent and electroluminescent and thus are being considered as materials for light-emitting diodes.¹⁸⁶

Experimental

^1H , ^{13}C , and ^{29}Si -NMR spectra were acquired on a Varian VXR-300 spectrometer. In order to assure the quantitative features of the ^{13}C and ^{29}Si -NMR spectra, the relaxation agent chromium(III) acetylacetonate was used in CDCl_3 with relaxation delay of 5 seconds. TMS was used as the external standard for ^{29}Si -NMR. Solid state ^{13}C -NMR spectra were obtained at 75.4 MHz on Bruker MSL300 spectrometer.

Routine GC-IR-MS spectra were obtained on a Hewlett Packard 5970 GC-IR-MS spectrometer. Other IR spectra were obtained on an IBM/Bruker IR-98 spectrometer. UV spectra were obtained on a Shimadzu UV-2101PC UV-VIS spectrometer. The ESR spin density was measured using a Bruker DSR 220X-band spectrometer with a slitted wall for optical access.

Polymer molecular weight were determined by gel permeation chromatography (GPC) with 6 Microstyrigel columns in series of 500 A, 2×10^3 A, 2×10^4 A, 2×10^5 A. THF was used as eluent at a flow rate of 1 mL/min. The system was calibrated by polystyrene standards. GPC analyses were performed on a Perkin-Elmer series 601 LC equipped with Beckman solvent delivery system, a Walter Associate R401 refractive index detector and a Viscotek viscometer. Differential scanning calorimetry (DSC) analyses were performed on a Du Pont 910 Differential Scanning Calorimeter.

THF was distilled from lithium aluminum hydride right before use. Other reagents were used as received from Aldrich Chemical Co. unless specified otherwise.

General preparation of dilithium acetylene (19). A 250 mL 2-necked oven-dried round-bottom flask, equipped with addition funnel, condenser, and magnetic stirrer, was charged with dry THF (20 mL) under argon flow and then cooled to -78°C . After n-butyllithium solution (24.0 mL, 2.5 M in hexane, 60 mmol) was transferred to the flask, trichloroethylene (1.80 mL, 20 mmol) was added dropwise. When the addition was finished, the reaction

temperature was raised to room temperature and stirred for another two hours. A white slurry was obtained.

Synthesis of 1,1,4,4-tetraphenyl-1,2,3-butatriene (2b). To the white slurry of dilithium acetylene (20 mmol) (vide supra), benzophenone (7.288 g, 40 mmol) in 20 mL dry THF was added at room temperature. The reaction mixture was refluxed for two hours and then poured into a mixture of 100 mL ether and 100 mL 2.0 M HCl acid. The separated organic layer was then washed with water twice and dried over sodium sulfate. After removal of the solvents, 1,1,4,4-tetraphenyl-2-butyne-1,4-diol (**20**) was obtained as a slightly yellow solid in quantitative yield (the weight of the product was always slightly higher than quantitative due to a small amount of THF remaining in the product even after drying at 67°C and 0.25 mmHg). m.p. 197°C (Lit.¹⁷², 196-197°C); FTIR (KBr disk) ν (cm⁻¹) 3528(m, broad, OH), 3346(m), 3167(m), 3084(m), 3057(m), 3024(m), 2972(w), 2871(w), 1597(m), 1488(s), 1450(vs), 991(s), 781(s), 746(s), 696(vs); ¹H-NMR (300 MHz, CDCl₃) δ 2.99(s, 2H), 7.10-7.55(m, 20H); ¹³C-NMR (75.429 MHz, CDCl₃) δ 74.02(2C), 89.51(2C), 125.52(8C), 127.28(4C), 127.84(8C), 144.25(4C).

In a 100 mL oven-dried round-bottom flask, equipped with magnetic stirrer and septum, diol **20** (1.17 g, 3 mmol), SnCl₂·(H₂O)₂ (1.13 g, 5 mmol), THF (10 mL) and ether (20 mL) were mixed under argon flow after which 20 mL 1.0 M HCl in ether was injected dropwise by syringe. After stirring at room temperature for one hour, considerable yellow precipitate was formed. The precipitate was filtered and washed with dilute hydrochloric acid twice and methanol once and dried under vacuum. 1,1,4,4-tetraphenyl-1,2,3-butatriene (**2b**) (0.90g, 85% yield) was obtained as bright yellow crystals. m.p. 237°C (lit.^{104a} 237°C); MS (Kratos MS50) *m/z* 357(30, M+1), 356(100, M), 276(10) 178(46); HRMS calculated for C₂₈H₂₀ *m/z* 356.15650, measured 356.15601 (Kratos MS50); FTIR (KBr disk) ν (cm⁻¹) 3055(m), 1952(w), 1890(w), 1811(w), 1591(m), 1489(s), 1441(s), 771(vs), 692(vs); ¹H-NMR (300 MHz, CDCl₃) δ 7.30-7.60(m, 20H); ¹³C-NMR (75.429 MHz, CDCl₃) 122.35(2C),

127.67(4C), 128.12(8C), 129.11(8C), 138.39(4C), 151.59(2C); UV-VIS (THF, nm) λ_{\max} (ϵ) 419 (4.07×10^4), 316(4.63×10^3), 271(3.49×10^4).

Synthesis of poly(*p*-phenylene-1,4-diphenyl-2-butyn-1,4-diol) (22). In a 250 mL oven-dried 2-necked round-bottom flask, equipped with addition funnel, condenser, and magnetic stirrer, dilithium acetylene (19) (20 mmol in 40 mL THF) was prepared according to the above described procedure. To the dianion solution was added *p*-dibenzoylbenzene (Lancaster) (21, 5.727 g, 20 mmol) dissolved in THF (100 mL) and the reaction mixture was refluxed overnight. The reaction mixture changed from a white slurry to a clear brown solution and finally to a clear red solution. After work up procedures similar as for compound 20, the slightly yellow polymer was obtained in quantitative yield after drying at 67°C under vacuum (0.25 mmHg). GPC: $M_w = 3.62 \times 10^3$, $M_n = 2.67 \times 10^3$, PDI = 1.36; FTIR (KBr disk) $\nu(\text{cm}^{-1})$ 3339(s, very broad, OH), 3059(m), 3028(m), 2974(m), 2872(m), 1650(m), 1598(m), 1489(s), 1448(vs), 1406(s), 1213(s), 1178(s), 1049(s), 1031(s), 1002(s), 895(s), 835(s), 762(s), 700(vs); $^1\text{H-NMR}$ (300 MHz, CDCl_3) δ 3.70(s, broad, 2H), 7.11 and 7.40 (two broad peaks, 20 H); $^{13}\text{C-NMR}$ (75.429 MHz, CDCl_3) δ 73.97(2C), 89.62(2C), 125.63, 127.45, 127.95, 129.80, 143.90; DSC study shows that 22 has an endothermic peak at $\sim 110^\circ\text{C}$ and an exothermic peak at $\sim 266^\circ\text{C}$.

Synthesis of poly(*p*-phenylene-1,4-diphenyl-1,2,3-butatriene) (23). A 100 mL oven-dried round-bottom flask, equipped with magnetic stirrer and septum, was charged with polymer 22 (0.936 g, 3 mmol), $\text{SnCl}_2(\text{H}_2\text{O})_2$ (1.13 g, 5 mmol), THF (20 mL), and ether (20 mL). Under argon flow and stirring, 20 mL 1.0 M HCl/ether solution was injected dropwise by syringe. The color of the solution changed from slightly yellow to red and then to purple. Stirring at room temperature was continued for another 2 hours. The purple polymer was filtered, washed with dilute aqueous HCl and methanol and vacuum dried to yield 0.7 g of 23 (84% yield). Polymer 23 is only partially soluble in CHCl_3 , THF, toluene and benzene. FTIR (KBr disk) $\nu(\text{cm}^{-1})$ 3053(m), 3026(m), 1944(w), 1659(m), 1595(s), 1499(m), 1487(s),

1442(m), 1279(s), 920(m), 910(m), 839(m), 764(s), 696(vs); $^1\text{H-NMR}$ (300 MHz, CDCl_3) two broad peaks partially overlapped δ 7.60, 7.40; Magic angle spinning at 2488, 3530, 4012 Hz, cross polarization with a contact time of 3 ms, recycle delay of 6 seconds were used respectively for solid state $^{13}\text{C-NMR}$ of polymer 23. Number of scans was 1584, 1256, 2224. $^{13}\text{C-NMR}$ (75.429 MHz) δ 122.73, 128.31, 138.38, 151.34; UV-VIS (THF) strong absorption from 400 nm to 550 nm and tailing to 650 nm; DSC shows that the polymer starts exothermic reaction at -103°C before it melts or softens.

Synthesis of *p*-alkoxybromobenzene (24a, b). A 1.0 L oven-dried round-bottom flask, equipped with condenser and magnetic stirrer, was charged with *p*-bromophenol (34.6 g, 200 mmol), K_2CO_3 (69.0 g, 500 mmol), 1-bromohexane (33.7 mL, 240 mmol) or 1-bromododecane (57.7 mL, 240 mmol), and methyl ethyl ketone (500 mL). The reaction mixture was refluxed for 80 hours. After filtration, the salts were washed with hot toluene (100 mL). After removal of organic solvents, the excess 1-bromohexane was removed by vacuum distillation. *p*-Hexoxybromobenzene (24a) was obtained as viscous liquid (50.43 g, 98% yield). GC-MS m/z 258(13, M+2), 256(13, M), 174(99), 172(100); HRMS m/z calculated for $\text{C}_{10}\text{H}_{17}\text{BrO}$ 256.04628, measured 256.04692 (Kratos MS 50); GC-FTIR $\nu(\text{cm}^{-1})$ 2939(s), 2876(m), 1578(w), 1488(vs), 1387(w) 1277(s), 1238(vs), 1169(m), 1073(m), 1007(m), 823(m); $^1\text{H-NMR}$ (300 MHz, CDCl_3) δ 0.85(t, $J = 6.6$ Hz, 3H), 1.20-1.45(m, 6H), 1.70(p, $J = 6.6$ Hz, 2H), 3.83(t, $J = 6.6$ Hz, 2H), 6.68, 6.71, 7.27, 7.30 (AB quartet, $J = 9.0$ Hz, 4H); $^{13}\text{C-NMR}$ (75.429 MHz, CDCl_3) δ 13.20(1C), 21.74(1C), 24.81(1C), 28.27(1C), 30.69(1C), 67.37(1C), 111.64(1C), 115.44(2C), 131.32(2C), 157.31(1C).

For *p*-dodecoxybromobenzene(24b), after the removal of the solvents, the resulting white crystals were washed with methanol and dried under vacuum (quantitative yield). m.p. 33°C . GC-MS m/z 342(8, M+2), 340(8, M), 174(99), 172(100), 71(11), 69(13), 57(29), 55(33); HRMS m/z calculated for $\text{C}_{18}\text{H}_{29}\text{BrO}$ 340.14018, measured 340.14043 (Kratos MS50); GC-FTIR $\nu(\text{cm}^{-1})$ 2932(vs), 2863(s), 1585(w), 1488(s), 1385(w), 1275(m),

1238(s), 1169(w), 1071(w), 1006(w), 822(w); ¹H-NMR (300 MHz, CDCl₃) δ 0.89(t, J = 6.6 Hz, 3H), 1.20-1.50(m, 18 H), 1.77(p, J = 6.6 Hz, 2H), 3.91(t, J = 6.6 Hz, 2H), 6.76, 6.79, 7.34, 7.37 (AB quartet, J = 9.0 Hz, 4H); ¹³C-NMR (75.429 MHz, CDCl₃) δ 13.78(1C), 22.33(1C), 25.62(1C), 28.80(1C), 29.00(2C), 29.19(1C), 29.22(1C), 29.26(1C), 29.28(1C), 31.55(1C), 67.87(1C), 112.14(1C), 115.90(2C), 131.79(2C), 157.83(1C).

Synthesis of 1,4-bis(*p*-alkoxybenzoyl)benzene (26a, b). A 500 mL oven-dried round bottom flask, equipped with condenser, addition funnel, and magnetic stirrer, was charged with magnesium (5.832 g, 240 mmol). The magnesium was stirred overnight under slow argon flow to be activated. After dry THF (150 mL) was charged, 1,2-dibromoethane (0.1 mL) was added to initiate the reaction. *p*-Hexoxybromobenzene (51.4 g, 200 mmol) or *p*-dodecoxybromobenzene (68.2 g, 200 mmol) in THF (100 mL) was added at a speed that the reaction is under mild refluxing. Stirring was continued for another 20 minutes after the addition was finished. To the above Grignard solution (25a,b), 1,4-dicyanobenzene (11.78 g, 92 mmol) and copper (I) bromide (0.5 g) were added in one portion under argon flow. As soon as copper (I) bromide was added, there was a lot of bubbling and the reaction mixture quickly solidified. Another 100 mL THF was transferred to the flask and the solid was broken up with a spatula. Refluxing for one hour produced a sticky mixture which was slowly added to 300 mL 15% cold sulfuric acid in a 2 L beaker with stirring. The black slurry turned to a yellow solid and an additional 150 mL more 15% sulfuric acid was added to break up the precipitate. After refluxing the whole work up mixture for 3 hours, the white crystals floating on the solution were filtered and then washed with water three times and ether twice. After vacuum drying in the presence of phosphorous pentoxide, 1,4-bis(*p*-hexoxybenzoyl)benzene (26a, 40.1 g, 90% yield) or 1,4-bis(*p*-dodecoxybenzoyl)benzene (26b, 51.0 g, 82% yield) was obtained.

For 1,4-bis(hexoxybenzoyl)benzene (26a): m.p.169-170°C. MS (Kratos MS50) *m/z* 487(18, M+1), 486(50, M), 402(14), 318(37), 232(15), 142(35), 127(89), 121(77), 85(100),

67(67), 59(72); HRMS m/z cal. for $C_{32}H_{38}O_4$ 486.27701, measured 486.27683 (Kratos, MS50); FTIR (KBr disk) $\nu(\text{cm}^{-1})$ 2955(m), 2937(m), 2862(m), 1641(vs), 1602(s), 1578(w), 1506(w), 1310(m), 1286(m), 1252(s), 1178(m), 1155(m), 1028(m), 930(m), 868(m), 841(m), 746(m), 700(m); $^1\text{H-NMR}$ (300 MHz, CDCl_3) δ 0.911(t, $J = 6.9$ Hz, 6H), 1.25-1.55(m, 12H), 1.82(p, $J = 6.9$ Hz, 4H), 4.05(t, $J = 6.6$ Hz, 2H), 6.95, 6.98, 7.83, 7.86 (AB quartet, $J = 9.0$ Hz, 8H), 7.82 (s, 4H); $^{13}\text{C-NMR}$ (75.429 MHz, CDCl_3) δ 13.39(2C), 21.92(2C), 24.99(2C), 28.38(2C), 30.86(2C), 67.73(2C), 113.54(4C), 128.65(6C), 132.00(4C), 140.37(2C), 162.54(2C), 194.17(2C).

For 1,4-bis(*p*-dodecoxybenzoyl)benzene (26b): m.p.142-143°C. MS (Kratos MS50) m/z 656(10, M+2), 655(45, M+1), 654(100, M), 629(18), 486(29), 318(26), 121(73), 94(54), 57(55), 55(40); HRMS m/z cal. for $C_{44}H_{62}O_4$ 654.46481, measured 654.46295 (Kratos MS50); FTIR (film on KBr) $\nu(\text{cm}^{-1})$ 2954(m), 2918(s), 2848(s), 1639(vs), 1605(s), 1578(m), 1506(m), 1471(m), 1464(m), 1310(m), 1286(m), 1254(m), 1177(m), 1155(m), 868(m), 841(m), 744(m), 700(m); $^1\text{H-NMR}$ (300 MHz, CDCl_3) δ 0.88(t, $J = 6.6$ Hz, 6H), 1.20-1.55(m, 36H), 1.82(p, $J = 6.9$ Hz, 4H), 4.05(t, $J = 6.6$ Hz, 4H), 6.95, 6.98, 7.82, 7.86 (AB quartet, $J = 9.0$ Hz, 8H), 7.82 (overlapped, s, 4H); $^{13}\text{C-NMR}$ (75.429 MHz, CDCl_3) δ 13.87(2C), 22.43(2C), 25.72(2C), 28.84(2C), 29.09(4C), 29.30(2C), 29.32(2C), 29.37(2C), 29.39(2C), 31.65(2C), 68.12(2C), 113.94(4C), 129.06(6C), 132.40(4C), 140.81(2C), 162.98(2C), 194.60(2C).

Synthesis of poly(*p*-phenylene-1,4-bis(*p*-hexoxyphenyl)-2-butyn-1,4-diol) (27a). 27a was synthesized in quantitative yield following the same procedure as for the synthesis of polymer 22. $M_w = 3.72 \times 10^3$, PDI = 1.40; FTIR (film on KBr) $\nu(\text{cm}^{-1})$ 3429(s, broad, OH), 3039(w), 2954(vs), 2931(vs), 2860(s), 1645(w), 1607(s), 1585(m), 1508(vs), 1470(m), 1304(s), 1248(vs), 1174(s), 1018(s), 831(s); $^1\text{H-NMR}$ (300 MHz, CDCl_3) 0.92(s, broad, 6H), 1.34(s, broad, 12H), 1.72(s, broad, 4H), 3.81(s, broad, 4H), 3.99(s, broad, 2H), 6.68(s, broad, 4H), 7.37(s, broad, 8H); $^{13}\text{C-NMR}$ (75.429 MHz, CDCl_3) (the assignment of peaks is

similar as that for polymer **27b** in Fig. 8) δ 13.68(2C), 22.22(2C), 25.31(2C), 28.80(2C), 31.22(2C), 67.56(2C), 73.55(2C), 89.53(2C), 113.63, 125.48, 126.90, 129.17, 129.49, 132.29, 136.21, 143.98, 157.98; DSC shows two small endothermic peaks at 69°C and 103°C before an exothermic reaction starts at 237°C.

Synthesis of poly(*p*-phenylene-1,4-bis(*p*-dodecoxyphenyl)-2-butyne-1,4-diol) (**27b**). **27b** was synthesized in quantitative yield following the same procedure as for the synthesis of polymer **22**. $M_w = 4.44 \times 10^3$, PDI = 1.32; FTIR (film on KBr) $\nu(\text{cm}^{-1})$ 3423(s, broad, OH), 3039(w), 2926(vs), 2854(vs), 1645(m), 1604(s), 1508(vs), 1468(s), 1418(m), 1402(m), 1306(s), 1250(vs), 1175(s), 1107(m), 1018(m), 831(s); $^1\text{H-NMR}$ (300 MHz, CDCl_3) δ 0.89(s, broad, 6H), 1.27(s, broad, 36H), 1.71(s, broad, 4H), 3.83(s, broad, 4H), 3.99(s, broad, 2H), 6.72(s, broad, 4H), 7.39(s, broad, 8H); $^{13}\text{C-NMR}$ (75.429 MHz, CDCl_3) (see Fig. 8 for peak assignments) δ 13.48(2C), 22.02(2C), 25.37(2C), 28.70-29.00(14C), 31.24(2C), 67.30(2C), 73.25(2C), 89.28(2C), 113.33, 125.20, 126.63, 129.16, 131.96, 135.82, 143.73, 148.41, 157.77, 162.16, 194.57; DSC shows two small endothermic peaks at 82°C and 113°C before an exothermic reaction starts at 196°C.

Synthesis of poly(*p*-phenylene-1,4-bis(*p*-hexoxyphenyl)-1,2,3-butatriene) (**28a**). **28a** was synthesized following the similar procedure to synthesize **23** except the final polymer was precipitated from methanol because the polymer has much better solubility than **23**. FTIR (film on KBr) $\nu(\text{cm}^{-1})$ 2930(s), 2858(m), 1948(m), 1649(w), 1601(s), 1549(w), 1506(s), 1468(m), 1298(m), 1248(vs), 1173(s), 1110(w), 1016(w), 833(m); $^1\text{H-NMR}$ (300 MHz, CDCl_3) δ 0.91(s, broad, 6H), 1.35(three peaks overlapped, broad, 12H), 1.80(s, broad, 4H), 4.00(s, broad, 4H), 6.93(s, broad, 4H), 7.55(m, broad, 8H); $^{13}\text{C-NMR}$ (75.429 MHz, CDCl_3) δ 13.84(2C), 22.39(2C), 25.51(2C), 29.03(2C), 31.38(2C), 67.90(2C), 114.21, 120.93, 129.09, 129.80, 130.55, 132.28, 136.71, 138.60, 142.63, 148.59, 149.99, 158.96, 162.61; UV-VIS (THF, nm): $\lambda_{\text{max}}(\epsilon) = 548 (1.21 \times 10^4)$, 486 (1.37×10^4), 437 (1.62×10^4), and the

absorption tails until 700 nm ($\epsilon = 5.68 \times 10^2$); DSC analysis shows that an exothermic reaction starts at 154°C before it melts or softens.

Synthesis of poly(*p*-phenylene-1,4-bis(*p*-dodecoxyphenyl)-1,2,3-butatriene) (28b). 28b was synthesized following the similar procedure as for the synthesis of polymer 28a. FTIR (KBr disk) $\nu(\text{cm}^{-1})$ 2924(vs), 2853(s), 1942(m), 1649(m), 1601(s), 1506(s), 1468(m), 1393(w), 1298(m), 1250(vs), 1175(m), 833(m); $^1\text{H-NMR}$ (300 MHz, CDCl_3) δ 0.89(s, broad, 6H), 1.28(two peaks overlapped, broad, 36H), 1.81(s, broad, 4H), 4.01(s, broad, 4H), 6.95(s, broad, 4H), 7.55(m, broad, 8H); $^{13}\text{C-NMR}$ (75.429 MHz, CDCl_3) 13.85(2C), 22.40(2C), 25.77(2C), 29.08 overlapped with 29.35(14C total), 31.63(2C), 67.83(2C), 113.75, 114.16, 120.70, 128.67, 129.00, 129.71, 130.45, 132.20, 136.61, 138.29, 142.47, 148.49, 149.90, 158.88, 162.53, 194.63; UV-VIS(THF, nm): λ_{max} (ϵ) = 543 (1.24×10^4), 483 (1.51×10^4), 437 (1.69×10^4), and the UV absorption tails until 700 nm (at 700 nm, $\epsilon = 4.08 \times 10^2$); DSC analysis shows that an exothermic reaction starts at 125°C before it melts or softens.

.

Synthesis of 1,1-diphenyl-2-propyn-1-ol (29). In a 250 mL oven-dried, argon-flushed round bottom flask equipped with addition funnel and magnetic stirrer, 6.37 g of benzophenone (35 mmol) and 50 mL THF were charged. Ethynyl magnesium chloride (140 mL, 0.5 M in THF, 70 mmol, 100% excess) was added dropwise. After stirring overnight, an aliquot was taken by syringe and quenched with dilute acid. According to GC-MS analysis compound 29 was the only product.

The reaction solution was poured into a mixture of 200 mL ether and 100 mL 2.0 M cold HCl acid. The organic layer was washed with acid one more time, then water twice, dried over sodium sulfate. After removal of solvents, the product was obtained as a slightly yellow oil which slowly crystallized out to give colorless crystals (m.p. 46-48°C, lit.¹¹³ 47°C, 100% yield). GCMS m/z 209(8, M+1), 208(53, M), 207(44), 189(20), 179(32), 178(26), 165(21), 131(47), 130(46), 105(19), 103(15), 102(18), 78(24), 77(41), 53(100); GC-FTIR ν

(cm^{-1}) 3632(s), 3323(vs), 3071(vs), 3040(s), 1598(m), 1490(s), 1450(s), 1330(s), 1260(s), 1170(s), 1034(s), 983(s), 891(s).

Synthesis of 1,1,6,6-tetraphenyl-2,4-hexadiyn-1,6-diol (30). CuCl (0.5 g) and acetone (10 mL) were charged into a 25 mL round bottom flask under argon flow. TMEDA (0.25 mL) was injected by syringe and the reaction mixture was stirred for one hour after which the blue/green clear solution was ready to use as oxidative coupling catalyst.

To a 250 mL oven-dried 2-necked round bottom flask, equipped with dry-ice condenser and magnetic stirrer, compound 29 (4.16 g, 20 mmol) and THF (50 mL) were added with stirring and slow oxygen bubbled flow, catalyst solution (10 mL, from above) was injected. After 5 hour of reaction, the green reaction mixture was poured into a mixture of 100 mL ether and 50 mL 2.0 M aqueous HCl. The organic layer was washed one more time with acid, twice with water, and then dried over sodium sulfate. After removal of the organic solvents, compound 30 was obtained in quantitative yield as a viscous oil. MS (Kratos MS 50) m/z 414(0.5, M), 309(16), 203(12), 182(14), 105(100), 77(65); HRMS cal. for $\text{C}_{30}\text{H}_{22}\text{O}_2$ 414.16198, measured 414.16263 (Kratos MS 50); FTIR (KBr disk) ν (cm^{-1}) 3412(broad, s, OH), 3061(w), 3028(w), 2926(w), 1599(m), 1491(s), 1450(vs), 1337(s), 1163(s), 1042(s), 1003(s), 891(m), 766(s), 698(vs), 642(s); $^1\text{H-NMR}$ (300 MHz, CDCl_3) δ 3.49(s, 2H), 7.28-7.57(m, 20H); $^{13}\text{C-NMR}$ (75.429 MHz, CDCl_3) δ 70.55(2C), 74.29(2C), 82.26(2C), 125.59(8C), 127.53(4C), 127.90(8C), 143.53(4C).

Synthesis of 1,1,6,6-tetraphenyl-1,2,3,4,5-hexapentaene (31). In a 100 mL oven-dried round bottom flask equipped with magnetic stirrer and septum, compound 30 (2.07 g, 5 mmol), $\text{SnCl}_2(\text{H}_2\text{O})_2$ (2.031 g, 9 mmol), ether (30 mL), and THF (15 mL) were charged. With stirring, 30 mL 1.0 M HCl/ether solution was injected dropwise by a syringe. The color of the solution turned to red. After stirring at room temperature for 2 hours, the precipitated red solid was filtered and washed with dilute HCl and methanol. After drying under vacuum, 1.25 g of compound 31 was obtained. A second crop, 0.20 g of lower purity was recovered from

the filtrate (total yield 77%). DSC analysis for compound **31** shows an exothermic reaction starts at 168°C before it melts (lit.^{104a} m.p. 301°C). MS (Kratos MS 50) *m/z* 381(19, M+1), 380(55, M), 302(14), 149(20), 129 (14), 111(17), 109(14), 97(38), 83(56), 69(79), 55(100); HRMS *m/z* cal. for C₃₀H₂₀ 380.15650, measured 380.15644 (Kratos MS 50); FTIR (KBr disk) $\nu(\text{cm}^{-1})$ 3053(w), 2000(w), 1593(w), 1487(m), 1450(m), 770(s), 765(s), 694(vs); ¹H-NMR (300 MHz, CDCl₃) δ 7.35-7.60 (m, 20H); ¹³C-NMR (75.429 MHz, CDCl₃) δ 124.33(2C), 126.90(2C), 128.22(8C), 128.28(4C), 129.01(8C), 137.68(4C), 148.94(2C).

Synthesis of Compound 32. Compound **32a** or **32b** were synthesized in quantitative yield from the reaction of **26a** or **26b** with ethynyl magnesium chloride following the same procedure as for the synthesis of compound **29**.

Characterization for compound 32a: MS (Kratos MS 50) *m/z* 539(29, M+1), 538(73, M), 521(11), 512(13), 486(20), 318(22), 308(20), 307(36), 290(14), 232(15), 224(18), 223(39), 173(14), 171(14), 147(100), 121(80); HRMS *m/z* cal. for C₃₆H₄₂O₄ 538.30831, measured 538.30861 (Kratos MS 50); FTIR (film on KBr) $\nu(\text{cm}^{-1})$ 3447(broad, s, OH), 3290(s, $\equiv\text{C-H}$), 3039(w), 2955(s), 2932(s), 1892(w), 1609(s), 1583(m), 1510(vs), 1470(m), 1302(m), 1248(vs), 1175(s), 1051(m), 989(s), 831(s), 652(m); ¹H-NMR (300 MHz, CDCl₃) δ 0.90(t, J = 6.9 Hz, 6H), 1.33(m, 8H), 1.43(m, 4H), 1.76(p, J = 6.9 Hz, 4H), 2.84 (-C \equiv C-H, s, 2H), 2.89 (-OH, s, 2H), 3.92(t, J = 6.6 Hz, 4H), 6.83(d, J = 9.3 Hz, 4H), 7.48(d, J = 9.0 Hz, 4H), 7.55(s, 4H); ¹³C-NMR (75.429 MHz, CDCl₃) δ 13.63(2C), 22.17(2C), 25.26(2C), 28.75(2C), 31.13(2C), 67.59(2C), 73.31(2C), 75.12(2C), 86.15(2C), 113.68(4C), 125.46(4C), 126.88(4C), 135.80(2C), 143.67(2C), 158.33(2C).

Characterization of 32b. MS (Kratos MS 50) *m/z* (the molecular ion was not observed) 628(5), 540(5), 262(11), 240(9), 205(17), 94(100), 77(19); FTIR (film on KBr) $\nu(\text{cm}^{-1})$ 3437(broad, s, OH), 3288(s, $\equiv\text{C-H}$), 3038(w), 2957(s), 2853(s), 1892(w), 1609(s), 1583(s), 1508(s), 1468(s), 1418(m), 1302(s), 1252(s), 1175(s), 1051(s), 989(s), 903(s), 829(s),

721(m), 654(s); $^1\text{H-NMR}$ (300 MHz, CDCl_3) δ 0.90(t, $J = 6.6$ Hz, 6H), 128-1.45(m, 36H), 1.78(m, 4H), 2.83 ($-\text{C}\equiv\text{C}-\text{H}$, s, 2H), 3.12 ($-\text{OH}$, s, broad, 2H), 3.92(t, $J = 6.6$ Hz, 4H), 6.82(d, $J = 9.0$ Hz, 4H), 7.48(d, $J = 9.0$ Hz, 4H), 7.54(s, 4H); $^{13}\text{C-NMR}$ (75.429 MHz, CDCl_3) δ 13.76(2C), 22.31(2C), 25.64(2C), 28.84(2C), 28.98(d, 4C), 29.25(t, 8C), 31.53(2C), 67.63(2C), 73.31(2C), 75.04(2C), 86.26(2C), 113.71(4C), 125.49(4C), 126.91(4C), 135.92(2C), 143.74(2C), 158.33(2C).

Synthesis of polymer 33a and 33b. Polymer 33a or 33b were synthesized from the oxidative coupling reaction of compound 32a or 32b following the same procedure as for the synthesis of compound 30.

Characterization of polymer 33a. GPC: $M_w = 2.18 \times 10^4$, $M_n = 8.31 \times 10^3$, PDI = 2.62; FTIR (film on KBr) ν (cm^{-1}) 3427(broad, s, OH), 3039(w), 2955(s), 2932(s), 1609(s), 1583(m), 1508(vs), 1470(m), 1304(m), 1248(vs), 1175(s), 1049(m), 1016(m), 989(m), 829(s); $^1\text{H-NMR}$ (300 MHz, CDCl_3) δ 0.87(s, broad, 6H), 1.29(s, broad, 12H), 1.68(s, broad, 4H), 3.81(s, broad, 4H), 6.70(s, broad, 4H), 7.32(s, broad, 8H); $^{13}\text{C-NMR}$ (75.429 MHz, CDCl_3) δ 13.59(2C), 22.12(2C), 25.21(2C), 28.68(2C), 31.11(2C), 67.56(2C), 70.58(2C), 73.87(2C), 82.34(2C), 113.70(4C), 125.56(4C), 126.94(4C), 135.22(2C), 143.17(2C), 158.16(2C); DSC: small endothermic peak at 89.5°C, exothermic reaction starts at 164°C.

Characterization of 33b. GPC: $M_w = 2.80 \times 10^4$, $M_n = 9.11 \times 10^3$, PDI = 3.07; FTIR (film on KBr) ν (cm^{-1}) 3422(broad, s, OH), 3038(w), 2924(vs), 2854(vs), 1609(s), 1583(w), 1508(vs), 1468(m), 1248(vs), 1175(s), 1016(m), 989(m), 829(s); $^1\text{H-NMR}$ (300 MHz, CDCl_3) δ 0.88(t, $J = 6.6$ Hz, 6H), 1.26(s, broad, 36H), 1.70(s, broad, 4H), 3.83(s, broad, 4H), 6.72(s, broad, 4H), 7.30(s, broad, 8H); $^{13}\text{C-NMR}$ (75.429 MHz, CDCl_3) δ 13.85(2C), 22.41(2C), 25.76(2C), 29.10-29.37(14C), 31.64(2C), 67.75(2C), 70.75(2C), 74.03(2C),

82.49(2C), 113.86(4C), 125.72(4C), 127.10(4C), 135.35(2C), 143.37(2C), 158.37(2C);

DSC: endothermic peak at 106°C, exothermic reaction starts at 131°C.

Synthesis of polymer 34a and 34b. In a 100 mL oven-dried round bottom flask, equipped with magnetic stirrer and septum, 1.608 g of polymer 33a (or 2.112 g of polymer 33b) (3 mmol), $\text{SnCl}_2 \cdot (\text{H}_2\text{O})_2$ (1.129 g, 5 mmol), THF (20 mL), and ether (20 mL) were charged under argon flow. 20 mL 1.0 M HCl/Ether solution was injected slowly into the above reaction by a syringe. The reaction solution turned purple immediately. After stirring at room temperature for four hours, the homogeneous solution was poured into 100 mL methanol. The precipitated black polymer was filtered and washed with dilute hydrochloric acid and then methanol. **The entire work up should be performed as fast as possible. The polymer, after methanol washing, should be immediately vacuum dried.**

No matter how fast the work up is, polymer 34a obtained (1.2 g, 80% yield) can not be redissolved in common organic solvents.

Polymer 34b obtained (1.96 g 97% yield) is readily soluble in common organic solvents such as THF or toluene. To preserve its solubility, polymer 34b needs to be kept under argon or vacuum.

Characterization of polymer 34a. FTIR (KBr disk) ν (cm^{-1}) 3036(w), 2953(s), 2858(m), 2000(w), 1601(s), 1506(vs), 1468(m), 1292(m), 1248(vs), 1173(s), 1018(m), 831(s); Solid state ^{13}C -NMR δ 12.82, 21.52, 24.58, 28.24, 30.23, 66.60, 113.00, 128.48, 157.48; UV-VIS (THF, nm): $\lambda_{\text{max}} = 509, 432, 378$ nm, strong UV absorption tails until 800 nm; DSC: an exothermic reaction starts at 148°C.

Characterization of 34b. FTIR (film on KBr) ν (cm^{-1}) 3038(w), 2924(vs), 2853(s), 2002(w), 1601(s), 1506(s), 1468(m), 1294(m), 1248(vs), 1173(s), 1018(m), 831(s); ^1H -NMR (300 MHz, CDCl_3) δ 0.88(s, broad, 6H), 1.27(s, broad, 36H), 1.78(s, broad, 4H), 3.99(s, broad, 4H), 6.93(s, broad, 4H), 7.51(s, broad, 8H); ^{13}C -NMR (75.429 MHz, CDCl_3)

δ 13.53, 22.09, 25.46, 29.02, 31.31, 67.48, 113.51, 129.99 (broad), 136.64 (weak), 145.68 (weak), 148.59 (weak), 158.73; UV-VIS(THF, nm): λ_{\max} (ϵ) = 507 (1.49×10^4), 431 (1.19×10^4), 377 (1.14×10^4), UV absorption tails until 800 nm (at 750 nm, $\epsilon = 1.09 \times 10^3$); DSC: an exothermic reaction starts at 105°C.

Synthesis of benzil monoanil (37). In a 250 mL oven-dried round bottom flask, equipped with magnetic stirrer, Dean-Stark trap and condenser, benzil (21.0 g, 100 mmol), aniline (9.3 g, 100 mmol), *p*-toluene sulfuric acid (0.125 g), and benzene (50 mL) were charged. The mixture was refluxed overnight while the water formed was distilled out by azeotropic distillation.

After removal of all the solvents, the products were recrystallized twice in a mixture of 150 mL hexane, 20 mL benzene. 20.4 g of yellow crystal was obtained (72% yield), m.p. 97-100 °C. FTIR (film on KBr) ν (cm^{-1}) 3060(m), 1673(vs), 1622(s), 1617(vs), 1578(s), 1484(s), 1448(s), 1228(s), 1195(s), 1173(s), 766(s), 693(vs); $^1\text{H-NMR}$ (300 MHz, CDCl_3) 6.89-7.92 (m, 25H); $^{13}\text{C-NMR}$ (75.429 MHz, CDCl_3) δ 120.21(2C), 124.46(1C), 127.90(2C), 128.40(2C), 128.60(4C), 129.05(2C), 131.49(1C), 134.12(1C), 134.39(1C), 134.82(1C), 148.96(1C), 166.01(1C), 197.36(1C).

Synthesis of compound 38. To a white slurry of dilithium acetylene (19) (10 mmol in 20 mL THF) made according to procedure described earlier, benzil monoanil (37, 5.7 g, 20 mmol) dissolved in 25 mL THF was added dropwise. After the addition the reaction mixture was refluxed overnight.

The reaction mixture was then poured into a mixture of 100 mL THF and 200 mL 2.0 M HCl acid and the mixture was refluxed for one hour. The aqueous layer was extracted with two portions of 100 mL ether, the combined organic layer was washed with water twice and dried over sodium sulfate.

After removal of the organic solvents, the product was redissolved in 50 mL THF in a 100 mL round bottom flask. Trimethylchlorosilane (2.53 mL, 20 mmol) and imidazole (5.44

g, 80 mmol) were added. The reaction mixture was stirred overnight. The reaction mixture was then added to a mixture of 100 mL ether and 100 mL 2.0 M HCl acid, the organic layer was washed with water twice, dried over sodium sulfate. After removal of all the organic solvents, the product was purified on a silica gel column (hexanes: ethyl acetate = 10:1).

The product has two isomers (*meso* and *dl* pair). One isomer was crystallized out from hexanes as slightly yellow crystals. m.p. 130-132°C. FTIR (film on KBr) ν (cm⁻¹) 3087(m), 2957(m), 1700(vs), 1597(m), 1448(s), 1252(vs), 1154(s), 1126(s), 1101(s), 1074(s), 876(vs), 846(vs), 755(s), 651 (s); ¹H-NMR (300 MHz, CDCl₃) δ -0.05(s, 18H), 7.26-7.97(m, 20H); ¹³C-NMR (75.429 MHz, CDCl₃) δ 0.92(6C), 79.76(2C), 89.22(2C), 125.98(4C), 127.60(4C), 128.09(2C), 128.40(4C), 130.48(4C), 132.34(2C), 133.58(2C), 140.53(2C), 194.54(2C); MS (Kratos MS50) *m/z* 590(4, M), 485(42), 380(13), 105(100), 73(44); HRMS *m/z* cal. for C₃₆H₃₈O₄Si₂ 590.23087, measured 590.23092 (Kratos MS50).

NMR spectra of the other isomer was obtained by subtraction of the spectra of the above isolated isomer from the spectra of the mixture. ¹H-NMR (300 MHz, CDCl₃) δ 0.04(s, 18H), 7.29-7.97(m, 20H); ¹³C-NMR (75.429 MHz, CDCl₃) δ 1.08(6C), 79.76(2C), 89.30(2C), 125.92(4C), 127.57(4C), 128.07(2C), 128.28(4C), 130.44(4C), 132.32(2C), 133.70(2C), 140.43(2C), 194.57(2C).

Synthesis of diketone 39. In a 1 liter oven-dried round bottom flask, equipped with magnetic stirrer and condenser, 4-hydroxybenzophenone (39.6 g, 200 mmol), 1,10-dibromodecane (30.0 g, 100 mmol), potassium carbonate (55.2 g, 400 mmol), and DMF (500 mL) were added. The reaction mixture was refluxed for 24 hours at ~160°C.

The reaction mixture was poured into 3L H₂O to afford a white precipitate. After stirring for 5-10 minutes, the reaction was left standing for 4 hours. The precipitate was filtered and washed with distilled water twice and ethanol three times, and then vacuum dried to give 50.91 g product 39 (95% yield). m.p. 135-136°C. MS (Kratos MS 50) *m/z* 534(4, M), 337(30), 324(21), 211(47), 198(53), 183(21), 121(100), 105(71); HRMS *m/z* cal. for C₃₆H₃₈O₄ 534.27701, measured 534.27736 (Kratos MS 50); FTIR (KBr disk) ν (cm⁻¹)

2937(s), 2922(m), 1641(vs), 1603(vs), 1576(m), 1506(m), 1308(s), 1290(vs), 1175(m), 1150(m), 1018(s), 939(m), 849(s), 795(m), 694(s); $^1\text{H-NMR}$ (300 MHz, CDCl_3) δ 1.35-1.52(m, 12H), 1.82(p, $J = 7.2$ Hz, 4H), 4.04(t, $J = 6.3$ Hz, 4H), 6.95(d, $J = 8.7$ Hz, 4H), 7.46-7.56(m, 6H), 7.75 (d, $J = 7.8$ Hz, 4H), 7.82(d, $J = 8.7$ Hz, 4H); $^{13}\text{C-NMR}$ (75.429 MHz, CDCl_3) δ 25.66(2C), 28.79(2C), 29.01(2C), 29.15(2C), 67.95(2C), 113.68(4C), 127.89(4C), 129.40(4C), 129.56(2C), 131.57(2C), 132.26(4C), 138.00(2C), 162.51(2C), 195.25(2C).

Synthesis of polymer 40. To a 250 mL oven-dried 2-necked round bottom flask, equipped with condenser, addition funnel and magnetic stirrer, diketone 39 (21.36 g, 40 mmol) and THF (40 mL) were added. Dilithium acetylene slurry (40 mmol, 80 mL THF) was transferred into the flask. THF (10 mL) was used to wash the dilithium acetylene flask and then transferred to the reaction mixture. The reaction mixture was then refluxed for 36 hours. The reaction mixture was poured into a mixture of 200 mL ether and 100 mL cold 2.0 M HCl. The organic layer was washed with dilute HCl one more time and then with water twice, dried over sodium sulfate. After removal of the organic solvents and drying under vacuum, 23.0 g of polymer 40 was obtained (a little more than the theoretical yield 22.4 g because of small amount of THF was not removed by vacuum drying according to NMR). GPC: $M_w = 2.20 \times 10^4$, $M_n = 8.10 \times 10^3$, PDI = 2.72; FTIR (film on KBr) ν (cm^{-1}) 3441(broad, m, OH), 3060(w), 2930(s), 2854(m), 1609(s), 1508(vs), 1491(m), 1304(m), 1248(vs), 1175(s), 1032(m), 829(m), 698(m); $^1\text{H-NMR}$ (300 MHz, CDCl_3) δ 1.32-1.45(m, broad, 12H), 1.77(m, broad, 4H), 3.56 (-OH, broad, 2H), 3.89(t, broad, 4H), 6.78(d, $J = 8.4$ Hz, 4H), 7.28(m, 6H), 7.45(d, $J = 8.1$ Hz, 4H), 7.56(d, $J = 7.2$ Hz, 4H); $^{13}\text{C-NMR}$ (75.429 MHz, CDCl_3) δ 25.68(2C), 28.89(2C), 28.99(2C), 29.13(2C), 67.66(2C), 73.87(2C), 89.64(2C), 113.80(4C), 125.65(4C), 127.05(4C), 127.28(2C), 127.92(4C), 136.56(2C), 144.69(2C), 158.27(2C); DSC: melts at $\sim 58^\circ\text{C}$ (maximum at the endothermic peak), an exothermic reaction starts at $\sim 196^\circ\text{C}$.

Synthesis of polymer 41. To a 100 mL oven-dried round bottom flask, equipped with magnetic stirrer and septum, polymer 40 (2.80 g, 5 mmol), $\text{SnCl}_2 \cdot 2\text{H}_2\text{O}$ (2.031 g, 9 mmol), THF (30 mL), and ether (20 mL) were added. An HCl/ether solution (30 mL, 1.0 M) was injected slowly to the above mixture, and the reaction mixture was then stirred overnight.

The precipitated polymer was filtered and the filtrate was added to 200 mL methanol to precipitate more polymer. The combined crops were redissolved in THF and reprecipitated in methanol to afford 2.16 g of yellow powder (82% yield). GPC: $M_w = 1.87 \times 10^4$, $M_n = 8.43 \times 10^3$, PDI = 2.22; FTIR (film on KBr) ν (cm^{-1}) 3056(m), 2928(s), 2854(s), 1653(m), 1601(s), 1505(vs), 1470(m), 1443(m), 1296(s), 1249(vs), 1175(s), 1029(m), 833(s), 766(s), 738(s), 696(s), 620(s); $^1\text{H-NMR}$ (300 MHz, CDCl_3) δ 1.36-1.48(two broad peaks overlapped, 12H), 1.81(s, broad, 4H), 4.00(s, broad, 4H), 6.90(d, $J = 8.4$ Hz, 4H), 7.36(s, broad, 6H), 7.48(s, broad, 4H), 7.56(s, broad, 4H); $^{13}\text{C-NMR}$ (75.429 MHz, CDCl_3) δ 25.36(2C), 28.68(6C), 67.37(2C), 113.68(4C), 120.27(2C), 126.98(2C), 127.64(4C), 128.66(4C), 129.88(4C), 130.56(2C), 138.38(2C), 149.20(2C), 158.29(2C); UV-VIS (THF, nm): λ_{max} (ϵ) = 405 (1.29×10^4), 276 (2.33×10^4), and the absorption tails until 550 nm; DSC: two endothermic peaks observed at 89°C and 161°C, but examination by polarized microscopy revealed that the entire polymer body does not melt.

Synthesis of 42. To a 250 mL oven-dried 2-necked round bottom flask, equipped with magnetic stirrer, condenser and addition funnel, diketone 39 (5.34 g 10 mmol) and THF (40 mL) were added. Ethynyl magnesium chloride (80 mL, 0.5 M in THF, 100% excess) was added to the reaction. The reaction mixture was heated with a heat gun until the whole reaction mixture became a clear solution which was then stirred overnight.

The reaction mixture was poured into a mixture of 100 mL ether and 50 mL 2.0 M HCl acid. The organic layer was washed with water twice, dried over sodium sulfate. After removal of the organic solvents, 5.86 g of 42 was obtained (quantitative yield) as a viscous liquid. MS (Kratos MS 50) m/z 586(22, M), 491(19), 463(13), 368(24), 337(32), 223(62), 207(93), 121(94), 105(100); HRMS m/z cal. for $\text{C}_{40}\text{H}_{42}\text{O}_4$ 586.30831, measured 586.30955

(Kratos MS 50); FTIR (film on KBr) ν (cm^{-1}) 3449(broad, m, OH), 3287(m, $\equiv\text{C-H}$), 3058(w), 2928(s), 2854(m), 1609(s), 1508(vs), 1498(m), 1448(m), 1302(m), 1248(vs), 1175(s), 1049(m), 986(m), 829(s), 760(m), 698(s); $^1\text{H-NMR}$ (300 MHz, CDCl_3) δ 1.32-1.44(m, 12H), 1.76(p, $J = 6.6$ Hz, 4H), 2.85 ($-\text{C}\equiv\text{CH}$, s, 2H), 3.22 ($-\text{OH}$, s, 2H), 3.92(t, $J = 6.6$ Hz, 4H), 6.84 (d, $J = 9.3$ Hz, 4H), 7.31(m, 6H), 7.49(d, $J = 9.0$ Hz, 4H), 7.60(m, 4H); $^{13}\text{C-NMR}$ (75.429 MHz, CDCl_3) δ 25.65(2C), 28.85(2C), 28.96(2C), 29.10(2C), 67.63(2C), 73.49(2C), 74.98(2C), 86.42(2C), 113.73(4C), 125.60(4C), 126.98(4C), 127.33(2C), 127.87(4C), 136.24(2C), 144.40(2C), 158.34(2C).

Synthesis of polymer 43. CuCl (0.5 g) and acetone (10 mL) were charged into a 25 mL round bottom flask under argon flow. TMEDA (0.25 mL) was injected by syringe and the reaction was stirred for another hour before use.

To a 250 mL oven-dried round bottom flask, equipped with dry-ice condenser, magnetic stirrer and septum, diacetylene 42 (5.86 g, 10 mmol) and THF (50 mL) were added. Under stirring and slow O_2 bubbled flow, 10 mL catalyst solution from above was injected. The reaction was stirred under O_2 flow for overnight.

The reaction mixture was poured into a mixture of 100 mL ether and 50 mL 2.0 M HCl acid. The organic layer was washed with dilute acid one more time, water twice and dried over sodium sulfate. After removal of all the organic solvents, and vacuum drying, the product was obtained as a slightly yellow powder in quantitative yield. GPC: $M_w = 1.30 \times 10^4$, $M_n = 5.07 \times 10^3$, PDI = 2.58; FTIR (film on KBr) ν (cm^{-1}) 3439(broad, s, OH), 3059(w), 2929(s), 2855(s), 1607(s), 1508(vs), 1448(m), 1302(m), 1248(vs), 1175(s), 1046(m), 988(m), 830(s), 760(m), 737(m), 699(s); $^1\text{H-NMR}$ (300 MHz, CDCl_3) δ 1.32-1.45(m, broad, 12H), 1.75(m, broad, 4H), 3.04(s, broad, OH), 3.92 (t, $J = 6.3$ Hz, 4H), 6.83(d, $J = 8.7$ Hz, 4H), 7.31(m, 6H), 7.43(d, $J = 8.1$ Hz, 4H), 7.54(d, $J = 8.1$ Hz, 4H); $^{13}\text{C-NMR}$ (75.429 MHz, CDCl_3) δ 25.62(2C), 28.81(2C), 28.93(2C), 29.07(2C), 67.65(2C), 70.65(2C), 74.20(2C), 82.53(2C), 113.84(4C), 125.70(4C), 127.11(4C), 127.58(2C),

127.97(4C), 135.63(2C), 143.73(2C), 158.48(2C); DSC: it melts at 72°C, an exothermic reaction starts at 194°C.

Synthesis of polymer 44. To a 100 mL oven-dried round bottom flask, equipped with magnetic stirrer and septum, polymer 43 (2.92 g, 5 mmol), THF (30 mL), and ether (15 mL) were added. HCl/ether (30 mL, 1.0M) was injected to the reaction slowly. The solution turned red immediately. Shortly after the addition of acid, polymer precipitated out. After stirring at room temperature for one and half hours, the precipitated polymer was filtered out as an elastomer-like material which can not be dissolved in THF or toluene.

The filtrate was poured into 200 mL of methanol and only very little polymer was obtained from the filtrate. The polymer can not be dissolved in either THF or toluene. The combined polymer weighted 2.40 g (84% yield). Solid state ^{13}C -NMR (75.429 MHz) MAS = 4572 Hz and 4081 Hz respectively, δ 25.31, 29.25, 67.40, 114.14, 128.24, 137.15, 146.53, 158.86; UV-VIS (taken from the reaction solution, THF, nm) $\lambda_{\text{max}} = 509, 428, 375, 277, 254$ and the absorption tails until 600 nm.

Synthesis of bisphenolcumulene 45. To a 250 mL oven-dried round bottom flask, equipped with magnetic stirrer and septum, 4-hydroxybenzophenone (19.8 g, 100 mmol), *t*-butyldimethylchlorosilane (18.06 g, 120 mmol), imidazole (17.0 g, 250 mmol), and dry DMF (55 mL) were added. The reaction was stirred for 48 hours at room temperature and then poured into a mixture of 150 mL of hexanes and 100 mL of 2.0 M of HCl acid. The organic layer was washed with water, NaCl solution twice, and dried over sodium sulfate. After removal of the organic solvents and flashing through a silica gel column (hexanes: ethyl acetate = 10:1), 4-(*t*-butyldimethylsiloxy)benzophenone obtained was directly used for next step after vacuum drying. GCMS m/z 313(3, M+1), 312(13, M), 256(14), 255(48), 105(100), 77(37); GC-FTIR ν (cm^{-1}) 3069(w), 2940(m), 2868(w), 1676(s), 1597(s), 1504(s), 1268(vs), 1168(m), 915(vs), 830(m).

In a 250 mL oven-dried round bottom flask, dilithioacetylene (20 mmol in 40 mL THF) was made according to procedures described earlier. To this dianion solution was added 4-*t*-butyldimethylsiloxy-benzophenone (12.48 g, 40 mmol) dissolved in THF (35 mL). The reaction solution became clear immediately. After stirring overnight, the reaction mixture was poured into a mixture of 200 mL ether and 100 mL 2.0 M HCl acid. The organic layer was washed twice with water, dried over sodium sulfate. After removal of the organic solvents, the diol precursor obtained was directly used for next step.

To a 250 mL oven-dried round bottom flask, equipped with magnetic stirrer and septum, the diol precursor (4.55 g, 7 mmol) obtained from the last step, SnCl₂·2H₂O (2.70 g, 12 mmol), ether (50 mL), and THF (25 mL) were charged. HCl/ether solution (50 mL, 1.0 M) was injected slowly. After stirring at room temperature for 2 hours, 100 mL of ether was added to the reaction. The mixture was washed with water three times and dried over sodium sulfate. After removal of the organic solvents, the silyl protected cumulene was obtained as a yellow solid. (Note: it cannot be precipitated out from methanol).

To the solution of silyl protected cumulene (the product from last step, 4.31 g, 3 mmol) in THF (50 mL), tetrabutylammonium fluoride (TBAF) (3.13 g, 12 mmol) was added. After stirring at room temperature for 2 hours, 100 mL of ether was added. And the solution was then washed with water three times, dried over sodium sulfate, and concentrated by a rotary evaporator. The product was precipitated out in 200 mL of hexanes. Bisphenolcumulene **45** was obtained as a yellow powder (2.28 g, 84% yield). Compound **45** does not melt before a thermal reaction starts at 161 °C. MS (Kratos MS50) *m/z* 389(35, M+1), 388(100, M), 387(10), 294(4), 198(4), 194(11), 121(4); HRMS *m/z* cal. for C₂₈H₂₀O₂ 388.14633, measured 388.14629 (Kratos, MS50); FTIR (KBr disk) ν (cm⁻¹) 3275(broad, m, OH), 3050(w), 1652(vs), 1551(m), 1506(s), 1437(m), 1223(m), 1169(m), 1103(m), 832(s) 761(s), 691(s); ¹H-NMR (300 MHz, DMSO) δ 6.82-7.47(m, 18H), 9.84(broad, OH, 2H); ¹³C-NMR (75.429 MHz, DMSO) δ 115.66(4C), 120.33(2C), 128.70-128.81(12C), 130.16(4C), 138.38(2C), 148.29(2C), 157.76(2C); UV-VIS (THF, nm) λ_{max} (ϵ) = 432 (5.67 × 10⁴), 279 (5.34 × 10⁴).

Synthesis of polymer 46. Bisphenolcumulene 45 (0.338 g, 1 mmol), NaOH (0.16 g, 4 mmol), H₂O (12.0 mL), tetrabutylammonium chloride (0.222 g, 0.8 mmol) were added into a 100 mL 3-necked round bottom flask equipped with a mechanical stirrer. Under vigorous stirring, adipoyl chloride (0.183 g, 1 mmol) in 5 mL dichloethane was injected by syringe. Red polymers precipitated out immediately. After stirring for another 10 minutes, hexanes (5 mL) were added to the reaction. The polymer was then filtered and washed many times with water to get rid of the red color. After vacuum drying, 0.40 g of yellow powder was obtained (80% yield). GPC results: $M_w = 8.14 \times 10^3$, $M_n = 3.57 \times 10^3$, PDI = 2.17; FTIR (film on KBr) ν (cm⁻¹) 3055(w), 2947(w), 2870(w), 1757(vs), 1595(w), 1499(vs), 1204(vs), 1165(vs), 1122(vs), 910(m), 844(m), 766(m), 695(s); ¹H-NMR (300 MHz, CDCl₃) δ 1.93(s, broad, 4H), 2.68(s, broad, 4H), 7.13(d, J = 6.9 Hz, 4H), 7.36(s, broad, 6H), 7.55(s, broad, 8H); ¹³C-NMR (75.429 MHz, CDCl₃) δ 24.04(2C), 33.77(2C), 121.34(4C), 121.59(2C), 127.89(2C), 128.25(4C), 129.13(4C), 130.15(4C), 136.07(2C), 138.25(2C), 150.12(2C), 151.33(2C), 171.41(2C); DSC: two endothermic peaks at 142°C and 161°C, however, examination by polarized microscopy revealed that the entire polymer body does not melt before an exothermic reaction started at 214°C; UV-VIS (THF, nm) $\lambda_{max}(\epsilon) = 440(2.71 \times 10^4)$, 285 (1.78 x 10⁴).

Synthesis of polymer 47. Bisphenolcumulene 45 (0.388 g, 1 mmol), dichlorodihexylsilane (0.269 g, 1 mmol, Hüls America, Inc.), imidazole (0.408 g, 6.0 mmol), and dry THF (10 mL) were added into a 25 mL round bottom flask equipped with condenser and magnetic stirrer under an argon atmosphere. After refluxing overnight, the reaction mixture was poured into a mixture of ether (50 mL) and HCl acid (50 mL, 2.0 M). The organic layer was washed with water twice, then dried over sodium sulfate. After removal of the organic solvents, 0.58 g of yellow polymer was obtained (quantitative yield). GPC: $M_w = 6.76 \times 10^3$, $M_n = 3.11 \times 10^3$, PDI = 2.17; FTIR (film on KBr) ν (cm⁻¹) 3056(w), 2954(s), 2923(vs), 2855(s), 1598(s), 1503(vs), 1446(m), 1264(vs), 1249(vs), 1170(s), 1102(m), 919(s), 840(s), 766(s), 696(s); ¹H-NMR (300 MHz, CDCl₃) δ 0.82-0.95 (m, broad, 10H),

1.33-1.53 (m, broad, 16H), 6.96-7.62 (m, 18H); $^{13}\text{C-NMR}$ (75.429 MHz, CDCl_3) (for some of the hexyl carbons, *Z* and *E* cumulene isomers can be resolved) δ 12.94-14.82 (3 peaks, 4C), 22.35-22.51(2 peaks, 4C), 31.08-32.63(4 peaks, 4C), 119.40(4C), 120.95(2C), 127.45(2C), 128.02(4C), 129.05(4C), 130.38(4C), 132.35(2C), 138.66(2C), 150.07(2C), 153.95(2C); $^{29}\text{Si-NMR}$ (59.591 MHz, CDCl_3 , TMS as external standard) δ : *cis* and *trans* isomer cumulene is resolved -10.12(1Si), -2.85(1Si). UV-VIS (THF, nm) λ_{max} (ϵ) = 424 (2.58×10^4), 275 (2.32×10^4); DSC analysis shows that polymer 47 does not melt or soften before an exothermic reaction starts at $\sim 197^\circ\text{C}$.

Synthesis of 1.1.4.4-tetraphenyl-1.3-butadiene (48). Compound 48 was synthesized according to a literature procedure.¹⁷⁸ 1,14,4-Tetraphenyl-1,2,3-butatriene (2b, 0.25 g), zinc powder (1.25 g), zinc chloride (0.5 g), THF (10 mL), and water (1 mL) were charged into a 25 mL round bottom flask equipped with magnetic stirrer and condenser. The reaction was refluxed overnight. After the addition of 20 mL of dilute HCl acid, the reaction mixture was extracted with three portions of 20 mL of toluene. The combined toluene solution was dried over sodium sulfate. After removal of all the solvents, a yellow powder was obtained. $^1\text{H-NMR}$ (300 MHz, CDCl_3) δ 6.71(s, 2H), 7.07-7.51(m, 20H); $^{13}\text{C-NMR}$ (75.429 MHz, CDCl_3) δ 125.82(2C), 127.20(2C), 127.34(2C), 127.54(4C), 127.97(4C), 128.07(4C), 130.52(4C), 139.68(2C), 142.29(2C), 143.83(2C).

Synthesis of 1.1.6.6-tetraphenyl-1.3.5-hexatriene (50). 1,1,6,6-tetraphenyl-1,2,3,4,5-hexapentaene (31) (0.19 g, 0.5 mmol), zinc powder (1.0 g), zinc chloride (0.4 g), THF (6 mL), and water (1 mL) were charged into a 25 mL round bottom flask. The reaction was stirred at room temperature. In contrast to the literature where the reaction finished in 10 minutes,¹⁷⁸ the red color of the reaction solution did not disappear even after 2 hours (the size of the zinc powder particles could have played a role here). So the reaction was stirred overnight and the reaction solution turned yellow. 20 mL 2.0 M of HCl acid was added to the reaction, and three portions of 20 mL of toluene was used to extract the product. After

removal of the solvents and vacuum drying, the product was obtained as yellow powder (0.18 g, 93% yield). m.p. 162-165°C. ¹H-NMR (300 MHz, CDCl₃) δ 6.43(double doublet, J₁ = 7.8 Hz, J₂ = 3.0 Hz, 2H), 6.64(double doublet, J₁ = 7.8 Hz, J₂ = 3.0 Hz, 2H), 7.15-7.31(m, 20H); ¹³C-NMR (75.429 MHz, CDCl₃) δ 127.10(8C), 127.83-128.03(three peaks, 10C), 130.20(4C), 132.23(2C), 139.36(2C), 141.66(2C), 142.48(2C); MS (Kratos MS 50) 384(36, M), 217(29), 215(47), 204(54), 182(40), 178(71), 167(91), 165(54), 152(24), 115(37), 105(49), 91(34), 81(30), 77(35), 71(100); HRMS *m/z* cal. for C₃₀H₂₄ = 384.18780, measured = 384.18865 (Kratos MS50); UV-VIS (THF, nm) λ_{max} (ε) = 372 (2.40 × 10⁴), 261 (2.60 × 10⁴), 255 (3.28 × 10⁴).

Synthesis of compound 51.^{104a} To a white slurry of dilithioacetylene (20 mmol in 40 mL THF) (vide supra), *p*-bromobenzopenone (10.44 g, 40 mmol) in THF (50 mL) was added. After refluxing overnight, the reaction mixture was poured into a mixture of 200 mL of ether and 100 mL 2.0 M of HCl. The organic layer was washed with acid one more time, water twice and then dried over sodium sulfate. After removal of the organic solvents, the diol precursor was obtained in quantitative yield as a white powder: m.p. 138-140°C; MS (Kratos MS 50) *m/z* 532(35, M+4-H₂O), 530(66, M+2-H₂O), 529(33), 528(32, M-H₂O), 502(21), 347(12), 345(13), 265(14), 185(32), 183(34), 105(100), 77(20); HRMS *m/z* cal. for C₂₈H₂₀O₂Br₂ 545.98300, measured 545.9844 (Kratos MS50); FTIR (KBr disk) ν (cm⁻¹) 3361(broad, m, OH), 3067(w), 1483(s), 1447(s), 1398(m), 1213(m), 1136(m), 1074(m), 1010(s), 920(m), 843(s) 762(s), 737(s), 698(s); ¹H-NMR (300 MHz, CDCl₃) δ 3.10(broad, -OH, s, 2H), 7.30-7.56(m, 18H); ¹³C-NMR (75.429 MHz, CDCl₃) δ 73.85(2C), 89.54(2C), 121.64(2C), 125.60(4C), 127.53(4C), 127.83(2C), 128.23(4C), 131.16(4C), 143.45(2C), 143.87(2C).

Diol precursor from above (2.74 g, 5 mmol), SnCl₂·2H₂O (2.031 g, 9 mmol), THF (55 mL), and ether (30 mL) were added into a 250 mL round bottom flask. HCl/ether solution (30 mL, 1.0 M) was injected. After stirring at room temperature for 2 hours, the solution was poured into 200 mL of methanol; the yellow precipitate was filtered, washed with dilute HCl

acid, methanol, and dried under vacuum. 1.76 g of compound **51** was obtained (70% yield). When heated, it turns black at 244°C (lit.^{104a} m.p. 268°C). MS (Kratos MS 50) *m/z* 516(54, M+4), 514(100, M+2), 512(52, M), 354(18), 352(10), 350(10), 277(19), 276(21), 258(30), 176(33); FTIR (KBr disk) $\nu(\text{cm}^{-1})$ 3051(w), 1576(w), 1481(vs), 1393(m), 1105(s), 1107(s), 829(vs), 766(s), 694(s); ¹H-NMR (300 MHz, CDCl₃) δ 7.35-7.55(m, 18H); ¹³C-NMR (75.429 MHz, CDCl₃) δ 121.81(2C), 122.02(2C), 128.08(2C), 128.32(4C), 129.04(4C), 130.58(4C), 131.39(4C), 137.33(2C), 137.84(2C), 151.30(2C); HRMS *m/z* cal. for C₂₈H₁₈Br₂ = 513.97561, measured = 513.97447 (Kratos MS50).

Synthesis of diethynyldihexylsilane (52). Dichlorodihexylsilane (5.38 g, 20 mmol) and THF (20 mL) were added into a 250 mL round bottom flask equipped with a magnetic stirrer and addition funnel. Ethynyl magnesium chloride (120 mL, 0.5 M solution in THF) was added to the reaction. After stirring overnight, the reaction solution was poured into a mixture of 100 mL of hexanes and 100 mL 2.0 M of HCl acid. The organic layer was washed with water twice, and dried over sodium sulfate. After removal of the solvents, the product was obtained in quantitative yield as a liquid. MS (Kratos MS 50) *m/z* 248(0.5, M), 222(22), 164(28), 163(100), 138(34), 136(23), 135(72), 122(21), 121(78); HRMS *m/z* cal. for C₁₆H₂₈Si = 248.19603, measured = 248.19568 (Kratos MS50); FTIR (film on KBr) $\nu(\text{cm}^{-1})$ 3294(vs, $\equiv\text{C-H}$), 2959(vs), 2924(vs), 2041(vs, $-\text{C}\equiv\text{C}-$), 1466(s), 1406(m), 1379(m), 1342(m), 1182(m), 1101(m), 995(m), 960(m), 847(m), 758(vs), 679(vs); ¹H-NMR (300 MHz, CDCl₃) δ 0.75(t, J = 7.5 Hz, 4H), 0.88(t, J = 6.9 Hz, 6H), 1.26-1.50(m, 16H), 2.46($-\text{C}\equiv\text{C-H}$, s, 2H); ¹³C-NMR (75.429 MHz, CDCl₃) δ 13.94(4C), 22.36(2C), 23.17(2C), 31.24(2C), 32.45(2C), 84.83(2C), 94.91(2C); ²⁹Si-NMR (59.591 MHz, CDCl₃, TMS as the external standard) - 33.52(1Si).

Synthesis of polymer 53. Compound **52** (0.514 g, 1 mmol), diethynyldihexylsilane (0.248 g, 1 mmol), PdCl₂(PPh₃)₂ (14 mg), CuI (10 mg), and toluene (35 mL) were added to a 50 mL round bottom flask equipped with condenser and magnetic stirrer. After the system

was filled with argon by freezing and thawing technique, 1,8-diazabicyclo[5,4,0]undec-7-ene (DBU) (1.0 mL) was injected and the reaction was refluxed for 6 hours. The solution was then added dropwise into 200 mL of methanol through a glass wool filter (to get rid of any insoluble materials). The precipitated yellow-brown polymer was then washed with 2.0 M HCl acid twice, water twice, methanol twice, and vacuum dried. 0.55 g of polymer **53** was obtained (92% yield). GPC: $M_w = 1.77 \times 10^4$, $M_n = 6.97 \times 10^3$, PDI = 2.53; FTIR (film on KBr) ν (cm^{-1}) 3057(w), 3031(w), 2955(s), 2924(vs), 2856(s), 2156(s), 1597(w), 1501(m), 1182(w), 1076(m), 839(s), 766(s), 696(s); $^1\text{H-NMR}$ (300 MHz, CDCl_3) δ 0.90(s, broad, 10H), 1.34-1.58(three peaks overlapped, 16H), 7.38-7.52(two peaks overlapped, broad, 18H); $^{13}\text{C-NMR}$ (75.429 MHz, CDCl_3) δ 13.91 and 14.54 (two peaks, 4C), 22.35-23.43 (three peaks, 4C), 31.27-32.46 (three peaks, 4C), 90.89(2C), 106.25(2C), 122.02-122.50(two peaks, 4C), 128.26-129.14(three peaks, 14C), , 131.39-131.92(two peaks, 4C), 137.90-138.72(two peaks, 4C), 151.20(2C); $^{29}\text{Si-NMR}$ (59.591 MHz, CDCl_3 , TMS as external standard) -30.70 (1Si); DSC results: endothermic peak at 142°C, exothermic reaction starts at 185°C; UV-VIS (THF, nm) λ_{max} (ϵ) = 453 (4.14×10^4), 305 (4.12×10^4).

Synthesis of compound 54. Compound **54** was synthesized from the reduction of compound **48** by $\text{Zn/ZnCl}_2/\text{H}_2\text{O}$. Compound **54** consists of 3 stereoisomers (*Z-Z*, *E-E*, *Z-E*) with ca. 1:1:1 ratio according to $^1\text{H-NMR}$. MS (Kratos MS 50) m/z 518(53, M+4), 516(100, M+2), 514(52, M), 356(7), 279(11), 278(12), 277(8), 276(9), 247(14), 166(13), 165(17); HRMS m/z cal. for $\text{C}_{28}\text{H}_{20}\text{Br}_2 = 515.99126$, measured = 515.99121(Kratos MS50); FTIR (KBr disk) ν (cm^{-1}) 3059(w), 3028(w), 1907(w), 1483(vs), 1443(m), 1391(m), 1346(w), 1155(w), 1101(w), 1072(s), 1030(s), 905(m), 827(vs), 768(s), 700(s); $^1\text{H-NMR}$ (300 MHz, CDCl_3) δ 6.71(s), 6.73(t, $J = 16.2$ Hz), 6.74(s) (these five peaks correspond to the two vinyl hydrogen from 3 isomers, two singlets from *Z-Z* and *E-E* isomers, one triplet from *Z-E* isomer, three isomers have an ca. 1: 1: 1 ratio), 7.0-7.57 (m, 18H); $^{13}\text{C-NMR}$ (75.429 MHz, CDCl_3) δ 121.33, 121.48, 125.54, 125.87, 127.40, 127.59, 127.99, 128.12, 129.00, 130.27, 131.03, 131.24, 132.05, 138.36, 138.83, 140.95, 141.53, 142.91, 143.19.

Synthesis of polymer 55. Polymer 55 was synthesized from the coupling of compound 54 (a mixture of three isomers) and diethynyldihexylsilane in 75% yield following the same procedure as that for the synthesis of polymer 53. GPC: $M_w = 6.89 \times 10^3$, $M_n = 3.85 \times 10^3$, PDI = 1.79; FTIR (film on KBr) ν (cm^{-1}) 3076(m), 2953(s), 2923(s), 2855(s), 2156(s), 1504(s), 1074(m), 837(vs), 767(s), 700(vs); $^1\text{H-NMR}$ (300 MHz, CDCl_3) δ 0.87 (two peaks overlapped, broad, 10H), 1.30(two peaks overlapped, broad, 16H), 6.77(s, broad, 2H), 7.14-7.56 (m, 18H); $^{13}\text{C-NMR}$ (75.429 MHz, CDCl_3) δ 13.60, 14.24, 16.15, 22.04, 22.40, 23.09, 30.99, 32.34, 89.74, 92.94, 103.93, 106.00, 121.45, 125.70, 127.71, 127.78, 130.05, 130.95, 131.39, 138.62, 141.35, 143.23, the ^{13}C spectrum was complicated by isomers of the butadiene unit; $^{29}\text{Si-NMR}$ (59.591 MHz, CDCl_3 , TMS as external standard) -10.12 (1Si); DSC: an exothermic reaction starts at 165°C; UV-VIS (THF, nm) λ_{max} (ϵ) = 370 (3.76×10^4), 274 (2.92×10^4).

Synthesis of 1.6-bis (*p*-bromophenyl)-1.6-diphenyl-1.2.3.4.5-hexapentaene (56). *p*-Bromobenzophenone (5.22 g, 20 mmol) in 40 mL THF was charged into a 250 mL round bottom flask equipped with magnetic stirrer and addition funnel. Ethynyl magnesium chloride (80 mL, 0.5 M, 40 mmol, 100% excess) was added. After stirring overnight, the mixture was poured into a mixture of 100 mL of ether and 100 mL of 2.0 M HCl acid. The organic layer was washed with water twice and dried over sodium sulfate. After removal of the solvents, 1-(*p*-bromophenyl)-1-phenyl-2-propyn-3-ol obtained was directly used for the next step. MS (Kratos MS 50) m/z 286(9, M), 285(18), 207(84), 189(27), 179(37), 178(39), 131(24), 130(19), 105(17), 77(29), 53(100); HRMS m/z cal. for $\text{C}_{15}\text{H}_{11}\text{OBr}$ 285.998396, measured 285.998840 (Kratos MS50); FTIR (film on KBr) ν (cm^{-1}) 3543(broad, m), 3427(broad, m), 3292(s, $\equiv\text{C-H}$), 3061(w), 1487(vs), 1448(s), 1396(s), 1331(m), 1165(m), 1072(s), 1051(s), 1013(s), 895(s), 822(vs), 760(vs), 698(vs), 661(s); $^1\text{H-NMR}$ (300 MHz, CDCl_3) δ 2.89($\text{C}\equiv\text{C-H}$, s, 1H), 3.14(broad, s, -OH, 1H), 7.28-7.60(m, 9H); $^{13}\text{C-NMR}$ (75.429 MHz, CDCl_3) δ 73.31(1C), 75.67(1C), 85.48(1C), 121.44(1C), 125.43(2C), 127.36(2C), 127.63(1C), 127.97(2C), 130.89(2C), 143.14(1C), 143.53(1C).

CuCl (0.5 g) and acetone (10 mL) were charged into a 25 mL round bottom flask under argon flow. 0.25 mL TMEDA was injected by syringe and the reaction was stirred for another hour before use.

A 250 mL 2-necked round bottom flask equipped with dry-ice condenser, magnetic stirrer was charged with of 1-(*p*-bromophenyl)-1-phenyl-2-propyn-3-ol (5.74 g, 20 mmol) from last step and THF (50 mL). Under stirring and slow O₂ bubbled flow, 10.0 mL catalyst solution from the above reaction was injected. The reaction was stirred for 5 hours under O₂ flow and then poured into a mixture of 100 mL ether with 100 mL 2.0 M HCl acid. The organic layer was washed with water twice and dried over sodium sulfate. After removal of the solvents, the diol precursor was directly used for the next step. MS (Kratos MS 50) *m/z* 572(1, M), 554(4), 465(3), 387(6), 289(5), 260(26), 231(22), 202(31), 185(42), 183(42), 157(14), 105(100), 77(48); HRMS *m/z* cal. for C₃₀H₂₀O₂Br₂ 571.98109, measured 571.98274 (Kratos MS50); FTIR (film on KBr) ν (cm⁻¹) 3387(broad, s, OH), 3061(w), 1599(m), 1387(m), 1487(vs), 1448(s), 1396(s), 1178(m), 1161(m), 1072(m), 1049(s), 1011(vs), 991(s), 893(m), 820(s), 758(s), 698(vs); ¹H-NMR (300 MHz, CDCl₃) δ 3.50(broad, OH, s, 2H), 7.29-7.55(m, 18H); ¹³C-NMR (75.429 MHz, CDCl₃) δ 70.91(2C), 74.14(2C), 82.16(2C), 121.90(2C), 125.72(4C), 127.61(4C), 128.06(2C), 128.27(4C), 131.20(4C), 142.78(2C), 143.23(2C).

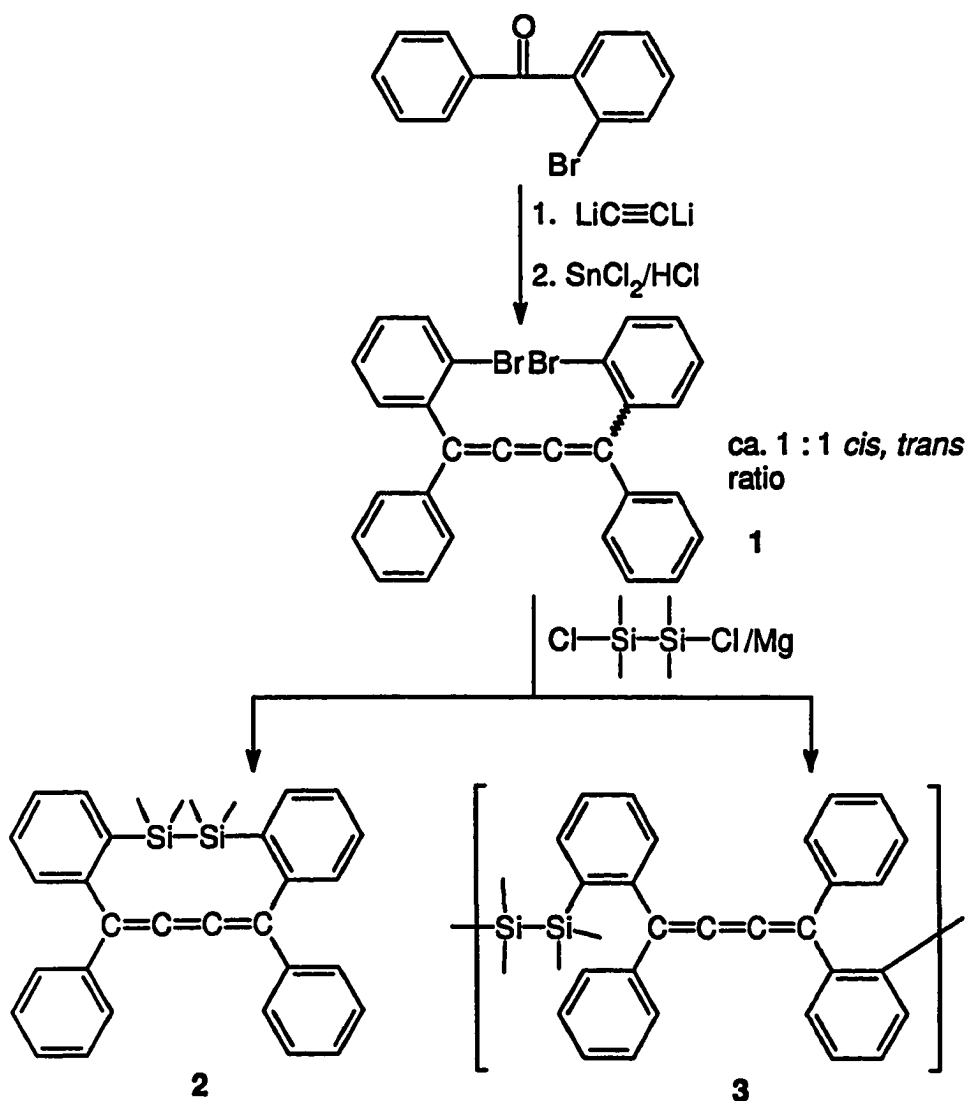
The diol precursor (5.72 g, 10 mmol) from last step, SnCl₂·2H₂O (4.062 g, 18 mmol), THF (30 mL), and 60 mL ether were charged into a 250 mL round bottom flask equipped with magnetic stirrer and septum. HCl/ether (60 mL, 1.0 M) was injected. After stirring at room temperature for 2 hours, the solution was added to 200 mL methanol. After filtration and vacuum drying, compound **56** was obtained as a red powder (4.8 g, 89% yield). The product does not melt before ~160°C when the material turns black. FTIR (KBr disk) ν (cm⁻¹) 3049(w), 1576(w), 1483(s), 1445(m), 1398(m), 1178(m), 1070(s), 1028(vs), 906(m), 827(s), 764(s), 696(s); ¹H-NMR (300 MHz, CDCl₃) δ 7.35-7.56(m, 18H); ¹³C-NMR (75.429 MHz, CDCl₃) δ 122.51(2C), 123.56(2C), 126.93(2C), 128.32(4C), 128.57(2C), 128.87(4C), 130.40(4C), 131.38(4C), 136.52(2C), 137.14(2C), 148.68(2C).

Synthesis of compound 57. Compound 57 was synthesized from the reduction of compound 56 by the Zn/ZnCl₂/H₂O system following the same procedure as that for the synthesis of compound 50. Compound 50 also contains *Z* and *E* isomers as shown in proton NMR (maximum 6 isomers). ¹H-NMR (300 MHz, CDCl₃) δ 6.09-6.75(m, 4H), 7.09-7.58(m, 18H); ¹³C-NMR (75.429 MHz, CDCl₃) (very complicated ¹³C-NMR) δ 121.28, 121.38, 127.17, 127.48, 127.61, 127.99, 128.07, 128.17, 128.32, 128.74, 128.79, 130.21, 131.06, 131.28, 132.00, 132.30, 132.56, 138.33, 138.87, 140.63, 141.18, 141.58, 141.72, 141.77.

Synthesis of polymer 58. Polymer 58 was synthesized from the coupling of compound 57 (a mixture of *Z*, *E* isomers) and diethynyldihexylsilane in 70% yield following the same procedure as that for the synthesis of polymer 53. FTIR (film on KBr) ν (cm⁻¹) 3030(w), 2955(s), 2923(vs), 2855(s), 2156(s, -C≡C-), 1599(m), 1512(m), 1445(m), 1183(m), 1074(s), 837(s), 765(m), 700(s); ¹H-NMR (300 MHz, CDCl₃) δ 0.87 (s, broad, 10H), 1.27(m, broad, 16H), 6.50 (s, broad, 2H), 6.72 (s, broad, 2H), 7.20-7.55(m, broad, 18H); ¹³C-NMR (75.429 MHz, CDCl₃) δ 14.04-16.64(three peaks, 4C), 22.51(three peaks overlapped, 4C), 31.47(2C), 32.81(2C), 90.11, 93.30, 106.28(three peaks), 121.89, 127.45-131.34(six peaks overlapped), 139.04-142.26(four peaks overlapped); ²⁹Si-NMR (59.591 MHz, CDCl₃, TMS as external standard) -20.90, -14.29; UV-VIS (THF, nm) λ_{max}(ε)= 397 (3.00 x 10⁴), 261 (3.75 x 10⁴), 255 (4.24 x 10⁴); DSC analysis shows that polymer 58 does not soften or melt before an exothermic reaction starts at 173°C.

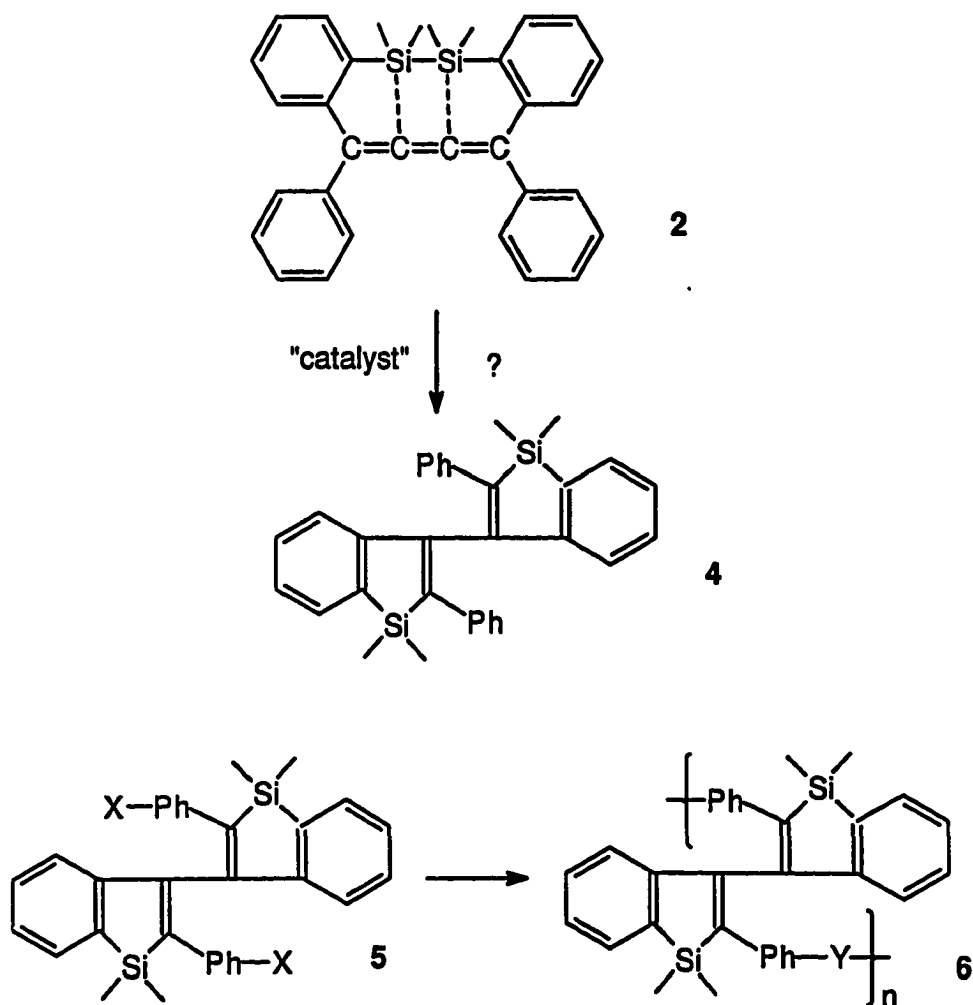
FUTURE WORK

1. Synthesis of cyclic cumulenes. The coupling of 1,4-bis(*o*-bromophenyl)-1,4-diphenyl-1,2,3-butatriene (**1**, 1 : 1 mixture of *cis*, *trans* isomers), which can be obtained from *o*-bromobenzophenone, with dichlorodisilane/magnesium should give cyclic cumulene **2** and polymer **3** (Scheme 1). The points of interest in cyclic cumulene **2** is the structural features and the possible catalytic addition of the Si-Si bond to the cumulene units.



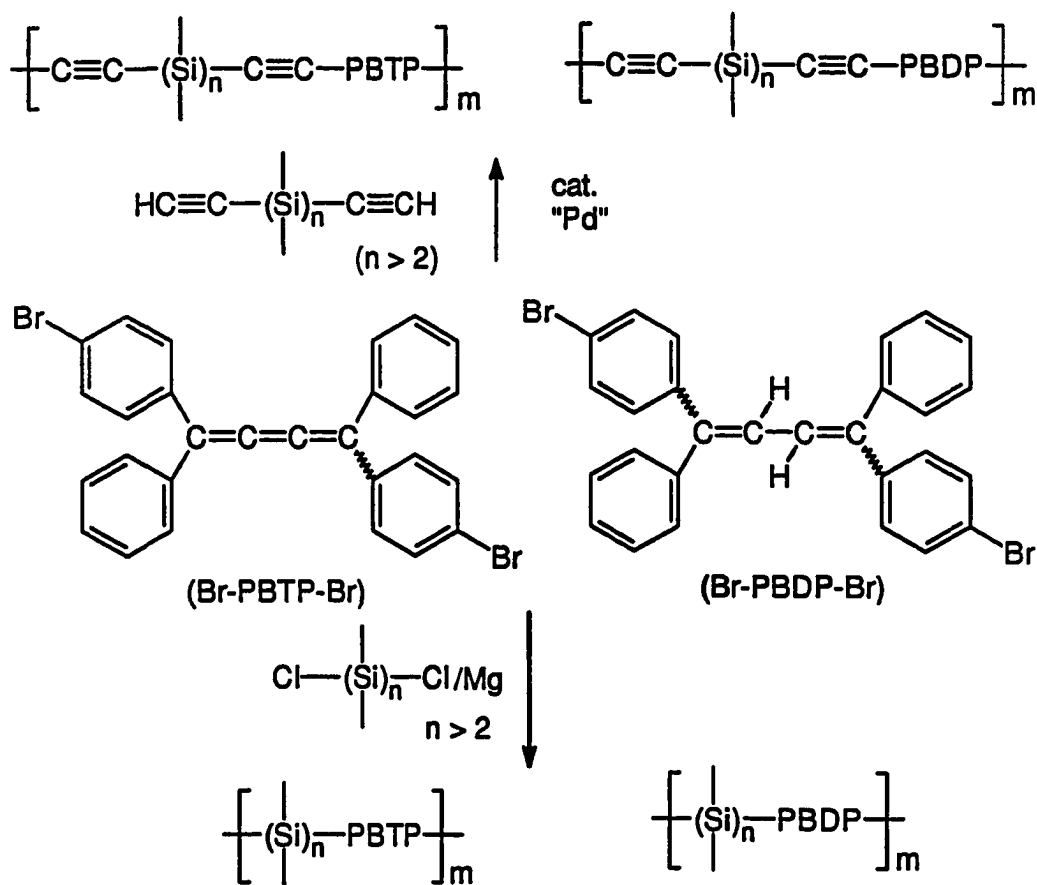
Scheme 1.

2. Synthesis of siloles from Si-Si addition to cumulenes. There is no report in literature about the addition of Si-Si bond to cumulene units which are very well studied for Si-Si addition to alkenes, alkynes, allenes, and butadienes. It would be interesting to see if compound **2** can undergo intramolecular Si-Si addition to the central double bond of the cumulene unit to give compound **4**. If this reaction is successful, polymers containing benzosilole units (**6**) can be synthesized from compound **5**, a monomer where two functional groups are introduced to the 2-phenyl positions (Scheme 2).



Scheme 2.

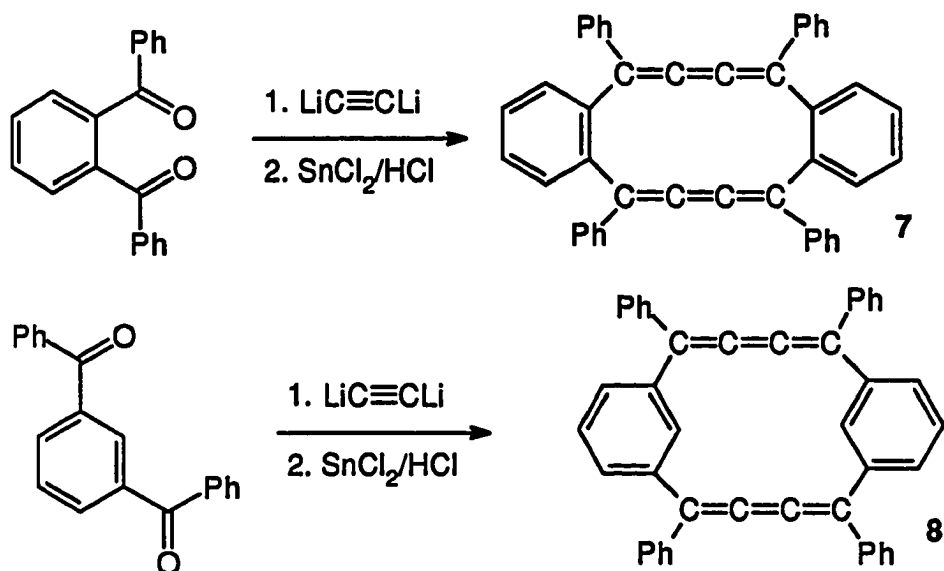
3. Synthesis of 1,2,3-butatriene and 1,3-butadiene-containing polymers for σ - π conjugation studies. 1,2,3-Butatriene and 1,3-butadiene-containing polymers can be synthesized (Scheme 3) for σ - π conjugation studies and for comparative studies.



Scheme 3.

4. Synthesis of macrocyclics containing cumulene units. Reaction of 1,2 or 1,3-dibenzoylbenzene with dilithium acetylene followed by reduction by tin(II) chloride under acidic conditions, could yield linear polymers, macrocyclics **7** and **8**, as well as larger cyclics (Scheme 4). Macrocyclics **7** and **8** are interesting not only because of their potential large

third order nonlinear response but the other chemistry they can be involved in such as their abilities to form complex with metals as well.



Scheme 4.

REFERENCES

1. Special issue on the strained organic compounds, *Chem. Rev.* **1989**, 89.
2. a) Greenberg, A.; Liebman, J. F. *Strained Organic Compounds*; Academic Press: New York, **1978**.
b) Wiberg, K. B. *Angew. Chem., Int. Ed. Engl.* **1986**, 25, 312.
3. Haase, J.; Krebs, A. *Z. Naturforsch* **1972**, 27a, 624.
4. Johnson, R. P.; Daoust, K. J. *J. Am. Chem. Soc.* **1995**, 117, 362.
5. a) Adams, R. D.; Chen, G.; Qu, X.; Wu, W.; Yamamoto, W. *J. Am. Chem. Soc.* **1992**, 114, 10977.
b) Adams, R. D.; Chen, G.; Qu, X.; Wu, W. *Organometallics* **1993**, 12, 4117.
6. Pang, Y.; Schneider, A.; Barton, T. J.; Gordon, M. S.; Carroll, M. T. *J. Am. Chem. Soc.* **1992**, 114, 4920.
7. Ando, W.; Hojo, F.; Sekigawa, S.; Nakayama, N.; Shimizu, T. *Organometallics* **1992**, 11, 1009.
8. Haase, J.; Krebs, A. *Z. Naturforsch* **1971**, 26a, 1190.
9. Johnson, R. P. *Chem. Rev.* **1989**, 89, 1111.
10. Price, J. D.; Johnson, R. P. *J. Org. Chem.* **1991**, 56, 6372.
11. Pang, Y.; Petrich, S. A.; Young, V. G. Jr.; Gordon, M. S.; Barton, T. J. *J. Am. Chem. Soc.* **1993**, 115, 2534.
12. Shimizu, T.; Hojo, F.; Ando, W. *J. Am. Chem. Soc.* **1993**, 115, 3111.
13. a) Skattebol, L. *Tetrahedron Lett.* **1961**, 167.
b) Skattebol, L. *Acta Chem. Scand.* **1963**, 1683.
14. DehmLow, E. V.; Stiehm, T. *Tetrahedron Lett.* **1990**, 1841.
15. Imgartinger, H.; Jager, H. U. *Tetrahedron Lett.* **1976**, 3595.
16. Baird, M. S.; Reese, C. B. *Tetrahedron* **1976**, 32, 2153.
17. Masamune, S.; Chin, C. G.; Hojo, K.; Seider, R. T. *J. Am. Chem. Soc.* **1967**, 89, 4804.
18. Eisenhuth, L.; Hopf, H. *Chem. Ber.* **1975**, 108, 2635.

19. D'Amore, M. B.; Bergman, R. G. *J. Am. Chem. Soc.* **1969**, *91*, 5694.
20. Crystal data for **24** (*meso*) at -50°C : $a = 8.768(2)\text{\AA}$, $b = 11.291(3)\text{\AA}$, $c = 11.726(3)\text{\AA}$, $\alpha = 104.74(2)^{\circ}$, $\beta = 102.42(2)^{\circ}$, $\gamma = 111.42(2)^{\circ}$, $\text{vol} = 982.1(4)\text{\AA}^3$, triclinic with space group $P1$, $Z = 1$, $\rho = 1.01\text{gcm}^{-3}$. The structure was solved by direct methods, $R = 0.049$ and $R_w = 0.068$ for 2272 reflections with $F_0^2 > 3.0\sigma(F_0^2)$.
21. Crystal data for **26** at -60°C : $a = 12.244(2)\text{\AA}$, $c = 10.523(2)\text{\AA}$, $\text{vol} = 1577.5(7)\text{\AA}^3$, tetragonal with space group $P4_22_12$, $Z = 2$, $\rho = 1.013\text{gcm}^{-3}$. The structure was solved by direct methods, $R = 0.031$ and $R_w = 0.046$ for 1063 reflections with $F_0^2 > 2.0\sigma(F_0^2)$.
22. Kloster-Jensen, E.; Wirz, J. *Helv. Chim. Acta* **1975**, *58*, 162.
23. For a review of "proximity interaction of acetylenes" see: Misuni, S.; Kaneda, T. in *The Chemistry of the Carbon-Carbon Triple Bond*; Patai, S. Ed.; John Wiley & Sons: Chichester, **1978**; Chapter 16.
24. Stierman, T. J.; Johnson, R. P. *J. Am. Chem. Soc.* **1985**, *107*, 3971.
25. Brandsma, L. *Preparative Acetylenic Chemistry*; Elsevier: New York, 2nd Ed., **1988**, 35.
26. Lin, J.; Pang, Y.; Young, V. G. Jr.; Barton, T. J. *J. Am. Chem. Soc.* **1993**, *115*, 3794.
27. Hojo, F.; Shimizu, T.; Ando, W. *Chem. Lett.* **1993**, 1171.
28. Raghavachari, K.; Frisch, M. J.; Pople, J. A.; Schleyer, P. V. R. *Chem. Phys. Lett.* **1982**, *85*, 145.
29. Nobes, R. H.; Radom, L.; Rodwell, W. R. *Chem. Phys. Lett.* **1980**, *74*, 269.
30. Pople, J. A.; Raghavachari, K.; Frisch, M. J.; Binkley, J. S.; Schleyer, P. V. R. *J. Am. Chem. Soc.* **1983**, *105*, 6389.
31. Jensen, J. H.; Morokuma, K.; Gordon, M. S. *J. Chem. Phys.* **1994**, *100*, 1981.
32. Chan, T. H.; Massuda, D. *J. Am. Chem. Soc.* **1977**, *99*, 936.
33. Barton, T. J.; Yeh, M. H. *Tetrahedron Lett.* **1987**, *28*, 6421.
34. Eaton, P.E.; Hoffmann, K. *J. Am. Chem. Soc.* **1987**, *109*, 5285.
35. Warner, P. M. *Chem. Rev.* **1989**, *89*, 1067.
36. Eaton, P. E.; White, A. J. *J. Org. Chem.* **1990**, *55*, 1321.

37. Steward, J. J. P.; Dewar, M. J. *Quantum Chemistry Program Exchange*, program MOPAC, No. 445.
38. Chen, N.; Jones, M. Jr. *J. Phys. Org. Chem.* **1988**, *1*, 305.
39. Chen, N.; Jones, M. Jr. *Tetrahedron Lett.* **1989**, *30*, 6969.
40. Eaton, P. E.; Appell, R. B. *J. Am. Chem. Soc.* **1990**, *112*, 4055.
41. White, W. R.; Platz, M. S.; Chen, N.; Jones, M. Jr. *J. Am. Chem. Soc.* **1990**, *112*, 7794.
42. Chen, N.; Jones, M. Jr.; White, W. R.; Platz, M. S. *J. Am. Chem. Soc.* **1991**, *113*, 4981.
43. Conlin, R. H.; Huffaker, H. B.; Kawk, Y. *J. Am. Chem. Soc.* **1985**, *107*, 731.
44. Barton, T. J.; Groh, B. L. *Organometallics* **1985**, 575.
45. Ishikawa, M.; Matsuzawa, S. *J. Chem. Soc. Chem. Commun.* **1985**, 588.
46. Barton, T. J. *Dow Corning Corporation Lecture Series* **1988**, 273.
47. Power, M. D. "Thermal rearrangments of unsaturated and strained organosilanes and their hydrocarbon counterparts", *Ph. D. Thesis*, Iowa State University, Ames, Iowa, **1989**.
48. Ermer, O.; Lifson, S. *Tetrahedron* **1974**, *30*, 2425.
49. Zhang, X. "A search for thermal isomerization of olefins to carbenes", *Ph. D. Thesis*, Iowa State University, Ames, Iowa, **1990**.
50. Roth, W. R. *J. Org. Chem.* **1987**, *52*, 5636.
51. a). Boatz, J. A.; Gordon, M. S.; Hildrbrandt, R. L. *J. Am. Chem. Soc.* **1988**, *110*, 352;
b). Boatz, J. A.; Gordon, M. S. *J. Phys. Chem.* **1988**, *920*, 3037.
52. For the most recent review on silicon carbide preceramic polymers see: Laine, R. M.; Babonneau, F. *Chem. Mater.* **1993**, *5*, 260.
53. Laine, R. M. *Aspects of Homogeneous Catalysis*; Ugo, R. Ed.; Kluwer Academic: Dordrecht, Netherlands, **1990**, Vol. 7, pp 37-63.
54. Wu, H. -J.; Interrante, L. V. *Chem. Mater.* **1989**, *1*, 564, and references cited therein.
55. Smith, T. L. *U. S. Patent* 4,631,179, **1986**.

56. a) Wu, H. -J.; Interrante, L. V. *Macromolecules* **1992**, *25*, 1840.
b) Interrante, L. V.; Wu, H. -J.; Apple, T.; Shen, Q.; Ziemann, B.; Narsavage, D. M.; Smith, K. *J. Am. Chem. Soc.* **1994**, *116*, 12085.
57. Bacqué, E.; Pillot, J. P.; Birot, M.; Dunoguès, J. *Macromolecules* **1988**, *21*, 30.
58. Bacqué, E.; Pillot, J. P.; Birot, M.; Dunoguès, J. *Macromolecules* **1988**, *21*, 34.
59. Bacqué, E.; Pillot, J. P.; Birot, M.; Dunoguès, J.; Lapouyade, P.; Bouillon, E.; Pailler, R. *Chem. Mater.* **1991**, *3*, 348.
60. a) Nametkin, N. S.; Vdovin, V. M.; Poletaev, V. A.; Zav'yalov, V. I. *Dokl. Akad. Nauk SSSR*, **1967**, *175*, 1068.
b) Vdovin, V. M.; Grinberg, P. L.; Babich, E. D. *Dolk. Acad. Nauk SSSR* **1965**, *161*, 268.
c) Gilman, G. Atwell, W. H. *J. Am. Chem. Soc.* **1964**, *86*, 2687.
61. Vdovin, V. M.; Pushchevaya, K. S.; Belikova, N. A. Sultanov, R.; Plate, A. F.; Petrov, A. *D. Dolk. Akad. Nauk SSSR* **1961**, *136*, 96.
62. Weyenberg, D. R.; Nelson, L. E. *J. Org. Chem.* **1965**, *30*, 2618.
63. Liao, C. X.; Weber, W. P. *Macromolecules* **1992**, *25*, 1639.
64. Theurig, M.; Weber, W. P. *Polymer Bulletin* **1992**, *28*, 17.
65. Theurig, M.; Sargeant, S. J.; Manuel, G.; Weber, W. P. *Macromolecules* **1992**, *25*, 3834.
66. Flowers, M. C.; Gusel'nikov, L. E. *J. Chem. Soc. B* **1968**, 419.
67. Davidson, I. M. T.; Fenton, A. M.; Jackson, P.; Lawrence, F. T. *J. Chem. Soc. Chem Commun.* **1982**, 806.
68. Egger, K. W.; Cocks, A. T. *Helv. Chim. Acta.* **1973**, *56*, 1516.
69. (a) Weuerchke, S. G.p Chandrasekhar, J.; Joegenson, W. L. *J. Am. Chem. Soc.* **1985**, *107*, 1496.
(b) Block, E.; Yench, A. J.; Aslam, M.; Eswarakrishnan, V.; Luo, L.; Sano, A. *J. Am. Chem. Soc.* **1988**, *110*, 4748.
70. Chesick, J. P. *J. Phys. Chem.* **1961**, *65*, 2170.
71. Doering, W. V. E.; Gilbert, J. C. *Tetrahedron Suppl.* **1966**, *7*, 397.
72. Cousseau, J. *Synthesis* **1980**, 805.

73. Noller, C. R.; Dinsmore, R. *Organic Synthesis Vol. 2* 1943, 358.
74. Baldwin, A. C.; Davidson, I. M. T.; Howard, A. V. *J. Chem. Soc.; Faraday Trans. 1* 1975, 71, 972.
75. Davidson, I. M. T.; Eaton, G.; Hughes, K. J. *J. Organomet. Chem.* 1988, 347, 17.
76. Pang, Y.; Ijadi-Maghsoodi, S.; Barton, T. J. *Macromolecules* 1993, 26, 5671.
77. Sommer, L. H.; Bailey, D. L.; Bailey, D. L.; Geldberg, G. M.; Buck, C. E.; Bye, T. S.; Evans, F. J.; Whitmore, F. C. *J. Am. Chem. Soc.* 1954, 76, 1613.
78. Ottolenghi, A.; Fridkin, M.; Zilkha, A. *Can. J. Chem.* 1963, 41, 2977.
79. Rieke, R. D. *Acc. Chem. Res.* 1977, 10, 301.
80. Uang, S.; Jones, P. R. *XXIV Organosilicon Symposium*, April 12-13, 1991, 96, El Paso, Texas.
81. Davidson, I. M. T.; Ijadi-Maghsoodi, S.; Lawrence, F. T.; Auner, N. *Organometallics* 1986, 3, 431.
82. Hamon, D. P. G. *J. Am. Chem. Soc.* 1968, 90., 4513.
83. Lee-Ruff, E. *Can. J. Chem.* 1972, 50, 952.
84. Morton, D. R.; Turro, N. *J. Am. Chem. Soc.* 1973, 95, 3947.
85. LaLancette, E. A. *J. Org. Chem.* 1964, 29, 2957.
86. a) Brook, A. G.; Bassindale, A. R. "Organic Chemistry" DeMayo, P., Ed.; Academic Press; New York, 1980; Essay No. 9.
b) Shimizu, H.; Gordon, M. S. *Organometallics* 1994, 13, 186.
87. Sargeant, S. J.; Zhou, S. Q.; Manuel, G.; Weber, W. P. *Macromolecules* 1992, 25, 2832.
88. Williams, J. K.; Benson, R. E. *J. Am. Chem. Soc.* 1962, 84, 1257.
89. Sakurai, H.; Tobita, H.; Nakadaria, Y. *Chem. Lett.* 1982, 1251.
90. Berry, R. S. *J. Chem. Phys.* 1963, 38, 1934.
91. Robin, M. B.; Hart, R. R.; Kuebler, N. A. *J. Chem. Phys.* 1966, 44, 1803.
92. Hirayama, K. *Handbook of Ultraviolet and Visible Absorption Spectra of Organic Compounds* 1967, New York, Plenum Press Data Division.

93. It was also reported that compound **82** was synthesized by photodimerization of 3-methyl-1,2-butadiene (Slobodin, Y. M., *Zh. Organ. Chem.*, **1988**, *24*, 1556.). However, the ¹³C-NMR data they reported (24.16, 111.74, 144.36 ppm) were exceedingly different from ours.
94. a) Barton, T. J.; Lin, J.; Zhang, X.; Ijadi-Maghsoodi, Shimizu, H.; Gordon, M. S. *J. Am. Chem. Soc.* to be submitted.
b) Lin, J.; Ijadi-Maghsoodi, S.; Barton, T. J. *Polym. Prepr.* **1995**, *36*(1), 501.
95. a) Williams, D. J. Ed. *Nonlinear Optical Properties of Organic and Polymeric Materials*, ACS Symposium Series 233, American Chemical Society, Washington, D.C., **1983**.
b) Reinhardt, B.A., *trends in Poly. Sci.*, **1993**, *1*, 5.
96. Most recent review on third-order nonlinear optical effects in organic systems: Bredas, J. L.; Adant, C.; Tackx, P.; Persoons, A.; Pierce, B. M. *Chem. Rev.*, **1994**, *94*, 243.
97. Kajzar, F.; Etemad, S.; Baker, G. L.; Messier, J. *Solid State Commun.* **1987**, *63*, 1113.
98. Singh, B. P.; Prasad, P. N.; Karasz, F. E. *Polymer*, **1988**, *29*, 1940.
99. Prasad, P. N.; Swiatkiewicz, J.; Pflieger, J. *Mol. Cryst. Liq. Cryst.* **1988**, *160*, 53.
100. Rao, D. N.; Chopra, P.; Ghosal, S. K.; Swiatkiewicz, J.; Prasad, P. N. *J. Chem. Phys.* **1986**, *84*, 7049.
101. Lee, C. Y-C.; Swiatkiewicz, J.; Prasad, P. N., Mehta, R.; Bai, S. J. *Polymer* **1991**, *32*, 1195.
102. Agrawal, A. K.; Jenekhe, S. A.; Vanherzeele, H.; Meth, J. S. *J. Phys. Chem.* **1992**, *96*, 2837.
103. Osaheni, J. A.; Jenkhe, S. A.; Vanherzeele, H.; Meth, J. S. Sun, Y.; Macdiarmid, A. G. *J. Phys. Chem.* **1992**, *96*, 2830.

104. Reviews on cumulenes:

- a) Fisher, H. *The Chemistry of Alkenes*; Patai, S. Ed.; Wiley-Interscience Publishers: London, 1964; Chapter 13, p1025-1159.
 - b) Murray, M. *Methoden Org. Chem.* (Houben-Weyl) 1977, 5/2a, p 973-1076.
 - c) Hopf, H. *The Chemistry of Ketenes, Allenes and Related Compounds*, Part 2; Patai, S. Ed.; Wiley-Interscience Publishers: Chichester, 1980, Chapter 20, p 779-901.
 - d) Brandsma, L.; Verkruijsse, H. D. *Synthesis of Acetylenes, Allenes and Cumulenes*, Elsevier Scientific Publishing Company, New York, 1981, p45-46, p126-130.
105. Berkovitch-Yellin, Z.; Leiserowitz, L. *J. Am. Chem. Soc.* 1975, 97, 5627.
106. Irgartinger, H.; Jäger, H.-U. *Angew. Chem., Int. Ed. Engl.* 1976, 15, 562.
107. Irgartinger, H.; Kurda, E.; Rodewald, H.; Berndt, A.; Bolze, R.; Schlüter, K. *Chem. Ber.* 1982, 115, 967.
108. Irgartinger, H.; Goetzmann, W. *Angew. Chem., Int. Ed. Engl.* 1986, 25, 340.
109. Ewing, D. W.; Pfeiffer, G. V.; *Chem. Phys. Letters* 1982, 86, 365.
110. Liang, C.; Allen, L. C. *J. Am. Chem. Soc.* 1991, 113, 1873.
111. Cognacq, J.-C.; Chodkiewicz, W. *Bull. Soc. Chim. Fr.* 1966, 1999.
112. Rauss-Godineau, J.; Chodkiewicz, W.; Cadiot, P. *Bull. Soc. Chim. Fr.* 1966, 2877.
113. Rauss-Godineau, J.; Chodkiewicz, W.; Cadiot, P. *Bull. Soc. Chim. Fr.* 1966, 2885.
114. Skowronski, R.; Chodkiewicz, W.; Cadiot, P. *Bull. Soc. Chim. Fr.* 1967, 4235.
115. Medvedeva, A. S.; Chichkareva, G. G.; Demina, M. M.; Vyazankin, N. S. *Izv. Akad. Nauk SSSR, Ser. Khim.* 1987, 695.
116. Karich, G.; Jochims, J. C. *Chem. Ber.* 1977, 110, 2680.
117. Stang, P. J.; White, M. R. *J. Am. Chem. Soc.* 1981, 103, 5429.
118. Bestmann, H. J.; Schmid, G. *Tetrahedron Lett.* 1975, 4025.
119. a) Nader, F. W.; Brecht, A. *Angew. Chem. Int. Ed. Engl.* 1986, 25, 93.
b) Nader, F. W.; Brecht, A.; Kreis, S. *Chem. Ber.* 1986, 119, 1208.
120. For a review on carbon suboxide, see: Kappe, T.; Ziegler, E. *Angew. Chem. Int. Ed. Engl.* 1974, 13, 491.

121. Kleijn, H.; Tigchelaar, M.; Bullee, R. J.; Elsevier, C. J.; Meijer, J.; Vermeer, P. J. *Organometal. Chem.* **1982**, 329.
122. Kunieda, T.; Takizawa, T. *Chem. Pharm. Bull.* **1977**, 25, 1809.
123. Iyoda, M.; Tanaka, S.; Otani, H.; Nose, M.; Oda, M. *J. Am. Chem. Soc.* **1988**, 110, 8494.
124. Chow, H.-F.; Cao, X.-P.; Leung, M.-K. *J. Chem. Soc. Perkin Trans. I* **1995**, 193.
125. Roth, W. R.; Humbert, H.; Wegener, G.; Erker, G.; Exner, H.-D. *Chem. Ber.* **1975**, 168, 1655.
126. a) Ripoll, J. L. *Chem. Commun.* **1976**, 235.
b) Ripoll, J. L.; Thuillier, A. *Tetrahedron*, **1977**, 33, 1333.
127. For an excellent review on radialenes see: Hopf, H.; Maas, G. *Angew. Chem. Int. Ed. Engl.* **1992**, 31, 931.
128. Kloster-Jensen, K.; Wirz, J. *Angew. Chem. Int. Ed. Engl.* **1973**, 12, 671.
129. Heinrich, B.; Roedig, A. *Angew. Chem. Int. Ed. Engl.* **1968**, 7, 375.
130. a) Koster, S. K.; West, R. *J. Chem. Soc. Chem. Comm.* **1971**, 1380.
b) Koster, S. K.; West, R. *J. Org. Chem.* **1975**, 40, 2300.
131. Nader, F. W.; Wacker, C.-D.; Irgartinger, H.; Huber-Patz, U.; Jahn, R.; Rodewald, H. *Angew. Chem. Int. Ed. Engl.* **1985**, 24, 852.
132. Uhler, R. O.; Schechter, H.; Tiers, G. V. D. *J. Am. Chem. Soc.* **1962**, 84, 3397.
133. Berkoovitch-Yellin, Z.; Lahav, M.; Leiserowitz, L. *J. Am. Chem. Soc.* **1974**, 96, 918.
134. Kaftory, M.; Agmon, I.; Ladika, M.; Stang, P. J. *J. Am. Chem. Soc.* **1987**, 109, 782.
135. Basak, S.; Srivastava, S.; LeNoble, W. J. *J. Org. Chem.* **1987**, 52, 5095.
136. a) Stang, P. J.; Learned, A. E. *J. Chem. Soc. Chem. Commun.* **1988**, 301.
b) Learned, A. E.; Arif, A. M.; Stang, P. J. *J. Org. Chem.* **1988**, 53, 3122.
137. a) Hartzler, H. D. *J. Am. Chem. Soc.* **1971**, 93, 4527.
b) Iyoda, M.; Oda, M.; Kai, Y.; Kanehisa, N.; Kasai, N. *Chem. Lett.* **1990**, 2147.
138. Review on molecular and polymeric carbon allotropes: Diederich, F.; Rubin, Y. *Angew. Chem. Int. Ed. Engl.* **1992**, 31, 1101.

139. Kertesz, M.; Koller, J.; Azman, A. *J. Chem. Phys.* **1978**, *2779*.
140. Karpfen, A. *J. Phys. C* **1979**, *C12*, 3227.
141. Rice, M. J.; Bishop, A. R.; Campbell, D. K. *Phys. Rev. Lett.* **1983**, *51*, 2136.
142. Akagi, K.; Nishiguchi, M.; Shirakawa, H.; Furukawa, Y.; Harada, I. *Synth. Met.* **1987**, *17*, 557.
143. Mel'nichenko, V. M.; Sladkov, A. M.; Nikulin, Y. N. *Russ. Chem. Rev.* **1982**, *51*, 421.
144. Smith, P. P. K.; Buseck, P. R. *Science (Washington, D. C.)* **1982**, *216*, 984.
145. a) Eastmond, R.; Johnson, T. R.; Walton, D. R. W. *Tetrahedron* **1972**, *28*, 4601.
b) Eastmond, R.; Walton, D. R. W. *Tetrahedron* **1972**, *28*, 4691.
c) Johnson, T. R.; Walton, D. R. W. *Tetrahedron* **1972**, *28*, 5221.
146. Hoffmann, R. *Tetrahedron* **1966**, *22*, 521.
147. Pitzer, K. S.; Clementi, E. *J. Am. Chem. Soc.* **1959**, *81*, 4477.
148. Bernholc, J.; Phillips, J. C. *J. Chem. Phys.* **1986**, *85*, 3258.
149. Zahradnik, R.; Hobza, P.; Burcl, R.; Hess, B. A. Jr.; Radziszewski, J. G. *J. of Mol. Struct. (Theochem)* **1994**, *313*, 335.
150. Diederich, F.; Rubin, Y.; Knobler, C. B.; Whetten, R. L.; Schriver, K. E.; Houk, K. N.; Li, Y. *Science (Washington, D. C.)* **1989**, *245*, 1088.
151. Parasuk, V.; Almlöf, J.; Feyereisen, M. W. *J. Am. Chem. Soc.* **1991**, *113*, 1049.
152. Reviews on polydiacetylenes:
a) Bässler, H.; Sixl, H.; Enkelmann, V. *Advances in Polymer Science: No. 63 Polydiacetylenes*, Cantow H.-J. Ed., Springer-Verlag Berlin Heidelberg **1984**.
b) Bloor, D.; Chance, R. R. Ed. *Polydiacetylenes*, Nato ASI Series Series E: Applied Sciences-No. 102, Martinus Nijhoff Publishers, **1985**.
c) Sandman, D. J. *trends in Poly. Sci.*, **1994**, *2*, 44.
d) Tsibouklis, J.; Feast, W. J. *trends in Poly. Sci.*, **1993**, *1*, 16.
153. Sandman, D. J.; Tripathy, S. K.; Elman, B. S.; Samuelson, L. A. *Synth. Met.* **1986**, *15*, 229.
154. Karpfen, A. *J. Phys. C.* **1980**, *C13*, 5673.

155. Eckert, H.; Yesinowski, J. P.; Sandman, D. J.; Velazquez, C. S. *J. Am. Chem. Soc.* **1987**, *109*, 761.
156. Skotheim, T. A. Ed. *Handbook of conducting polymers*, M. Dekker, New York, **1986**.
157. a) Dory, M.; Bodart, V.P.; Delhalle, J.; André, J.-M.; Bredas, J.L. *Nonlinear Optical Properties of Polymers*; Heeger, A.J.; Orenstein, J.; Ulrich, D.R., Ed.; Materials Research Society, Pittsburgh, **1988**; p239.
- b) Bodart, V.P.; Delhalle, J.; Dory, M.; Fripiat, J. G.; André, J.-M. *J. Opt. Soc. Am. B* **1987**, *4*, 1047.
158. Beratan, D. N.; Onuchic, J. N.; Perry, J. W. *J. Phys. Chem.* **1987**, *91*, 2696.
159. Chopra, P.; Carlacci, L.; King, H.F.; Prasad, P.N. *J. Phys. Chem.* **1989**, *93*, 7120.
160. Albert, I. D. L.; Pugh, D.; Morley, J. O.; Ramasesha, S. *J. Phys. Chem.* **1992**, *96*, 10160.
161. Shi, R. F.; Zhou, Q. L.; Heflin, J. R.; Zamani-Khamiri, Garito, A. F. *Nonlinear Optics* **1994**, *6*, 305.
162. Kminek, I.; Klimovic, J.; Prasad, P.N., *Chem. Mater.* **1993**, *5*, 357.
163. Ermer, S.; Lovejoy, S.; Leung, D.; Altman, J.C.; Avon, K.; Spitzer, R.; Hansen, G., *SPIE Proceedings* **1990**, 1337, 89.
164. Ermer, S.; Lovejoy, S.; Leung, D.; Spitzer, R.; Hansen, G.; Stone, R., *SPIE Proceedings* **1991**, 1560, 120.
165. Ijadi-Maghsoodi, S.; Pang, Y.; Barton, T. J. *J. of Poly. Sci.: Part A: Poly. Chem.* **1990**, *28*, 955.
166. Van Dongen, J. P. C. M.; De Bie, M. J. A.; Sture, R. *Tetrahedron Lett.* **1973**, *16*, 1371
167. Giesa, R.; Schulz, R. C. *Makromol. Chem.* **1990**, *191*, 857.
168. Weiberth, F. J.; Hall, S. S. *J. Org. Chem.* **1987**, *52*, 3901.
169. Ni, Q.-X.; Shinar, J.; Vardeny, Z. V.; Grigoras, S.; Pang, Y.; Ijadi-Maghsoodi, S.; Barton, T. J. *Phys. Rev.* **1991**, *B 44*, 5939.
170. Soos, Z. G.; Eternad, S.; Galvão, D. S.; Ramasesha, S. *Chem. Phys. Lett.* **1992**, *194*, 341.

171. For a detailed theoretical and experimental description of Z-scan technique, see:
Sheik-Bahae, M.; Said, A. A.; Wei, T.-H.; Hagan, D. J.; Van Stryland, E. W. *IEEE J. Quantum Electron.* **1990**, *26*, 760.
172. Wittig, G.; Harborth, G. *Ber. Dtsch. Chem. Ges.* **1944**, *77*, 306; Wittig, G.; Harborth, G. *ibid* **1946**, *79*, 311.
173. Jones, G. E.; Kendrick, D. A.; Holmes, A. B. *Org. Synth.* **1987**, *65*, 32.
174. a) Lee-Ruff, E. *Can. J. Chem.* **1972**, *50*, 952.
b) Morton, D. R.; Turro, N. J. *J. Am. Chem. Soc.* **1973**, *95*, 3947.
c) Sidky, M. M.; Mahran, M. R. H.; Abdou, W. M.; Hafez, T. S. *Egypt. J. Chem.* **1984**, *27(6)*, 810.
175. Yang, Z.; Sokolik, I.; Karasz, F. E. *Macromolecules* **1993**, *26*, 1188.
176. Morgan, P. W. *Macromolecules* **1970**, *3*, 536.
177. Kuhn, R.; Fischer, F. *Chem. Ber.* **1961**, *94*, 3060.
178. Kishigami, S.; Tanaka, K.; Toda, F. *Chem. Lett.* **1990**, 1877.
179. For the most recent review on organic electroluminescent devices based on organic polymers, see: Kido, J. *trens in Poly. Sci.* **1994**, *2* (10), 350.
180. a) Ding, Y. "Synthesis and study of acetylenic polymers", *Ph. D thesis*, Iowa State University, Ames, Iowa, **1994**.
b) Moroni, M.; Le Moigne, J.; Luzzati, S. *Macromolecules* **1994**, *27*, 562.
181. Soos, Z. G.; Ramasesha, S.; Galvão, D. S. *Phys. Rev. Lett.* **1993**, *71*, 1609.
182. Schmidt, M. W.; Baldrige, K. K.; Boatz, J. A.; Jensen, J. H.; Koseki, S.; Gordon, M. S.; Nguyen, K. A.; Windus, T. L.; Elbert, S. T. *QCPE Bulletin* **1990**, *10*, 52.
183. Lin, J.; Ijadi-Maghsoodi, S.; Barton, T. J.; Meyer, R. K.; Benner, R. E.; Vardeny, Z. V.; Wei, X.; Smith, A. V.; Shinar, J. *Polym. Prepr.* **1994**, *35(2)*, 832.
184. Lin, J.; Ijadi-Maghsoodi, S.; Barton, T. J. *Polym. Prepr.* **1995**, *36(1)*, 499.
185. Meyer, R. K.; Benner, R. E.; Vardeny, Z. V.; Wei, X.; Lin, J.; Barton, T. J. *Mol. Cryst. Liq. Cryst.* **1994**, *256*, 605.
186. Barton, T. J.; Lin, J.; Ma, Z. to be submitted.

ACKNOWLEDGMENTS

This dissertation could not have been accomplished without the inspiration and assistance of many people both named and unnamed. First, I would like to thank Professor Thomas J. Barton for the great three and half years I have spent in this research group. From the stentorian Professor Barton, I have gained a wealth of knowledge about chemistry, betting (mainly on chemistry), flying, English, and humor. His encouragement and support will always be greatly appreciated.

I would like, also, to express my appreciation to the members of Barton research group, both past and present for their friendship and help. Especially, I would like to thank Dr. Yi Pang for his hands-on help when I first joined this group; Dr. Sina Ijadi-Maghsoodi for his invaluable advice and daily help; Mrs. Kathie Hawbaker, for her kind help on many occasions; Ms. Kellie L. Campbell for correcting the English of this thesis and numerous other technical submissions of mine.

In addition, many of our collaborators contributed to this work and they are as follows: Professor Zev V. Vardeny, Professor R. E. Benner, and Mr. Ron Meyer at the University of Utah who studied the third-order nonlinear optical properties of cumulene-containing polymers; Professor Joseph Shinar and Dr. Andy Smith from the Department of Physics at ISU who conducted the ESR studies and luminescent property studies; Professor Mark S. Gordon and Mr. Hideaki Shimizu from the Department of Chemistry at ISU who performed the theoretical study for the olefin to carbene isomerization; Mr. Zhongxin Ma in our group who worked on the theoretical comparison for butatriene and butadiene containing polymers.

I would also like to thank Dr. Victor G. Young, Jr. for the crystallographic results, Dr. Dave Scott and Dr. Karen Ann Smith for their assistance in NMR spectroscopy, Dr. Kamel Harrata, Ms. Jan Beane, and Mr. Charles Baker for mass spectroscopic data reported in this thesis.

Moreover, I would like to use this work to commemorate my parents. Their support and sacrifices throughout my education have always been a great inspiration for me. I would also

like to thank my brothers and sisters for their encouragement, financial assistance through my education, and taking care of my parents.

Finally, I want to express my warmest appreciation to my wife, Linghua, for her love, encouragement, and understanding. It would have been impossible to finish this work without her full support.

Financial support for this work from the Director of Energy Research, Office of Basic Energy Sciences of DOE, National Science Foundation is gratefully acknowledged. Also, I would like to thank the Department of Chemistry and the donors for The Henry Gilman Fellowship which paid for my last year of study at Iowa State.

This work is performed at Ames Laboratory which is operated for U. S. Department of Energy by Iowa State University under contract No. W-7405-ENG-82. The United States government has assigned the DOE report number IS-T1738 for this thesis.